Generation of „LYmph Node Derived Antibody Libraries“ (LYNDAL): a concept for recovering human monoclonal antibodies with therapeutic potential

Von der Fakultät Energie-, Verfahrens- und Biotechnik der Universität Stuttgart
zur Erlangung der Würde eines Doktors der
Naturwissenschaften (Dr. rer. nat.)
genehmigte Abhandlung

Vorgelegt von
Philipp Johannes Diebolder
aus Geislingen an der Steige

Hauptberichter:	Prof. Dr. Roland E. Kontermann
Mitberichter:	PD Dr. Jürgen Krauss

Tag der mündlichen Prüfung: 11. April 2014

Institut für Zellbiologie und Immunologie
Universität Stuttgart
2014

Preface

This dissertation was conducted at the National Center for Tumor Diseases (NCT) Heidelberg, Department of Medical Oncology in the research group of Dr. Michaela A. E. Arndt and PD Dr. Jürgen Krauss ("Antibody-based Immunotherapeutics"). This work has in part been funded by the Bundesministerium für Bildung und Forschung (BMBF; 01EZ0934) and the Klaus Tschira Stiftung (KTS, 00.150.2009). Patient material, i.e., lymph nodes and blood samples, were provided within cooperation by Prof. Dr. Christel Herold-Mende (Department of Neurosurgery, Heidelberg University Hospital, Germany), Dr. Gerhard Dyckhoff, and PD Dr. Philippe A. Federspil (both Department of Otorhinolaryngology, Heidelberg University Hospital, Germany). Parts of this dissertation have been published:

Diebolder P, Keller A, Haase S, Schlegelmilch A, Kiefer JD, Karimi T, Weber T, Moldenhauer G, Kehm R, Eis-Hübinger AM, Jäger D, Federspil PA, Herold-Mende C, Dyckhoff G, Kontermann RE, Arndt MA, Krauss J (2014) Generation of "LYmph Node Derived Antibody Libraries" (LYNDAL) for selecting fully human antibody fragments with therapeutic potential. MAbs 6: 130-146.

Table of contents

Abbreviations

aa	Amino acid(s)
ACV	Acyclovir
ADC	Antibody drug conjugate
ADCC	Antibody-dependent cell-mediated cytotoxicity
ADCP	Antibody-dependent cellular phagocytosis
AIDS	Acquired immunodeficiency syndrome
ALL	Acute lymphoblastic leukemia
Amp^r	Ampicillin resistance
AR	Amphiregulin
ATCC	American Type Culture Collection
ATP	Adenosine triphosphate
B	Bursa of Fabricius; bone marrow
B. anthracis	*Bacillus anthracis*
BLyS	B lymphocyte stimulator
bp	Base pairs
BSA	Bovine serum albumin
BTC	Betacellulin
C5	Complement component 5
CD	Cluster of differentiation
CDC	Complement-dependent cytotoxicity
cDNA	Complementary deoxyribonucleic acid
CDR	Complementarity determining region
CH	Heavy chain constant domain
CIP	Calf intestinal alkaline phosphatase
CL	Light chain constant domain
CMC	Carboxymethyl cellulose
CMV	Cytomegalovirus
CNS	Central nervous system
ColE1	Origin of replication of plasmid Colicin E1
CPE	Cytopathic effect
CpG	Cytosine-phosphate-guanine
CTLA-4	Cytotoxic T lymphocyte antigen 4
D	Diversity
DEPC	Diethyl pyrocarbonate
DMEM	Dulbecco's modified Eagle's medium
DMSO	Dimethyl sulfoxide

DNA	Deoxyribonucleic acid
dNTP	Deoxynucleoside triphosphate
DPBS	Dulbecco's phosphate-buffered saline
DSMZ	German Collection of Microorganisms and Cell Cultures
DTT	1,4-Dithiothreitol
E	Early
E. coli	*Escherichia coli*
EBV	Epstein–Barr virus
EC	Effective concentration
EC_{50}	Half maximal effective concentration
EDC	1-Ethyl-3-(3-dimethylaminopropyl)carbodiimide
EDTA	Ethylenediaminetetraacetic acid
EGF	Epidermal growth factor
EGFR	Epidermal growth factor receptor
ELISA	Enzyme-linked immunosorbent assay
EpCAM	Epithelial cell adhesion molecule
EPGN	Epigen
EPR	Epiregulin
ERK	Extracellular signal-regulated kinase
EtOH	Ethanol
Fab	Fragment antigen-binding
FACS	Fluorescence-activated cell sorting
FBS	Fetal bovine serum
Fc	Fragment crystallizable
FDA	Food and Drug Administration
FITC	Fluorescein isothiocyanate
FPLC	Fast protein liquid chromatography
FR	Framework region
g	Glycoprotein
GP	Glycoprotein
HAMA	Human anti-mouse antibody
HAT	Hypoxanthine-aminopterin-thymidine
HB-EGF	Heparin-binding EGF-like growth factor
HCV	Hepatitis C virus
HEK	Human embryonic kidney
HER	Human epidermal growth factor receptor
HGPRT	Hypoxanthine-guanine phosphoribosyl transferase
HHV	Human herpesvirus

HIV	Human immunodeficiency virus
HPI	Helicase-primase inhibitor
HPV	Human papillomavirus
HRG	Heregulin
HSA	Human serum albumin
HSE	Herpes simplex encephalitis
HSV	Herpes simplex virus
HuMAb	Human monoclonal antibody
IC_{50}	Half maximal inhibitory concentration
IE	Immediate early
Ig	Immunoglobulin
IGF	Insulin-like growth factor
IL	Interleukin
IMAC	Immobilized metal ion affinity chromatography
IPTG	Isopropyl β-D-1-thiogalactopyranoside
J	Joining
JAK	Janus kinase
kb	Kilo base pairs
KRAS	Kirsten rat sarcoma viral oncogene homolog
KSHV	Kaposi's sarcoma-associated herpesvirus
L	Late
LAT	Latency-associated transcript
LB	Lysogeny broth
LYNDAL	Lymph node derived antibody libraries
M	Marker
M13 origin	Origin of replication of bacteriophage M13
mAb	Monoclonal antibody
MEK	Mitogen-activated protein kinase kinase
MFI_{max}	Maximum median fluorescence intensity
MLP	Adenovirus major late promoter
MOA	Mechanism of action
MOI	Multiplicity of infection
MPBS	Milk phosphate-buffered saline
mpELISA	Monoclonal phage enzyme-linked immunosorbent assay
mRNA	Messenger ribonucleic acid
mTOR	Mechanistic target of rapamycin
Myc	Myelocytomatosis oncogene
NA	Not approved

NC	Negative control; not calculable; not calculated
ND	Not determined
NHS	N-hydroxysuccinimide
No.	Number(s)
NRG	Neuregulin
NSCLC	Non-small cell lung cancer
OD	Optical density
o/n	Overnight
OriP	Epstein-Barr virus origin of plasmid replication
P	Primer
PA	Protective antigen
PAGE	Polyacrylamide gel electrophoresis
PBS	Phosphate-buffered saline
PBST	Phosphate-buffered saline Tween 20
PC	Positive control
pCMV	Cytomegalovirus promoter
PCR	Polymerase chain reaction
PD-1	Programmed cell death-1
PEG	Polyethylene glycol
PEI	Polyethylenimine
pelB	Pectate lyase B
PES	Polyethersulfone
PFA	Phosphonoformic acid
PI3K	Phosphatidylinositide 3-kinase
pLac	Lactose promoter
PLC	Phospholipase C
ppELISA	Polyclonal phage enzyme-linked immunosorbent assay
PRNT	Plaque reduction neutralization test
R	Round
Raf	Rapidly accelerated fibrosarcoma
RANKL	Receptor activator of NF-κB ligand
Ras	Rat sarcoma
RBS	Ribosome binding site
RNA	Ribonucleic acid
rpm	Revolutions per minute
RPMI	Roswell Park Memorial Institute medium
RSV	Respiratory syncytial virus
RT	Room temperature

RTK	Receptor tyrosine kinase
RT-PCR	Reverse transcription-polymerase chain reaction
RU	Response units
SA	Splice acceptor sequence
scFv	Single-chain variable fragment
SD	Standard deviation; splice donor sequence
SDS	Sodium dodecyl sulfate
SE	Standard error
SEC	Size-exclusion chromatography
SFCA	Surfactant-free cellulose acetate
SOB	Super optimal broth
SOC	Super optimal broth with catabolite repression
SP	Sodium phosphate
SPR	Surface plasmon resonance
STAT	Signal transducer and activator of transcription
STD	Sexually transmitted disease
T	Thymus
t.u.	Transducing units
TEV	Tobacco etch virus protease cleavage site
TGF-α	Transforming growth factor alpha
TK	Tyrosine kinase
TKI	Tyrosine kinase inhibitor
TM	Transmembrane
TMB	3,3',5,5'-Tetramethylbenzidine
TNF	Tumor necrosis factor
TPL	Adenovirus tripartite leader sequence
UV	Ultraviolet
V	Variable
VEGF	Vascular endothelial growth factor
VH	Heavy chain variable domain
VL	Light chain variable domain
VSV	Vesicular stromatitis virus
VZV	Varicella zoster virus
YT	Yeast extract tryptone

Summary

The development of efficient strategies for generating human monoclonal antibodies with therapeutic potential remains a major challenge in the antibody technology field. In present thesis, an applicable approach has been developed for recovering such antibodies from antigen-encountered, human B cell repertoires. As the source for variable antibody genes, immunoglobulin G (IgG)-derived B cell repertoires from lymph nodes of 20 head and neck cancer patients were employed for cloning individual antibody libraries. Sequence analysis of “Lymph Node Derived Antibody Libraries” (LYNDAL) revealed a naturally occurring distribution pattern of rearranged antibody sequences that represent all known variable gene families and most functional germline sequences. To demonstrate the feasibility of presented approach, test selections against distinct therapeutic targets have been performed including the viral glycoprotein B of herpes simplex virus type 1 (HSV-1) and human epidermal growth factor receptor (EGFR) being frequently overexpressed in head and neck cancer. Panning of LYNDAL from donors with target-specific IgG serum titers delivered 34 anti-gB-1 and seven anti-EGFR single-chain variable fragments (scFvs) with unique sequences. Sequence analysis revealed extensive somatic hypermutation of enriched clones as result of natural affinity maturation. Target specificity was confirmed by binding antiviral scFvs to common glycoprotein B variants from HSV-1 and HSV-2 strains and by binding EGFR-specific scFvs to various EGFR-overexpressing cancer cell lines. The majority of analyzed scFvs bound to the targets with nanomolar affinity as determined on recombinant proteins as well as on protein variants in their natural context. Therapeutic potential of LYNDAL antibodies was evaluated by functional *in vitro* assays testing either the virus neutralizing capacity or the potential for mediating tumor cell growth inhibition. From eight scFvs with HSV-neutralizing capacity, the most potent antibody neutralized 50% HSV-2 at 4.5 nM as dimeric $(scFv)_2$. One of the EGFR-specific antibodies showed auspicious anti-proliferative effects on tumor cells. Using SKOV-3 tumor cells, 50% of the EGF-induced cell growth promoting effect was inhibited at 6.2 nM of bivalent scFv-Fc. In conclusion, the LYNDAL approach is useful for recovering fully human antibodies with therapeutic potential and is expected to be extendable to others than the here evaluated targets.

Zusammenfassung

Die Entwicklung effizienter Strategien zur Herstellung humaner monoklonaler Antikörper mit therapeutischem Potential bleibt eine große Herausforderung innerhalb der Antikörper-Technologiebranche. In der vorliegenden Arbeit wurde eine effektive Methode entwickelt, mit welcher Antikörper aus natürlich immunisierten, humanen B-Zell-Repertoires gewonnen werden können. Als Quelle für die variablen Bereiche der Antikörpergene wurden Immunglobulin G (IgG)-abgeleitete B-Zell-Repertoires aus Lymphknoten von 20 Kopf- und Hals-Tumorpatienten entnommen, um daraus individuelle Antikörper-Bibliotheken herzustellen. Eine Sequenzanalyse der *LYmph Node Derived Antibody Libraries* (LYNDAL) ergab ein natürliches Verteilungsmuster an rearrangierten Antikörpersequenzen, wobei alle humanen Antikörperfamilien und die meisten funktionalen Keimbahnsequenzen identifiziert werden konnten. Um die Effizienz der präsentierten Methode zu demonstrieren, wurden Test-Selektionen gegen unterschiedliche therapeutische Antigene durchgeführt, einschließlich dem viralen Glykoprotein B von Herpes Simplex Virus Typ 1 (HSV-1) und dem humanen Epidermalen Wachstumsfaktor Rezeptor (EGFR), welcher häufig bei Kopf- und Halstumoren überexprimiert vorliegt. Selektionen mit LYNDAL von Spendern mit Antigen-spezifischen IgG Serum-Titer lieferten insgesamt 34 unterschiedliche anti-gB-1 und sieben anti-EGFR *single-chain variable fragments* (scFvs). Sequenz-Analysen zeigten, dass die angereicherten Klone zahlreiche somatische Hypermutationen aufwiesen, was auf eine natürliche Affinitätsreifung hindeutet. Die Antigen-Spezifität konnte durch Bindung der antiviralen scFvs an ubiquitäre HSV-1- und HSV-2-Varianten von Glykoprotein B bzw. im Falle der EGFR-spezifischen scFvs anhand von EGFR überexprimierenden Tumorzelllinien nachgewiesen werden. Der Großteil der analysierten scFvs besaß nanomolare Affinitäten gegenüber den Zielantigenen und zwar sowohl zu rekombinanten Protein als auch zu Proteinvarianten im natürlichen, therapeutischen Kontext. Das therapeutische Potential der LYNDAL-Antikörper wurde in In-Vitro-Experimenten überprüft, wobei entweder die virale Neutralisationseffizienz oder das Potential zur Tumorzellwachstums-Inhibition getestet wurde. Von insgesamt acht scFvs mit nachgewiesener HSV-Neutralisation-Kapazität konnte der potenteste Antikörper 50% der HSV-2 Partikel bei einer eingesetzten Konzentration von 4.5 nM als dimeres $(scFv)_2$ neutralisieren. Einer der EGFR-spezifischen Antikörper zeigte

vielversprechende anti-proliferative Eigenschaften, wobei der durch EGF-induzierte, wachstumsfördernde Effekt gegenüber SKOV-3 Tumorzellen mit 6.2 nM an bivalentem scFv-Fc halbiert werden konnte. Schlussfolgernd kann gesagt werden, dass die entwickelte Methode hilfreich ist, um vollständig humane Antikörper mit therapeutischem Potential zu generieren. Es wird darüber hinaus erwartet, dass das Konzept verwendet werden kann, um Antikörper gegen bis dato noch nicht untersuchte Antigene zu gewinnen.

1 Introduction

1.1 Medical need of human monoclonal antibodies

With the invention of the hybridoma technology for generating monoclonal antibodies (mAbs) in 1975 [1], immunotherapy with mAbs or antibody-based drugs evolved to a powerful therapeutic intervention of the modern medicine. However, first therapeutic trials showed limited success because the applied murine antibodies induced host immune responses (human anti-mouse antibodies, HAMAs) leading to reduced therapeutic efficacy [2-4]. To diminish immune reactions of animal-derived mAbs, technologies for chimerization [5,6] and humanization [7] have been developed. Moreover, recent approaches enable the generation of even fully human antibodies. Although the most of mAbs being approved in the EU and/or US are still animal-derived, the vast of the latest approved mAbs are of human origin (**Table 1**). Today, human monoclonal antibodies (HuMAbs) have emerged to the fastest growing class of antibody-derived therapeutics entering clinical trials [8,9] indicating that the dominance of HuMAbs as therapeutics will further increase. In general, the majority of the currently approved mAbs are intended for the treatment of immunological disorders and cancer (**Table 1**) but several hundred mAbs being in clinical development are directed against a much broader panel of targets and diseases. Based on the still high medical need for fully human antibody therapeutics, this thesis aimed in the development of an applicable and efficient approach for generating HuMAbs with therapeutic potential.

Table 1. Therapeutic mAbs being approved or in review in the EU and/or US.

International non-proprietary name	Trade name; company	Target; type[a]	Indication first approved	Year of EU (US) approval
Muromonab-CD3	Orthoclone Okt3; Janssen-Cilag	CD3; murine IgG2a	Reversal of kidney transplant rejection	1986[b] (1986[c])
Abciximab	Reopro; Janssen Biotech, Eli Lilly	GPIIb/IIIa; chimeric IgG1 Fab	Prevention of blood clots in angioplasty	1995[b] (1994)
Rituximab	MabThera, Rituxan; Biogen Idec, Genentech	CD20; chimeric IgG1	Non-Hodgkin's lymphoma	1998 (1997)
Basiliximab	Simulect; Novartis	IL2R; chimeric IgG1	Prevention of kidney transplant rejection	1998 (1998)
Daclizumab	Zenapax; Genentech	IL2R; humanized IgG1	Prevention of kidney transplant rejection	1999 (1997);[c]
Palivizumab	Synagis; MedImmune, AbbVie	RSV; humanized IgG1	Prevention of respiratory syncytial virus infection	1999 (1998)
Infliximab	Remicade; Janssen Biotech	TNF; chimeric IgG1	Crohn disease	1999 (1998)
Trastuzumab	Herceptin; Genentech	HER2; humanized IgG1	Breast cancer	2000 (1998)
Alemtuzumab	MabCampath, Campath-1H; Genzyme	CD52; humanized IgG1	Chronic myeloid leukemia	2001 (2001)
Adalimumab	Humira; AbbVie	TNF; human IgG1, phage-produced	Rheumatoid arthritis	2003 (2002)
Tositumomab-I131	Bexxar; GlaxoSmithKline	CD20; murine IgG2a	Non-Hodgkin lymphoma	NA (2003)
Efalizumab	Raptiva; Genentech, Merck	CD11a; humanized IgG1	Psoriasis	2004 (2003);[c]
Cetuximab	Erbitux; Bristol-Myers Squibb, Eli Lilly, Merck	EGFR; chimeric IgG1	Colorectal cancer	2004 (2004)
Ibritumomab tiuxetan	Zevalin; Biogen Idec, Bayer	CD20; murine IgG1	Non-Hodgkin lymphoma	2004 (2002)
Omalizumab	Xolair; Genentech, Norvartis	IgE; humanized IgG1	Asthma	2005 (2003)
Bevacizumab	Avastin; Genentech	VEGF; humanized IgG1	Colorectal cancer	2005 (2004)
Natalizumab	Tysabri; Biogen Idec, Perrigo	alpha4 integrin; humanized IgG4	Multiple sclerosis	2006 (2004)
Ranibizumab	Lucentis; Genentech, Norvartis	VEGF; humanized IgG1 Fab	Macular degeneration	2007 (2006)
Panitumumab	Vectibix; Amgen	EGFR; human IgG2, mouse-produced	Colorectal cancer	2007 (2006)
Eculizumab	Soliris; Alexion	C5; humanized IgG2/4	Paroxysmal nocturnal hemoglobinuria	2007 (2007)

International non-proprietary name	Trade name; company	Target; type[a]	Indication first approved	Year of EU (US) approval
Certolizumab pegol	Cimzia; UCB	TNF; humanized Fab, pegylated	Crohn disease	2009 (2008)
Golimumab	Simponi; Janssen-Cilag, Merck	TNF; human IgG1, mouse-produced	Rheumatoid and psoriatic arthritis, ankylosing spondylitis	2009 (2009)
Canakinumab	Ilaris; Novartis	IL1b; human IgG1, mouse-produced	Muckle-Wells syndrome	2009 (2009)
Catumaxomab	Removab; Trion, Fresenius	EpCAM/CD3; rat-mouse bispecific mAb	Malignant ascites	2009 (NA)
Ustekinumab	Stelara; Janssen-Cilag	IL12/23; human IgG1, mouse-produced	Psoriasis	2009 (2009)
Tocilizumab	RoActemra, Actemra; Genentech	IL6R; humanized IgG1	Rheumatoid arthritis	2009 (2010)
Ofatumumab	Arzerra; Genmab	CD20; human IgG1, mouse-produced	Chronic lymphocytic leukemia	2010 (2009)
Denosumab	Prolia; Amgen	RANKL; human IgG2, mouse-produced	Bone Loss	2010 (2010)
Belimumab	Benlysta; MedImmune, GlaxoSmithKline	BLyS; human IgG1, phage-produced	Systemic lupus erythematosus	2011 (2011)
Ipilimumab	Yervoy; Medarex, Bristol-Myers Squibb	CTLA-4; human IgG1, mouse-produced	Metastatic melanoma	2011 (2011)
Brentuximab vedotin	Adcetris; Seattle Genetics, Millennium	CD30; chimeric IgG1, immunoconjugate	Hodgkin lymphoma	2012 (2011)
Pertuzumab	Perjeta; Genentech	HER2; humanized IgG1	Breast Cancer	2013 (2012)
Raxibacumab	(Pending); MedImmune, GlaxoSmithKline	*B. anthrasis* PA; human IgG1, phage-produced	Anthrax infection	NA (2012)
Trastuzumab emtansine	Kadcyla; Genentech	HER2; humanized IgG1, immunoconjugate	Breast cancer	In review (2013)
Vedolizumab	Entyvio; Millennium	alpha4beta7 integrin; humanized IgG1	Ulcerative colitis, Crohn disease	In review (NA)

[a]All murine, chimeric, and humanized antibodies were originally derived from murine hybridomas. The technology for the generation of HuMAbs (shaded in gray) is indicated. [b]Country-specific approval; approved under concertation procedure. [c]Voluntarily withdrawn from market. BLyS, B lymphocyte stimulator; C5, complement component 5; CD, cluster of differentiation; CTLA-4, cytotoxic T lymphocyte antigen 4; EGFR, epidermal growth factor receptor; EpCAM, epithelial cell adhesion molecule; GP, glycoprotein; IL, interleukin; NA, not approved; PA, protective antigen; RANKL, receptor activator of NF-κb ligand; RSV, respiratory syncytial virus; TNF, tumor necrosis factor; VEGF, vascular endothelial growth factor. Adapted from [10].

1.2 Current technologies for generation of HuMAbs

Over the past 30 years, monoclonal antibody technology has rapidly progressed and several powerful and competing technologies for generation of fully human mAbs are now available [11]. Currently, the vast majority of clinically investigated HuMAbs are either produced by immunization of transgenic mice that are equipped with the human antibody gene repertoires (**Figure 1 A**) [12,13] or by preparing combinatorial antibody libraries (**Figure 1B**) [14]. Although based on human genes, both technologies can deliver mAbs that possess (cross-) reactivity to human antigens due to missing depletion mechanisms in transgenic mice or due to de novo VH/VL combinations in combinatorial libraries. More recently, other methodologies have been developed or refined, e.g., the efficient immortalization of human B cells [15,16] now allowing the efficient generation of human hybridomas (**Figure 1C**) [17] and the expression-cloning of physiological variable (V) gene pairings from blood-derived human B cells of infected individuals (**Figure 1D**) [18]. Both latter techniques allowed the production of antiviral HuMAbs with high therapeutic potential, e.g., against influenza virus [19,20] and human immunodeficiency virus (HIV) [21-24] that can be hardly obtained from not immunologically challenged repertoires. Indeed, employing immortalized memory B cell populations delivered potent neutralizing HuMAbs even decades after antigen exposure as shown for survivors of the 1918 pandemic influenza virus [20]. Actually, immortalization and antigen baiting approaches are currently mainly focused on memory B cells [11]. However, antibody secreting plasmablasts that were collected from the blood during an active immune response have also been used as source for the rapid cloning of high affinity HuMAbs [19,25]. These technologies always require immunized B cell populations thus excluding several targets a priori, e.g., many human antigens and toxins. Most limiting, sorted B cell repertoires as well as immunized mice can only be used once for screening towards a disease-related antigen. In contrast, combinatorial libraries can be employed for a theoretical unlimited number of targets.

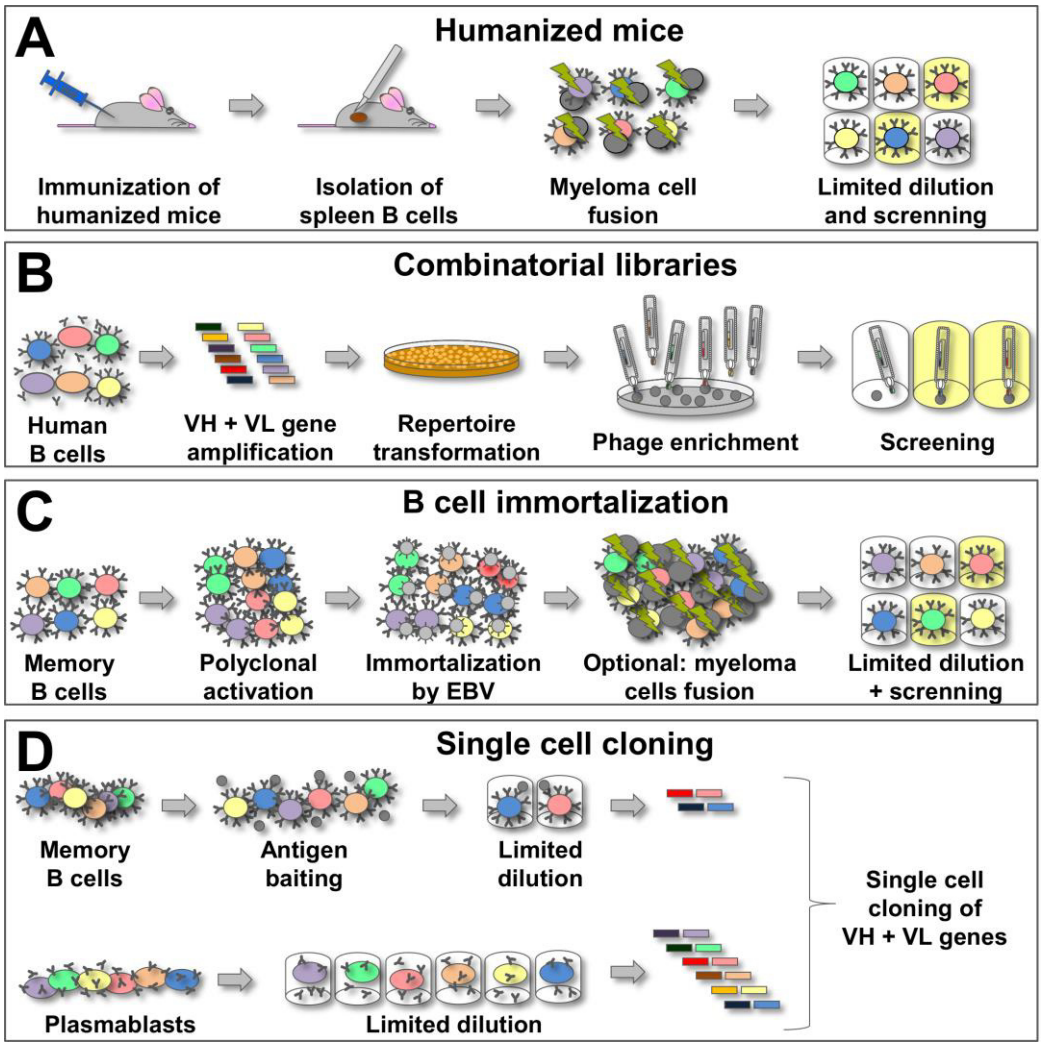

Figure 1. Most common technologies for generating human therapeutic mAbs. (**A**) In humanized mice, murine antibody loci are replaced by human counterparts. Antigen-specific immune response is induced by immunization followed by fusion of spleen B lymphocytes with myeloma cells. HGPRT-positive hybridomas are selected in HAT medium, and culture supernatants of hybridomas are screened for antigen-specific HuMAbs. (**B**) For generation of combinatorial antibody libraries, human B cell repertoires are used for reverse transcription (RT)-PCR amplification of VH and VL genes that are randomly cloned into appropriate vector systems. After electroporation into *E. coli* bacteria, antibody fragment-presenting phage libraries are produced by superinfection with helper phage. Antigen-enriched binders are then screened for specific monoclonal phage antibodies. (**C**) Immortalization of isolated human B cells is archived by polyclonal *in vitro* activation using CpG followed by EBV transformation. Optionally, human hybridomas are produced by electrofusion with myeloma cells. After limited dilution, single cells are screened for desired specificities. (**D**) In single-cell expression cloning, RT-PCR of single cells is applied for cloning V genes into mammalian cell expression vector systems. As source, either antigen-specific memory B cells or unselected plasmablasts are employed.

1.3 Antibody selection platforms

Today, various platform technologies are used for the selection of HuMAbs from combinatorial libraries [14,26]. As a common principle, rearranged antibody genes are randomly cloned into appropriate vector systems for presentation of selectable antibodies (IgG) or fragments (scFvs, Fabs) followed by enrichment of specific binders. The current display technologies can be roughly grouped into *in vitro* systems, such as phage display [27,28] or ribosome display [29,30], and into *in vivo* techniques employing bacteria [31-34], yeast [35,36], and mammalian cells [37,38]. Although all these approaches seem to be valuable, displaying antibody repertoires on bacteriophages, however, has evolved into the most successful selection platform today because it offers highly versatile technological options. Beside the choice of various antibody formats, the display valency can be easily controlled which directly leads to improved selection efficacies. Thus, the most common type 3+3-derived phagemid system allows for adapting the number of presented antibody fragments depending on the employed helper phage strain. For instance, the hyperphage system can theoretically improve antigen binding activity up to 400-fold by oligomeric display when compared to the mostly monovalent fragment presentation using pIII wild-type encoding helper phages [39]. Moreover, phage display provides various selection strategies that are clearly limited for the other platforms. Predominantly, panning is performed on recombinant targets being immobilized onto plastic surfaces [40-42], but more sophisticated methodologies can be employed, e.g., capturing in solution [43,44], *in vivo* selection [45], and panning using target-expressing cells [46] or tissues [47]. Further advantages of phage display includes that it is technically robust, inexpensive, and allows the automation of the selection and screening process [26,48]. In 2002, the first fully human phage display-derived mAb adalimumab was FDA-approved for the treatment of rheumatic and chronic inflammatory bowel diseases followed by belimumab and raxibacumab for the treatment of systemic lupus erythematosus and inhalational anthrax infection, respectively. Today, other phage display-derived mAbs are currently at advanced stages of clinical development and may reach market approval within the next few years.

1.3.1 Antibody repertoires: immune libraries

Combinatorial antibody repertoires are usually grouped into immune, naïve, and (semi-) synthetic libraries depending on the gene source used for construction. Immune libraries are often cloned from IgG mRNA of patients or vaccinated donors and intended for recovering of mAbs that have undergone natural affinity maturation. As a main strength, the cloned repertoires can be usually relative small in size (10^5-10^7 members) since cloning from peripheral blood during an ongoing infection guarantees a large number of disease-related plasmablasts [49]. Indeed, the construction of various immune libraries against a wide range of disease-related targets has been reported [50-63], and many high affinity HuMAbs have been isolated from immunized repertoires. Such isolated antibodies may be therapeutically valuable since affinity maturation during the course of an antigen-encountered immune response can lead to advantageous functional properties and improved fine-specificities over immunologically unchallenged repertoires [64,65]. Although the natural pairing of immunoglobulin heavy and light chains are often lost during library construction, combinatorial immune libraries may also be useful for the retrospective characterization of the natural antibody response to infections [66,67]. Nevertheless, combinatorial immune repertoires are generally small in size and therefore restricted to targets for that natural immune responses occurred within donors.

1.3.2 Antibody repertoires: non-immune libraries

To be more flexible concerning the number of exploitable targets, the field moved continuously towards generating commonly usable large non-immune libraries with highly diverse repertoires. The first such libraries were mostly cloned from the IgM B cell mRNA to capture the naïve or primary immune response [40,68-70] because these antibody genes are known to be barely mutated and should be capable to recognize a wide panel of epitopes. However, naïve and primary repertories are generally not the most productive for successful isolation of high affinity autoantibodies because the human immune system may be depleted from self-binding sequences to prevent the development of autoimmune diseases [71]. To solve this problem, artificial sequence diversity was either introduced into the highly diverse complementarity determining regions (CDRs) of natural repertoires thus constructing semi-synthetic libraries [72-74] or, less frequent, artificial frameworks

were completed with naturally occurring sequences [75]. In the end, several complete synthetic libraries were generated that enabled the isolation of high affinity mAbs with specificities against a huge panel of antigens inclusively many human-derived proteins [76-80]. As the major drawback, however, non-immune libraries have in general to be large in size because the probability to discover high affinity antibodies for any target increases with the size and diversity of the used antibody library [81,82]. For example, Griffiths and coworkers showed that large libraries (>10^{10} members) can yield in antibodies with affinities in the range of a secondary immune response (<10 nM) [72]. As a result, most current commercial libraries consist of antibody repertoires of 10^{11}-10^{12} clones [79,80,83-85] that allow the selection of HuMAbs with even picomolar affinities for multiple targets inclusively for antigens of human origin. However, cloning of large libraries is time-consuming and elaborate because the cloned repertoires have to be introduced into *E. coli* bacteria by ususally hundreds of electroporations. Moreover, the mentioned complexities of the latest state-of-the-art libraries represent an upper limit for library construction since larger phage-displayed repertoires can not be efficiently handled during selection and smaller libraries with more defined repertoires might be preferable. Most importantly, current single-pot libraries usually do not contain rearrangements that were developed during the course of a humoral immune response. As a matter of fact, the thus selected antibodies have usually not undergone natural somatic hypermutations that lead to increased affinities.

1.4 Immunological targets

This thesis aimed at developing an applicable strategy for generation of human monoclonal antibodies exploitable for immunotherapy. The elaborated LYNDAL concept was proved by antibody selections employing two different therapeutic targets, glycoprotein B of herpes simplex virus (HSV) type 1 and human epidermis growth factor receptor. Therefore, the following sections describe the therapeutic relevance of these antigens as well as the current standard of care options for treating diseases being associated with these antigens.

1.5 Herpes simplex virus

The human pathogenic herpes simplex virus type 1 and type 2 (HSV-1 and HSV-2) are dermatotropic and neurotropic DNA viruses with a high prevalence in the adult world population (HSV-1: 55-85%, HSV-2: 10-25%) [86-90]. HSV-1 and HSV-2 are closely related members of the family of human herpesviruses which also includes varicella-zoster virus (VZV), cytomegalovirus (CMV), Epstein-Barr virus (EBV), human herpesviruses 6 and 7 (HHV-6 and HHV-7), and Kaposi's sarcoma-associated herpesvirus (KSHV).

1.5.1 HSV entry and replication

Herpesviruses possess complex virions of different size but all share the same basic morphology that consists of four distinct concentric layers: the inner core composed of the virus DNA is housed in an icosahedral capsid that is surrounded by tegument proteins and the envelope membrane bearing virus encoded glycoproteins (**Figure 2A**) [91].

Productive HSV replication starts with virion binding to host epithelial cells. Attachment is initiated by interaction of the virions glycoproteins B (gB) and C (gC) to heparan sulfate moieties on the host cell membrane. Virion attachment is further stabilized by binding of the main receptor glycoprotein D (gD) to different host receptors including nectin 1. Receptor binding triggers conformational changes within gD that leads to activation of the herpesvirus-conserved core fusion machinery consisting of trimeric gB and the heterodimer gH/gL. Fusion is a highly complex so far poorly understood process despite knowing that gB acts as main fusogen being regulated by the gH/gL complex [92]. Fusion protein gB shows structural homology and similar fold to other viral fusion proteins and may undergo large conformational changes during fusion. Thus far, the crystallographic structure of noncovalently-linked trimeric gB of HSV-1 (gB-1) was solved that is regarded to represent the post-fusion conformation of the protein (**Figure 2B**) [93] whereas the pre-fusion structure is still elusive. It remains to be understood how gB undergoes the substantial folding changes [92] but transition from the pre-fusion to the post-fusion conformation and further conformational changes of the fusion machinery finally induce membrane fusion of the virus envelope with the host plasma membrane. Then, the nucleocapsid

is released into the cell cytoplasm and rapidly transported along microtubules to the nuclear pores where the HSV genome is delivered into the nucleus [91]. After circulation of the HSV genome, the HSV genes are gradually expressed. In the first phase, the immediate early (IE) genes are transcribed by the host RNA polymerase II supported by viral transcription factor VP16 [91]. Produced mRNA encoded for further five transcription factors with roles in switching on the early (E) and late (L) genes encoding for gene products essentially for virus DNA replication and virus structural proteins, respectively [94]. Virus genome is amplified as concatemer in a rolling circle replication. Virion assembly starts with formation of empty procapsids that are loaded with concatemer DNA in genome-length by entering via the capsid portal [94]. Upon acquiring some tegument proteins in the nucleus, the nucleocapsids bud through the inner and outer nucleus membranes into the cytoplasm where the remainders of the tegument proteins are added. The virion envelope with embedded glycoproteins is acquired through budding into the Golgi compartment followed by the transport within vesicles to the plasma membrane. Finally, the matured virions are released from the cell by membrane fusion [94].

Besides the infection by free released particles, HSV virions can spread from cell-to-cell over direct cell contacts. This is an efficient way of HSV virions for moving across epithelial cells or neuronal junctions because the virions are protected from neutralizing antibody responses by tight and adherent junctions [92]. Direct cell-to-cell spread is a complex and poorly understood process that involves the proteins of the fusion machinery and other additional proteins, such as the heterodimerc gE/gI complex [95].

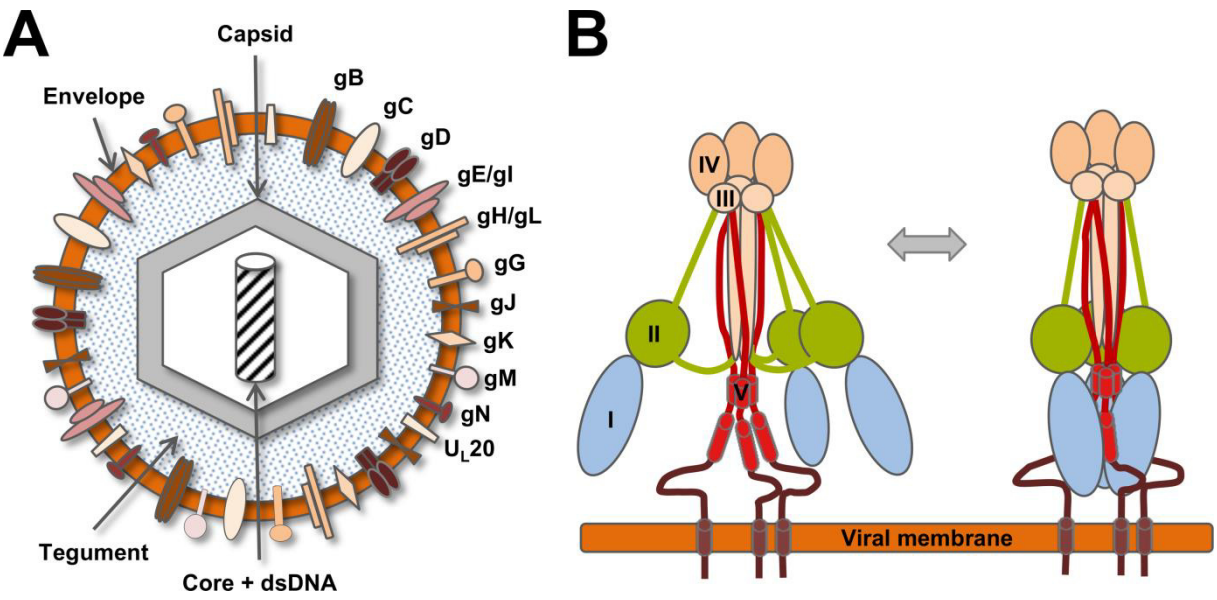

Figure 2. Schematic structures of the HSV virion and HSV glycoprotein B. (**A**) The herpes simplex virion is an enveloped virus, i.e., the icosahedral capsid containing the HSV genome is shielded by tegument proteins and a host-derived lipid bilayer. In the figure, only the 13 distinct envelope embedded glycoproteins are shown. (**B**) The schematic model of HSV-1 glycoprotein B shows how it may refold during the fusion process. The potential pre-fusion (left) and post-fusion state (right) is deducted from crystal structure experiments and comparisons with other viral fusion mechanisms as well leading to the hypothesis that gB refolds in an umbrella-like fashion. Figure 2B was adapted from [93].

1.5.2 Latent HSV infections

One hallmark of HSV is its capability to establish latent infections of neurons that persist life-long in the host. Virus transmission mostly occurs by body fluids of infected individuals or by direct skin contact to regions with actively replicating virions even without visible lesions. Primary infections of usually oral or genital mucosa are mostly asymptomatic. Viruses may replicate in epithelial cells and enter innervating sensory neurons where they start travelling along the axon to the neuronal body in ganglion tissue, e.g., trigeminal ganglia and sacral ganglia. Once in the neuron, the virus establishes latent infections without production of infection particles. During latency, the virus genome persists as circular, double-stranded episom [96]. Latency is accompanied by synthesis of virus RNA known as latency-associated transcripts (LATs). These transcripts are further processed to a series of microRNAs that ensure the survival of the infected neuron by avoiding immune surveillance and inhibition of apoptosis [94]. Virus activation can be induced upon the proper stimulus, e.g.,

physical and psychical stresses, ultraviolet light, and immunosuppression. Activation from latency results in travelling of the viral capsid back down the axon and finally in another round of productive replication at or near the primary site of infection [91].

1.5.3 HSV immunoepidemiology

HSV belongs to the most prevalent infectious agents in humans and is source of different diseases [97]. The most common form, herpes labiablis, is mainly mediated by HSV-1 usually causing recurrent facial herpes that can vary in severity. Primary orofacial infections are mostly acquired early in childhood but other body regions can also be affected, e.g., fingers or thumbs (herpetic whitlow), head, extremities, and the trunk after skin-to-skin contact (herpes gladiatorum). Recurrent outbreaks can differ in frequency and severity and even asymptomatic forms may allow spreading to susceptible individuals. Genital herpes is a common sexually transmitted disease (STD) with estimated half a billion infected individuals worldwide that is predominantly caused by HSV-2 [98]. However, HSV-1 has recently emerged as the prominent causative agent of genital herpes in some developed countries [99]. Genital infection can be painful due to herpes ulceration, moreover, causing substantial psychological morbidity [100]. Genital herpes infection can increase the risk of susceptibility to other sexually transmitted diseases, e.g., 3-fold for acquiring HIV [101]. Furthermore, short bursts of subclinical HSV reactivations are frequent despite antiviral therapy [102] and may be responsible for rapidly transmission of genital herpes to sexual partners. Vertical transmission of the herpes simplex virus from mother to newborn can cause neonatal herpes that is associated with eye or skin lesions but can also be fatal by causing meningoencephalitis, disseminated infection, or fetal malformations [99]. Although the incidence for neonatal herpes is low [103], it causes significant morbidity and mortality in infected newborns despite antiviral therapies. In fact, the mortality rate among untreated infants with disseminated or central nervous system HSV infection is more than 50% [104]. In common, herpes simplex encephalitis (HSE) in older children, adolescents, and adults is a rare disease (about 1 in 300.000), however, HSE remains one of the most devastating infections of the central nervous system with high rates of recurrence despite available antiviral therapy [105]. HSV is also associated with a variety of ocular diseases, e.g., herpes keratitis. The estimated annual incidence of herpes keratitis is around 1.5 million with around 40,000 cases of severe visual impairment

[106]. Indeed, HSV is the leading cause of infectious blindness in the developed world [107]. Although shedding of HSV-1 to the eyes may occur often in infected individuals, the vast majority remains asymptomatic. However, recurrent symptomatic infections can range from rare episodes to outbreaks occurring monthly or even more frequently [97].

1.5.4 Current treatment options for HSV

Today acyclovir (ACV) is widely used as gold standard for prevention and treatment of HSV infections representing a potent and safe drug with almost no side effects [108]. Being a nucleoside analogue, ACV is selectively converted by the viral thymidine kinase into acyclo-guanosine monophosphate. Cellular kinases further mediate phosphorylation into the active triphosphate form that lead to termination of the DNA replication due to lack of a 3'OH group. Acyclovir is indicated for the treatment of the most HSV-caused diseases as well as for the prophylaxis in immunocompromised individuals or cancer patients undergoing chemotherapy. Depending on the medical indication, acyclovir is marketed as topical cream, tablet, ophthalmic ointment, and when high ACV concentrations are needed, as intravenous injection due to its poor oral bioavailability. Alternatively to acyclovir, the acyclic guanosine analogue penciclovir is also widely used for HSV treatment because its active triphosphate form may persist longer within the host cells. To avoid intravenous applications, prodrug formulations valaciclovir and famciclovir have been developed that possess greater oral bioavailability than ACV and penciclovir, respectively. However, the wide use of nucleoside analogues in HSV treatment and prophylaxis has raised concern about the development of resistance [106]. Several studies analyzing the resistance to acyclovir revealed that it is low (~0.3%) in immunocompetent individuals [109] but much higher in immunocompromised [110-112] particularly in HIV patients or recipients of stem cell transplants with 4% and 11%, respectively [109]. Resistance to ACV is mostly associated with mutations of the viral thymidine kinase (>95%) and rarely due to mutations of the viral DNA polymerase. As a result, ACV-resistant HSV strains are almost always cross-resistant to the other thymidine kinase-dependent drugs, i.e., penciclovir and prodrug formulations [113]. Resistant infections are usually managed by foscarnet (phosphonoformic acid, PFA), but resistance to this drug has also been documented [109,114-116]. Patients excreting strains being resistant to both ACV and PFA are

usually treated with the acyclic nucleoside phosphonate cidofovir [117-119]. Although intravenous injected foscanet and cidofovir have been successfully applied for treatment of resistant strains, nephrotoxicity is a serious side effect to these drugs and applicable therapeutic alternatives are required [116].

1.5.5 Alternative approaches to treat HSV

Nucleoside analogues-resistant HSV strains predominantly originate from mutations within the viral thymidine kinase [116,120,121]. Novel strategies for treatment of HSV infections include development of chemical drugs that act independently of the thymidine kinase, such as imiquimod, helicase-primase inhibitors (HPIs), and distamycin A [116]. Imiquimod, for example, is a toll-like receptor agonist leading to induction of cytokine production of lymphocytes, such as interferon alpha being known to have antiviral capacity and to show promising result in multiresistant patients [122]. Helicase-primase inhibitors were first identified by large screening programs [123] and represent a novel class of well-tolerated compounds targeting the HSV helicase-primase complex. These inhibitors possess high potency and low rate of resistance [124], but selection of pre-existing HPI resistance mutations may also occur [121].

Active immunotherapy by vaccination is actually the foremost goal to prevent especially genital HSV infections. However, despite persistent efforts during 50 years of investigation, thus far no potent vaccine could be developed [125]. This might mainly be caused by the highly complex nature and long coevolution of herpes viruses in man. Being neclected in the current vaccine development thus far, it is now assumed that a successful HSV vaccine will likely require enhancing a broader immune reponse including the innate, B cell, and T cell system as well [126,127]. Indeed, various clinical attempts for development of HSV-2 vaccines were undertaken employing inactivated viruses [128], virus components [129-131], glycoprotein subunits [132-134], and live attenuated viruses [135]. However, all failed in preventing of genital herpes infections and only a few vaccines could achieve some therapeutic effects [136]. Current promising HSV-2 vaccine strategies are mainly focused on HSV peptides, DNA vaccines, and attenuated/replication-defective virions [126,127,136,137], and it has to be seen whether these strategies can generate effective long-term immunity in humans. Generally, the development of a

prophylactic HSV vaccine might be difficult to reach because the induced immune response has to be more potent than that occurring in nature to prevent latent neuron infections. Therefore, it was suggested to focus on therapeutic vaccine development to reduce HSV shedding frequency and quantity [138].

1.5.6 Immunotherapy of HSV

Immunotherapy with polyclonal sera from convalescent or vaccinated individuals has been demonstrated to be efficient for prevention and treatment of various virus-mediated infectious diseases [139]. Although passive immunotherapy with universally pooled human IgG as well as hyperimmune preparations are available for several viral infections inclusively hepatitis A, hepatitis B, hepatitis C, rabies, and West Nile fever [140,141], such preparations do not exist for HSV. Furthermore, polyclonal antibody products possess several limitations, e.g., high content of non-neutralizing antibodies, batch to batch variations, limited number of potential donors, and risks being associated with contaminated blood products [140]. Thus, it is expected that polyclonal sera will be replaced by monoclonal antibody preparations in the future [141,142].

The only antiviral mAbs on the market is palivizumab which has been approved for the prophylaxis of respiratory syncytial virus (RSV) infection in high risk infants (**Table 1**). However, a vast effort is underway to develop more antiviral mAbs and there are currently many such mAbs in various stages of clinical development [143].

Virus neutralizing antibodies can inhibit viral infection by different modes of action. For instance, neutralizing antibodies can block virus entry either by binding to viral antigens essential for virus attachment to the target cell or by binding to cellular receptor and/or coreceptors. Enveloped viruses enter host cells by fusion of viral and host membranes what usually requires conformational changes of the viral proteins. Neutralizing antibodies may therefore block fusion at the post-binding/pre-fusion stage. Another mechanism is the inhibition of the release of progeny viruses through antibody binding to virion proteins on the infected cell surface.

Antibody valency can be important for antiviral activity, and it has been shown that virion cross-linking through bivalent (IgG) or multimeric (IgM or secretory IgA) antibody molecules essentially contribute to virus inactivation during the course of infection [141]. Furthermore, neutralizing efficacy of recombinant antibodies targeting

certain viral epitopes requires multivalency as it has been reported for an HSV gB-specific antibody [144] or a varicella zoster virus (VZV) gH-specific antibody [145]. In addition, antiviral antibody function may also require Fc-mediated effector functions like antibody-dependent cell-mediated cytotoxicity (ADCC) by natural killer cells, complement-dependent cytotoxicity (CDC), or antibody-dependent cellular phagocytosis (ADCP).

Regardless of the underlying mechanism, the best strategy for development of potent neutralizing antibodies was suggested to be the development of ultra-high affinity antibodies that target the most critical neutralization sites [140]. However, especially in the case of viruses with naturally occurring antigenic drift and antigenic shift, the emergence of viral escape mutants has to be considered in the course of antiviral mAb development [141]. Indeed, resistant RSV variants could be isolated from infants who were treated with palivizumab [146].

Thus far, several humanized or even fully human mAbs against HSV infections have been described [144,147-150] that showed partially promising therapeutic potential in *in vivo* studies in mice [151,152]. These antibodies were all directed against glycoprotein B or glycoprotein D, and one antibody could even prevent death of immunocompromised mice that had been infected with a mulitresistant HSV strain [152]. However, clinical evaluation of these antibodies is pending and their efficacy in humans has to be evaluated in the future. Moreover, it was assumed that neutralizing antibodies might be employed in the development of novel universal vaccines and other antiviral agents [153,154].

1.6 Antibody immunotherapy of cancer

Nowadays, cancer diseases have evolved to the leading cause of death in the economically developed world and the second leading cause of death in developing countries [155,156]. In 2008, cancer already accounted for about 12.7 million new cases and 7.6 million deaths [155]. The cancer burden is predicted to strongly increase in the future not only driven by growth and aging of the world population but also by adaption of cancer promoting behaviors, e.g., smoking and physical inactivity [155,156]. The leading sites being responsible for the most cancer deaths are lung, stomach, liver, colon, and breast [156]. Ongoing proceedings in cancer research now allow better treatment of tumor patients with increasing survival times for various

cancers. However, for other carcinomas the overall prognosis is still poor even when state-of-the-art therapies are applied. The success of current and coming therapeutic interventions strongly depends on the development of novel targeted therapeutics and personalized medicine. Starting in the 1990s, immunotherapy with monoclonal antibodies has proven to be successful for cancer treatment and has the large potential to further improve both life and survival times of cancer patients.

Thus far, 15 mAbs have been approved in the EU and/or US as cancer therapeutics. Nine of these are bivalent, monospecific IgGs as they can be found in nature, and six are non-canonical mAbs. Based on the success of mAbs in cancer therapy, currently more than 165 candidates are worldwide in clinical studies. About half of these candidates are canonical, full-length mAbs whereas the rest are modified antibodies, e.g., antibody drug conjugates (ADCs), bispecific antibodies, engineered antibodies, antibody fragments, or antibody domains [157]. In general, anticancer monoclonal IgGs can act via different mechanisms of action (MOAs) that are either mediated by the antigen binding site or by the Fc part (**Figure 3**). For example, cancer cell-specific IgGs can trigger Fc-mediated induction of cell death by natural effector functions, i.e., ADCC and CDC (**Figure 3A**). On the other side, antibody binding to cancer cell-expressed receptors may directly interfere with cell signaling leading to growth inhibition or cell death. This aim can also be achieved by antibody-mediated blocking of the natural receptor-ligand interaction (**Figure 3B**). Latest concepts also include indirect MOAs, e.g., immune checkpoint blockade where mAbs act as agonists for immune activation receptors or the other way round as antagonists of immune inhibitory receptors [158]. In contrast, recombinant antibody technology enables construction of engineered antibodies that are equipped with non-natural properties. For instance, protein- and glyco-engineering are mostly used for improvement of natural effector functions [157], e.g., half-life extension by protein sequence modifications or enhanced effector functions by de-fucosylation [159]. Moreover, chemical drug conjugation and recombinant antibody technology enable the combination of anticancer antibodies with novel effector functions, e.g., by coupling to therapeutic or cytotoxic payloads (**Figure 3C**). In ADCs for instance, monoclonal antibodies are attached via a cleavable linker to a cytotoxic drug (**Figure 3C**) [160]. The first US-approved drug conjugate was gemtuzumab ozogamicin, an IgG with DNA damaging payload. Gemtuzumab ozogamicin was indicated for treatment of acute myeloid leukemia but had to be withdrawn from market in 2010 due to

increased mortality in comparative confirmatory trial [161]. Technical improvements now allow the production of ADCs with increased safety and efficacy [162,163] recently leading to approval of two further anticancer ADCs (brentuximab vedotin, trastuzumab emtansine) (**Table 1**). Other strategies include targeted delivery of radioactive isotopes to cancer cells for example as shown for approved tositumomab-I131 and ibritumomab tiuxetan (**Table 1**) revealing promising results in treatment of non-Hodgkin lymphoma [164]. Novel strategies for cancer treatment are employing bispecific antibodies that are designed to bind two different targets (**Figure 3D**). Catumaxomab is the first EU-approved bispecific mAb for treatment of malignant ascites. This murine, trifunctional IgG allows retargeting of cytotoxic T cells to the tumor site via its variable domains simultaneously mediating natural effector functions by its Fc region [165]. Actually, several bispecific antibodies of various formats have entered clinical trials that mostly are employed for recruitment of effector cells to the tumor site [157], but several more dual targeting strategies are under preclinical investigation, e.g., targeting two receptors on cancer cells or retargeting of different effector functions [166].

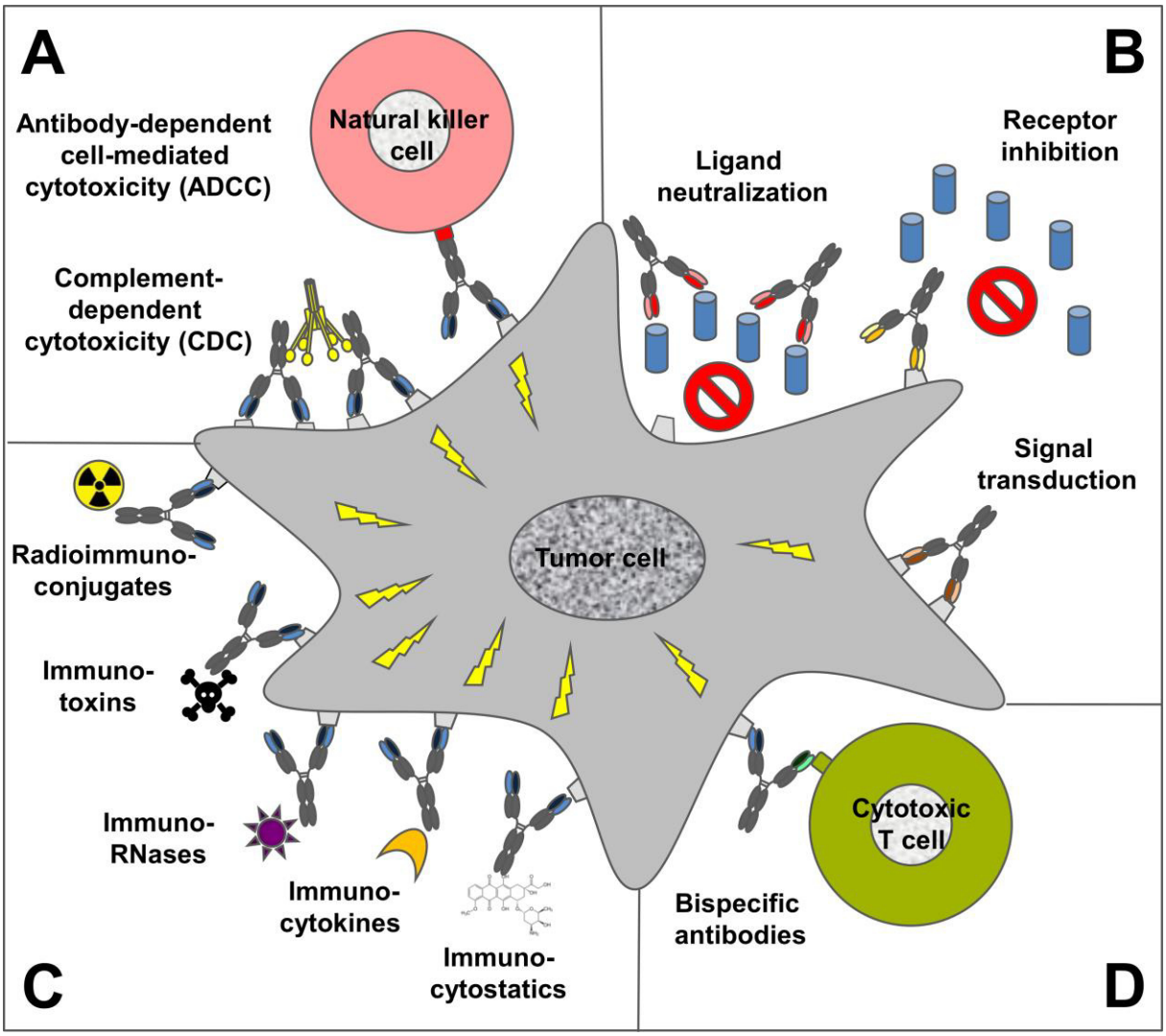

Figure 3. Various mechanisms of action used for therapeutic anticancer mAbs. (**A**) Natural effector functions as ADCC and CDC are mediated via the antibody Fc part that can induce cytotoxic effects on targeted tumor cells. (**B**) Therapeutic mAbs can act by influencing various regulatory mechanisms, e.g., by binding to cancer cell receptors to induce apoptotic signals or by blocking cell-growth stimulatory ligand-receptor interactions. (**C**) Coupling of antibodies or derived fragments to effector molecules (e.g., radioisotopes, toxins, RNases, cytokines, or chemical drugs) enables construction of immunotherapeutics that can mediate toxic effects in the targeted cancer cells. (**D**) Bispecific antibody constructs may act via several mechanisms, e.g., by retargeting of cytotoxic effector molecules or immune cells to the tumor site. Figure adapted from [167].

1.6.1 Targets of therapeutic anticancer mAbs

Today, cancer immunotherapy is focused on some well-validated antigens especially CD20, HER2, and EGFR that are targeted by 9 of the 14 EU/US-marketed anticancer mAbs (**Table 1**) [168]. CD20 is a glycosylated phosphoprotein expressed on B-cells. It is the target of four marketed mAbs or antibody radioimmunoconjugates that are all

indicated for therapy of leukemias and/or lymphomas. HER2 and EGFR are receptor tyrosine kinases (RTKs) that play important roles in cancer. Aberrant signaling by these two receptors are found in many cancers including those of the colon, lung [169], breast [170], and head and neck [171]. Of the three approved HER2-specific antibody drugs, widely employed trastuzumab has a major impact in treatment of HER2-positive breast cancer patients, and it significantly improves the overall survival times when combined with chemotherapy [172]. Currently, there are two EU/US-approved mAbs targeting the EGF receptor, chimeric cetuximab and human panitumumab. Both antibodies are indicated for the treatment of patients expressing KRAS wild-type colorectal cancers. Based on successful phase III clinical trials, cetuximab additionally obtained approval in 2008 for treatment of squamous cell carcinoma of the head and neck in combination with either radio- or chemotherapy [173,174]. Although the vast of mAb products undergoing clinical studies are still directed against these well-established targets, at least 89 other antigens are targeted by the currently clinical investigated mAbs most frequently angiopoietin 2, CD19 (both five times), CD22, HER3 (both four times), CD38, CD70, CEA, fibronectin, GD2, IGF-1 receptor, and PD-1 (all three times) [157].

1.6.2 EGFR: structure and signaling

Epidermal growth factor receptor is one of the four members of the EGFR family that are involved in various cellular processes, such as proliferation, differentiation, migration and apoptosis [175]. Structurally, the family members are composed of a cysteine-rich extracellular ligand-binding region, a hydrophobic transmembrane domain, and an intracellular segment with conserved tyrosine kinase domain and C-terminal tyrosine-rich tail. The EGFR family is regulated by multiple natural ligands. For example, seven ligands with binding specificity to EGFR are known today (**Table 2**). Based on crystal structures of the extracellular EGFR domain with and without activating ligand [176-178], a structural model of ligand-induced EGFR dimerization has been proposed (**Figure 4**) [179]. In the unligated state, the extracellular region adopts a tethered configuration that is in equilibrium with an extended form [180]. EGF-ligand binding to the extracellular EGFR domains I and III stabilize the extended conformation in which the dimerization domain II and IV are exposed that facilitate homodimerization as well as heterodimerization with the other family members. As a result of dimerization, the intracellular tyrosine kinase domains

can perform cross-phosphorylation of specific tyrosine residues in the C-terminal tail of the partnering receptor. Recruitment of phosphotyrosine-binding adaptor and effector proteins triggers downstream activation of a complex and diverse network of distinct signaling pathways including PI3K-mTOR, JAK-STAT, PLC, and Ras-Raf-MEK-ERK [181,182]. Ultimately, activation of the EGF receptor by growth factors induces various cellular processes, e.g., proliferation, angiogenesis, migration, survival, and adhesion [182,183].

Table 2. The EGFR family.

Receptor	Synonym(s)	Ligand(s)	Intrinsic tyrosine kinase activity
EGFR	ERBB-1; HER1	EGF, TGF-α, HB-EGF, AR, BTC, EPR, EPGN	Yes
HER2	ERBB2, Neu	None	Yes
HER3	ERBB3	HRG1+2, NRG 1+2	No
HER4	ERBB4	HRG1-4, NRG 1-4, HB-EGF, BTC, EPR	Yes

AR, amphiregulin; BTC, betacellulin; EGF, epidermal growth factor; EGFR, epidermal growth factor receptor; EPGN, epigen; EPR, epiregulin; HB-EGF, heparin-binding EGF-like growth factor; HER, human epidermal growth factor receptor; HRG, herregulin; NRG, neuregulin; TGF-α, transforming growth factor alpha.

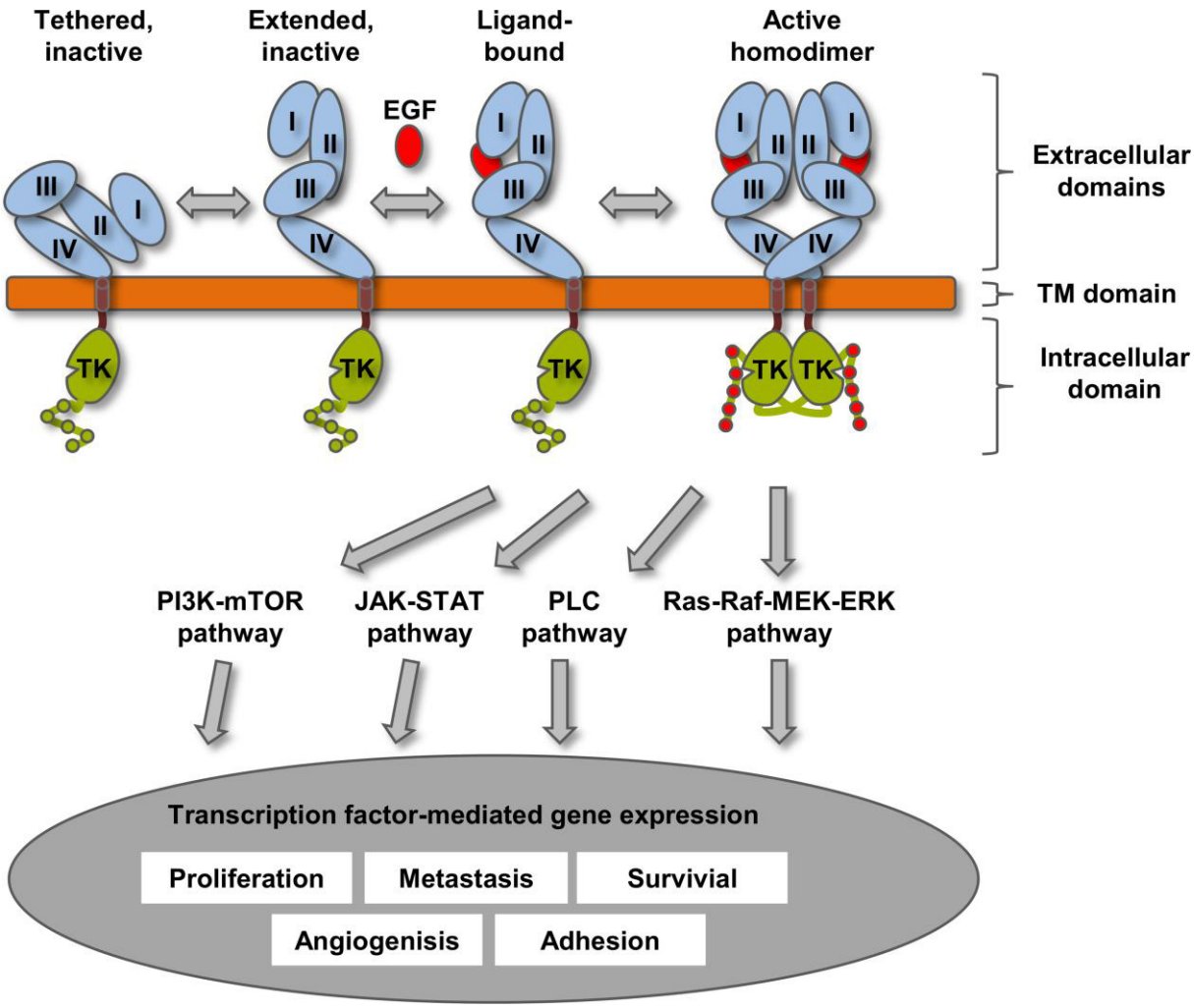

Figure 4. Model of ligand-induced EGFR homodimerization. The unligated extracellular region of the EGF receptor adopts an unactivated tethered conformation that is stabilized by interaction of the domain II and IV. After ligand binding to domain I and III, the extracellular region undergoes large conformational changes leading to exposure of the dimerization interface located mainly in domain II. Additional to the both structurally confirmed structures, conceptual intermediates are shown, i.e., the extended, unligated conformation and an extended, ligand-bound monomer. Ligand-induced receptor dimerization triggers autophosphorylation of intracellular tyrosine residues (green) to phospho-tyrosine residues (red). Ligand binding activates distinct signaling cascades that may stimulate cell growth and survival. EGF, epidermal growth factor; TK, tyrosine kinase; TM, transmembrane. Figure partly adapted from [180].

1.6.3 The role of EGFR in cancer

EGFR is encoded by a proto-oncogene, i.e., aberrant expression or mutations of the EGFR gene can promote cancer formation. Indeed, dysregulation of the EGFR signal may trigger mitogenic, anti-apoptotic, angiogenic, and proinvasive pathways that contribute to malignant transformation of affected cells. Several mechanisms are

known that can result in altered EGFR signaling including receptor overexpression, gene amplification, overexpression of EGFR ligands, activating mutations, and loss of negative regulatory mechanisms [184]. For instance, many malignancies show a high frequency of EGFR overexpression, i.e., more than the physiological normally expected 40,000-100,000 receptors/cell (**Table 3**) [185,186] that is often caused by gene amplification or the result of increased transcription and/or translation activity. Moreover, enhanced activity of the EGFR signaling can also be induced by increased levels of activating EGFR ligands either by autocrine or paracrine mechanisms [187]. Finally, EGFR is frequently altered in several tumor types, and most deletion and point mutations are predominantly clustered in areas of functional and regulatory importance, i.e., within the ligand binding domain, the kinase domain, and the C-terminal tail [188]. The most common EGFR alteration in human cancers is the type EGFRvIII mutation that is characterized by an in frame deletion of exons 2-7 leading to the expression of a truncated EGFR receptor. This gene mutation results in constitutive receptor dimerization with enhanced tumorigenicity [189]. The EGFRvIII mutation is often found in glioblastomas [190,191] but has also be identified in lung, breast, ovarian and other tumors types [188]. In general, EGFR expression has been reported to be associated with worse prognosis and poor clinical outcome [184,186].

Table 3. EGFR overexpression in human tumors.

Tumor type	Percentage of tumors overexpressing EGFR
Colon	25-77%
Head and neck	80-100%
Pancreatic	30-50%
Nonsmall cell lung carcinoma	40-80%
Breast	14-91%
Renal carcinoma	50-90%
Ovarian	35-70%
Glioma	40-63%
Bladder	31-48%

Table adapted from [185].

1.6.4 EGFR-targeted cancer therapy: current treatment options

The frequent aberrant activation of EGFR in human cancers makes it highly attractive for targeted cancer therapy. Hereby, two main classes of drugs are utilized, tyrosine kinase inhibitors (TKIs) and monoclonal antibodies. Two EGFR-specific TKIs, gefitinib (Iressa by AstraZeneca) and erlotinib (Trarceva by Roche/Genentech), have been approved by the FDA in 2003 for the treatment of non-small cell lung cancer (NSCLC). Both drugs are small compounds that inhibit the EGFR tyrosine kinase by binding to the adenosine triphosphate (ATP) binding site thereby preventing auto-phosphorylation and activation of the EGFR signaling [182]. Susceptibility of lung cancer patients to gefitinib and erlotinib was shown to be dependent on EGFR activating mutations of the tyrosine kinase domain [192]. However, these mutations are rare and only increasingly found in certain types of NSCLC and adenocarcinomas. In contrast, lapatinib (Tykerb/Tyverb by GlaxoSmithKline) with dual specificity to EGFR and HER2 accounts for a broader spectrum of anticancer activity and improved efficacy [182]. Based on a clinical trial confirming the efficacy of lapatinib in combined chemotherapy [193], it was approved for the treatment of HER2-positive breast cancer in 2007 [194].

Therapeutic EGFR-specific antibodies target the extracellular receptor region and mainly act via inhibition of the receptor-mediated downstream signaling. Mechanistically, several distinct MOAs for therapeutic mAbs have been reported inclusively blockade of ligand binding, inhibition of receptor dimerization, stabilization of the tethered conformation, and prevention of adopting the extended receptor conformation [180,195]. Apart from inhibition of downstream signaling cascades, EGFR-specific mAbs can also induce receptor internalization, degradation, and prolonged down regulation [182,196]. Finally, some therapeutic EGFR-specific IgGs also induce Fc-mediated effector functions inclusively ADCC and CDC.

Currently, two anti-EGFR mAbs are marketed in the EU and US, chimeric cetuximab and human panitumumab. Cetuximab originally derived from parental monoclonal antibody 225 that was produced by hybridoma technology using carcinoma cell line A431 for mouse immunization. The X-ray structure of the cetuximab-derived Fab fragment in complex with the extracellular region of EGFR revealed that the antibody epitope lies on receptor domain III and overlaps with the EGF binding site [197]. Additionally, cetuximab acts by sterically blocking the receptor from adopting the

extended conformation [180,197]. In addition to the prevention of EGFR signaling, ADCC is considered to be an essential MOA of cetuximab [167,198]. Treatment with cetuximab revealed to be clinically beneficial for EGFR-positive KRAS wild-type colorectal cancer patients [199]. Based on improved overall survival times in clinical trials [173,174], cetuximab was approved for the treatment of head and neck cancers as combined radiotherapy or in combination with platinum-based therapy [167]. Beside skin toxicity due to cross-reactivity to healthy skin cells [167], cetuximab is known to possibly induce fatal reaction during treatment inclusively serious infusion reactions and cardiopulmonary arrest.

Panitumumab is a human antibody produced by humanized mice. It possesses an approximately 8-fold greater affinity to EGFR than cetuximab (K_D = 0.05 nM versus K_D = 0.39 nM) [200]. Panitumumab acts over similar receptor inhibiting mechanisms as cetuximab because both share overlapping epitopes. In contrast to IgG1 antibody cetuximab, panitumumab is an IgG2 and may be therefore less potent in ADCC activation. Panitumumab has been shown to be beneficial in treatment of KRAS wild-type colorectal cancer showing improved progression-free survival in combination with chemotherapy but also as monotherapy [201]. Although completely human and no occurrence of hypersensitivity reactions, unexpected severe toxicities have been observed during combination therapy with anti-VEGF antibody bevacizumab and chemotherapy that is probably caused by unknown pharmacokinetic or pharmacodynamic interactions between the used drugs [201,202].

1.7 Aims

The goal of the present thesis was the development of an applicable concept for effective generation of human monoclonal antibodies with therapeutic potential. The concept should include design and generation of antibody libraries cloned from repertoires of tumor patients to allow selection of cancer-specific autoantibodies. In contrast to most other antibody immune libraries, the concept should also allow recovering of high affinity antibodies to other therapeutic targets where immunization has occurred within donor patients.

2 Materials and methods

2.1 Materials

2.1.1 Instruments

Balances:	**Suppliers:**
Analytical balance AB104-S/FACT	Mettler-Toledo, Greifensee, Switzerland
Analytical balance BP 301 S	Sartorius, Göttingen, Germany
Precision balance 440-33N	Kern&Sohn, Balingen, Germany
Precision balance AJ-2200CE	Shinko Denshi, Jakarta, Indonesia

Centrifuges:	**Suppliers:**
Heraeus Fresco 21	Thermo Fisher Scientific, Waltham, MA, USA
Heraeus Megafuge 1.0, 1.0R, 16R, and 40R	Thermo Fisher Scientific, Waltham, MA, USA
Heraeus Multifuge 4KR	Thermo Fisher Scientific, Waltham, MA, USA
J2-HC and J2-MC	Beckman Coulter, Brea, CA, USA
Mikro 200, 200 R, and Rotina 420 R	Andreas Hettich GmbH, Tuttlingen, Germany
5415 R	Eppendorf, Hamburg, Germany

CO_2 incubators and shaker:	**Suppliers:**
HERAcell 150	Thermo Fisher Scientific, Waltham, MA, USA
NU-5500E	NuAire, Plymouth, MN, USA
Orbital shaker Multitron Pro	INFORS HT, Bottmingen, Switzerland

Cryo conservation:	**Suppliers:**
Cryo freezing container	Thermo Fisher Scientific, Waltham, MA, USA
Cryo tank Biosafe MD	Cryotherm, Kirchen, Germany
Cryogenic refrigerator LS750	Taylor-Wharton, Theodore, AL, USA

Developing machine:	**Supplier:**
CURIX 60	Agfa HealthCare, Mortsel, Belgium

Dispenser:	**Supplier:**
Multipette plus	Eppendorf, Hamburg, Germany

Dot blot system:	**Supplier:**
System Minifold I	GE Healthcare, Little Chalfont, UK

Electro blotting systems:	**Suppliers:**
Power supply PowerPac HC High-Current	Bio-Rad Laboratories, Hercules, CA, USA
Trans-BlotSD Semi-Dry Transfer Cell	Bio-Rad Laboratories, Hercules, CA, USA

Electrophoresis systems:	**Suppliers:**
Power supply peqPOWER E250	PEQLAB Biotechnologie, Erlangen, Germany
Power supply PowerPac 300, and Basic	Bio-Rad Laboratories, Hercules, CA, USA
System (Mini-) Sub-Cell GT	Bio-Rad Laboratories, Hercules, CA, USA
System Maxi ExW	PEQLAB Biotechnologie, Erlangen, Germany
System XCell SureLock Mini-Cell	Life Technologies, Carlsbad, CA, USA

Electroporation systems:	**Supplier:**
Gene Pulser Xcell, and MicoPulser	Bio-Rad Laboratories, Hercules, CA, USA

Flow cytometer:	**Supplier:**
BD FACSCanto II	BD Biosciences, San Jose, CA, USA

FPLC system:	**Supplier:**
ÄKTA FPLC system	GE Healthcare, Little Chalfont, UK

Freezers:	**Suppliers:**
GP 1366 Premium	Liebherr, Bulle, Switzerland
Gram BioLine BioMidi RF 625	Gram, Swanley, UK
Innova U725	Eppendorf, Hamburg, Germany
LGUex 1500 MediLine	Liebherr, Bulle, Switzerland
MDF-U5386S	Panasonic, Kadoma, Japan

Gel visualization and documentation:	**Suppliers:**
Gel documentation system Quantum ST4	Vilber Lourmat, Marne-la-Vallée, France
UV light transilluminator TM-20	UVP, Upland, CA, USA

Heating blocks:	**Suppliers:**
HBT-2 131 and TH 21	DITABIS, Pforzheim, Germany
HX-1 and HX-2	PEQLAB Biotechnologie, Erlangen, Germany

Hemocytometer:	**Supplier:**
Neubauer improved	Karl Hecht, Sondheim, Germany

Homogenizer:	**Supplier:**
Handheld homogenizer TissueRuptor	Qiagen, Hilden, Germany

Incubator shakers:	**Suppliers:**
Innova 40 and Innova 44	Eppendorf, Hamburg, Germany
Minitron	INFORS HT, Bottmingen, Switzerland

Magnetic stirrers:	**Suppliers:**
IKA Combimag RCT	IKA-Werke, Staufen, Germany
MMS-3000	Biosan, Riga, Latvia
MR Hei-Standard	Heidolph Instruments, Schwabach, Germany
RCT basic	IKA-Werke, Staufen, Germany
2mag MIX 1 XL	2mag AG, München, Germany

Microbiological incubators:	**Supplier:**
Heraeus B6 and B6060	Thermo Fisher Scientific, Waltham, MA, USA

Microplate readers:	**Supplier:**
GENios Plus and Infinite 200 PRO	Tecan Group, Männedorf, Switzerland

Microplate washer:	**Supplier:**
ELx405	BioTek, Winooski, VT, USA

Microscopes:	**Supplier:**
Inverted microscope CKX31 and CKX41	Olympus, Tokyo, Japan

Microwaves:	**Suppliers:**
NN-E203WB	Panasonic, Kadoma, Japan
R-239 W-A	Sharp Corporation, Osaka, Japan

Multichannel pipettes:	**Suppliers:**
Eppendorf Research pro (1200 µl) (8-channel)	Eppendorf, Hamburg, Germany
PIPETMAN Neo (20 µl, 200 µl) (8-channel)	Gilson, Middleton, WI, USA
Rainin Pipet-Lite LTS (200 µl) (12-channel)	Mettler-Toledo, Greifensee, Switzerland

PCR-Workstation:	**Supplier:**
UVC/T-M-AR UV-cabinet	Biosan, Riga, Latvia

pH meters:	**Suppliers:**
PB-11	Sartorius, Göttingen, Germany
SevenEasy	Mettler-Toledo, Greifensee, Switzerland

Photometers:	**Suppliers:**
BioPhotometer plus	Eppendorf, Hamburg, Germany
NanoDrop ND-1000 spectrophotometer	Thermo Fisher Scientific, Waltham, MA, USA
UV/visible spectrophotometer Ultrospec 1100 pro	GE Healthcare, Little Chalfont, UK

Pipette controllers:	**Suppliers:**
Accu-jet	BRAND GmbH, Wertheim, Germany
Easypet	Eppendorf, Hamburg, Germany
Pipetus	Hirschmann, Eberstadt, Germany
Swiftpet plus	PZ HTL, Warsaw, Poland

Plate shakers:	**Supplier:**
DSG 304/M4 and TCR 190	Heidolph Instruments, Schwabach, Germany

Refrigerators:	**Supplier:**
FKEX 5000 MediLine and FKS 3600 ProfiLine	Liebherr, Bulle, Switzerland

Roller mixer:	**Supplier:**
RM5-30V	CAT Ingenieurbüro, Staufen, Germany

Rotator:	**Supplier:**
Multi Bio RS-24	Biosan, Riga, Latvia

Rocking shakers:	**Suppliers:**
DRS-12	neoLab, Heidelberg, Germany
Rocky 1000	Labortechnik Fröbel, Lindau, Germany
UltraRocker	Bio-Rad Laboratories, Hercules, CA, USA

Shaker:	**Supplier:**
Bacterial shaker 3005	GFL, Burgwedel, Germany

Single channel pipettes:	**Suppliers:**
Pipetman Classic and Neo (2 µl, 10 µl, 20 µl, 200 µl, and 1000 µl)	Gilson, Middleton, WI, USA
peqPETTE (10 µl, 100 µl, 200 µl, and 1000 µl)	PEQLAB Biotechnologie, Erlangen, Germany
DISCOVERY Comfort (10 µl, 20 µl, 100 µl, 200 µl, and 1000 µl)	PZ HTL, Warsaw, Poland

Sterile benches:	**Supplier:**
HERAsafe KS 18 and KSP 12	Thermo Fisher Scientific, Waltham, MA, USA

Surface plasmon resonance system	**Supplier:**
Biacore 2000 instrument	GE Healthcare, Little Chalfont, UK

Test tube shakers:	**Suppliers:**
PV-1	Grant Instruments, Shepreth, UK
Reax 1R and 1DR	Heidolph Instruments, Schwabach, Germany
Vortex-Genie 2	Scientific Industries, Bohemia, NY, USA

Thermocyclers:	**Suppliers:**
peqSTAR 96 Universal Gradient	PEQLAB Biotechnologie, Erlangen, Germany
PTC-0200 DNA Engine Cycler	Bio-Rad Laboratories, Hercules, CA, USA

Water baths:	**Suppliers:**
GFL-1003	GFL, Burgwedel, Germany
Heating Circulator MC-26	JULABO, Seelbach, Germany
RM 6 T	LAUDA, Lauda-Königshofen, Germany
Shaking water bath type 1083	Peter Oehmen GmbH, Essen, Germany

2.1.2 Consumables

Common consumables:	**Suppliers:**
Blood collection system S-Monovette with clotting accelerator	Sarstedt, Nümbrecht, Germany
Blotting papers	Bio-Rad Laboratories, Hercules, CA, USA GE Healthcare, Little Chalfont, UK
Bottle Top Vacuum Filter (500 ml, 0.2 µm, PES or SFCA), for common solution filtration	Thermo Fisher Scientific, Waltham, MA, USA
Bottle Top Vacuum Filter (150 ml, 45 µm, PES), for helper phage filtration	Thermo Fisher Scientific, Waltham, MA, USA
Chemical film Curix HT1.000G Plus	Agfa HealthCare, Mortsel, Belgium
Gauze swabs	Karl Beese, Barsbüttel, Germany
Gloves	Semperit, Wien, Austria VWR, Radnor, PA, USA
Indicator strips	Macherey-Nagel, Düren, Germany
Needles	BD Biosciences, San Jose, CA, USA
Ni-NTA spin columns	QIAGEN, Hilden, Germany
Nitrocellulose membranes	Carl Roth, Karlsruhe, Germany GE Healthcare, Little Chalfont, UK
Parafilm	Bemis, Neenah, WI, USA
Scalpels	FEATHER**,** Osaka, Japan
SDS-PAGE precast protein gels 12%	Expedeon, Harston, UK
Sensor Chips CM5	GE Healthcare, Little Chalfront, England
Syringe Filters (0.20 µm, Minisart NML)	Sartorius, Göttingen, Germany
Syringe Filters (0.22 µm, Millex-GV)	Merck KGaA, Darmstadt, Germany

Plastic and glass implements:	**Suppliers:**
Beakers	BRAND, Wertheim, Germany KAVALIERGLASS, Praha, Czech Republic
Cell culture flasks (T25, T75, T175)	Greiner Bio-One, Kremsmünster, Austria
Cell culture plates (6-well, 24-well, 48-well)	Greiner Bio-One, Kremsmünster, Austria
Cell culture plate (96-well), F-bottom and U-bottom	Greiner Bio-One, Kremsmünster, Austria
Centrifuge tubes (250 ml, 500 ml)	Beckman Coulter, Brea, CA, USA
Chromatography columns and lids	Bio-Rad Laboratories, Hercules, CA, USA
Conical tubes (15 ml, 50 ml)	Greiner Bio-One, Kremsmünster, Austria
Cryogenic storage vials (2 ml)	Greiner Bio-One, Kremsmünster, Austria Thermo Fisher Scientific, Waltham, MA, USA

Plastic and glass implements:	Suppliers:
Cuvettes, semi-micro	Ratiolab, Dreieich, Germany
Dispenser tips (2.5 ml, 10 ml, 25 ml)	Eppendorf, Hamburg, Germany
Erlenmeyer flasks (0.3 l, 0.5 l, 1 l, 2 l), glass	Kavalierglass, Praha, Czech Republic SCHOTT, Stafford, UK
Erlenmeyer flasks (125 ml), disposable	VWR, Radnor, PA, USA
Glass beads, for bacteria plating	Carl Roth, Karlsruhe, Germany
Glass bottle (0.25 l, 0.5 l, 1 l, 2l)	SCHOTT, Stafford, UK
Hemocytometer, disposable	NanoEnTek, Seoul, South Korea
Immuno ELISA plates MaxiSorp (96-well)	Thermo Fisher Scientific, Waltham, MA, USA
Immuno tubes MaxiSorp	Thermo Fisher Scientific, Waltham, MA, USA
Inoculation needles, disposable	Greiner Bio-One, Kremsmünster, Austria
Measuring cylinders (0.25 l, 1 l, 2 l)	BRAND, Wertheim, Germany KAVALIERGLASS, Praha, Czech Republic
Micro tubes (1.5 ml, 2 ml)	BRAND, Wertheim, Germany Eppendorf, Hamburg, Germany Sarstedt, Nümbrecht, Germany
Pasteur capillary pipettes (230 mm)	Wu, Mainz, Germany
Reagent reservoirs (50 ml)	Corning Incorporated, Corning, NY, USA
Rubber caps, for sealing SPR tubes	GE Healthcare, Little Chalfront, England
Serological pipets (5 ml, 10 ml, 25 ml, 50 ml)	Corning Incorporated, Corning, NY, USA
Syringes (1 ml, 2 ml, 5 ml, 10 ml)	BD Biosciences, San Jose, CA, USA

2.1.3 Chemicals, kits, and commercial reagents

Chemicals:	Suppliers:
Agar	Sigma-Aldrich, St. Louis, MO, USA
Agarose	PEQLAB Biotechnologie, Erlangen, Germany
Ammonium chloride (NH_4Cl)	Carl Roth, Karlsruhe, Germany
Ampicillin sodium salt ($C_{16}H_{18}N_3NaO_4S$)	Carl Roth, Karlsruhe, Germany
Aqua ad iniectabilia	B. Braun, Melsungen, Germany
Carboxymethylcellulose sodium salt	Carl Roth, Karlsruhe, Germany
Citric acid ($C_6H_8O_7$)	Carl Roth, Karlsruhe, Germany
Coomassie Brilliant Blue R-250 ($C_{45}H_{44}N_3NaO_7S_2$)	Carl Roth, Karlsruhe, Germany
Crystal violet ($C_{25}H_{30}ClN_3$)	Carl Roth, Karlsruhe, Germany
D(+)-glucose anhydrous ($C_6H_{12}O_6$)	Carl Roth, Karlsruhe, Germany
D(+)-sorbose ($C_6H_{12}O_6$)	Carl Roth, Karlsruhe, Germany
DEPC (diethyl pyrocarbonate; $C_6H_{10}O_5$)	Carl Roth, Karlsruhe, Germany

Chemicals:	**Suppliers:**
Disodium hydrogen phosphate (Na_2HPO_4)	Carl Roth, Karlsruhe, Germany
DMSO (dimethyl sulphoxide; C_2H_6OS)	Carl Roth, Karlsruhe, Germany
DTT (1,4-dithiothreitol; $C_4H_{10}O_2S_2$)	Carl Roth, Karlsruhe, Germany
EDTA (ethylenediaminetetraacetic acid, disodium salt dihydrate; $C_{10}H_{14}N_2Na_2O_8x2H_2O$)	Merck KGaA, Darmstadt, Germany
Ethanol 96% (C_2H_6O), denatured	Carl Roth, Karlsruhe, Germany
Ethanol (C_2H_6O), extra pure	Carl Roth, Karlsruhe, Germany
Formaldehyde 37% (CH_2O)	Carl Roth, Karlsruhe, Germany
Glycine ($C_2H_5NO_2$)	Carl Roth, Karlsruhe, Germany
Glycerol ($C_3H_8O_3$)	Carl Roth, Karlsruhe, Germany
Glycogen	Thermo Fisher Scientific, Waltham, MA, USA
HEPES ($C_8H_{18}N_2O_4S$)	Carl Roth, Karlsruhe, Germany
Hydrochloric acid (HCl)	Carl Roth, Karlsruhe, Germany
Imidazole ($C_3H_4N_2$)	Sigma-Aldrich, St. Louis, MO, USA
IPTG (isopropyl β-D-1-thiogalactopyranoside; $C_9H_{18}O_5S$)	Carl Roth, Karlsruhe, Germany
Isopropanol (C_3H_8O)	Carl Roth, Karlsruhe, Germany
Kanamycin sulphate ($C_{18}H_{36}N_4O_{11}xH_2SO_4$)	Carl Roth, Karlsruhe, Germany
Magnesium chloride hexahydrate ($MgCl_2x6H_2O$)	Carl Roth, Karlsruhe, Germany
Magnesium sulphate ($MgSO_4$)	Carl Roth, Karlsruhe, Germany
Methanol (CH_3OH)	Carl Roth, Karlsruhe, Germany
Milk powder	Carl Roth, Karlsruhe, Germany
Polyethylene glycol 6000	Carl Roth, Karlsruhe, Germany
Potassium chloride (KCl)	Carl Roth, Karlsruhe, Germany
Potassium dihydrogen phosphate (KH_2PO_4)	Carl Roth, Karlsruhe, Germany
SDS (sodium dodecyl sulfate; $C_{12}H_{25}NaO_4S$)	Carl Roth, Karlsruhe, Germany
Sodium azide (NaN_3)	Sigma-Aldrich, St. Louis, MO, USA
Sodium acetate ($C_2H_3NaO_2$)	Carl Roth, Karlsruhe, Germany
Sodium chloride (NaCl)	Carl Roth, Karlsruhe, Germany
Sodium dihydrogen phosphate monohydrate ($NaH_2PO_4xH_2O$)	Carl Roth, Karlsruhe, Germany
Sodium hydroxide (NaOH)	Carl Roth, Karlsruhe, Germany
Sucrose ($C_{12}H_{22}O_{11}$)	Carl Roth, Karlsruhe, Germany
Sulfuric acid (H_2SO_4)	Carl Roth, Karlsruhe, Germany
Thiamine hydrochloride ($C_{12}H_{17}ClN_4OSxHCl$)	Carl Roth, Karlsruhe, Germany
Trichloromethane ($CHCl_3$)	Carl Roth, Karlsruhe, Germany
Tris-base ($C_4H_{11}NO_3$)	Carl Roth, Karlsruhe, Germany

Chemicals:	**Suppliers:**
Tris hydrochloride (Tris-HCl; $C_4H_{11}NO_3$xHCl)	Carl Roth, Karlsruhe, Germany
Trypton/peptone, ex casein	Carl Roth, Karlsruhe, Germany
Tween 20	Carl Roth, Karlsruhe, Germany
Yeast extract	Carl Roth, Karlsruhe, Germany

Commercial kits:	**Suppliers:**
Amine Coupling Kit	GE Healthcare, Little Chalfront, England
EndoFree Plasmid Maxi Kit	QIAGEN, Hilden, Germany
First Strand cDNA Synthesis Kit	Thermo Fisher Scientific, Waltham, MA, USA
Gel Filtration Calibration Kit, low molecular weight	GE Healthcare, Little Chalfront, England
KAPAHiFi PCR Kit	PEQLAB, Erlangen, Germany
KAPA2G PCR ReadyMix with Dye	PEQLAB, Erlangen, Germany
QIAGEN Plasmid Midi and Maxi Kit	QIAGEN, Hilden, Germany
QIAprep Spin Miniprep Kit	QIAGEN, Hilden, Germany
QIAquick PCR Purification Kit	QIAGEN, Hilden, Germany
QIAquick Gel Extraction Kit	QIAGEN, Hilden, Germany
RNAlater TissueProtect Tubes	QIAGEN, Hilden, Germany
RNeasy Lipid Tissue Midi Kit	QIAGEN, Hilden, Germany

Commercial reagents:	**Suppliers:**
AlamarBlue Cell Viability Reagent	Life Technologies, Carlsbad, CA, USA
Bradford reagent	Bio-Rad Laboratories, Hercules, CA, USA
Decontamination solution DNA-ExitusPlus	AppliChem, Darmstadt, Germany
Decontamination solution RNase-ExitusPlus	AppliChem, Darmstadt, Germany
Deoxynucleotide solution mix (all 10 mM)	New England Biolabs, Ipswich, MA, USA
DNA stain GelRed	Biotium, Hayward, CA, USA
ECL immunoblot substrate kit	Thermo Fisher Scientific, Waltham, MA, USA
Ethidium bromide solution UltraPure (10 mg/ml)	Life Technologies, Carlsbad, CA, USA
Nickel sepharose 6 Fast Flow for IMAC	GE Healthcare, Little Chalfont, UK
Photographic developer G153	Agfa HealthCare, Mortsel, Belgium
Photographic fixer G354	Agfa HealthCare, Mortsel, Belgium
SDS running buffer RunBlue RAPID (20x)	Expedeon, Harston, UK
Surfactant P20	GE Healthcare, Little Chalfont, UK
TAE electrophoresis buffer (50x)	AppliChem, Darmstadt, Germany
TMB ELISA Substrate Kit	Thermo Fisher Scientific, Waltham, MA, USA

Markers and loading dyes:	Suppliers:
DNA gel loading buffer	New England Biolabs, Ipswich, MA, USA
DNA ladder (100 bp and 1000 bp)	New England Biolabs, Ipswich, MA, USA
Protein LDS sample buffer RunBlue (4x)	Expedeon, Harston, UK
Protein ladder Spectra Multicolor, broad range	Thermo Fisher Scientific, Waltham, MA, USA
RNA gel loading buffer	Thermo Fisher Scientific, Waltham, MA, USA
RNA ladder, broad range	Thermo Fisher Scientific, Waltham, MA, USA

Reagents for cell culture:	Suppliers:
DMEM, high glucose	Life Technologies, Carlsbad, CA, USA
Dulbecco's PBS (DPBS) without Ca^{2+} and Mg^{2+}	GE Healthcare, Little Chalfront, England
Fetal bovine serum (FBS), heat-inactivated	GE Healthcare, Little Chalfront, England
FreeStyle F17, without L-glutamine	Life Technologies, Carlsbad, CA, USA
Geneticindisulfate (G418) solution (50 mg/ml)	Carl Roth, Karlsruhe, Germany
Kolliphor P188	Sigma-Aldrich, St. Louis, MO, USA
L-glutamine 200 mM (100x)	Life Technologies, Carlsbad, CA, USA
Opti-MEM reduced serum medium	Life Technologies, Carlsbad, CA, USA
Penicillin/streptomycin solution (100x)	GE Healthcare, Little Chalfront, England

Reagents for cell culture:	Suppliers:
PEI (polyethylenimine, molecular weight: 25,000)	PolySciences, Warrington, PA, USA
RPMI-1640	GE Healthcare, Little Chalfront, England
Sodium pyruvate solution (100 mM)	Sigma-Aldrich, St. Louis, MO, USA
TN1 (tryptone N1)	Organotechnie, La Courneuve, France
Trypan blue stain (0.4%)	Life Technologies, Carlsbad, CA, USA
Trypsin/EDTA solution (0.05%)	Life Technologies, Carlsbad, CA, USA

2.1.4 Media, buffers, and solutions

Common solutions:	Compositions:
MPBS	20 g/l milk powder, in PBS
PBS (10x)	1.4 M NaCl, 27 mM KCl, 101 mM Na_2HPO_4, 18 mM KH_2PO_4, in dH_2O
PBST	0.5 ml/l Tween 20, in PBS

Media for bacterial culture:	**Compositions:**
Induction medium	2xYT supplemented with glucose stock solution, 1 ml/l ampicillin stock solution, 0.25 ml/l kanamycin stock solution, 0.5 ml/l IPTG stock solution
LB high salt	10 g/l trypton, 5 g/l yeast extract, 10 g/l NaCl, in dH_2O, autoclaved
Minimal plates	15 g agar autoclaved in 880 ml dH_2O, 10 ml glucose stock solution, 1 ml $MgSO_4$ (1 M in H_2O), 1 ml thiamine (2 mg/ml in H_2O), 100 ml M9 solution
M9 solution	58 g/l Na_2HPO_4, 30 g/l KH_2PO_4, 5 g/l NaCl, 10 g/l NH_4Cl, in dH_2O, adjusted to pH 7.2, filter-sterilized
SOB	5 g/l yeast extract, 20 g/l tryptone, 10 mM NaCl, 2.5 mM KCl in dH_2O, adjusted to pH 7.0 with 1 M NaOH prior to autoclaving, addition of 10 mM $MgSO_4$, 10 mM $MgCl_2$ just before use
SOC	SOB, 20 mM glucose
Top agar	2xYT supplemented with 7.5 g/l agar, autoclaved
2xYT	16 g/l trypton, 10 g/l yeast extract, 5 g/l NaCl, in H_2O, autoclaved
2xYT-GA	2xYT supplemented with glucose stock solution, 1 ml/l ampicillin stock solution
2xYT-GA agar	2xYT supplemented with 15 g/l agar, 100 g/l glucose stock solution, 1 ml/l ampicillin stock solution
2xYT-GK agar	2xYT supplemented with 15 g/l agar, 100 ml/l glucose stock solution, 1 ml/l kanamycin stock solution

Solutions for bacterial culture:	**Compositions:**
Ampicillin stock solution	100 mg/ml ampicillin sodium salt, in dH_2O, filter-sterilized
Glucose stock solution	200 g/l glucose, in dH_2O, filter-sterilized
IPTG stock solution	1 M in dH_2O, filter-sterilized
Kanamycin stock solution	100 mg/ml kanamycin sulphate, in dH_2O, filter-sterilized
Lysozyme solution	50 mg/ml lysozyme, in dH_2O
Periplasmic preparation buffer	30 mM Tris-HCl, in dH_2O, adjusted to pH 8.0, 1 mM EDTA, 200 g/l sucrose

Solutions for cell culture:	**Compositions:**
Carboxymethyl cellulose (CMC) solution	2/3 volume DMEM (100 ml/l FBS, 10 ml/l penicillin/ streptomycin) and 1/3 volume CMC solution (20 g/l in PBS)
Crystal violet solution	200 mg/l crystal violet dissolved in 1 ml ethanol, filled up with dH_2O
Formaldehyde solution	135 ml/l formaldehyde stock solution (37%), diluted in PBS
Freezing medium	100 µl/ml DMSO, in FBS
Freezing medium (HEK 293-6E)	100 µl/ml DMSO, in F17 culture medium without G418

Solutions for cell culture:	**Compositions:**
Kolliphor P188 stock solution	100 g/l Kolliphor P188, in dH_2O, filter-sterilized
PEI transfection reagent	1 mg/ml PEI dissolved at pH 2.0, in dH_2O, adjusted to pH 7.0, filter-sterilized
TN1 feeding medium	200 g/l, in F17 culture medium without G418, filter-sterilized

Solutions for phage display:	**Compositions:**
PEG-NaCl	200 g/l polyethylene glycol 6000, 2.5 M NaCl, in dH_2O
Phage elution buffer	0.1 M glycine-HCl, 0.5 M NaCl, in H_2O, adjusted to pH 2.2, filter-sterilized
Phage neutralization buffer	1 M Tris-HCl, in H_2O, adjusted to pH 9.5, filter-sterilized
Trypsin solution	10 µg/ml, in DPBS

Solutions for protein purification:	**Compositions:**
Protein A binding buffer	100 mM NaH_2PO_4 x H_2O, 100 mM NaCl, 10 mM EDTA, in dH_2O, adjusted to pH 7.0, filter-sterilized
Protein A elution buffer	100 mM citric acid, in dH_2O, adjusted to pH 3.0, filter-sterilized
Protein A neutralization buffer	1 M Tris-base, in dH_2O, adjusted to pH 9.0, filter-sterilized
Semi-dry blotting buffer	48 mM Tris-base, 38 mM glycine, 200 ml/l methanol, 1.3 mM SDS, in dH_2O, adjusted to pH 9.4, filter-sterilized
SP IMAC buffer	20 mM sodium phosphate, 0.5 M NaCl, in dH_2O, adjusted to pH 7.4
SP-10 IMAC binding buffer	SP buffer, 10 mM imidazole, adjusted to pH 7.4, filter-sterilized
SP-30 IMAC wash buffer	SP buffer, 30 mM imidazole, adjusted to pH 7.4, filter-sterilized
SP-500 IMAC elution buffer	SP buffer, 500 mM imidazole, adjusted to pH 7.4, filter-sterilized

Solutions for protein work:	**Compositions:**
Coomassie solution	70 mg/l Coomassie Brilliant Blue G-250, in dH_2O, 35 mM HCl
DTT solution (10x)	2.5 M DTT, in dH_2O
FACS buffer	20 ml/l FBS, 1 g/l NaN_3, in DPBS

Solution for SPR:	**Composition:**
Running buffer	10 mM HEPES, 150 mM NaCl, 0.5 ml/l Surfactant P20, adjusted to pH 7.0, degassed prior to use by filtration

Solution for RNA work:	**Composition:**
DEPC solution	1 g/l DEPC, in dH_2O, autoclaved

2.1.5 Software and online tools

The subsequent tables show the software (**Table 4**), online tools, and databases (**Table 5**) that were used in this thesis.

Table 4. Computer programs.

Software	Description	Supplier/developer
BIAevaluation 4.1.1	Evaluation of surface plasmon resonance data	GE Healthcare, Little Chalfront, England
Cromas Lite 2.01	Sequence evaluation	Technelysium, South Brisbane, Australia
EndNote X6	Reference manager	Thomson Reuters, New York, NY, USA
FACSDiva	Acquisition and analysis of flow cytometer data	BD Biosciences, San Jose, CA, USA
Geneious R6.1	Vector visualization	Biomatters, Auckland, New Zealand
GIMP 2.8	Figure preparation	GIMP Team (http://www.gimp.org/)
GraphPad Prism 5	Statistical analysis	GraphPad Software, La Jolla, CA, USA
MS Exel 2010	Data evaluation and chart creation	Microsoft, Redmond, WA, USA
MS PowerPoint 2010	Figure drawing and preparation	Microsoft, Redmond, WA, USA
MS Word 2010	Text processing	Microsoft, Redmond, WA, USA
Unicorn 5.10	FPLC control and operating software	GE Healthcare, Little Chalfront, England
Win MDI 2.9	Flow cytometry data evaluation	Joe Trotter (http://facs.scripps.edu/software.html)
XFluor4	Data processing of used plate reader	Tecan, Männedorf, Switzerland

Table 5. Online tools and databases.

Online tool/database	Description	Homepage
ClustalW2	Multiple alignment of protein or nucleic acid sequences	http://www.clustal.org/clustal2/ [203]
DNAPLOT	Alignment of V genes to the VBASE database	http://www2.mrc-lmb.cam.ac.uk/vbase/dnaplot2.php
ExPASy ProtParam	Computation of various physicochemical parameters (e.g., molecular weight, extinction coefficient, etc.) of an entered protein sequence	http://web.expasy.org/protparam/ [204]
ExPASy Translate	Translation of nucleotide to amino acid sequences	http://web.expasy.org/translate/
IMGT/GENE-DB	Database for human immunoglobulin genes	http://www.imgt.org/IMGT_GENE-DB/GENElect?livret=0 [205]
IMGT/V-QUEST	Alignment of V genes to the IMGT/V-QUEST database	http://www.imgt.org/IMGT_vquest/vquest [206]
Phylogeny.fr	Phylogenetic analysis of entered sequences	http://www.phylogeny.fr/ [207]
UniProt Knowledgebase	Database of protein sequences inclusively functional information	http://www.uniprot.org/
VBASE2	Database of human antibody genes	http://www.vbase2.org/vbquery.php [208]
VBASE2 Fab Analysis	Alignment of Fab or scFv sequences to the VBASE2 database	http://www.vbase2.org/vbscAb.php
VBASE	Database of functional human antibody genes	http://www2.mrc-lmb.cam.ac.uk/vbase/alignments2.php

2.1.6 Antibodies, enzymes, and proteins

Antibodies, enzymes, and proteins that were used within this thesis are subsequently listed (**Table 6**, **Table 7**, and **Table 8**). Schematic representations of the herein listed proteins are depicted in **Figure 5**.

Table 6. Antibodies and antibody conjugates.

Specificity (epitope)	Description (concentration/dilution)	Supplier (catalog #)
Coat protein pIII of phage M13 (ATDYGAAIDGF)	Mouse monoclonal IgG clone 10C3 used for detection of pIII fusions in immunoblot (0.5 µg/ml in MPBS)	MoBiTec, Göttingen, Germany (PSKAN3)
Coat protein pVIII of phage M13	Mouse monoclonal peroxidase conjugate used for detection of phage antibodies in ELISA (1:5,000 in MPBS)	GE Healthcare, Little Chalfront, UK (27-9421-01)
Coat protein pVIII of phage M13 (AEGDDPAKAAFDSLQASAT)	Mouse monoclonal IgG2b clone B6-FE2 used for the estimation of the number of phage particles (0.1 µg/ml in MPBS)	PROGEN, Heidelberg, Germany (61997)
Glycoprotein B of herpes simplex virus	Mouse or humanized monoclonal IgG clone 2c used as control in PRNT	Group “Antibody-based Immunotherapeutics”, Department of Medical Oncology, NCT, Heidelberg, Germany
Human EGFR	Chimeric monoclonal IgG1 cetuximab used as control for EGFR expression on tumor cells in flow cytometry	Merck KGaA, Darmstadt, Germany
Human IgG Fc	Mouse monoclonal IgG clone 5A9 conjugated to peroxidase and used for detection of IgGs in serum ELISA (0.4 µg/ml in MPBS)	Abcam, Cambridge, UK (ab7499)
Human IgG Fc	Rabbit polyclonal IgG conjugated to FITC and used as secondary antibody for detection of scFv-Fcs and IgG cetuximab in flow cytometry (3 µg/ml in FACS buffer)	Jackson ImmunoResearch Laboratories, West Grove, PA, USA (309-096-008)
Human IgG Fc	Rabbit polyclonal IgG conjugated to peroxidase and used for detection of scFv-Fcs in dot blot and immunoblot (0.04 µg/ml in MPBS)	Jackson ImmunoResearch Laboratories, West Grove, PA, USA (309-035-008)
Mouse IgG Fc	Goat polyclonal IgG conjugated to FITC and used as secondary antibody for detection of scFvs in flow cytometry (7.5 µg/ml in FACS buffer)	Jackson ImmunoResearch Laboratories, West Grove, PA, USA (115-095-008)
Mouse IgG Fc	Goat polyclonal IgG conjugated to peroxidase and used as secondary antibody for detection of scFvs in immunoblot (0.02 µg/ml in MPBS) or for determination of phage titer in ELISA (0.04 µg/ml in MPBS)	Jackson ImmunoResearch Laboratories, West Grove, PA, USA (115-035-008)

Specificity (epitope)	Description (concentration/dilution)	Supplier (catalog #)
Myc peptide (EQKLISEEDL)	Mouse monoclonal IgG clone 9E10 used for detection of expressed scFvs in immunoblot (2 µg/ml in MPBS) or in flow cytometry (5 µg/ml in FACS buffer)	Dr. Gerhard Moldenhauer, Translational Immunology Unit, German Cancer Research Center, Heidelberg, Germany
Myc peptide (EQKLISEEDL)	Mouse monoclonal IgG1 clone 9E10 conjugated to peroxidase and used for detection of scFv-pIII fusions in dot blot (1 µg/ml in MPBS)	Roche Diagnostics, Basel, Switzerland (11 814 150 001)

Table 7. Enzymes.

Enzyme	Description (activity)	Supplier
Alkaline phosphatase from calf-intestinal (CIP)	Dephosphorylation of expression vectors pAB1 and pYD11 (10 units/µl)	New England Biolabs, Ipswich, MA, USA
Antarctic phosphatase	Dephosphorylation of pagemid vector pHENIS (5 units/µl)	New England Biolabs, Ipswich, MA, USA
Lysozyme from hen egg white	Hydrolysis of bacteria cell walls used for periplasmic extraction of produced scFvs (50 units/µg)	Roche Diagnostics, Basel, Switzerland
Pfu DNA Polymerase	PCR amplification of antibody genes for library construction (2.5 units/µl)	Thermo Fisher Scientific, Waltham, MA, USA
ApaLI	Restriction enzyme used for library cloning (50 units/µl)	New England Biolabs, Ipswich, MA, USA
BstNI	Restriction enzyme used for fingerprint analysis (10 units/µl)	New England Biolabs, Ipswich, MA, USA
EcoRV	Restriction enzyme used for scFv-Fc subcloning (20 units/µl)	New England Biolabs, Ipswich, MA, USA
NarI	Restriction enzyme used for scFv-Fc subcloning (5 units/µl)	New England Biolabs, Ipswich, MA, USA
NotI	Restriction enzyme used for scFv subcloning (10 units/µl)	New England Biolabs, Ipswich, MA, USA
NotI-HF (high fidelity enzyme)	Restriction enzyme used for library cloning (100 units/µl)	New England Biolabs, Ipswich, MA, USA
SfiI	Restriction enzyme used for library cloning and scFv subcloning (20 units/µl)	New England Biolabs, Ipswich, MA, USA
XhoI	Restriction enzyme used for library construction (20 units/µl)	New England Biolabs, Ipswich, MA, USA
T4 DNA Ligase	Ligation of DNA fragments for cloning (1 unit/µl)	Thermo Fisher Scientific, Waltham, MA, USA
Trypsin from porcine pancreas	Elution of phage antibodies from selection antigen EGFR	Sigma-Aldrich, St. Louis, MO, USA

Table 8. Proteins.

Protein	Description	Supplier (catalog #)
BSA (albumin from bovine serum)	Lyophilized powder with 96% purity prepared by heat shock fractionation and used as specificity control in ELISA	Sigma-Aldrich, St. Louis, MO, USA (A9647)
EGF (human epidermal growth factor)	1 mg/ml solution (20 mM citrate buffer, pH 3.5) with >95% purity recombinantly expressed by *E. coli* and used for proliferation assays	Life Technologies, Carlsbad, CA, USA (PHG0311L)
EGFR (human extracellular domain of epidermal growth factor receptor)	Lyophilized powder with >90% purity recombinantly expressed by Sf9 insect cells and used for detection of EGFR-specific IgGs in serum ELISA	ProSpec-Tany TechnoGene, Rehovot, Israel (PKA-3449)
EGFR-Fc (human extracellular domain of epidermal growth factor receptor coupled to human IgG1 Fc)	Lyophilized powder with >90% purity recombinantly expressed by mouse myeloma cell line NSO and used for EGFR-specific antibody selection from libraries	R&D Systems, Minneapolis, MN, USA (344-ER-050)
Fc (region of human IgG1)	Lyophilized powder with >95% purity recombinantly expressed by mouse myeloma cell line NSO and used as specificity control in ELISA and preabsorption of phages during antibody selection	R&D Systems, Minneapolis, MN, USA (110-HG-100)
gB-1 (ectodomain of glycoprotein B of human herpes simplex virus type 1, KOS strain)	Recombinantly expressed by baculovirus-infected insect cells, diluted in PBS, and used for EGFR-specific antibody selection from libraries	Prof. Dr. Roselyn J. Eisenberg and Prof. Dr. Gary H. Cohen, Department of Microbiology, University of Pennsylvania, PA, USA
HSA (albumin from human serum)	Lyophilized powder with ≥99% purity used as specificity control in ELISA	Sigma-Aldrich, St. Louis, MO, USA (A3782)
Lysozyme (from chicken egg white)	Lyophilized powder prepared by crystallization and and used as specificity control in ELISA	Sigma-Aldrich, St. Louis, MO, USA (62971)
Ovalbumin (albumin from chicken egg white)	Lyophilized powder with ≥98 purity prepared by crystallization and used as specificity control in ELISA	Sigma-Aldrich, St. Louis, MO, USA (A5503)
Protein A	Lyophilized powder prepared from cell walls of *Staphylococcus aureus*, Cowan strain	Sigma-Aldrich, St. Louis, MO, USA (P3838)

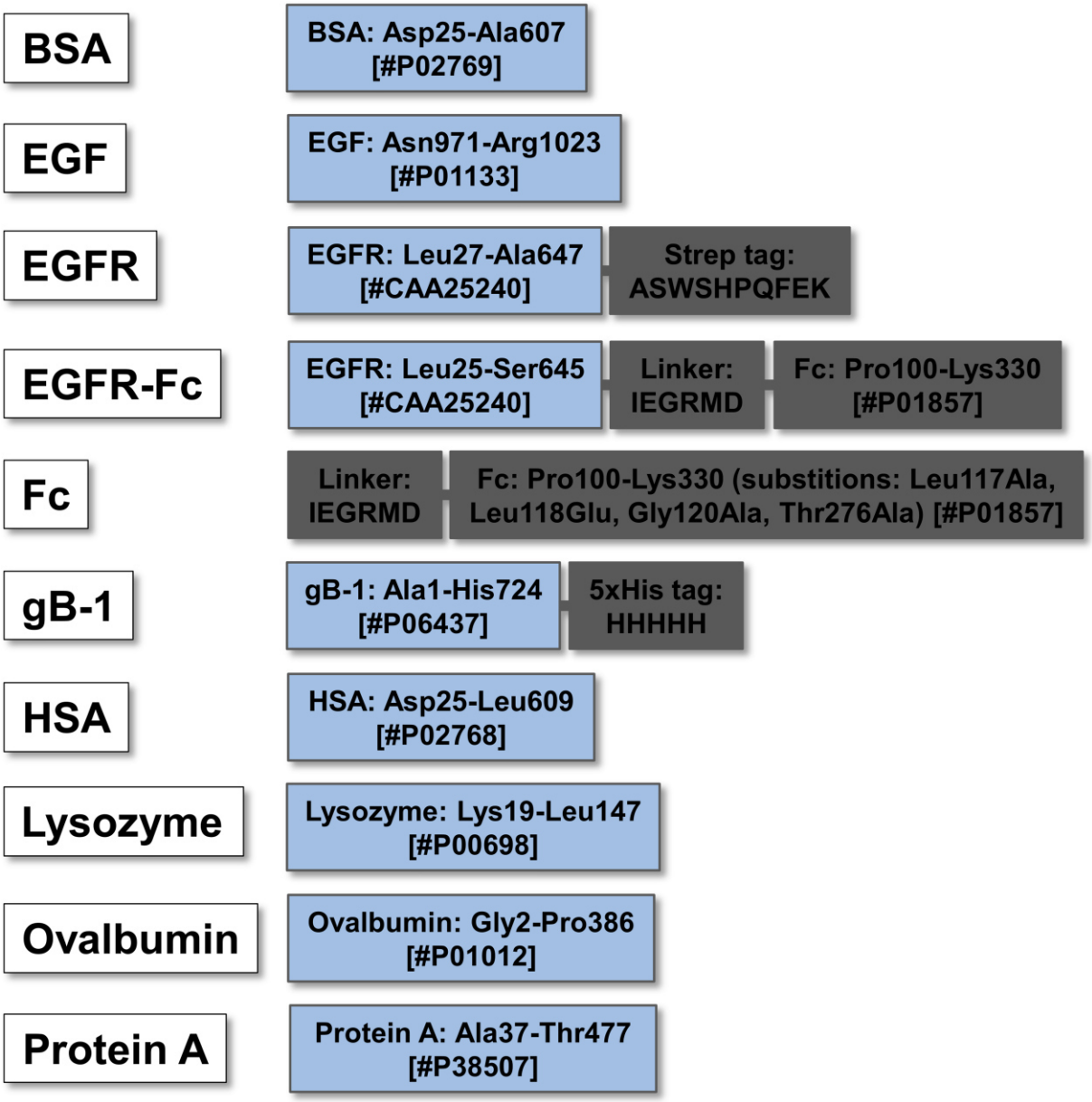

Figure 5. Schematic representation of used proteins. The accession numbers of the UniprotKB entries are given inclusively the first and last amino acid of the primary protein sequence (blue). Sequences of protein tags and domains used for detection (streptavidin, hexahistidine, myc, and human IgG Fc) are shaded in gray. Proteins with human IgG1 Fc region form disulfide-linked homodimers. The ectodomain of HSV-glycoprotein B is known to form homotrimers.

2.1.7 Chromatography columns

All used chromatographic columns were purchased from GE Healthcare (Little Chalfront, UK) and are described in **Table 9**.

Table 9. Chromatographic columns.

Column	Description
HiLoad 16/60 Superdex 75	Preparative gel filtration column, flow rate: 0.3-1.6 ml/min, maximal column pressure: 0.5 MPa, bed volume: 120 ml, loading capacity 5 ml, separation range (M_r): 3,000 to 70,000; used for SEC purification of scFvs
HiTrap rProtein A FF	Protein A affinity column, flow rate: <4 ml/min, maximal column pressure: 0.3 MPa, bed volume: 1 ml; used for protein A purification of scFv-Fcs
Superdex 75 10/300GL	Analytical gel filtration column, flow rate: 0.5-1 ml/min, maximal column pressure: 1.8 MPa, bed volume: 24 ml, loading capacity 25-500 µl, separation range (M_r): 3,000 to 70,000; used for SEC analysis of scFvs
Superdex 200 10/300 GL	Analytical gel filtration column, flow rate: 0.25-0.75 ml/min, maximal column pressure: 1.5 MPa, bed volume: 24 ml, loading capacity 25-500 µl, separation range (M_r): 10,000 to 60,000; used for SEC analysis of scFv-Fcs

2.1.8 Primers

All oligonucleotides were purchased in either desalted or cartridge-purified (>40 bases) quality from Life Technologies (Carlsbad, CA, USA). Primers for recloning of isolated scFvs into the scFv-Fc antibody format, for sequencing, and for colony PCR are depicted in **Table 10**.

Table 10. Primers for cloning of antibody fragments, sequencing, and colony PCR

No.	Name	Seqence (5'-3')
P91	LMB3long	CAGGAAACAGCTATGACCATGATTAC
P92	fdseqlong	GACGTTAGTAAATGAATTTTCTGTATGAGG
P93	LMB2long	GTAAAACGACGGCCAGTGAATTC
P94	M13-RP	CAGGAAACAGCTATGACC
P95	scFv-Fc-H28-fwd-NarI	TATAGGCGCCGAGGTGCAGCTGTTGGAGTC
P96	scFv-Fc-H28-rev-EcoRV	TATATTTGATATCCACTTTGGTCCCTTG
P97	scFv-Fc-E6-fwd-NarI	TederspATAGGCGCCCAGGTCACCTTGAAGGAGTC
P98	scFv-Fc-E6-rev-EcoRV	TATAGATATCTAGGACGGTGACCTTGGTCC
P99	scFv-Fc-IZI08-fwd-NarI	TATAGGCGCCGAAGTGCAGCTGGTTGAAAGC
P100	scFv-Fc-IZI08-rev-	TATAGATATCTTTAATTTCCAGTTTGGTGCCCGC
P101	pYD11-fwd	CAAGTTTGCCGCCACCATGG
P102	pYD11-rev	GGGAAGAGGAAGACTGACGG

2.1.9 Vectors

In **Table 11**, the used plasmid vectors are briefly described. The corresponding vector maps are depicted in the appendix section (**Figure 45**, **Figure 46**, and **Figure 47**).

Table 11. Vectors.

Vector	Description	Supplier
pHENIS	Derivative of phagemid vector pHEN [210] used for generation of antibody phage display libraries by cloning of human antibody genes as scFv-pIII fusions	Prof. Dr. Roland E. Kontermann, Institute of Cell Biology and Immunology, University of Stuttgart, Germany
pAB1 [209]	Derivative of vector pUC119 used for bacterial expression of soluble scFvs into the periplasm of *E. coli*	Prof. Dr. Roland E. Kontermann, Institute of Cell Biology and Immunology, University of Stuttgart, Germany
pYD11	Derivative of vector pTT [211] used for transient expression of scFv-Fc antibodies by mammalian cells into the culture medium	National Research Council, Montréal, Quebec, Canada

2.1.10 Eukaryotic and prokaryotic cells

Bacteria and cell lines that were utilized for molecular cloning, recombinant protein expression, binding analysis, and virus infection/production are listed in **Table 12**.

Table 12. Bacteria and cell lines.

Cell line(s)	Organism	Description	Culture medium	Supplier (catalog #)
A431	*Homo sapiens*	Adherently growing cell line established from epidermoid carcinoma and used for cell binding analyses	DMEM (100 ml/l FBS, 10 ml/l penicillin/ streptomycin)	ATCC, Manassas, VA, USA (CRL-1555)
HEK 293-6E	*Homo sapiens*	Suspension cell line established from embryonic kidney cells and used for transient protein expression	F17 (10 ml/l Kolliphor P188 stock solution, 20 ml/l L-glutamine stock solution, 0.5 ml G418 solution)	National Research Council, Montréal, Quebec, Canada
HNO97, HNO199, HNO210, HNO211, HNO223, HNO410	*Homo sapiens*	Adherently growing, primary patient cell lines established from head and neck carcinomas and used for cell binding analyses	DMEM (100 ml/l FBS, 10 ml/l penicillin/ streptomycin)	Prof. Dr. Christel Herold-Mende, Department of Neurosurgery, Heidelberg University Hospital, Germany

Cell line(s)	Organism	Description	Culture medium	Supplier (catalog #)
Jurkat	*Homo sapiens*	Suspension cell line established from acute T cell leukemia and used for cell binding analyses	RPMI (100 ml/l FBS, 10 ml/l penicillin/ streptomycin)	ATCC, Manassas, VA, USA (TIB-15)
MCF7	*Homo sapiens*	Adherently growing cell line established from breast adenocarcinoma and used for cell binding analyses	DMEM (100 ml/l FBS, 10 ml/l penicillin/ streptomycin)	ATCC, Manassas, VA, USA (HTB-22)
NALM-6	*Homo sapiens*	Suspension cell line established from acute lymphoblastic leukemia (ALL) and used for cell binding analyses	DMEM (100 ml/l FBS, 10 ml/l penicillin/ streptomycin)	DSMZ, Braunschweig, Germany (ACC 128)
Raji	*Homo sapiens*	Suspension cell line established from Burkitt's lymphoma and used for cell binding analyses	RPMI (100 ml/l FBS, 10 ml/l penicillin/ streptomycin)	ATCC, Manassas, VA, USA (CCL-86)
SKOV-3	*Homo sapiens*	Adherently growing cell line established from adenocarcinoma and used for cell binding analyses	DMEM (100 ml/l FBS, 10 ml/l penicillin/ streptomycin)	ATCC, Manassas, VA, USA (HTB-77)
TG1	*Escherichia coli*	Bacteria strain used for preparation of phage display libraries, general (sub-) cloning, and recombinant periplasmic protein expression	Minimal plates (only maintaining)	Agilent Technologies, Santa Clara, CA, USA (200123)
UDSCC2	*Homo sapiens*	Adherently growing cell line established from HPV-associated head and neck carcinoma and used for cell binding analyses	RPMI (100 ml/l FBS, 10 ml/l penicillin/ streptomycin, 10 ml/l sodium pyruvate)	Prof. Dr. Thomas Hoffmann, Department of Otorhinolaryngology, University Hospital of Essen, Germany
Vero	*Cercopithecus aethiops*	Adherently growing cell line established from epithelial kidney and used for virus production or infection studies	DMEM (100 ml/l FBS, 10 ml/l penicillin/ streptomycin)	ATCC, Manassas, VA, USA (CCL-81)
93VU1047T	*Homo sapiens*	Adherently growing cell line established from HPV-associated head and neck carcinoma and used for cell binding analyses	DMEM (100 ml/l FBS, 10 ml/l penicillin/ streptomycin)	Dr. Renske Steenbergen, Department of Pathology, VU University Medical Center, Amsterdam, the Netherlands

2.1.11 Phages and viruses

The different phage and virus types and strains are summarized in **Table 13**.

Table 13. Viruses and phages.

Virus/phage	Description	Supplier
HSV-1, strain F [212]	Established laboratory strain propagated in Vero cells	Prof. Dr. Anna-Maria Eis-Hübinger, Institute of Virology, University of Bonn Medical Center, Germany
HSV-2, strain G [212]	Established laboratory strain propagated in Vero cells	Prof. Dr. Anna-Maria Eis-Hübinger, Institute of Virology, University of Bonn Medical Center, Germany
Hyperphage (M13 K07ΔpIII) [39]	Helper phage for superinfection of phagmid containing libraries; enabled oligovalent scFv presentation as pIII fusions on phages due to missing pIII wild-type protein during phage assembly	PROGEN, Heidelberg, Germany
VCSM13	Helper phage for superinfection of phagmid containing libraries; enabled monovalent scFv presentation as pIII fusions on phages	Agilent Technologies, Santa Clara, CA, USA

2.2 Patient material

2.2.1 Ethics statement

All patient samples, lymph nodes and blood, were taken according to ethical guidelines and patient's informed consent. Control sera of healthy individuals were obtained after donor's informed consent.

2.2.2 Lymph nodes

Human lymph nodes were chosen as the antibody gene source for construction of LYNDAL. Single cervical tumor-draining lymph nodes were obtained from 20 individuals with squamous cell head and neck carcinoma undergoing surgery in cooperation with Prof. Dr. Christel Herold-Mende (Department of Neurosurgery, Heidelberg University Hospital, Germany), Dr. Gerhard Dyckhoff, and PD Dr. Philippe A. Federspil (both Department of Otorhinolaryngology, Heidelberg University Hospital, Germany). Immediately after surgical removal, individual lymph nodes were transferred into RNAlater reagent and cooled down to stabilize RNA. Amount of isolated lymph nodes were quantified and sliced lymphatic tissue submerged in RNAlater reagent o/n at 4°C. Long-time storage was done at –20°C following the manufacturer's instructions until the corresponding donor library was constructed.

2.2.3 Sera

Frozen sera samples of LYNDAL donors were obtained from cooperation partners, aliquoted (10 µl), and stored at -20°C. Blood from control individuals was taken using the S-Monovette blood collection system. The blood was allowed to clot for up to 1 h at room temperature (RT). After centrifugation (1500 rpm, 15 min, 4°C), layers containing the blood sera were taken, aliquoted, and frozen. To guarantee the same procedure for LYNDAL donors, control sera were thawed once and stored at -20°C.

2.3 Library construction

2.3.1 RNA preparation

Individual lymph nodes were thawed to RT and mechanically disrupted by using a handheld homogenizer. Total RNA was isolated from lymphatic tissue by using an RNeasy Lipid Tissue Midi Kit and stored at -80°C. Concentration and purity of extracted RNA was assessed by measurement of absorbance in a spectrophotometer. Integrity of purified RNA was analyzed on an agarose gel using formamide containing loading dye and RNA ladder.

2.3.2 cDNA preparation

Single stranded cDNA for the amplification of human antibody genes was synthesized from RNA that was isolated from donor lymph nodes. Typically, 30 µg total RNA per donor was reversely transcribed using a First Strand cDNA Synthesis Kit according to the manufacturer's protocol. Independent reactions with 5 µg total RNA were performed using either supplied oligo$(dT)_{18}$ primer or random hexamer primers. The products of the cDNA synthesis were separately pooled for each donor and subsequently stored at -80°C.

2.3.3 Primer design

Ninety primers (P1-P90) for the generation of LYNDAL were designed for cloning the complete IgG repertoire of human donors. To guarantee the utmost stringency during gene amplification, a maximum of two degenerated nucleotide positions per primer were included. The used forward primers amplified human V genes of all functional sequences as notated in VBASE and corresponded to the first (5') seven or eight amino acids. These primers were used in combination with a set of reverse primers that were designed employing the Kabat database [213] and either bound to the CH1 genes (115-121) of all human IgG subclasses or to the CL genes of the human kappa (109-116) and lambda (121-128) light chains. For the cloning of amplified V genes, a further set of primers was designed for adding SfiI/XhoI or ApaLI/NotI encoding overhangs at the VH and VL fragments, respectively. Forward primers of this second set reamplified the original sequences whereas the corresponding

reverse primers bound to the last (3') seven (JH: 106-112, JK: 101-107, and JL: 101-107) amino acids of human J segments as being notated in VBASE.

2.3.4 Amplification of antibody genes

VH, VL-kappa, and VL-lambda encoding gene repertoires were separately amplified from the prepared cDNA by a first set of independent PCR reactions (1st PCRs). Genes of the VH domain were amplified during 13 reactions per donor by combining a single forward primer (P1-P13) with a mix of reverse primers (P14+P15) according to the following pipette scheme:

Reagent	**Single reaction (µl)**
Donor cDNA	1
Forward primer [25 µM]	1
Reverse primer mix [20 µM]	2
10x buffer with $MgSO_4$	5
dH_2O	39.2
dNTP mix [10 mM]	1
Pfu DNA polymerase	0.8

Antibody light chains were amplified in 12 (VL-kappa) or 14 (VL-lambda) independent reactions per donor by combining a single forward primer (kappa: P16-P27, lambda: P29-P42) with reverse primer P28 (kappa) or P43 (lambda):

Reagent	**Single reaction (µl)**
Donor cDNA	1
Forward primer [25 µM]	1
Reverse primer [25 µM]	1
10x buffer with $MgSO_4$	5
dH_2O	40.2
dNTP mix [10 mM]	1
Pfu DNA polymerase	0.8

The antibody subsets (VH, VL-kappa, and VL-lambda) were amplified during 30 PCR cycles by using the following PCR program:

Step	Temperature (°C)	Time
Initial denaturation	94	3 min
Denaturation	94	30 sec
Annealing	55	1 min
Elongation	72	2 min
Final elongation	72	10 min
Cooling	4	Unlimited time

Successful amplification of the variable antibody genes was verified by analytical agarose gel (1.5%) electrophoresis.

2.3.5 Restriction site addition

Addition of the artificial cloning sites was independently performed for the VH, VL-kappa, and VL-lambda subsets during a second set of PCRs (2^{nd} PCRs). SfiI (5') and XhoI (3') restriction sites were added at the amplified VH fragment in 13 independent reactions per donor by combining a single forward primer (P44-P56) with a mix of reverse primers (P57+P58) as follows:

Reagent	Single reaction (µl)
Unpurified products (1^{st} PCRs)	1
Forward primer [25 µM]	1
Reverse primer mix [20 µM]	2
10x buffer with $MgSO_4$	5
dH_2O	39.2
dNTP mix [10 mM]	1
Pfu DNA polymerase	0.8

ApaLI (5') and NotI (3') restriction sites were added to the amplified VL genes in 12 (kappa) or 14 (lambda) independent reactions per donor by combining a single forward primer (kappa: P59-P70, lambda: P74-P87) with a mix of reverse primers P71-P73 (kappa) or P88-P90 (lambda):

Reagent	Single reaction (µl)
Unpurified products 1st PCRs	1
Forward primer [25 µM]	1
Reverse primer mix [30 µM]	3
10x buffer with $MgSO_4$	5
dH_2O	38.2
dNTP mix [10 mM]	1
Pfu DNA polymerase	0.8

The introduction of restriction sites was performed with a similar PCR program as described for variable antibody gene amplification (section 2.3.5) by decreasing the number of PCR cycles to 15 and increasing the annealing temperature to 57°C. PCR-products (2 µl/reaction) were analyzed on analytical agarose gel (1.5%) for successful amplification followed by separation of the remaining products (one reaction/lane) on preparative 1.5% agarose gel. Indistinct bands with the size of the amplified variable genes (VH: ~400 bp, VL: ~350 bp) were sliced from ethidium bromide dyed gel and purified with a QIAquick Gel Extraction Kit employing one column for two lanes. Bound DNA was eluted with different volumes of supplied EB-buffer (VH: 40 µl, VL: 41.2 µl).

2.3.6 V gene preparation for cloning

Amplified VH genes from 2nd PCRs were firstly digested with the restriction enzyme SfiI for 6 h at 50°C in 7 reactions per donor according to following scheme:

Reagent	Volume (µl)
VHs after 2nd PCRs	38
NEB buffer 4 (10x)	5
BSA (10x)	5
SfiI (20 units/µl)	2

Products were purified by a QIAquick PCR Purification Kit and eluted in 40 µl of EB buffer per column. Subsequently, SfiI-digested heavy chains were cut with the restriction enzyme XhoI o/n at 37°C:

Reagent	Volume (µl)
SfiI-digested VHs	38
NEB buffer 4 (10x)	5
BSA (10x)	5
XhoI (20 units/µl)	2

Upon heat inactivation of XhoI for 20 min at 65°C, products were column-purified and eluted with 30 µl of EB buffer. DNA concentration of pooled VH fragments was measured by spectrophotometer, and products were stored at -20°C. Amplified VL genes from 2nd PCRs were firstly digested with ApaLI for o/n at 37°C in 6 (kappa) or 7 (lambda) reactions per donor:

Reagent	Volume (µl)
VHs after 2nd PCRs (kappa or lambda)	39.2
NEB buffer 4 (10x)	5
BSA (10x)	5
ApaLI (50 units/µl)	0.8

ApaLI-digested VL chains were column-purified and eluted with 41.6 µl of EB buffer per column. Subsequently, products were cut with restriction enzyme NotI for 6 h at 37°C:

Reagent	Volume (µl)
ApaLI-digested VLs (kappa or lambda)	39.6
NEB buffer 4 (10x)	5
BSA (10x)	5
NotI-HF (100 units/µl)	0.4

NotI was heat-inactivated for 20 min at 65°C, and purified products were eluted with 30 µl of EB buffer per column. Digested kappa and lambda fragments were separately pooled for each donor and stored at -20°C after determination of DNA concentration.

2.3.7 Vector preparation for VH cloning

Bacterial glycerol stock containing the pHENIS phagemid was streaked onto a 2xYT-GA selection plate, and the DNA was prepared from a grown single colony using a QIAGEN Plasmid Kit according to the manufacturer's protocol. Phagemid DNA (5 µg per sample) was firstly digested with the restriction enzyme SfiI for 6 h at 50°C:

Reagent	**Volume (µl)**
pHENIS DNA [5 µg]	X
NEB buffer 4 (10x)	5
BSA (10x)	5
SfiI (20 untis/µl)	1
dH_2O	Ad 50

Products (2 µl/reaction) were analyzed on analytical agarose gels (1%) and bands with the size of SfiI-digested phagmid (~4.6 kb) were purified from preparative agarose gels. After elution with 40.5 µl per column, DNA was cut with the restriction enzyme XhoI o/n at 37°C:

Reagent	**Volume (µl)**
SfiI-digested pHENIS DNA	38.5
NEB buffer 4 (10x)	5
BSA (10x)	5
XhoI (20 units/µl)	1.5

The restriction enzyme XhoI was heat-inactivated for 20 min at 65°C followed by elution of purified DNA from columns with 46 µl of EB buffer. SfiI/XhoI-cut phagemid was dephosphorylated by Antarctic phosphatase for 4 h at 37°C:

Reagent	**Volume (µl)**
SfiI/XhoI-digested pHENIS DNA	44
Antarctic phosphatase buffer (10x)	5
Antarctic phosphatase (5 units/µl)	1

Antarctic phosphatase was heat-inactivated for 5 min at 65°C and column-purified DNA eluted with 40 µl of EB buffer per sample. After analysis by analytical agarose gel (1%) electrophoresis, DNA concentration of pooled samples was measured before storing the double-digested and dephosphorylated phagemids at -20°C.

2.3.8 Cloning of VH repertoire

Fourfold molar excess of SfiI/XhoI-digested VH gene repertoire (~109 ng) was ligated into 300 ng double-digested phagmid pHENIS per reaction o/n at 16°C thus preparing 22 samples for each donor library:

Reagent	Volume (µl)
SfiI/XhoI-digested, dephosphorylated pHENIS DNA (300 ng)	X
Insert (SfiI/XhoI-digested VH)	Y
Ligation buffer (10x)	5
T4 Ligase (1 units/µl)	2
dH_2O	Ad 50

Upon heat inactivation of ligase for 10 min at 65°C, DNA samples were precipitated o/n at -20°C:

Reagent	Volume (µl)
Ligation mix	50
100% ice-cold EtOH	125
Sodium acetate pH 5.5 [3 M]	5
Glycogen (20 µg/µl)	2.5

Pellets of centrifuged DNA (20,000xg, 1 h, 4°C) were washed three times with 70% ice-cold ethanol (500 µl/sample) by repetitive centrifugation (20,000xg, 10 min, 4°C), decantation, and resuspension. Air-dried DNA was dissolved in dH_2O (4 µl/sample) and stored at -20°C until transformation in electrocompetent *E. coli* TG1 bacteria.

Cells were freshly prepared by inoculation of 10 ml of SOC medium per donor repertoire with single TG1 colonies that had grown on minimal plates. Cultures were incubated o/n at 37°C under shaking and analyzed for contamination by streaking 100 µl samples on 2xYT agar plates either containing ampicillin or kanamycin. SOB medium (1 l) was inoculated with o/n culture and grown at 37°C until OD_{600} of 0.6

was reached. Pelleted bacteria (3,000xg, 10 min, 4°C) were washed twice by resuspension of centrifuged cells with 400 ml ice-cold dH_2O followed by incubation of the cell suspension for 30 min on ice. Pelleted bacteria were washed with 50 ml of ice-cold 10% glycerol and the cell suspension was further incubated for 30 min on ice. Centrifuged cells were resuspended (2 ml ice-cold 10% glycerol) and aliquoted (50 µl) after adding 50 µl of 100% D-sorbose.

For the cloning of VH repertoires, 2 µl of cloned DNA were added to 50 µl of freshly prepared TG1 *E.coli* cells and incubated for 1 min on ice in prechilled electroporation cuvettes. Cells were transformed with VH-ligated phagmids in 44 reactions per donor by pulsing (1,800 Volt, 25 µF, 200 Ohm) and immediately mixed with 950 µl of prewarmed SOC (37°C) followed by growing for 1 h at 37°C. Pelleted bacteria (3,000xg 10 min, RT) were resuspended in 250 µl of SOC medium per sample and streaked on 145 mm 2xYTGA agar plates for growing at 30°C. The next day, transformed bacteria were harvested from the plates after adding 2xYT medium, and individual donor repertoires were stored as glycerol stocks (15% final) at -80°C.

Additionally, controls were prepared by electroporation of pUC18 DNA (10 pg, positive), dH_2O (negative), and ligated double-digested vector (religation) as described. One hundred µl of suited dilutions (positive: 2.5 µl in SOC, negative: undiluted, religation: 1 µl in SOC) were plated on small 2xYT-GA agar plates, and grown colonies were counted the next day.

2.3.9 Vector preparation for VL cloning

Plasmid DNA containing the VH repertoire was prepared from transformed glycerol stock by use of a Plasmid Maxi Kit. Two preparations with 5 ml of pelleted bacteria were performed per donor according to the manufacturer's protocol. Phagemid DNA (10 µg per sample) was firstly digested with the restriction enzyme ApaLI o/n at 37°C:

Reagent	**Volume (µl)**
pHENIS-VH DNA [10 µg]	X
NEB buffer 4 (10x)	5
BSA (10x)	5
ApaLI (50 U/µl)	1
dH_2O	Ad 50

After analyzing each sample by agarose gel electrophoresis, bands (~5 kb) corresponding to ApaLI-digested phagemid were purified from preparative agarose gel (1%). Column-purified DNA was eluted with 41.5 µl of EB buffer and subsequently cut with the restriction enzyme NotI o/n at 37°C:

Reagent	Volume (µl)
ApaLI-digested pHENIS-VH DNA	39.5
NEB buffer 4 (10x)	5
BSA (10x)	5
NotI-HF (100 units/µl)	0.5

NotI was heat-inactivated for 20 min at 65°C, and products were purified and eluted from columns with 45 µl of EB buffer. SfiI/XhoI-cut phagemid was dephosphorylated by Antarctic phosphatase for 4 h at 37°C:

Reagent	Volume (µl)
ApaLI/Not-digested pHENIS DNA	43
Antarctic phosphatase buffer (10x)	5
Antarctic phosphatase (5 units/µl)	2

Upon heat inactivation of Antartic phosphatase for 5 min at 65°C, double-digested and dephosphorylated phagemid DNA was analyzed by analytical gel (1%) electrophoresis followed by elution of column-purified DNA with 40 µl of EB buffer. DNA samples were separately pooled for each of the donors and stored at -20°C after DNA measurement.

2.3.10 Cloning of final libraries

The final libraries were prepared by randomly subcloning both kappa and lambda light chain repertoires into pHENIS phagemid carrying the corresponding VH donor repertoire. Ligation of ApaLI/NotI-digested VL-kappa or VL-lambda gene repertoires was performed exactly as described for VH cloning using 87 ng of insert per reaction. Two sublibraries (VH/VL-kappa or VH/VL-lambda) were generated per donor by transforming prepared DNA in at least 88 reactions and storing the final libraries glycerol stocks at -80°C.

2.4 Characterization of libraries

2.4.1 Determination of library sizes

Sizes of all sublibraries were estimated by counting transformed *E. coli* colonies from dilution plates. After electroporation of final library DNA into bacteria as described in chapter 2.3, two grown bacteria cultures per sublibrary were randomly chosen for preparing appropriate 1:10 serial dilutions in a SOC medium. One hundred µl of dilutions were streaked on 2xYT-GA agar plates and incubated at 30°C. The next day, plates with single colonies were counted and the averaged colony number was used to calculate the total size of the corresponding library.

2.4.2 Insert analysis

The number of library clones containing both variable antibody genes was assessed by colony PCR. Typically, 40 single colonies per sublibrary were picked with sterile pipette tips from dilution plates and transferred into a prepared PCR ReadyMix:

Reagent	**Volume (µl)**
KAPA2G PCR ReadyMix with Dye	12.5
Forward primer P91 [25 µM]	0.5
Reverse primer P92 [25 µM]	0.5
dH_2O	11.5
Template DNA	Picked single colony

PCR amplification was performed during 35 cycles:

Step	**Temperature (°C)**	**Time**
Initial denaturation	95	5 min
Denaturation	95	15 sec
Annealing	51	15 sec
Elongation	72	15 sec
Final elongation	72	5 min
Cooling	4	Unlimited time

Amplified products were analyzed by agarose gel (1.5%) electrophoresis, and library clones with intact scFv gene were identified by a fragment size of around 1 kb.

2.4.3 Sequence analysis

At least five clones per sublibrary with confirmed scFv gene (section 2.4.2) were randomly chosen for sequence analysis. Per clone, 5 ml of medium (LB high salt, 100 µg/ml ampicillin) was inoculated with 25 µl of medium containing the pipette tip that was used for the colony PCR mix infection. Grown o/n cultures were used for the preparation of plasmid DNA using a QIAprep Spin Miniprep Kit following the manufacturer's protocol. After measurement of the DNA concentration, scFv genes were sequenced by GATC Biotech (Konstanz, Germany) using the standard forward primer P94. Obtained sequence data were tested by software Chromas Lite for sequence inaccuracies, and variable genes were analyzed by the online tool DNAPLOT in order to identify the closest germline V, (D), and J segment genes and antibody families as listed in the VBASE sequence directory. Varieties in the complementarity determining regions (CDRs) were additionally analyzed employing the Fab Analysis tool that aligns the entered scFv sequences against the VBASE2 database. Relative gene family occurrences of sequenced library clones were calculated and compared with the average distribution of functional V gene entries of human antibody databases VBASE, VBASE2, and IMGT-GENE excluding non-functional reading frames, orphans, and pseudogenes.

2.4.4 Expression analysis

To evaluate the soluble expression of scFv-pIII fusions in *E. coli*, induced periplasmic preparations from random chosen clones were analyzed by both dot blot and immunoblot experiments. Library glycerol stocks were streaked on 2xYT-GA selection plates and single-grown colonies used for inoculation of 100 µl 2xYT-GA medium in 96-well microtiter plates. Induction plates containing fresh medium (0.1% glucose) were inoculated with grown cultures (o/n at 37°C, 150 rpm) and incubated for a further 3 h until the expression of scFv-pIII fusions was induced by adding 1 mM isopropyl beta-D-1-thiogalactopyranoside (IPTG). After o/n expression at 28°C, pelleted bacteria (3,000xg, 10 min, 4°C) were resuspended in periplasmic preparation buffer containing 50 µg/ml freshly prepared lysozyme and incubated for 30 min on ice until 10 mM $MgSO_4$ was added. Periplasmic preparations were clarified by centrifugation (3,000xg, 20 min, 4°C) and applied onto nitrocellulose membranes either using a semi-dry electroblotting system (30 min at 20 V) after separation of

reduced protein samples by 12 % SDS-PAGE or employing a dot blot system (100 µl/dot). Membranes were blocked for 1 h at RT and incubated with either peroxidase-conjugated anti-myc antibody (1 h; dot blot) or mouse anti-pIII antibody as first (o/n) and goat anti-mouse IgG conjugate as secondary antibody (1 h; immunoblot). After the single incubation steps, membranes were rinsed three times with PBST and once with PBS. Peroxidase activity was finally detected by chemiluminescence using ECL substrate (3 min) and chemical film.

2.5 Serum screening

LYNDAL donors with target-specific serum antibodies were identified by ELISA screening using proteins of interest. Recombinant gB-1 and EGFR were diluted in PBS to 1 µg/ml and 100 µl/well coated o/n at 4°C. Preincubated serum samples (1:100 in MPBS, 1 h at RT) were added to MPBS-blocked plates (400 µl/well, 2 h at RT) and incubated for 2 h at RT (100 µl/well). After washing the plates (3xPBST and 3xPBS), peroxidase-conjugated anti-human IgG Fc-specific antibody (100 µl/well) was applied for 1 h at RT. Freshly prepared TMB substrate solution was added to washed plates (100 µl/well) and reaction stopped by addition of 1 M sulfuric acid (50 µl/well). Absorbance signals were measured at 450 nm with 620 nm as the reference wavelength.

2.6 Antibody selection and screening

2.6.1 Helper phage preparation

For the amplification of strain VCSM13, serial dilutions (100 µl) of the phage stock preparation (1:10 in 2xYT medium) was mixed with equal volumes of a log phase TG1 culture (OD_{600} of 0.5) followed by incubation for 10 min at RT. Infected bacteria were transferred to 3 ml of melted top agar (42°C) and cast on prewarmed (37°C) 2xYT agar plates. After incubation o/n at 30°C, a single small plaque from the lawn was picked and transferred to 3 ml of 2xYT medium that was previously inoculated with 100 µl of TG1 o/n culture. Grown plaque (3 h at 37°C, 180 rpm) was used for inoculation of 500 ml of 2xYT medium followed by a further incubation for 1 h. After adding 25 µg/ml of kanamycin to the culture, helper phages were produced o/n at 37°C during shaking. Bacteria were pelleted (6,000xg, 30 min, 4°C), and the

phage-containing supernatant was heated (15 min at 65°C) and filtered (0.45 µm). Remaining cell debris was removed by centrifugation, and aliquoted phages (15 ml) were frozen for long-time storage to -20°C. Preparation was analyzed on control plates (2xYT-GA and 2xYT-GK) and the titer determined as described above by counting plaques from top agar plates.

2.6.2 Immunotube selection

Antibody repertoires of chosen donors were separately packaged by inoculating 2xYT-GA medium (200 ml/donor) with corresponding library stocks (start OD_{600} of 0.05-0.1). Log phase bacteria (OD_{600} of about 0.5) were either superinfected with helper phage VCSM13 or hyperphage at a multiplicity of infection (MOI) of 15 and 20, respectively. Infection of *E. coli* cells occurred at 37°C (30 min standing, 30 min shaking) and was verified by the spreading of bacteria samples (1 µl in 2xYT) onto 2xYT-GK agar plates. The expression of scFv-pIII fusions was induced by resuspension of pelleted bacteria (4,000xg, 15 min, RT) in equal volumes of glucose-free induction medium and incubation of combined libraries on a shaker for 6 h (helper phage rescue) or o/n (hyperphage rescue) at 28°C. After pelleting the bacteria at 4°C, phages were precipitated by adding 1/5 volume prechilled PEG solution to the supernatant followed by an incubation for 1 h (hyperhage) or o/n (helper phage) at 4°C. Pelleted phages (4,000xg, 45 min, 4°C) were carefully resuspended in the equal volume of icecold PBS, and remaining bacteria were removed in a further centrifugation step. After repeated precipitation for 1 h on ice, pelleted phages were resuspended in a reduced volume of prechilled PBS for concentrating by a factor of 200 compared with the original culture. Phage solution was centrifuged (20,000xg, 3 min, 4°C) to remove remaining cell debris and stored o/n at 4°C. Titer of phage solution was determined (section 2.6.3) and around 10^{12} t.u. (hyperphage) or 10^{13} t.u. (helper phage) were preincubated in MPBS for 1 h at RT. Phages were applied to a blocked immunotube (MPBS for 2 h at RT) that was previously coated (o/n at 4°C) with the recombinant target protein (12-20 µg/ml in 3 ml PBS). In the case of using chimeric EGFR-Fc, solutions were supplemented with the same concentration of recombinant Fc protein. Binding of phage antibodies occurred during overhead rotation for 90 min and 30 min rest at RT. Unbound phages were removed by washing five times with PBST as well as PBS. For VCSM13-packaged phages, bound phage antibodies were eluted with 1 ml of elution

buffer by incubation for 8 min at RT under constant rotation and transfer of the solution into a tube containing neutralization buffer (~ 130 µl) thus adjusting the final pH to 7.4. For hyperphage-packaged phages, elution was performed employing 1 ml of freshly prepared trypsin solution for 20 min at RT. Eluted phages were added to log phase TG1 (final volume: 10 ml) and an empty selection tube was additionally filled with 5 ml log phase bacteria to rescue non-eluted phages. After infection at 37°C, both cultures were combined and samples taken for the determination of eluted phage titer by spreading 100 µl of serial dilutions (1:10 in 2xYT) onto 2xYT-GA agar plates and counting grown colonies. Remaining cultures were centrifuged (2,000xg, 10 min, RT), resuspended in 1 ml of 2xYT medium and streaked on large square 2xYT-GA agar plates. On the next day, bacteria were harvested from plates after adding 2xYT medium and stored as glycerol stock at -80°C. Further rounds of selection were performed by preparing smaller start cultures (100-200 ml) always using helper phage for superinfection. In the following selection rounds, the stringency during panning was enhanced by employing less antigen for coating (4-10 µg/ml) and more wash cycles with PBST and PBS (per solution: 10x for round 2, 15x for round 3, and 20x for round 4).

2.6.3 Determination of phage titer

To determine the titer after rescuing with phage strain VCSM13, serial dilutions from log phase infected TG1 culture were prepared. Ten µl of a 10^{-6} phage dilution was added to 990 µl of log phase growing TG1 bacteria for infection at 37°C. Dilutions of infected bacteria (1:10) were prepared in a 2xYT medium and 100 µl plated on 2xYT-GA selection plates. The titer was determined on the next day by counting colonies.

The particle number of hyperphage-packaged libraries was determined by phage ELISA. The phage sample and serial PBS dilutions of a reference phage preparation with known titer were coated in duplicate (100 µl/well) o/n at 4°C and plates blocked with MPBS (200 µl/well) for 2 h at RT. After incubation of 100 µl/well with peroxidase-conjugated anti-pVIII antibody (PROGEN) for 1 h at RT, plates were washed (3xPBST, 3xPBS) and peroxidase-conjugated anti-mouse detection antibody applied (1 h at RT). Peroxidase activity was detected using TMB as described

(section 2.5), and the number of phages was calculated by comparison with the reference calibration curve.

2.6.4 Polyclonal phage ELISA

Successful enrichment of specific binders to target proteins was assayed by polyclonal phage ELISA (ppELISA). Microtiter plates were coated with target and control proteins (2-3 µg/ml in PBS) o/n at 4°C. After blocking with MPBS (400 µl/well) for 2 h at RT, rescued phage after the different selection rounds were diluted in PBS to 10^{11} t.u./well and incubated for 1 h at RT. Plates were washed (3xPBST and 3xPBS) and bound phages detected with 100 µl/well of peroxidase-conjugated anti-pVIII antibody (GE Healthcare) for 1 h at RT employing TMB solution as described (section 2.5).

2.6.5 Monoclonal phage ELISA

Binding efficacy of individually produced phage antibodies was determined by monoclonal phage ELISA (mpELISA). Glycerol stock from positively enriched panning rounds were streaked on 2xYT-GA agar plates, and grown single colonies were inoculated into 96-well microtiter plates containing 100 µl of 2xYT-GA. Cultures were shaken o/n at 37°C and used for inoculation (3 µl/well) of an infection plate with fresh medium storing the master clones by adding glycerol (50 µl/well 2YT-GA containing 45% glycerol) at -20°C. After incubation of infection plates (2 h, 37°C, 150 rpm), bacteria were superinfected with 10 µl of helper phages (10^8 t.u./well) at 37°C followed by resuspension of the pellets in induction medium (150 µl/well) to induce antibody-pIII expression o/n at 28°C under shaking. The next day, each clone was analyzed for binding to coated selection antigen (1-2 µg/ml in PBS) and control antigen (1-2 µg/ml human Fc in PBS or MBPS), respectively by incubation of blocked wells (MPBS for 1 h at RT) with 100 µl/well phage supernatant in MPBS for 1 h at RT. Detection was performed following the ppELISA protocol (section 2.6.4). Readings for target protein five times (EGFR) or ten times (gB-1) higher than the averaged signal for the control proteins were considered to be antigen-specific binding.

2.6.6 Identification of unique antibodies

Master clones from target-specific binders were spread out onto 2xYT-GA agar plates and grown colonies (2-3 per clone) were analyzed by colony PCR as described (section 2.4.2). Plasmids of clones with intact scFv gene were prepared with QIAprep Spin Miniprep Kit and used as templates for reamplification of scFv inserts:

Reagent	**Volume (µl)**
Phagemid DNA (normalized to 20 ng/µl)	0.5
Forward primer P91 [25 µM]	0.6
Reverse primer P92 [25 µM]	0.6
KAPAHiFi buffer (5x)	10
dNTP mix (10 mM each dNTP)	1.5
KAPAHiFi DNA polymerase (1 units/µl)	1
dH_2O	35.8

PCR amplification was performed during 30 cycles:

Step	**Temperature (°C)**	**Time**
Initial denaturation	95	5 min
Denaturation	98	20 sec
Annealing	51	15 sec
Elongation	72	1 min
Final elongation	72	5 min
Cooling	4	Unlimited time

Amplified fragments were column-purified and eluted with 40 µl of EB-buffer. DNA fingerprint was performed using the restriction enzyme BstNI (1 h at 60°C):

Reagent	**Volume (µl)**
Purified PCR product	X (~400 ng)
NEB buffer 2 (10x)	2.5
BSA (10x)	2.5
BstNI (10 units/µl)	0.5
dH_2O	Ad 25

Banding pattern was analyzed by agarose gel (2%) electrophoresis to identify unique clones.

2.6.7 Gene subcloning

One representative from clones with the same pattern was subcloned into expression vector pAB1 over restriction sites SfiI (5') and NotI (3'). Amplified fragments and vector were digested with SfiI for 2 h at 50°C:

Reagent	**Volume (µl) insert**	**Volume (µl) vector**
DNA	X (1 µg)	X (10 µg)
NEB buffer 4 (10x)	5	5
BSA (10x)	5	5
SfiI (20 untis/µl)	0.25	2.5
dH_2O	Ad 50	Ad 50

After elution of purified DNA samples from columns (41.5 µl of EB buffer), SfiI-cut inserts and vector were further digested with NotI for 2 h at 37°C:

Reagent	**Volume (µl) insert**	**Volume (µl) vector**
DNA	39.5	39.5
NEB buffer 4 (10x)	5	5
BSA (10x)	5	5
NotI (10 untis/µl)	0.5 (10 units/µl)	0.5 (100 units/µl)
dH_2O	Ad 50	Ad 50

Alkaline phosphatase (1 µl/reaction) was added to the vector after 1 h of digestion and enzyme NotI was heat-inactivated during 20 min at 65°C. Bands for SfiI/Not-digested insert (~0.75 kb) and vector (~3.3 kb) were extracted from agarose gels (vector: 1%, inserts: 1.5%) and ligated for 1 h at 22°C using a molar ration of vector to insert of around 3 to 1:

Ligation	Volume (µl)
SfiI/NotI-digested, dephosphorylated pAB1 (50 ng)	X
Insert (SfiI/NotI-digested insert)	Y
Ligation buffer (10x)	2
T4 Ligase (1 U/µl)	1
dH_2O	Ad 20

Upon heat inactivation of ligase for 10 min at 65°C, DNA samples were precipitated for 2 h at -80°C:

Reagent	Volume (µl)
Ligation	20
100% ice-cold EtOH	50
Sodium acetate, pH 5.5 [3 M]	2
Glycogen (20 µg/µl)	1

Precipitation and DNA transfer into bacteria were performed with the protocol used for library cloning (section 2.3.8) by electoporation of 4 µl DNA/sample into 50 µl of frozen TG1 *E. coli* cells. Samples of transformed bacteria (10 µl and 100 µl) were spread on 2xYT-GA agar plates and grown o/n at 34°C. Single grown colonies were analyzed by colony PCR for existence of intact scFv gene and used for inoculation of 6 ml LB high salt cultures for preparation of glycerol stock and plasmid DNA.

2.6.8 Sequence analysis

Germline sequences and respective antibody gene families were determined by DNAPLOT as described (section 2.4.3) followed by the construction of phylogenetic trees with the Phylogeny.fr web tool. Additionally, the level of somatic hypermutations within V genes was determined by analyzing the nucleotide sequences of the VH and VL domains with the IMGT/V-QUEST online tool.

2.7 Expression and purification of antibody fragments

2.7.1 Expression and purification of scFvs

Glycerol stocks of unique clones were spread on 2xYT-GA agar plates, and single grown colonies were used for inoculating 5 ml of 2xYT-GA o/n cultures (37°C, 180 rpm). The next day, 200 ml of medium (2xYT-GA, 1 g/l glucose) was inoculated with 1/100 volume of o/n cultures and cells were grown at 37°C until OD_{600} of 1 was reached. After adding 1 ml/l IPTG stock solution to the cultures, proteins were expressed while shaking o/n at 21°C. Bacteria were harvested by centrifugation (6,000xg, 15 min, 4°C) and resuspended in 3 ml of periplasmic preparation buffer, supplemented with 1 ml/l of freshly prepared lysozyme stock solution to induce cell lysis during incubation for 30 min on ice. Spheroblasts were stabilized by addition of 10 mM $MgSO_4$ followed by centrifugation (12,000xg, 20 min, 4°C) to clarify periplasmic fractions. Antibody fragments were dialyzed (12 kDa cutoff) o/n at 4°C against recommended NPI-10 buffer and purified by IMAC employing Ni-NTA spin columns following the manufacturer's protocol. The protein concentrations of the PBS-dialyzed and filtered (0.22 µm) solutions were determined by measurement of the absorbance at 280 nm in a NanoDrop 1000 spectrophotometer entering the calculated values of the molar extinction coefficient and molecular mass of each protein. For production of high quantities, the herein presented protocol was upscaled using 50 ml of periplasmic preparation buffer per liter of bacterial culture. Protein fractions were dialyzed against SP-10 IMAC binding buffer and loaded to an equilibrated column containing Ni-Sepharose 6 Fast Flow. IMAC purification was performed according to the manufacturer's recommendations using buffers with increased imidazole concentrations for washing (SP-30) and elution (SP-500). Eluted fractions were analyzed by Coomassie-stained SDS-PAGE (12%) under reducing conditions. Fractions containing purified fragments were pooled and dialyzed against PBS.

2.7.2 Cloning of scFv-Fcs

Selected antibodies were formatted into bivalent scFv-Fc format by inserting the scFv gene over NarI/EcoRV into the eukaryotic expression vector pYD11 that encodes the human Fc gene. ScFv genes were PCR-amplified from the corresponding pAB1 templates using fragment-specific primers (H28: P95+P96, E6: P97+P98, and IZI08: P99+P100) with overhangs encoding for artificial cleavage sites NarI (5') and EcoRV (3') analogously as described (section 2.6.6). Purified PCR amplicons and vector were firstly digested with NarI and for 2 h at 37°C:

Reagent	**Volume (µl): insert**	**Volume (µl): vector**
DNA	38	X (10 µg)
NEB buffer 4 (10x)	5	5
NarI (5 untis/µl)	1	2.5
dH_2O	Ad 50	Ad 50

NarI was heat-inactivated for 20 min at 65°C and column-purified DNA eluted with 39.5 µl of EB buffer. Samples were further digested with EcoRV for 2 h at 37°C adding 1 µl of alkaline phosphatase to the vector after 1 h:

Reagent	**Volume (µl): insert**	**Volume (µl): vector**
DNA	37.5	37.5
NEB buffer 3 (10x)	5	5
BSA (10x)	5	5
EcoRV (20 units/µl)	0.25	2.5
dH_2O	Ad 50	None

After heat inactivation of EcoRV (20 min at 80°C), bands with the sizes of digested scFv genes (~1 kb) and vector (~5 kb) were sliced from 1.5% agarose gels, and ligated DNA was transformed into *E. coli* cells as described (section 2.6.7). Colony PCR was performed according to the presented protocol (section 2.4.2) employing forward primer P101 and reverse primer P102 that both bind to the pYD11 vector backbone. Colonies with successfully cloned scFv genes were identified by fragment sizes of around 1 kb followed by sequencing of the prepared plasmid DNA using primer P101. For subsequent transfection of mammalian cells, endotoxin-free

plasmid DNA was prepared from a single-grown colony using an EndoFree Plasmid Maxi Kit according to the manufacturer's protocol.

2.7.3 Expression and purification of scFv-Fcs

ScFv-Fcs were transiently expressed in HEK293-E6 cells. Two days before transfection, HEK293-E6 cells were diluted to $0.5x10^6$ cells/ml with F17 culture medium (22.5 ml) in a 125 ml shaker flask, and the culture then maintained in an orbital shaker with a humidified atmosphere (5% CO_2 at 37°C). The day of transfection, 200 µl aliquots were taken for determining the cell density ($1.5\text{-}2.0x10^6$ cells/ml) and viability (>97%). DNA solutions were prepared by vortexing after adding 25 µg of plasmid DNA to 1.25 ml of transfection medium (prewarmed F17 culture medium). PEI solutions were similarly produced by adding of 50 µl PEI solution (50 µg) to another 1.25 ml of transfection medium and vortexing. PEI was transferred to the DNA solution and vortexed with 3 pulses of 1 sec each followed by 3 min incubation at RT. For transfection, the DNA-PEI complex was added to the cells and the flasks swirled immediately. Proteins were expressed by 120 h incubation on an orbital shaker at 37°C. After one day of protein expression, TN1 feeding medium was added to a final concentration of 5 g/l. Culture samples (300 µl) were taken every day to count the cell number and monitor the expression levels by dot blot analysis. Expression analysis was performed as described (section 2.4.4) by applying 100 µl/dot of centrifuged sample in comparison with serial dilutions of control IgG with known concentration followed by detection with a peroxidase-conjugated anti-human IgG Fc antibody (2 h at RT). Supernatants containing the expressed proteins were harvested by centrifugation (200xg, 10 min, RT) and purified by protein A chromatography using the FPLC system. Therefore, production supernatants were first dialyzed and then 1:2 diluted in protein A binding buffer. Filtered solutions (0.20 µm) were loaded on equilibrated HiTrap rProtein A FF columns (0.5 ml/min) according to the manufacturer's instructions. Proteins were eluted with protein A elution buffer and directly fractionated into wells containing 200-300 µl of protein A neutralization buffer. Fractions containing the constructs were pooled and pH tested by indicator strips. Proteins were dialyzed against PBS and concentrations of filter-sterilized proteins were determined.

2.7.4 SDS-PAGE

Purity of fragments was assessed by sodium dodecyl sulphate-polyacrylamide gel electrophoresis (SDS-PAGE) and Coomassie staining. Protein samples were prepared with reducing LDS sample buffer supplemented with dithiothreitol (DTT) solution before heating for 3 min to 90°C. Proteins were loaded on 12% precast gels using a prestained protein ladder and separated for about 1 h at 180 V. Gels were rinsed in dH_2O (3x in a microwave for 30 sec) before staining with heated Coomassie solution for about 1 h while shaking. Destaining of gels was carried out in dH_2O o/n.

2.7.5 Immunoblotting

Specific detection of antibody fragments was achieved by immunoblotting. After separation by SDS-PAGE (section 2.7.4), proteins were electroblotted onto nitrocellulose membranes for 30 min at 20 V using semi-dry blotting buffer. For detection of scFvs, blocked membranes (MPBS, 1 h, RT) were incubated with a mouse anti-myc antibody (o/n at 4°C) followed by detection with a goat anti-mouse IgG peroxidase conjugate (2 h at RT). ScFv-Fc fragments were detected with a peroxidase-conjugated anti-human IgG Fc antibody (o/n at 4°C). After the single incubation steps, membranes were rinsed three times with PBST and once with PBS. Peroxidase activity was finally detected by chemiluminescence using ECL substrate (3 min) and chemical film.

2.7.6 Size-exclusion chromatography

Size-exclusion chromatography (SEC) was performed using a FPLC ÄKTA system in combination with columns that had been calibrated with protein standards of known size. Oligomeric states of purified antibody fragments were analyzed either using column Superdex 75 10/300 GL (scFvs) or Superdex 200 10/300 GL (scFv-Fcs). Depending of the concentration of investigated fragments, 25-50 µl of samples were loaded and separated with PBS as mobile phase at a constant flow rate of 0.5 ml/min. Several scFvs were further purified by separation on the preparative SEC column HiLoad 16/60 Superdex 75. Between 2-5 ml per construct was loaded and separated with PBS as a mobile phase at a flow rate of 1 ml/min. Fractions

containing the monomeric proteins were pooled and partly concentrated with centrifugal filter units (10 kDa cutoff).

2.8 Cell culture techniques

2.8.1 Thawing cells

Vials with cryo-conserved cell line HEK293-6E were thawed in a water bath at 37°C and immediately transferred to 125 ml culture shaker flasks containing 16 ml of conditioned F17 medium without G418. Cells were grown in a humidified orbital shaker (5% CO_2, 37°C, 120 rpm) for about three days until a density of at least $1x10^6$ cells/ml was reached. As soon as a cell doubling time of about 24 h was established, medium was supplemented with 25 µg/ml of G418 for further cultivation.

Other cell lines were thawed and transferred to conical tubes containing 4 ml of fresh medium. For removing DMSO, cells were pelleted (5 min, 250xg, RT), resuspended in 10 ml of prewarmed medium, and transferred into two T25 tissue flasks containing 5 ml of fresh culture medium. After maintaining cells up to two days in a humidified cell culture incubator at 37°C with 5% CO_2, medium was exchanged and cells, depending on the density, were transferred to a new T75 flask for further culturing.

2.8.2 Cell cultivation

Cell line HEK293-E6 was cultivated in disposable 125 ml Erlenmeyer flasks in 40 ml of F17 culture medium in a humidified orbital shaker under constant conditions (5% CO_2, 37°C, 120 rpm) by dilution to $0.5x10^6$ cells/ml (2 days), to $0.25x10^6$ cells/ml (3 days), or to $0.125x10^6$ cells/ml (4 days) never allowing the maintenance cells to exceed $2x10^6$ cells/ml.

Other mammalian cell lines were maintained in T75 tissue culture flasks in 20 ml of the appropriate culture medium (**Table 12**) under constant conditions in a humidified cell culture incubator (5% CO_2, 37°C). Cells were passaged every 2-4 days depending on the cell line and density using prewarmed culture media and solutions by transfer into new cell culture flasks. Adherent cell lines were washed with 10 ml of PBS and detached with 2 ml of trypsin/EDTA solution for about 5 min at 37°C followed by addition of 8 ml of fresh medium. Both adherent and suspension cell lines

were counted using a hemocytometer and microscope after dead-live staining with trypan blue.

2.8.3 Cell freezing for storage

For freezing of cell line HEK293-E6, log phase cells (~1x10^6 cells/ml) were centrifuged (250xg, 5 min, RT) and gently homogenized in a suitable freezing medium to obtain the desired cell concentration (~1x10^7 cells/ml). Cell suspensions were aliquoted (1 ml/cryovial) and slowly frozen at 1°C/min to a temperature of –80°C in a cryo freezing container filled with isopropanol. The next day, vials were transferred to fluid nitrogen and stored in a cryo tank or cryogenic refrigerator.

Other cells lines for storage were grown in T75 flasks to 80-90% confluence (adherent) or vitality of more than 95% (suspension). Suspension cells were harvested by centrifugation (200xg, 10 min, RT) whereas adherent cells had to be detached by PBS washing and trypsinization prior to centrifugation. The cell number was determined and adjusted to 1x10^7/ml by resuspension in a freezing medium. Aliquoted cells were slowly frozen and stored as described above.

2.8.4 Virus propagation and titration

Stocks of herpes simplex viruses were propagated by infection of Vero cells with master stocks of laboratory strains HSV-1F or HSV-2G. The day before infection, Vero cells had been seeded with 2x10^5/ml (45 ml/T175 flask) in culture medium. Virus master stocks were defrosted from -80°C at RT and 0.6 x 10^6 virions diluted in 5 ml of serum-free Opti-MEM medium. Cells (2x10^7 per flask) were infected with an MOI of 0.3 by addition of inocula for 45 min at 37°C and gentle movement of the flasks every 15 min. After addition of 20 ml/flask prewarmed Opti-MEM medium, cells were maintained for 2 or 3 days until maximum cytopathic effect (CPE) was reached. For releasing virions, cells were frozen o/n at -80°C and defrost under occasional gentle shaking. Cells were removed by repeated centrifugation (twice, 3,500xg, 15 min, 4°C) and supernatant aliquoted for shock freezing in liquid nitrogen before transfer of virus preparations to -80°C for long-time storage.

Titers of virus preparations were determined by plaque assay using Vero cells. Therefore, 1x10^5 cells/well were seeded in 24-well plates and grown o/n at 37°C. The

next day, virus preparations were serially diluted 1:10 in DMEM medium (10^{-3} to 10^{-8}) and 100 µl/well applied in quadruple to PBS-washed cells. Upon incubation for 45 min at 37°C, inocula were removed and 1 ml/well of prewarmed CMC preparation was added to washed cells. Plates were further incubated for up to 3 days until plaques become visible. Cells were fixated by applying formaldehyde solution (500 µl/well, 5 min) and stained with crystal violet solution (500 µl/well, 2 min). After washing the cells once with PBS and twice with H_2O, titers were calculated by counting plaques.

2.9 Characterization of selected antibodies

2.9.1 Specificity by cell binding

Specificity of selected antibodies for binding to naturally occurring gB protein was evaluated by flow cytometry using Vero cells that had been infected with different human HSV strains (1F or 2G). Two days before infection, Vero cells had been seeded with $1.4x10^5$/ml of culture medium (45 ml/T175 flask) and grown at 37°C. For infection, virus stocks were thawed at RT and $6x10^7$ virions diluted in 5 ml of DMEM medium. Vero cells were washed with PBS and infected with an MOI of 3 by incubation of the inocula for 45 min at 37°C under gentle movement of the flask every 15 min. After infection, 20 ml of culture medium was applied to each flask and incubated for a further 16 to 20 h. The next day, cells were washed with PBS and detached with 4 ml of trypsin/EDTA solution for about 5 min at 37°C followed by the addition of 16 ml of fresh medium. After counting, cells were centrifuged (200xg, 3 min, RT) and diluted to $5x10^6$/ml in FACS buffer. Cell suspension was distributed into U-bottom microtiter plates with 100 µl per well and the pelleted cells were resuspended in 100 µl of FACS buffer containing 100 nM of purified scFvs. Upon incubation for 1h at RT on a rocker, cells were washed twice by resuspension of centrifuged cells (200xg, 3 min, RT) with 200 µl/well in a FACS buffer. Bound scFvs were labeled with mouse anti-myc-specific IgG for 45 min at 4°C followed by incubation of washed cells with FITC-conjugated anti-mouse IgG Fc for 15 min at RT in the dark. Cells were washed twice and resuspended samples (100 µl in FACS buffer) were transferred to FACS tubes containing 500 µl of FACS buffer. The fluorescence of 10,000 events/sample was measured on a flow cytometer, and the mean and median fluorescence intensities were calculated using FACSDiva

software. Unstained cells and cells incubated with detection system served as controls. To confirm specificity, selected gB-specific scFvs (1 nM) were preincubated with (control: without) 10-fold molar excess of recombinant gB-1 for 30 min at RT in FACS buffer and applied to HSV-1 infected Vero cells for measuring by flow cytomertry as described above.

Specific binding of EGFR-selected scFvs was analyzed by flow cytometry employing various cancer cell lines with tested EGFR status. To analyze the expression level of the EGF receptor, cultured cells were counted, diluted to $5x10^6$/ml in FACS buffer, and applied to U-bottom microtiter plates (100 µl/well) for staining with 100 µl/well of cetuximab (10 µg/ml in FACS buffer, 1 h at RT). Washed cells were labeled with FITC-conjugated anti-human IgG Fc antibody for 15 min at 4°C in the dark and fluorescence intensity measured as described. Specificity assays were performed as described above using a similar protocol by staining receptor-positive (HNO97, HNO199, HNO210, HNO211, HNO223, HNO410, UDSCC2, 93VU1047T SKOV-3, A431) and negative tumor cell lines (Jurkat, NALM-6, Raji, MCF7) with 300 nM of purified monomeric scFvs.

2.9.2 Antibody affinity by flow cytometry

Affinities of selected scFvs were determined by measurement of equilibrium binding curves by flow cytometry using either HSV-infected Vero cells with confirmed cell suface expression of gB or the A431 cancer cell line overexpressing EGFR. Flow cytomtery was mainly performed as described (section 2.9.1) by incubation of $5x10^5$ cells/well with 1:2 serial dilutions of monomeric scFvs (0.03–1000 nM in FACS buffer) in triplicate. Background fluorescence was subtracted from measured median fluorescence intensities, and relative affinities were calculated by nonlinear regression using GraphPad Prism software. Affinity was described by the half maximal effective concentration (EC_{50}).

2.9.3 Antibody affinity by SPR analysis

Binding kinetics were additionally measured by surface plasmon resonance employing a Biacore 2000 instrument. For affinity measurements of gB-specific scFvs, ligand gB-1 was immobilized on a CM5 sensor chip using amine coupling chemistry. The surface of flow cells 1 and 2 were activated for 7 min with a 1:1 mixture of 0.1 M NHS (N-hydroxysuccinimide) and 0.4 M EDC (1-ethyl-3-(3-dimethylaminopropyl) carbodiimide hydrochloride) at a flow rate of 5 µl/min. The ligand (100 µg/ml) in 10 mM sodium acetate, pH 4.7, was immobilized on flow cell 2 for 7 min at 5 µl/min to reach a density of 230 RU leaving flow cell 1 blank to serve as reference. Surfaces were blocked by injection of 1 M ethanolamine, pH 8.5, for 7 min at 5 µl/min. To measure kinetics, monomeric fractions of scFvs in running buffer were injected in increasing concentrations (1 nM, 10 nM, 50 nM, 100 nM, 200 nM, 500 nM, and 1000 nM) over both flow cells at a flow rate of 10 µl/min and a temperature of 25°C. Analytes were allowed to associate and dissociate for 3 min and 30 min, respectively. Surfaces were regenerated in running buffer for further 30 min. The data were globally fitted with the Langmuir 1:1 binding model using the BIAevaluation 4.1.1 software. Constants and errors were averaged from two independent determinations.

Affinity measurements of EGFR-specific scFvs were performed by amine coupling of protein A on a activated CM5 sensor chip. Protein A (300 µg/ml, 10 mM sodium acetate, pH 4.5) was immobilized for 7 min at 5 µl/ml on flow cells 1 and 2. After blocking the surfaces, EGFR-Fc in running buffer was captured at 5 µl/min on flow cell 2 with 20 µg/ml for 7 min (IZI08: 3 µg/ml, 1.5 min) reaching a density of 2680 RU (IZI08: 290 RU). Monomeric scFvs in running buffer were injected in increasing concentrations (0.1 nM, 1 nM, 10 nM, 50 nM, 100 nM, and 200 nM) over both flow cells at a flow rate of 10 µl/min and a temperature of 25°C. Analytes were allowed to associate and dissociate for 6 min (IZI08: 3 min) and 30 min (IZI08: 15 min), respectively. Surfaces were regenerated in running buffer for further 30 min (IZI08: 15 min). The data were globally fitted with the 1:1 binding mass transfer model using the BIAevaluation 4.1.1 software. Constants and errors were averaged from two independent determinations.

2.9.4 Virus neutralization assays

Neutralizing activity of gB-specific scFvs was determined in plaque reduction neutralization tests (PRNTs). The day before infection, Vero cells had been seeded in 6-well cell culture plates with $5x10^5$ cells/well that had been diluted in always 5 ml of prewarmed culture medium. The next day, HSV-1 preparations were freshly thawed from cryostock at RT and diluted to 600 PFU/ml in DMEM (2% FCS, penicillin/streptomycin). Virus preparations (280 µl) were preincubated with equal volumes of scFv dilutions (4 µM, i.e., 2 µM final concentrations) or PBS as control and incubated in 48-well plates for 1 h at 37°C. The virus antibody preparations (500 µl/well) were added to Vero cell monolayer that had been washed with 2 ml of PBS. After 45 min incubation at 37°C, the inocula were removed and cells washed with 3 ml of PBS and overlaid with 3 ml/well CMC of preparation. After 72, infected cells were fixed with formaldehyde solution (3 ml/well for 5 min) and stained with crystal violet solution (800 µl/well) for 2 min. Before counting the plaques, cells were washed once with PBS (2 ml/well) and twice with H_2O (5 ml and 2 ml per well). The percentage of neutralization was calculated as follows:

$$\% \text{ of neutralisation} = 100 - \left[\left(\frac{\text{Number of plaques: virus + antibody}}{\text{Number of plaques: virus only}} \right) \times 100 \right]$$

To further evaluate the neutralization capacity of antibody H28, serial dilutions (five 1:2.5 dilution steps, one well/plate with PBS control) of the different formats (scFv, $scFv_2$, scFv-Fc) and control IgG hu2c were prepared in PBS using different start concentrations depending on the analyzed antibody format (IgG hu2c: 200 nM, H28 $(scFv)_2$: 300 nM, H28 scFv and H28 scFv-Fc: 600 nM).

2.9.5 EGF competition assay

To analyze the capability of EGFR-specific scFvs to compete with EGF for binding to cellular expressed receptor, selected scFv monomers (300 nM) were preincubated with or without (control) a 2-fold molar excess of recombinant EGF in FACS buffer for 1 h at 4°C. A431 or SKOV-3 cells ($5x10^5$ cells/well) were incubated with prepared samples for 1 h at 4°C. Washed cells were stained and fluorescence detected as described (section 2.9.1) keeping the cells on ice to prevent EGF-induced receptor internalization.

2.9.6 Proliferation assays

The influence of EGFR-specific antibodies on cell proliferation was tested in an *in vitro* assay using SKOV-3 carcinoma cells. After trypsinization, 5,000 cells/well being diluted in 100 µl culture medium with reduced serum concentration (0.3% FCS) were seeded into the inner wells of 96-well F-bottom cell culture plates. Outer wells were filled up with PBS (400 µl/well) to reduce evaporation and plates were incubated for 24 h at 37°C. For prescreening, 50 µl/well of medium was removed the next day and replaced by 1:10 dilutions of scFv (0.002 nM to 2,000 nM) in DMEM medium that had been supplemented with 0.3% FCS and 2 nM EGF. After 72 h incubation, 10 µl/well of AlamarBlue Cell Viability Reagent was added and plates incubated for about 1.5 h at 37°C and 5% CO_2 until color change appeared for the control wells (proliferation medium without antibody) from blue (oxidized form, non-fluorescent) to red (reduced form, fluorescent). Metabolic activity was monitored by measuring the fluorescence signals at 535 nm excitation and 595 nm emission wavelength employing the Infinite 200 PRO reader. The anti-proliferative effect of EGFR-specific antibodies in the scFv-Fc or IgG format was evaluated following the presented protocol using changed antibody start concentrations (0.0002 nM, 0.02 nM, 2 nM, 10 nM, 20 nM, 100 nM, 200 nM).

3 Results

3.1 Concept of LYNDAL

In this thesis, a concept has been developed allowing the isolation of human monoclonal antibodies with therapeutic potential from antigen-encountered immune repertoires. Based on phage display technology, individual IgG antibody libraries were cloned from antibody gene pools of patients with squamous cell head and neck carcinoma undergoing surgery. Antibody gene information was isolated from single tumor-draining lymph nodes and the final library collection therefore termed as LYNDAL: “Lymph Node Derived Antibody Libraries”. Additionally, serum samples of corresponding patients were collected for identifying those donors with a strong IgG-based antibody response against therapeutic relevant targets. Finally, antibody libraries from donors with target-specific antibody response were combined for subsequent antibody selection. The LYNDAL concept is illustrated in **Figure 6**.

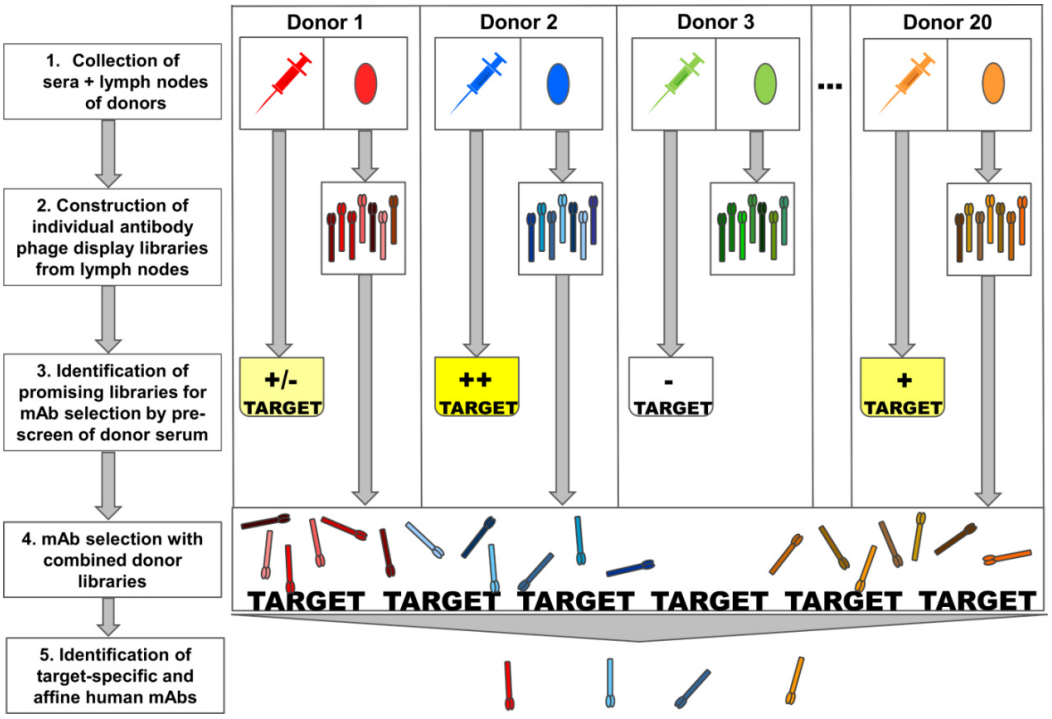

Figure 6. LYNDAL concept. Serum samples and lymph nodes were obtained from human donors. Antibody gene repertoires were amplified from lymph node-derived B cells and cloned as individual antibody phage display libraries. Donors with target-specific IgG antibody titer were identified by serum analysis and corresponding libraries were combined for the antibody selection.

3.2 Construction of libraries

The concept presented here includes the generation of individual combinable antibody libraries that were cloned from the IgG repertoires of donors who had been encountered with therapeutically useful target antigens. Together, these individual antibody libraries are forming the final library collection. A schematic overview about the cloning procedure of LYNDAL is depicted in **Figure 7** whereas the detailed protocol is described into the materials and methods section 2.3.

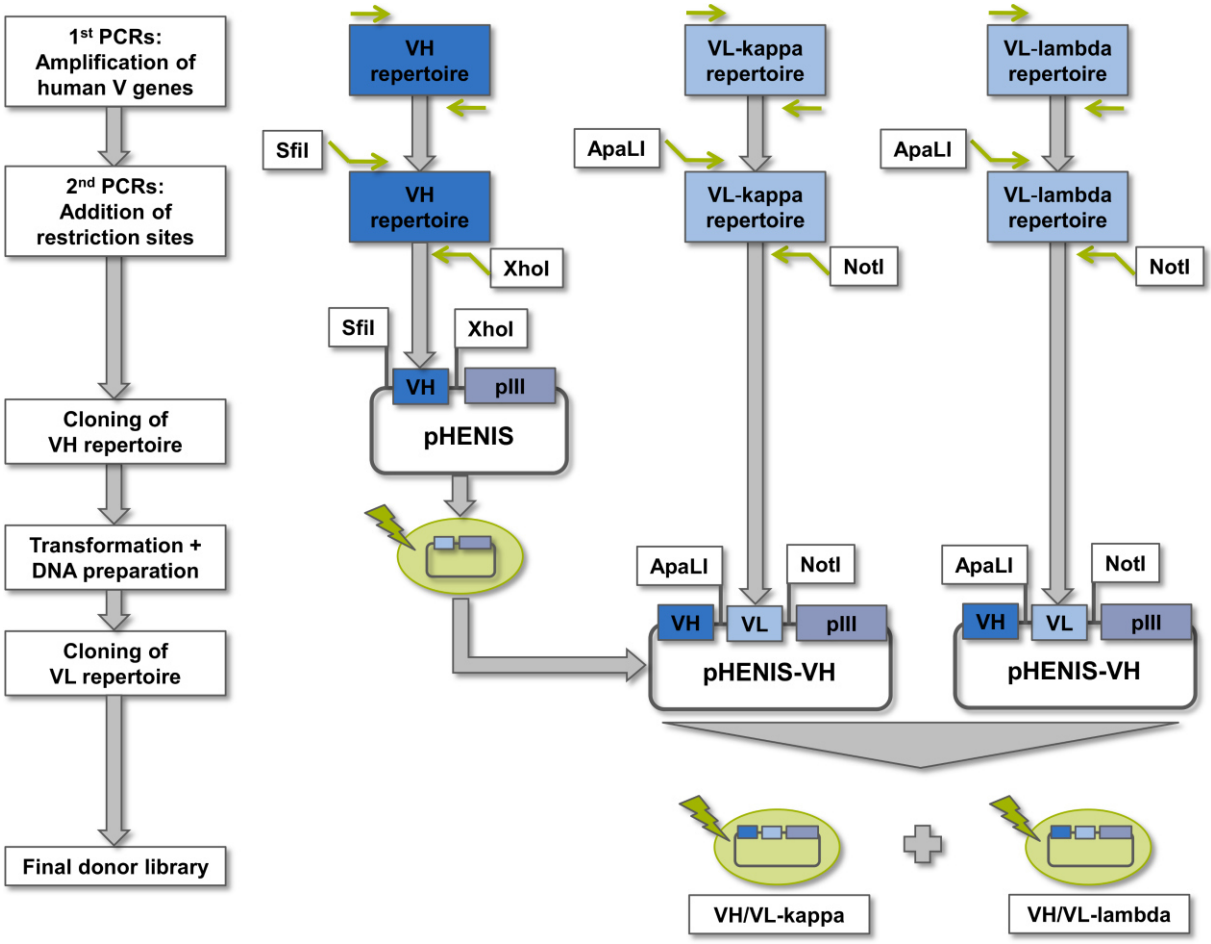

Figure 7. LYNDAL cloning strategy. IgG antibody repertoires of included donors were amplified from lymph node-derived cDNA in a two-step, semi-nested PCR strategy. In a first round of PCRs (1st PCRs), the VH, VL-kappa, and VL-lambda subsets were independently amplified. In a second round of PCRs (2nd PCRs), artificial cleavage sites were introduced at amplified fragments (VL: ApaL/NotI, VH: SfiI/XhoI). LYNDAL were cloned in a two-step strategy. First, the VH repertoire was cloned into phagemid pHENIS as SfiI/NotI fragments followed by transformation of *E. coli* cells and preparation of plasmid DNA. In a second cloning step, the VL repertoires were randomly introduced into the VH-repertoire containing phagemids as ApaLI/NotI fragments. Final libraries were obtained by *E. coli* transformation thus preparing two sublibraries per donor (VH/VL-kappa and VH/VL-lambda).

In summary, the individual variable IgG antibody genes were amplified in a two-step, semi-nested PCR strategy. Giving the fact that successful antibody selection mainly depends on the generation of high quality libraries, a sophisticated set of ninety PCR primers was designed to amplify all known antibody families and germline sequences as annotated in VBASE antibody database (**Table 14**). Each primer contained not more than two degenerated nucleotide positions to maximize specific gene amplification. In a first round of PCRs, the human antibody genes were separately amplified for the VH, VL-kappa, and VL-lambda subsets by combining one forward primer with a single reverse primer (VL-kappa and lambda) or a mix of reverse primers (VH). While the forward primers bound to the region encoding for the first amino acids of the variable domain, the reverse primers bound within the constant gene region of the CH1 or CL antibody domain. During a second round of PCRs, artificial restriction sites were added on reamplified variable antibody genes by using primers that encoded for additional nucleotide overhangs. Here, sets of reverse primers were used that bound to the J genes located upstream of the regions that had been used for initial amplification. Final libraries were generated by randomly combining the VH and VL antibody repertoires in phagemid vector pHENIS in a two-step cloning strategy. After insertion of the amplified VH genes, VL-kappa and VL-lambda genes were separately introduced and transformed in bacteria during at least 88 electroporations per donor thus preparing two independent sublibraries (VH/VL-kappa and VH/VL-lambda).

The gene assembly of the final library vector is shown in **Figure 8A**. The IgG repertoires of the LYNDAL donors were cloned in VH-VL orientation as scFv antibody fragments linked by a flexible 15 amino acid peptide. To enable the detection and purification of scFv antibody fragments, the original phagemid vector pHENIS contained sequences that encode for a C-terminal hexahistidine tag and myc peptide. The cloned scFv genes were separated from the phage pIII gene by an amber stop codon. Induced expression by an amber suppressor *E. coli* stain (e.g., TG1) finally allowed the periplasmic production of antibody fusion proteins consisting of an N-terminal located scFv antibody fragment and a C-terminal pIII M13 coat protein (**Figure 8B**). Soluble expressed scFv-pIII fusion served either for quality analysis of cloned LYNDAL, or for the presentation of selectable scFv-pIII fusion on the surface of filamentous phages (**Figure 8C**).

Table 14. Primer combinations for LYNDAL cloning.

No.	Name	Binding germline sequence	Description
P1	VH1/7-fwd	1-02, 1-08, 1-45, 1-46, 1-69, 1e, 7-4.1	1st PCRs: Amplification of VH fragments
P2	VH1A-fwd	1-45, 1-58	
P3	VH1B-fdw	1-24, 1f	
P4	VH1C-fdw	1-03, 1-18	
P5	VH2-fwd	2-05, 2-26, 2-70	
P6	VH3A-fwd	3-07, 3-09, 3-13, 3-15, 3-20, 3-21, 3-43, 3-48, 3-49, 3-64, 3-66, 3-72, 3-73, 3d	
P7	VH3B-fwd	3-53, 3-74	
P8	VH3C-fwd	3-11, 3-30, 3-30.3, 3-30.5, 3-33	
P9	VH3D-fwd	3-23	
P10	VH4A-fwd	4-04, 4-28, 4-30.1, 4-30.2, 4-30.4, 4-31, 4-39, 4-59, 4-61, 4b	
P11	VH4B-fwd	4-34	
P12	VH5-fwd	5-51, 5a	
P13	VH6-fwd	6-1	
P14	IgG-rev-1	CH1 (IgG1, IgG2, IgG3)	
P15	IgG-rev-2	CH1 (IgG4)	
P16	Vκ1A-fwd	A20, A30, L1, L5, L12, L14, L15, L19, O12/O2, O18/O8	1st PCRs: Amplification of VL-kappa fragments
P17	Vκ1B-fwd	L4, L8, L18	
P18	Vκ1C-fwd	L9, L11, L23	
P19	Vκ1D-fwd	L24	
P20	Vκ2A-fwd	A2, A18, A23, O11/O1	
P21	Vκ2B-fwd	A1, A17, A19/A3	
P22	Vκ3A-fwd	A11, A27, L2, L16	
P23	Vκ3B-fwd	L6, L20, L25	
P24	Vκ4-fwd	B3	
P25	Vκ5-fwd	B2	
P26	Vκ6A-fwd	A26/A10	
P27	Vκ6B-fwd	A14	
P28	Cκ-rev	CLκ	
P29	Vλ1A-fwd	1a, 1c, 1g	1st PCRs: Amplification of VL-lambda fragments
P30	Vλ1B-fwd	1b, 1e	
P31	Vλ1C-fwd	1e	
P32	Vλ2-fwd	2a2, 2b2, 2c, 2d, 2e	
P33	Vλ3A-fwd	3h, 3j, 3r	
P34	Vλ3B-fwd	3a, 3e, 3m(2), 3p, V2-19	
P35	Vλ3C-fwd	3l	
P36	Vλ3D-fwd	3m(1)	
P37	Vλ4-fwd	4a, 4b	
P38	Vλ5-fwd	5b, 5c, 5e	
P39	Vλ6-fwd	6a	
P40	Vλ7/8-fwd	7a, 7b, 8a	
P41	Vλ4/9-fwd	4c, 9a	
P42	Vλ10-fwd	10a	
P43	Cλ-rev	CLλ	

P44	VH1/7-fwd-SfiI	1-02, 1-08, 1-45, 1-46, 1-69, 1e, 7-4.1	2nd PCRs: Introducing of restriction sites at VH fragments
P45	VH1A-fwd-SfiI	1-45, 1-58	
P46	VH1B-fwd-SfiI	1-24, 1f	
P47	VH1C-fwd-SfiI	1-03, 1-18	
P48	VH2-fwd-SfiI	2-05, 2-26, 2-70	
P49	VH3A-fwd-SfiI	3-07, 3-09, 3-13, 3-15, 3-20, 3-21, 3-43, 3-48, 3-49, 3-64, 3-66, 3-72, 3-73, 3d	
P50	VH3B-fwd-SfiI	3-53, 3-74	
P51	VH3C-fwd-SfiI	3-11, 3-30, 3-30.3, 3-30.5, 3-33	
P52	VH3D-fwd-SfiI	3-23	
P53	VH4A-fwd-SfiI	4-04, 4-28, 4-30.1, 4-30.2, 4-30.4, 4-31, 4-39, 4-59, 4-61, 4b	
P54	VH4B-fwd-SfiI	4-34	
P55	VH5-fwd-SfiI	5-51, 5a	
P56	VH6-fwd-SfiI	6-1	
P57	JH1-2,4-5-rev-	JH1, JH4, JH5	
P58	JH3,6-rev-XhoI	JH3, JH6	
P59	Vκ1A-fwd-ApaI	A20, A30, L1, L5, L12, L14, L15, L19, O12/O2, O18/O8	2nd PCRs: Introducing of restriction sites at VL-kappa fragments
P60	Vκ1B-fwd-ApaI	L4, L8, L18	
P61	Vκ1C-fwd-ApaI	L9, L11, L23	
P62	Vκ1D-fwd-ApaI	L24	
P63	Vκ2A-fwd-ApaI	A2, A18, A23, O11/O1	
P64	Vκ2B-fwd-ApaI	A1, A17, A19/A3	
P65	Vκ3A-fwd-ApaI	A11, A27, L2, L16	
P66	Vκ3B-fwd-ApaI	L6, L20, L25	
P67	Vκ4-fwd-ApaI	B3	
P68	Vκ5-fwd-ApaI	B2	
P69	Vκ6A-fwd-ApaI	A26/A10	
P70	Vκ6B-fwd-ApaI	A14	
P71	Jκ1,2,4-fwd-NotI	Jκ1, Jκ2, Jκ4	
P72	Jκ3-rev-NotI	Jκ3	
P73	Jκ5-rev-NotI	Jκ5	
P74	Vλ1A-fwd-ApaI	1a, 1c, 1g	2nd PCRs: Introducing of restriction sites at VL lambda fragments
P75	Vλ1B-fwd-ApaI	1b, 1e	
P76	Vλ1C-fwd-ApaI	1e	
P77	Vλ2-fwd-ApaI	2a2, 2b2, 2c, 2d, 2e	
P78	Vλ3A-fwd-ApaI	3h, 3j, 3r	
P79	Vλ3B-fwd-ApaI	3a, 3e, 3m(2), 3p, V2-19	
P80	Vλ3C-fwd-ApaI	3l	
P81	Vλ3D-fwd-ApaI	3m(1)	
P82	Vλ4-fwd-ApaI	4a, 4b	
P83	Vλ5-fwd-ApaI	5b, 5c, 5e	
P84	Vλ6-fwd-ApaI	6a	
P85	Vλ7/8-fwd-ApaI	7a, 7b, 8a	
P86	Vλ4/9-fwd-ApaI	4c, 9a	
P87	Vλ10-fwd-ApaI	10a	
P88	Cλ-rev1-NotI	Jλ1	
P89	Cλ-rev2-NotI	Jλ2, λ3	
P90	Cλ-rev3-NotI	Jλ7	

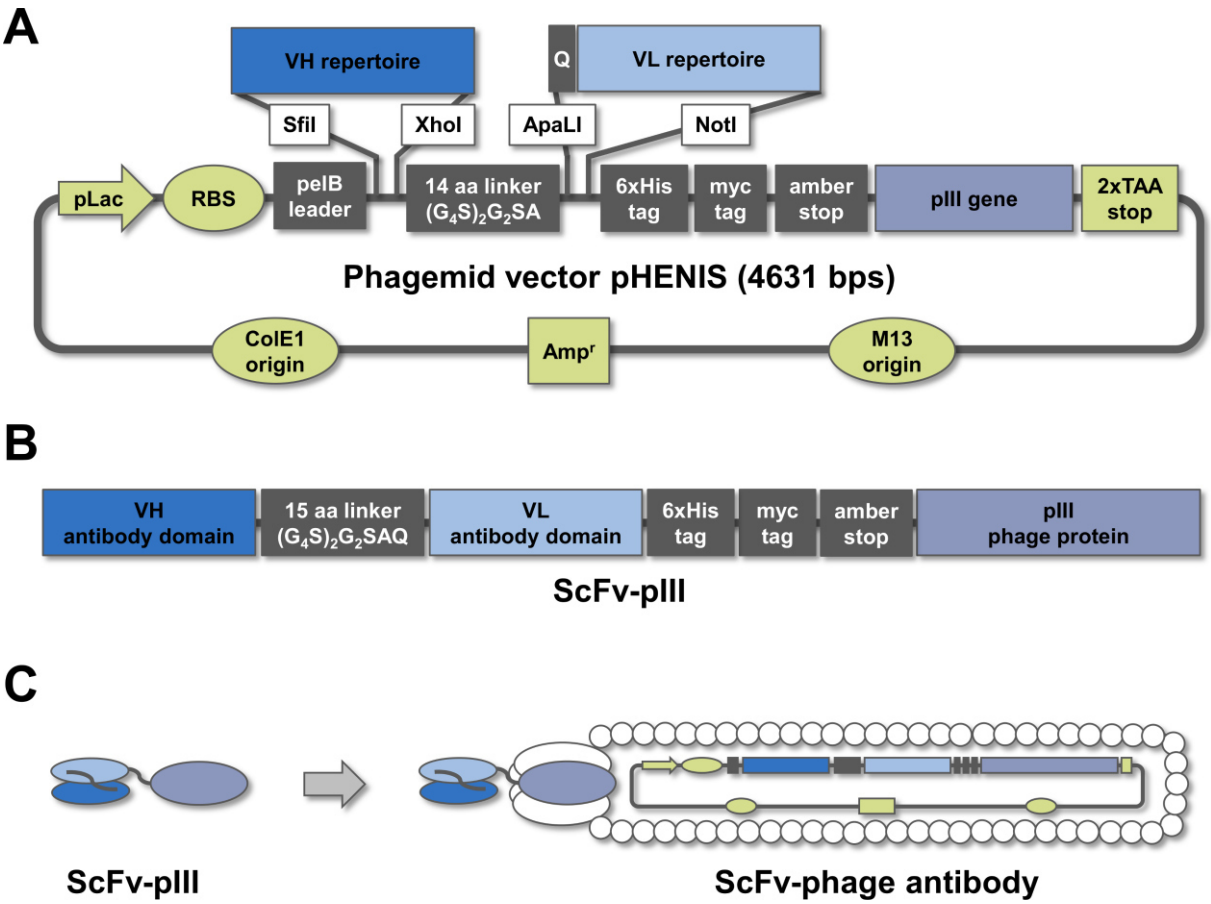

Figure 8. Maps of LYNDAL vector and derived proteins. (**A**) IgG donor repertoires were cloned into phagemid vector pHENIS as VH and VL repertoire using restriction sites SfiI/XhoI and ApaLI/NotI, respectively. Forward primers for the amplification of the VL repertoires added an additional codon encoding for the amino acid glutamine (Q). Thus, the vector-intrinsic scFv linker was completed to the 15 amino acid long peptide $(G_4S)_2G_2SAQ$ to enable the flexible assembly of the VH and VL domain. Since the pHENIS contained two origins of replication (ColE1 and M13), final LYNDAL phagemids are either capable of being propagated as bacterial plasmids or as phage DNA. For the selection of bacteria containing the vector DNA, phagemid encodes for selection marker ampicillin (Amp^r). After inducing the lactose promoter (pLac), protein translation is initiated by binding of ribosomes to the ribosome binding site (RBS) and is terminated by the double stop codon TAATAA. (**B**) Translated proteins are directed by the pelB (pectate lyase B) leader sequence into bacterial periplasm to support the correct folding of scFv-pIII fusion proteins. (**C**) After superinfection of plasmid carrying bacteria, scFv-pIII fusions are assembled within newly produced scFv-phage antibodies thus being usable for antibody selection.

In the end, 20 patients were included for construction of LYNDAL. As summarized in **Table 15**, the average weight of the collected patient lymph nodes was 223 mg. Preparation of lymphatic tissue delivered, on average, 2.2 µg/mg of highly pure total RNA as assessed from the absorbance spectra. All preparations showed distinct and prominent bands for intact ribosomal RNA without obvious degradation as analyzed by agarose gel electrophoresis (**Figure 9**).

Table 15. Weight and yields of prepared RNA from LYNDAL lymph nodes.

LYNDAL number	Patient number	Weight of lymph node (mg)	Yield RNA/weight lymph node (µg/mg)
1	485M	129	3.1
2	485N	398	2.0
3	485O	225	2.2
4	485Q	373	2.6
5	485S	313	3.2
6	485V	432	2.5
7	486C	118	0.2[a]
8	485I	401	1.2
9	486J	175	2.4
10	513	163	2.9
11	515	120	5.7
12	487M	107	0.6
13	488H	306	2.7
14	488G	107	0.6
15	ARJ	ND[b]	ND[b]
16	518	144	1.9
17	488C	333	1.7
18	504	134	2.2
19	488A	168	1.5
20	552	89	2.2

[a]Less efficient RNA isolation due to technical problems during homogenization. [b]ND: Not determined.

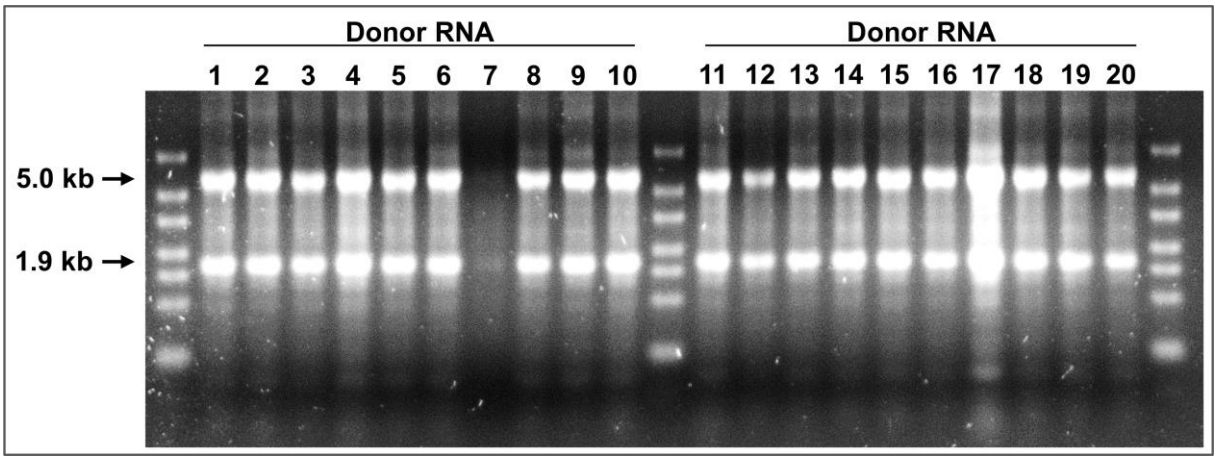

Figure 9. Integrity of LYNDAL donor RNA. Total RNA was isolated from single tumor non-infiltrated lymph nodes from head and neck cancer patients and analyzed on non-denaturing agarose gel using formamide-containing loading dye and RNA ladder. Bands for ribosomal 18S (~1.9 kB) and 28S (~5 kB) RNA are marked by arrows. Around two µg total RNA per lane was loaded with exception of donor 7 (0.4 µg) due to less yield during preparation.

Prepared RNA was partially transcribed into single-stranded cDNA and utilized for PCR amplification of patient´s IgG repertoires employing combinations of degenerated primes as shown in **Table 14**. All combinations enabled the amplification of fragments corresponding to genes of the VH, VL-kappa, and VL-lambda subset. Examples of successfully amplified V genes for five of the amplified patient repertoires (donor 2, 3, 5, 6, and 10) are shown in **Figure 10**. High amplification efficacy was observed for most primer combinations during the first set of PCRs. Only for two VL combinations (kappa: P22+P28, lambda: P34+P43) a less efficient amplification was observed for some donor repertoires. By introducing of cloning restriction sites during the second rounds of amplifications, the yields of amplified gene products usually further increased also for combinations with less efficient gene amplification during the first PCRs.

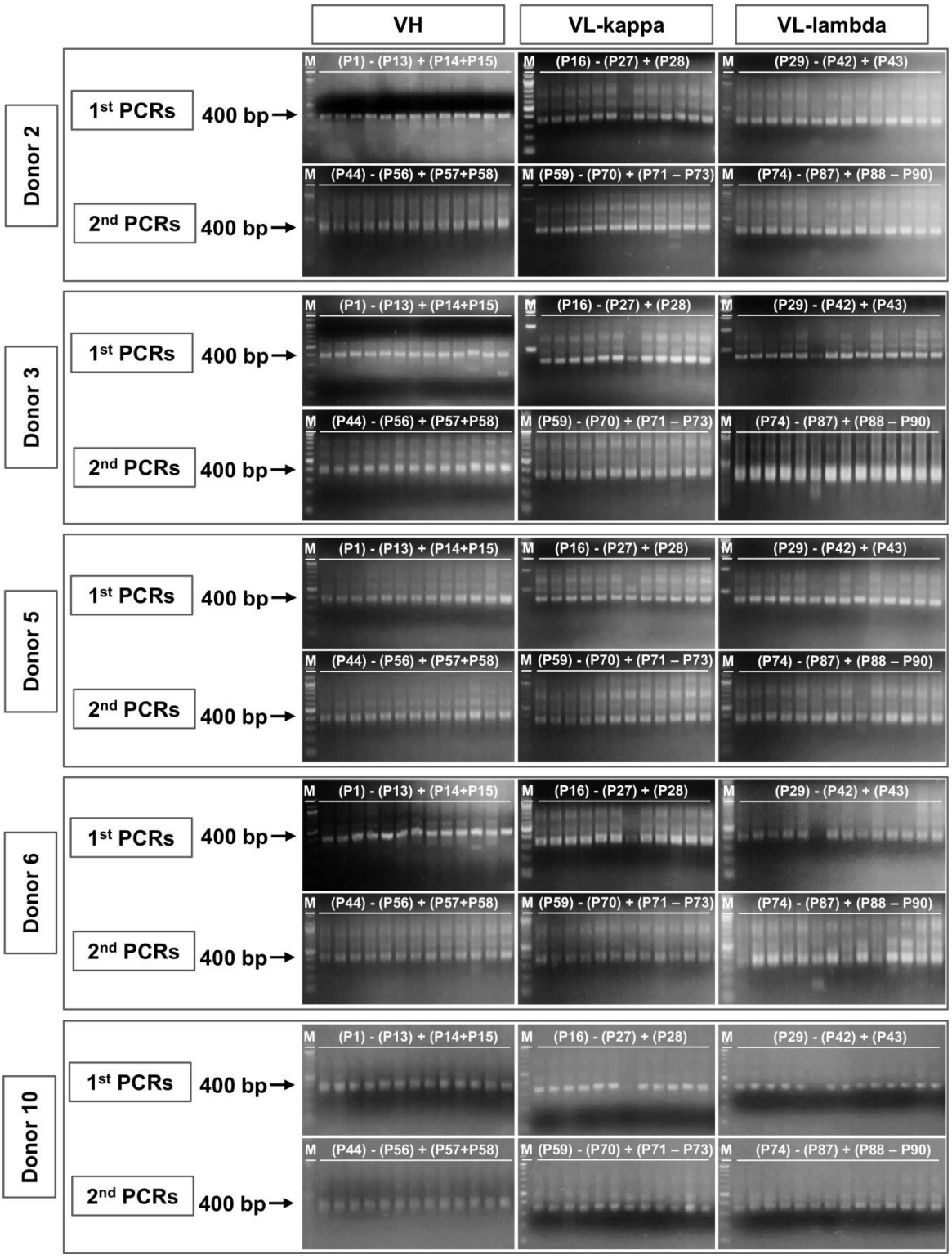

Figure 10. Amplification of antibody repertoires from LYNDAL donors. The IgG donor repertoires were amplified for the VH, VL-kappa, and VL-lambda subsets in a first round of independent PCRs followed by introduction of restriction sites during a second round of PCRs. Successful amplification was assessed by analyzing the products on agarose gels. Sizes of amplified V genes ranged between 350 and 400 bp. Amplified repertoires of five LYNDAL donors are shown. Used primer combinations are indicated. M, marker; P, primer.

After cloning individual VH repertoires, the corresponding vectors were efficiently transformed. The obtained complexities varied between $1.1x10^7$ and $9.7x10^8$ colonies per repertoire (mean = $3.5x10^8$) with only a small number of religations ranging from 0.2% to 8.5% (mean = 3.2%). By cloning both the kappa and lambda repertoires into vectors containing the corresponding VH donor repertoire, 40 final sublibraries were generated (20 VH/VL-kappa and 20 VH/VL-lambda repertoires, respectively). Sizes of all generated LYNDAL are listed in **Table 16**. Each sublibrary consisted, on average, of $1.1x10^8$ independent clones and $2.2x10^8$ for each donor repertoire. The final library collection comprises approximately $4.4x10^9$ clones containing 16.4% religations in total.

Table 16. Number of independent antibody clone within LYNDAL.

LYNDAL number	Patient number	Kappa library size ($x10^7$)	Lambda library size ($x10^7$)	Total size ($x10^7$)
1	485M	0.7	12.1	12.8
2	485N	4.4	2.0	6.4
3	485O	1.0	1.1	2.1
4	485Q	4.7	1.1	5.8
5	485S	1.1	2.9	4.0
6	485V	4.0	28.1	32.1
7	486C	2.7	2.6	5.3
8	486I	4.8	4.3	9.1
9	486J	8.6	16.6	25.2
10	513	16.3	5.2	21.5
11	515	9.6	15.7	25.3
12	487M	14.2	7.7	21.9
13	488H	3.9	13.1	17.0
14	488G	2.9	15.4	18.3
15	ARJ	7.3	4.2	11.5
16	518	29.3	2.6	31.9
17	488C	89.5	54.3	143.8
18	504	8.5	10.7	19.2
19	488A	3.9	3.9	7.8
20	552	4.5	11.3	15.8

Sublibrary sizes were determined by preparing serial dilutions from two random transformations and by extrapolating the number of grown colonies.

3.3 Characterization of libraries

Quality assessment of the library collection was performed on both gene and protein level since the successful antibody selection from phage display libraries depends on the expression of correctly folded antibody fragments on the phage surface. The percentage of clones encoding both variable domains as analyzed by colony PCR screening is summarized in **Table 17**. Of 1460 investigated colonies, on average, 67% (SD = ±12%) contained a complete scFv fragment with a similar proportion of kappa and lambda sublibraries with 71% and 65%, respectively.

Table 17. Presence of full-length scFv genes in LYNDAL determined by colony PCR.

LYNDAL number	Patient number	Kappa library (%)	Lambda library (%)	Total (%)
1	485M	55	70	63
2	485N	80	65	73
3	485O	70	53	58
4	485Q	33	70	45
5	485S	85	50	62
6	485V	55	28	41
7	486C	58	68	63
8	486I	60	75	68
9	486J	68	70	69
10	513	55	33	44
11	515	78	70	74
12	487M	83	68	75
13	488H	75	60	68
14	488G	63	68	65
15	ARJ	93	75	84
16	518	80	65	73
17	488C	85	65	75
18	504	83	88	85
19	488A	73	78	75
20	552	83	75	79

To evaluate the number of solubly expressed scFvs by *E. coli*, induced periplasmic preparations of randomly picked colonies from the LYNDAL collection were analyzed by both dot blot and immunoblot. As result, 82% (SD = ±16%) of 320 LYNDAL clones investigated by dot blot (**Figure 11A**) were expressed as antibody-pIII fusion proteins with comparable expression rates of kappa and lambda light chain sublibraries (80% and 83%, respectively) (**Table 18**). The proportion of detectable fusion proteins

for each sublibrary correlated well with that of full-length inserts as analyzed by the colony PCR screening (r = 0.75). Similar results were obtained in immunoblot analysis (**Figure 11B**). Expression of complete scFv-pIII fusion proteins were detected for 27 of 30 random chosen clones with positive dot blot signals. Taking together, around 73% of the LYNDAL members were successfully produced by *E. coli* as complete scFv-pIII fusion proteins. On the basis of these analyses, current LYNDAL collection is estimated to consist of 3.2×10^9 independent clones.

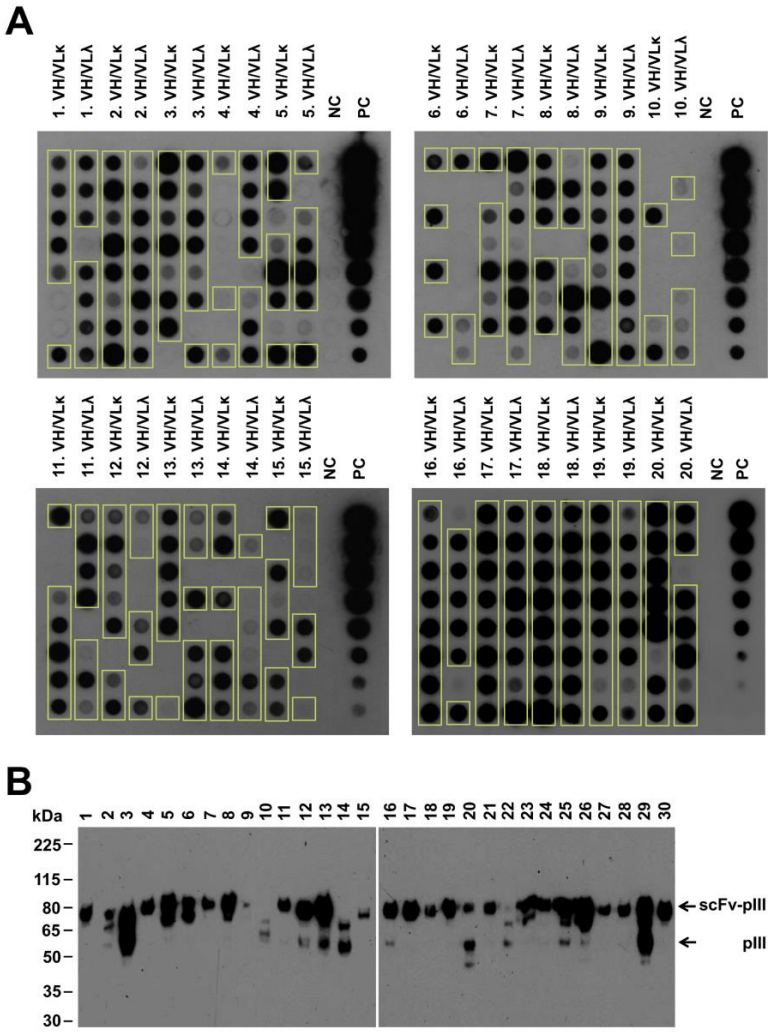

Figure 11. Expression analysis of antibody-pIII fusions within LYNDAL. Induced periplasmic fractions of randomly chosen colonies were analyzed by dot blot (**A**) and immunoblot (**B**). In dot blot screening using a myc tag-specific antibody peroxidase conjugate, 261 of 320 clones expressed detectable amounts of antibody-pIII fusion proteins (framed boxes). Growth medium served as negative control (NC) and a purified scFv as positive control (PC, 5 µg in 1:2 dilutions). Thirty clones with confirmed expression in dot blot were further analyzed in immunoblot using a pIII-specific monoclonal antibody for detection. All with exception of clones 10, 14, and 22 showed protein bands migrating at an apparent molecular weight of about 80 kDa corresponding to full-length scFv-pIII fusion proteins. Size of molecular marker is indicated.

Table 18. Producibility of antibody-pIII fusions in LYNDAL as determined by dot blot.

LYNDAL number	Patient number	Kappa library (%)	Lambda library (%)	Total (%)
1	485M	75	88	81
2	485N	100	100	100
3	485O	88	88	88
4	485Q	38	88	63
5	485S	75	75	75
6	485V	50	38	44
7	486C	75	100	88
8	486I	75	88	81
9	486J	100	100	100
10	513	38	63	50
11	515	75	88	81
12	487M	88	63	75
13	488H	75	75	75
14	488G	75	63	69
15	ARJ	75	75	75
16	518	100	75	88
17	488C	100	100	100
18	504	100	100	100
19	488A	100	100	100
20	552	100	88	94

The primer set used for LYNDAL cloning was designed for the PCR amplification of all known functional human antibody genes and families as annotated in the antibody sequence database VBASE. To assess the distribution and usage of germline genes and antibody families that were actually amplified by this primer set, 280 sequences of randomly picked LYNDAL colonies with confirmed scFv insert were analyzed. Noteworthy, investigated scFvs were derived from in total 90 out of the 117 VBASE listed functional antibody genes (**Figure 12**) including all 22 human antibody gene families (**Figure 13A**) and most VH (45 out of 51), VL-kappa (22 out of 35), and VL-lambda (23 out of 31) subsets (**Figure 13B**). The distribution pattern of analyzed functional sequences in LYNDAL was comparable to that of three large antibody databases (VBASE, VBASE2, and IMGT) being considered to reflect the natural distribution (**Figure 13C**). Apparent differences were observed for 4 families that occurred more frequently in either LYNDAL (i.e., VH6, Vκ4) or in the three databases (i.e., VH2, Vλ5).

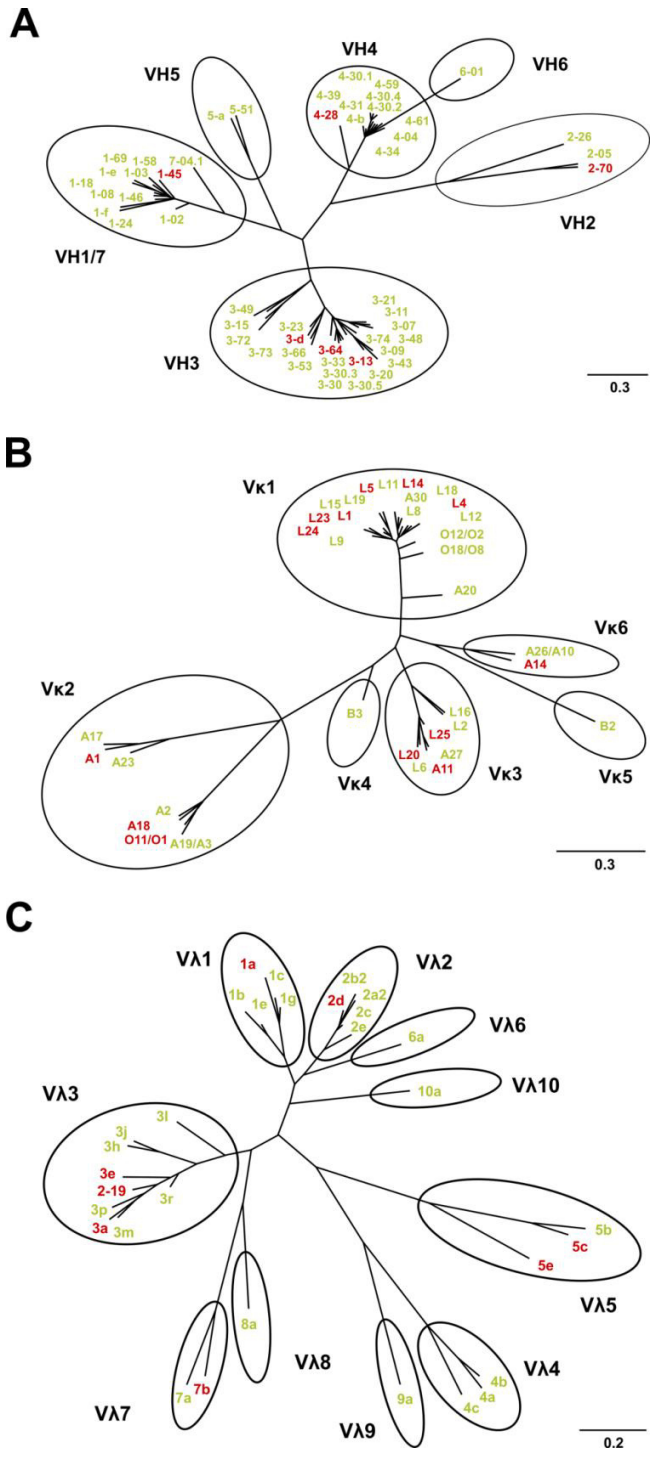

Figure 12. Phylogenetic analysis of LYNDAL sequences. Germline sequences of 280 randomly sequenced clones (142 VH/VL-kappa and 138 VH/VL-lambda) containing complete scFv genes were determined. Functional sequences from the VBASE database were used for drawing three unrooted phylogenetic trees for the VH (**A**), VL-kappa (**B**) and VL-lambda (**C**) subset employing the Phylogeny.fr web tool followed by grouping the sequences to the corresponding antibody families (black cycles). All functional sequences that were identified in the analyzed sample are marked green (77%), and non-represented germline sequences are labeled red. The nucleotide distance scales are indicated with a value of 20% distance for VL-lambda and of 30% distance for VH and VL-kappa, respectively.

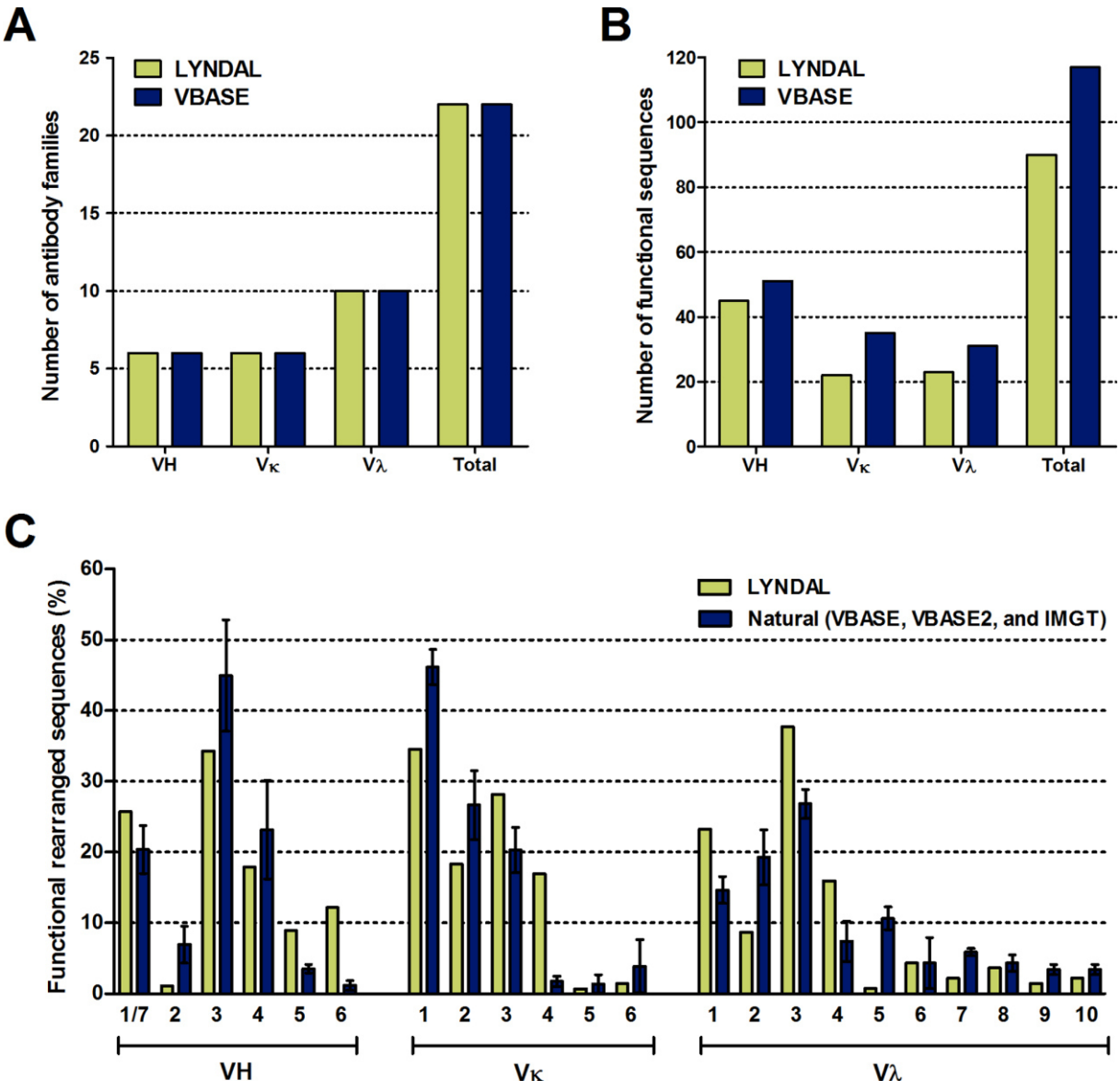

Figure 13. Usage of antibody germline sequences in LYNDAL. Sequences of 280 randomly chosen clones from all 40 sublibraries were determined. In the analyzed sample, all antibody families (**A**) and most functional VH (88%), VL-kappa (63%) and VL-lambda (74%) germline sequences (**B**) were identified when aligned to VBASE entries. Framework usage of native LYNDAL library was additionally compared to the distributions from three independent human antibody databases VBASE, VBASE2, and IMGT (**C**). Error bars of natural distribution are shown as standard deviations of mean values.

3.4 Selection of antiviral antibodies

To confirm the LYNDAL concept, it was assessed whether the pool of affinity-matured antibodies within the donor repertoires is directly accessible for antibody selection. As first target for antibody selection, envelope glycoprotein B of herpes simplex virus type 1 (gB-1) was chosen for panning because of the known high prevalence of HSV-1 of 83% in the German population [214]. To exclusively use HSV-experienced B cell repertoires for selecting gB-specific scFvs from LYNDAL, only donor libraries with high IgG titer against gB-1 were included. Therefore, serum samples from 17 LYNDAL donors were screened for reactivity to recombinant gB-1 by ELISA. Fourteen donor samples showed comparable absorbance signals to the HSV-infected control individuals, i.e., 82% of the investigated LYNDAL donors were tested positive for HSV antibodies (**Figure 14**).

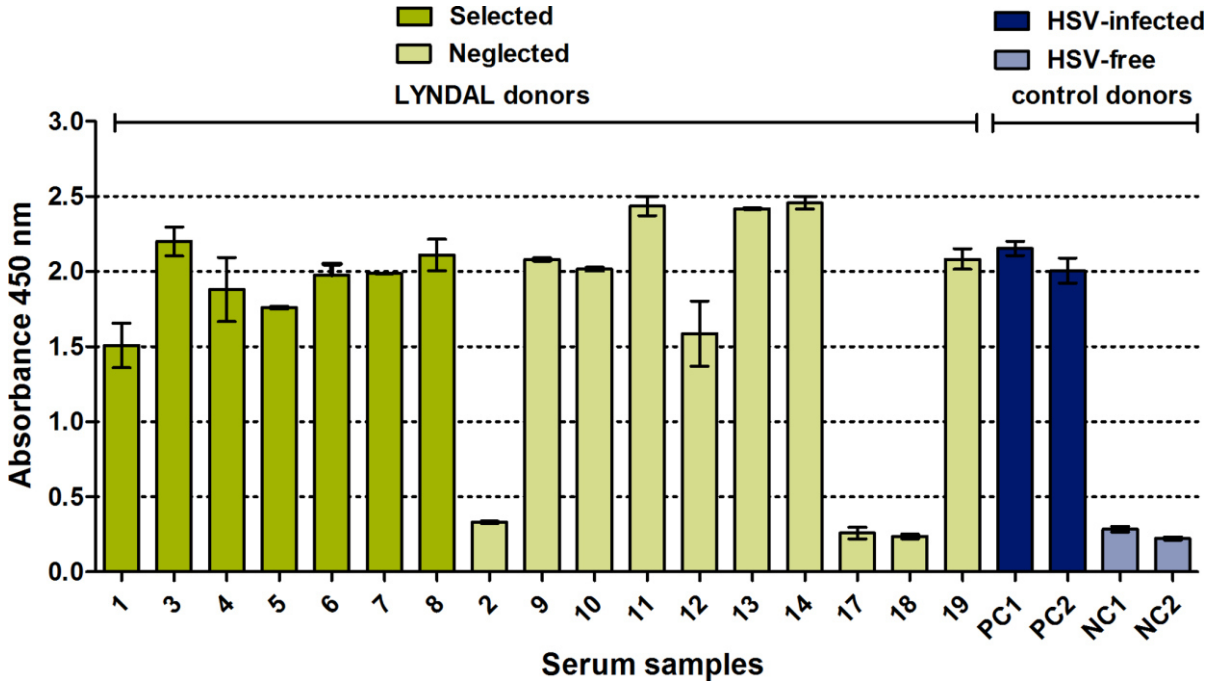

Figure 14. Serum-screening against target gB-1. To identify donors who have been encountered herpes simplex virus, sera from LNYDAL donors and from control individuals with known HSV infection status were screened by ELISA. Recombinant gB-1 was coated with 1 µg/ml and incubated with sera that had been diluted 1:100 in MPBS. HSV-specific IgG response was detected by using a peroxidase-conjugated antibody specifically recognizing human IgG Fc. Herpes infection status of LYNDAL donors was assessed by comparison of responses with those of HSV-infected individuals (dark blue) and healthy controls (bright blue), respectively. Bars of LYNDAL donors who were chosen for later antibody selection are marked in dark green whereas all bars from neglected donors are colored in bright green. Error bars represent the standard deviations of the mean.

LYNDAL from seven donors with high HSV-specific IgG titers were combined for antibody selection (donors 1, 3-8). Total size of the respective libraries was $7.1x10^8$ members. Specific binders against recombinant gB-1 were successfully enriched during three rounds of panning as evident from both the calculated enrichment factors (**Table 19**) and the corresponding ppELISA profile (**Figure 15A**). ELISA screening with monoclonal phages deriving from round 2 and 3 revealed increases of gB-specific scFv phage antibodies of 21% (20 out of 96; **Figure 15B**) and 34% (33 out of 96; **Figure 15C**), respectively. The subsequent fingerprint analysis of clones with confirmed scFv genes (**Figure 16**) lead to the identification of 34 individual binders out of 192 screened colonies, i.e., every 6th screened colony (17.7%) encoded for a gB-specific scFv with unique gene sequence.

Table 19. Enrichment factors.

Round	Used gB-1 concentration (µg/ml)	Input (t.u.)	Output (t.u.)	Ratio (out/in)	Enrichment (ratio n/ratio n-1)
1	20	$2.0x10^{13}$	$4.5x10^5$	$3.4x10^7$	NC
2	5	$2.1x10^{13}$	$2.3x10^7$	$1.7x10^5$	49
3	5	$3.2x10^{13}$	$3.2x10^8$	$1.5x10^4$	9

Phage numbers were calculated from selection plate-counted bacterial colonies before (input) and after (output) the single selection rounds as transducing units (t.u.) and used for the calculation of enrichment factors. NC, not calculable.

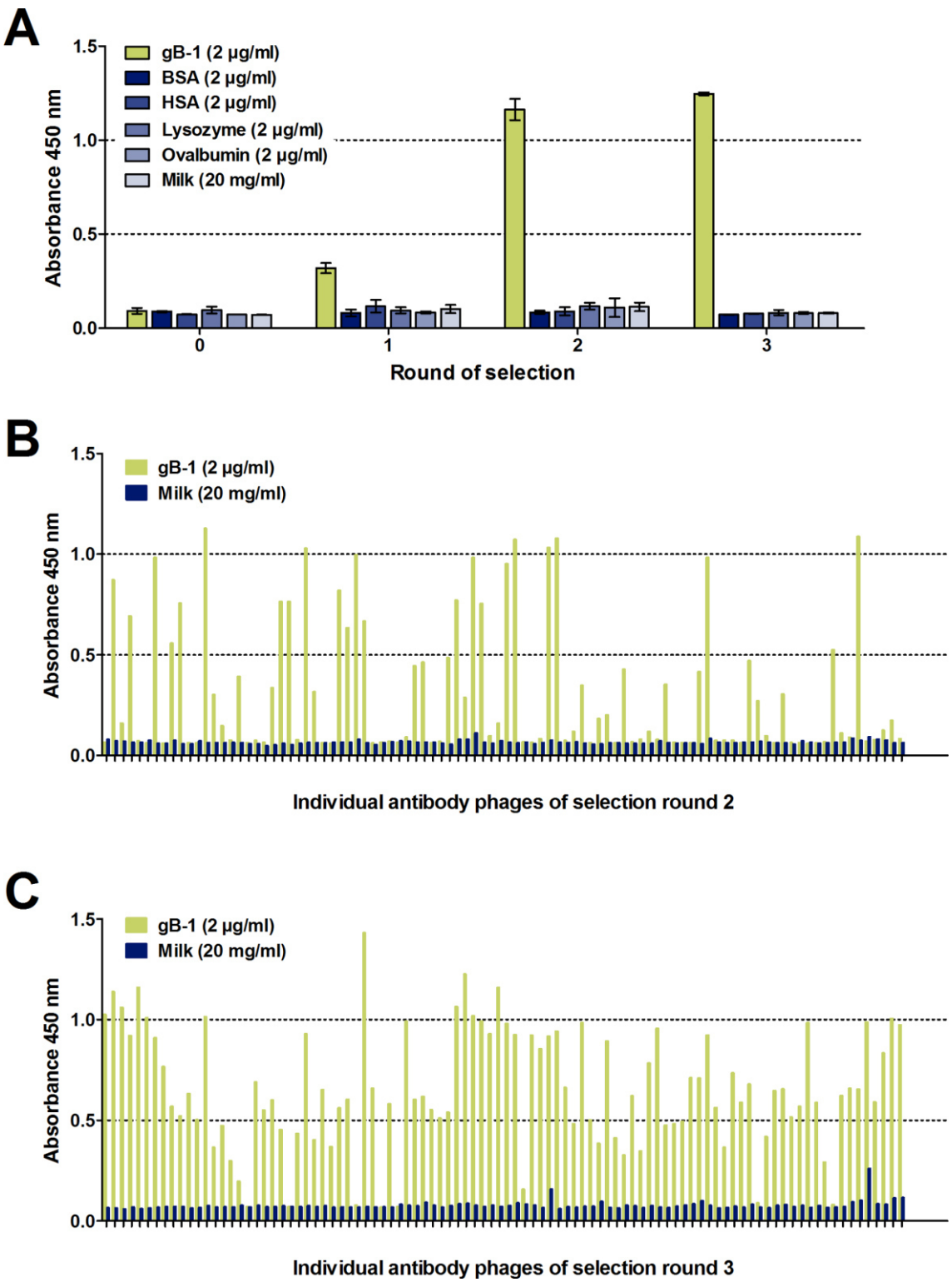

Figure 15. Enrichment of gB-specific LYNDAL antibodies. LYNDAL of seven donors with high anti-HSV titers were combined for panning against target gB-1. The enrichment of target-specific scFv phage antibodies during selection rounds 1 to 3 was confirmed in polyclonal phage ELISA (**A**) by binding rescued phages to target protein gB-1 or control antigens. The error bars represent standard deviations of duplicates. Screening of individual clones by monoclonal phage ELISA revealed an increase of specific binders between round 2 (**B**) and 3 (**C**). Phage antibodies were detected using an anti-phage peroxidase conjugate in combination with colorimetric substrate TMB.

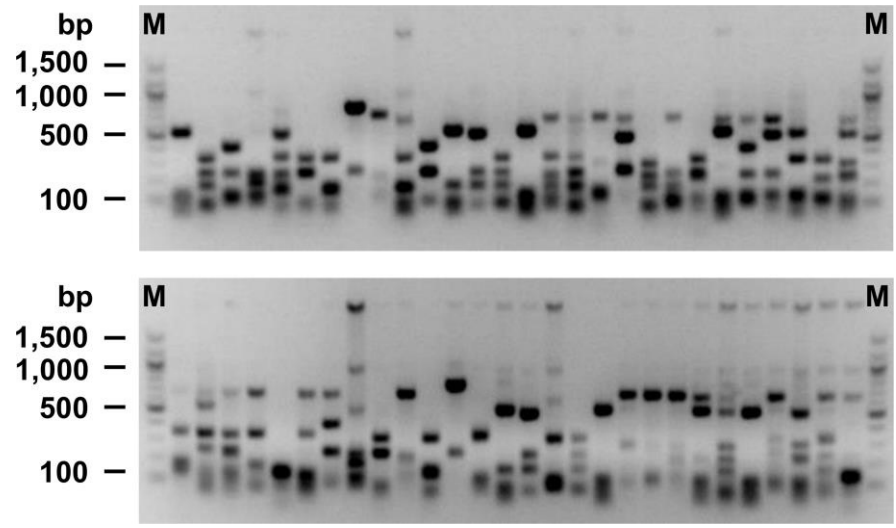

Figure 16. Fingerprint analysis. To identify unique gB-specific binders, individual clones with confirmed scFv gene and strong target-specific binding in mpELISA were PCR-amplified and digested with multicutting restriction enzyme BstNI. Sixty-four percent of the analyzed clones exhibited an individual banding pattern after separation on agarose gel. Bp, base pairs; M, marker.

Analysis of the variable genes revealed that the enriched gB-specific scFvs were derived from various germline genes (18 out of 117) and antibody families (9 out of 22) showing an exclusive usage of the VH1 or VH3 gene families and a preference for lambda light chains (**Figure 17**). Two selected clones possessed lambda light chains from germline sequences 5c and 5e that were not found in the investigated sample of unselected clones (**Figure 12C**). Analyzing the respective VH/VL parings, 22 out of 34 scFvs possessed a recurring combination, and some of the scFvs were likely derived from clonally related B cells. To further investigate the level of antigen-driven affinity maturation of the enriched gB-specific scFvs, the number of somatic hypermutations was determined for both the nucleotide (**Figure 18A**) and the amino acid sequences (**Figure 18B**). On average, the VH domains carried more amino acid exchange mutations than the VL domains (17.4 versus 8.6) with a calculated exchange mutation frequency of 18% and 9% for the VH and VL domains, respectively. Considering the number of nucleotide mutations (VH: 32.5, VL: 14.8), however, the frequency for non-silent mutations was comparable for both variable genes (VH: 54%, VL: 58%). When excluding CDR3 and FR4 regions for analysis, these mutations were predominantly accumulated within the CDRs (25%) and to a lower extent within the framework regions (11%) with the highest mutation frequency for the CDRH2 and CDRH1 followed by CDRL2 and CDRL1 (**Figure 18C**).

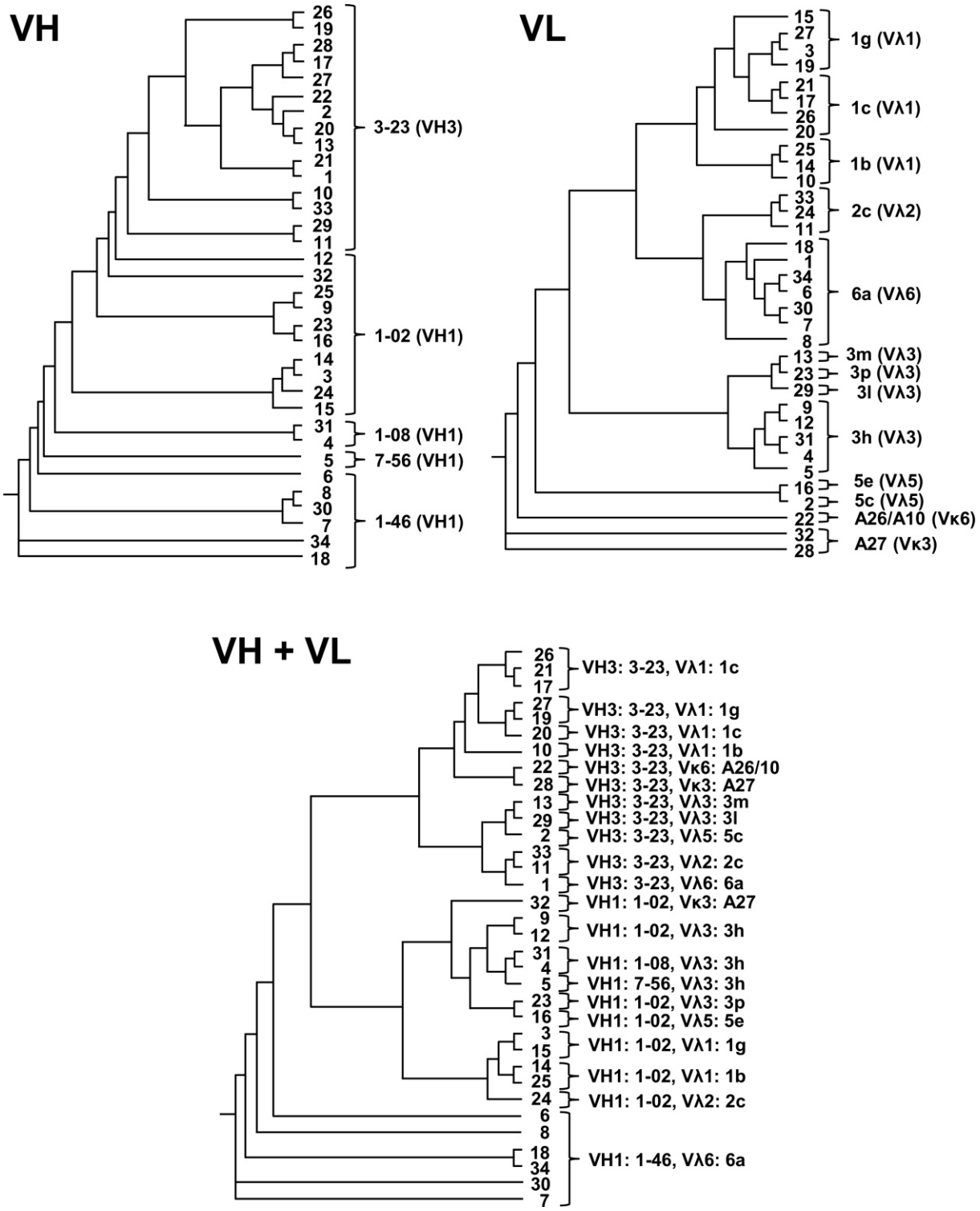

Figure 17. Sequence analysis of gB-specific LYNDAL scFvs. Germline sequences of the 34 enriched scFvs were determined and phylogenic relationships analyzed by drawing phenograms employing the Phylogenic.fr web tool. The germline sequences as well as corresponding antibody families are shown for each clone.

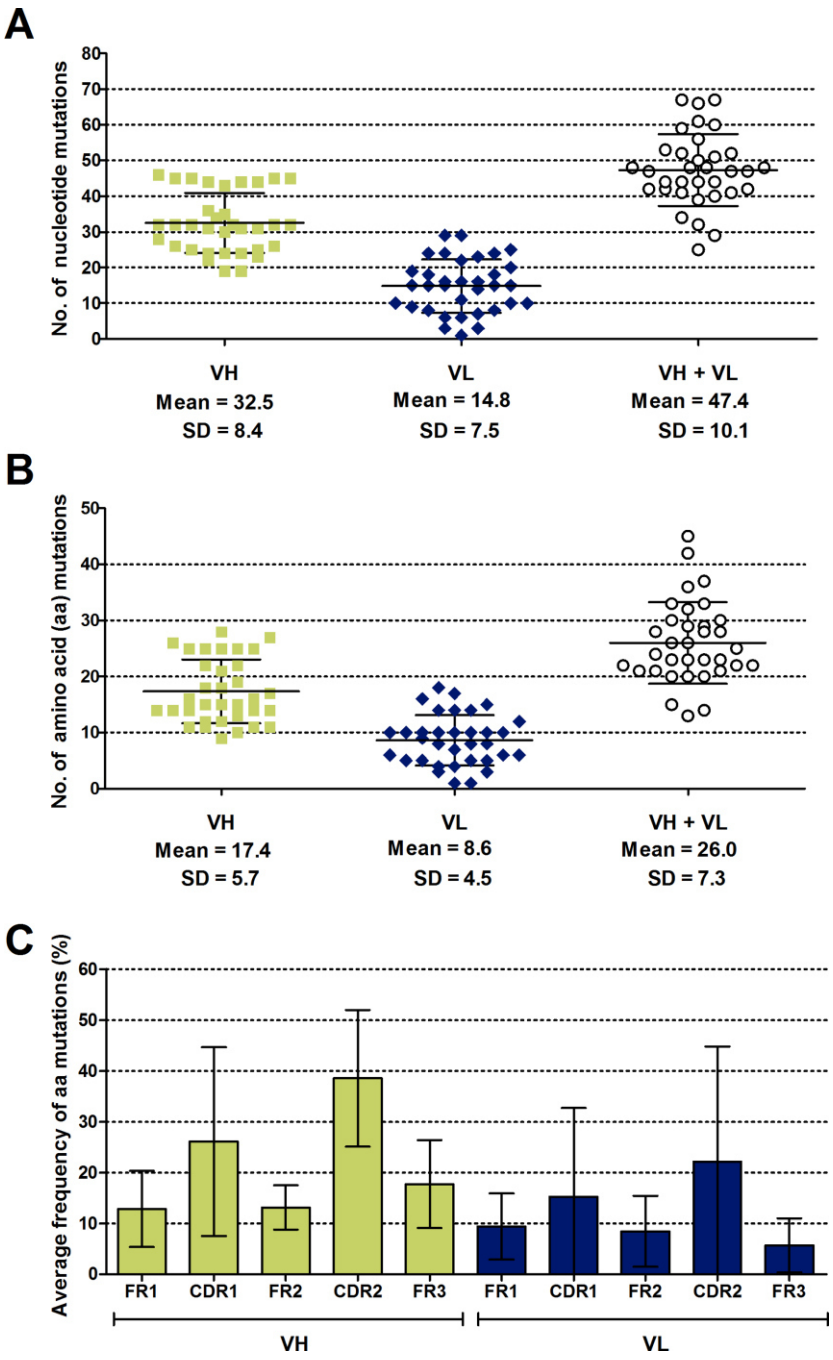

Figure 18. Analysis of somatic mutations within enriched gB-specific LYNDAL scFvs. Variable genes of the enriched 34 scFvs were aligned to the closest respective germline sequences and the number of nucleotide (**A**) and amino acid (**B**) mutations was determined. Mean values and corresponding standard deviations are shown for the VH (green squares), VL (blue diamonds), and combined VH/VL genes (black circles). The distribution of amino acid exchange mutations was analyzed separately for the VH (green) and VL (blue) domains (**C**). Mutation numbers of framework region (FR) 1-3 and complementarity determining region (CDR) 1+2 were determined and normalized to the length of each corresponding region. Results are presented as mean mutation frequency, i.e., the average probability of observing an amino acid mutation within the investigated segment when compared with its corresponding germline sequence. Error bars represent standard deviations of mean values.

For further analyses, scFv genes of specific binders were subcloned as SfiI/NotI fragments into the bacterial expression vector pAB1 containing C-terminal myc and hexahistidine tags for detection and purification purposes (**Figure 19**). ScFvs were solubly expressed in the periplasm of TG1 *E. coli* and purified from periplasmic extracts by IMAC. Coomassie-stained SDS-PAGE and immunoblot showed a high purity (>95%) for all specific detectable scFvs (**Figure 20**). The yield of IMAC purified scFvs varied from 0.4 to 4.3 mg/l of bacterial culture depending on the respective fragment (**Figure 21**). The vast majority of the investigated scFv antibody fragments showed mainly monomeric profiles after its separation by size exclusion chromatography (18 out of 24, i.e., 75%) and only a few associated further into higher molecular dimers, trimers, and aggregates (**Figure 22**).

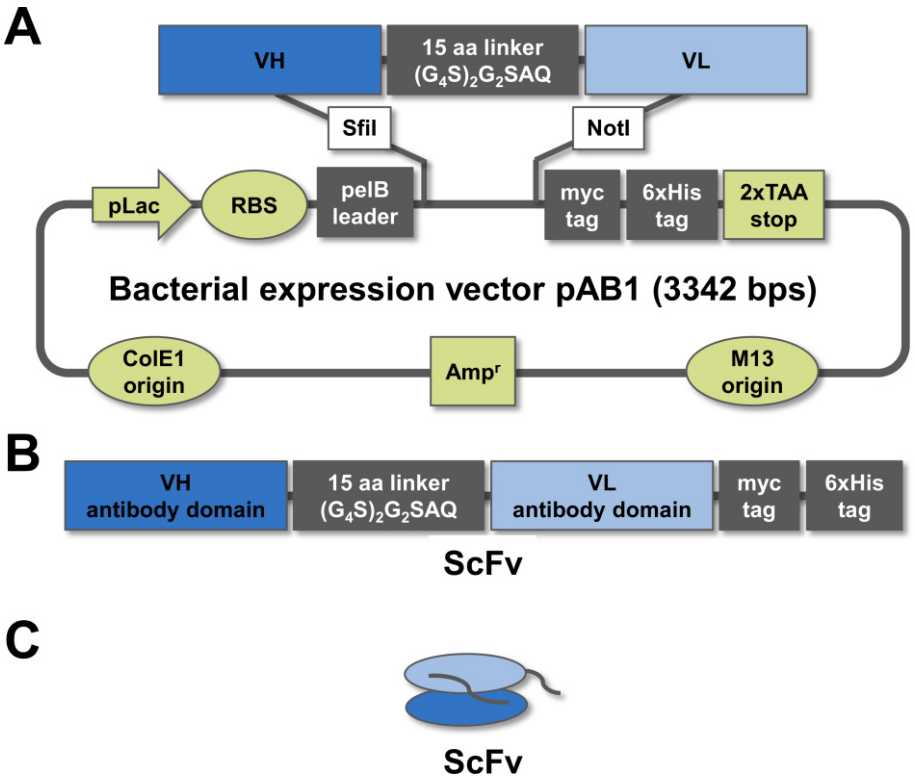

Figure 19. Maps of expression vector pAB1 and derived proteins. Target-enriched scFv genes were reamplified and subcloned into bacterial expression vector pAB1 as SfiI/NotI fragments (**A**). After induction of the lac promoter, translated proteins (**B**) are directed by the pelB leader sequence into the bacterial periplasm and folded to soluble scFv antibody fragments (**C**).

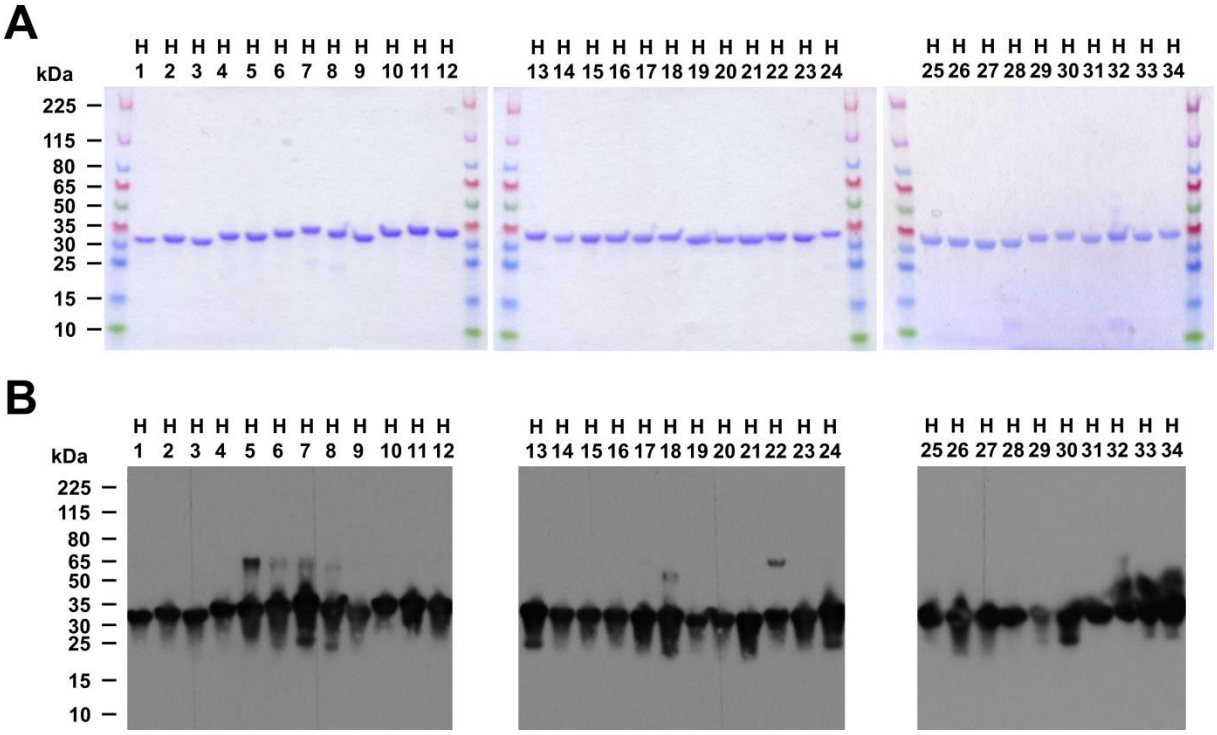

Figure 20. Characterization of gB-specific LYNDAL scFvs. All 34 gB-specific scFvs were expressed as soluble proteins in the periplasm of bacteria and purified by IMAC. Purity of scFvs (2 µg/lane) was assessed by Coomassie stained 12% SDS-PAGE (**A**). The integrity of corresponding products was confirmed by immunoblot loading 1 µg/lane of reduced scFv. Detection was performed with primary myc tag-specific antibody followed by secondary peroxidase conjugate (**B**).

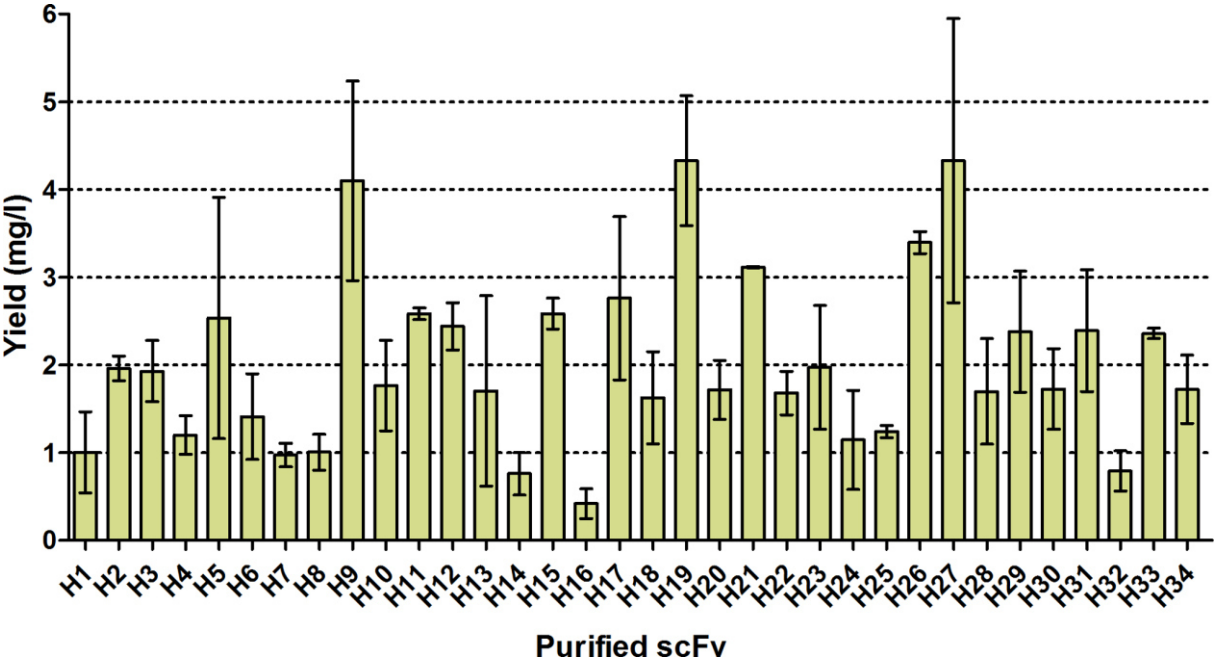

Figure 21. Expression yields of gB-specific LYNDAL scFvs. Antibody fragments were produced periplasmatically in bacteria, IMAC-purified, and sterile-filtered. Yields are given as mg protein per liter bacteria culture. Error bars represent the standard deviations of at least two independent productions.

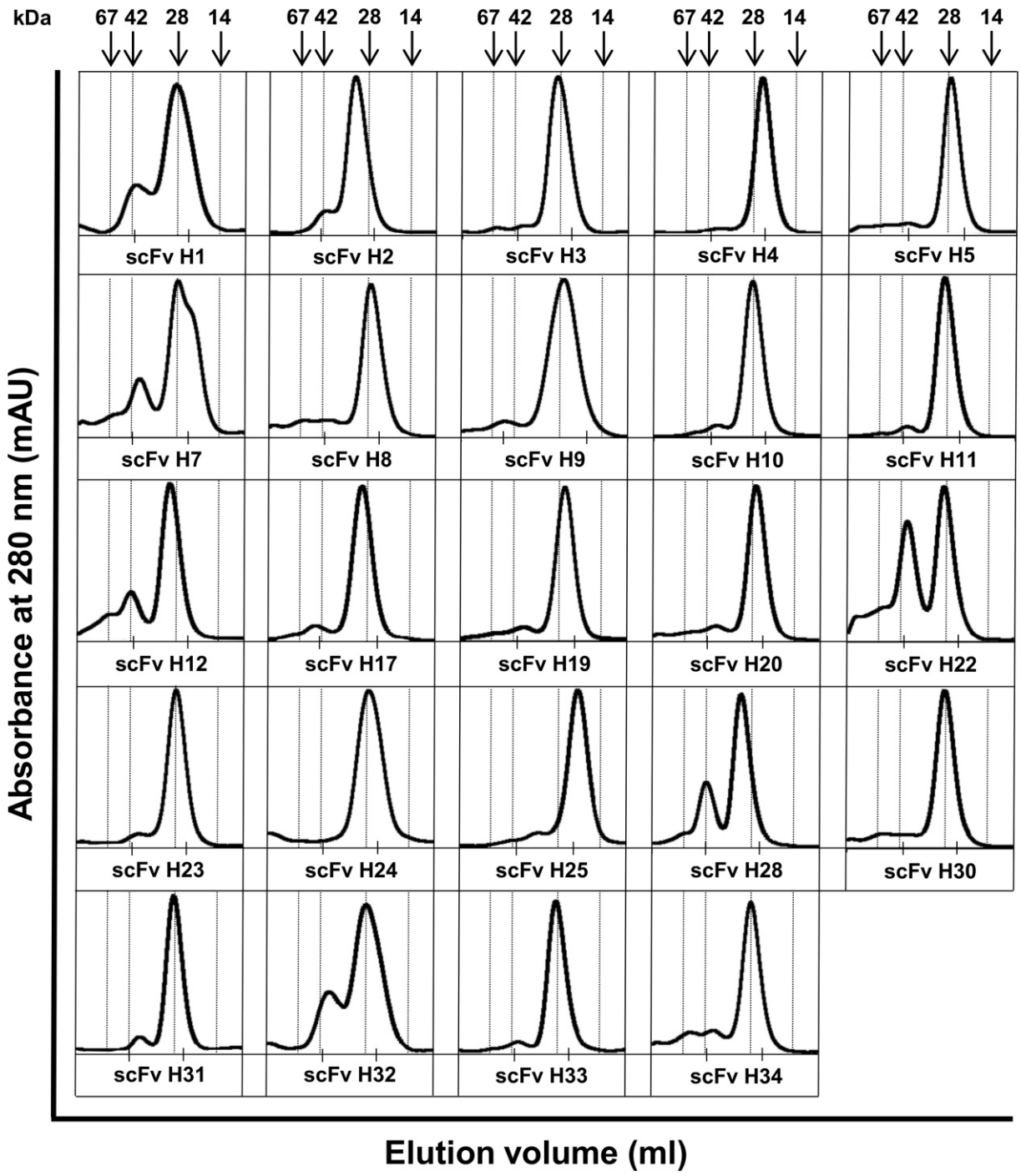

Figure 22. FPLC profiles of gB-specific LYNDAL scFvs. Antibody fragments were purified from periplasmic extracts by IMAC and separated on SEC column Superdex 75 10/300 GL. The x-axes show the elution volumes ranging from 8-14 ml and being segmented in 2 ml increments. All analyzed fragments exhibited a main peak corresponding to monomeric scFvs. Some fragments eluted with additional peaks indicating dimeric and higher oligomeric fractions. Arrows indicate molecular weights of the used calibration reference proteins BSA (67 kDa, 9.07 ml), ovalbumin (42 kDa, 9.86 ml), control scFv (28 kDa, 11.50 ml), and RNase A (14 kDa, 12.98 ml).

To analyze the specificity of enriched scFvs, flow cytomertry was performed using Vero cells that had been infected with either HSV-1 or HSV-2 in comparison with non-infected cells. As illustrated in **Figure 23**, all scFvs bound specifically to membrane-associated gB of both members of the herpes simplex virus family while no binding was found on uninfected Vero cells. Although LYNDAL was panned against the recombinant ectodomain of gB-1, the observed cross-reactivity of the enriched scFvs to HSV-2-derived gB is likely since both viral proteins share an overall amino acid homology of more than 87% (767 out of 882 aa). The received fluorescence intensities tended to be stronger on the HSV-2-infected cells probably due to their higher viral genome copy number compared to that of HSV-1-infected cells [144]. Nine out of 34 scFvs showed greater reactivity toward HSV-1- than to HSV-2-infected cells that may indicate recognition of non-shared epitopes. The six scFvs with the highest relative HSV-1-specific signals (H6, H7, H8, H18, H30, H34) seemed all to be clonally related since they possessed the same VH/VL germline combination (VH1: 1-46, Vλ6: 6a) with an overall amino acid homology of 89% (210 out of 235 aa) and a high similarity within the VH domains (121 out of 125 aa, i.e, 97%).

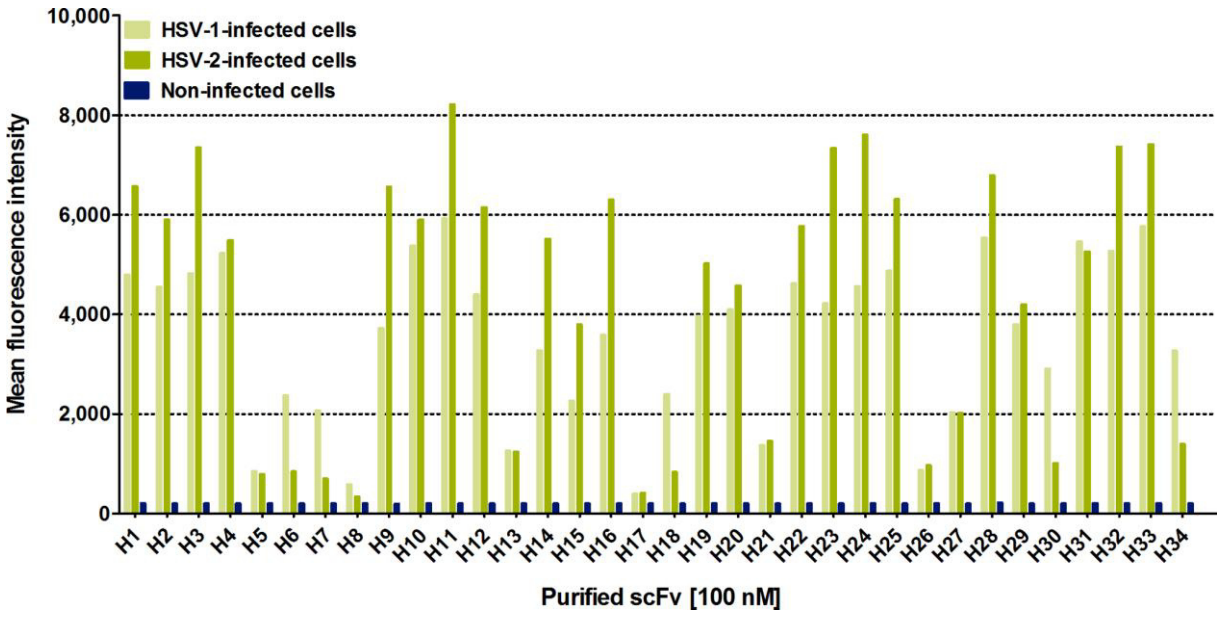

Figure 23. Binding analysis of gB-specific LYNDAL scFvs. Specificity of scFvs for binding to glycoprotein B of HSV-1- and HSV-2-infected Vero cells was assessed by flow cytometry compared to uninfected cells. Infection of Vero cells with HSV results in transfer of glycoprotein B to the host cell membrane thus allowing the detection by specific antibodies. Bound fragments were detected with myc-specific mouse antibody followed by anti-mouse FITC conjugate.

To assess the binding activities of the antiviral antibodies to the target antigen in its natural context, affinity measurements by flow cytometry of twelve randomly chosen scFvs monomers were performed on HSV-1-infected cells. Due to additional dimer formation in the FPLC elution profiles (**Figure 22**), monomeric fractions of two scFv preparations (H22 and H28) were first SEC-separated to guarantee the determination of the equilibrium constant of the monovalent binding. Equilibrium binding curves could be measured for all investigated scFv monomers (**Figure 24**). With exception of one, all investigated scFvs bound the target antigen with equilibrium constants in the nanomolar range reaching an EC_{50} of 3 nM for the most affine scFv (**Table 20**). Subsequent affinity measurements by surface plasmon resonance (SPR) employing recombinant gB-1 confirmed the tight binding (r = 0.90) of analyzed scFv (**Table 20**, **Figure 25**).

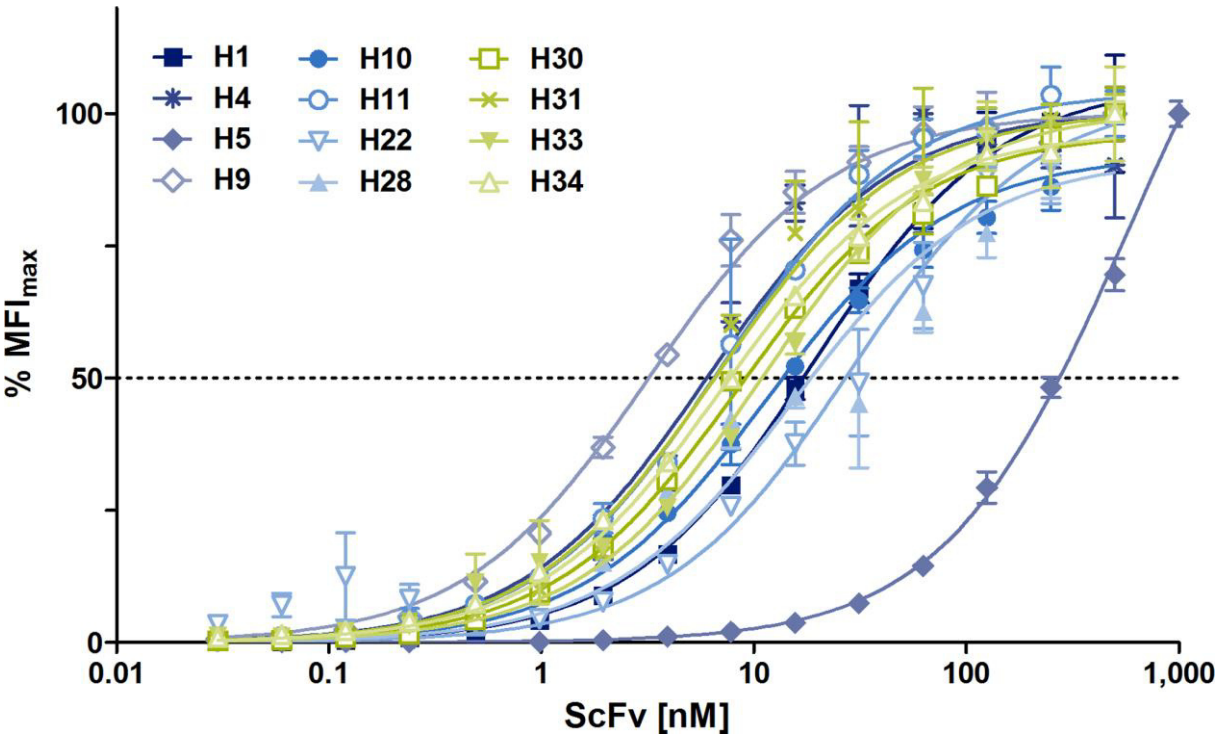

Figure 24. Equilibrium-binding curves for gB-specific scFvs. Binding activities of LYNDAL-selected antibodies to membrane-associated gB was measured by flow cytometry. Monomeric scFvs were titrated in triplicate on HSV-1-infected Vero cells and binding detected using a myc-specific mouse IgG followed by mouse-specific FITC conjugate. Averaged median fluorescence intensities were used for calculating nonlinear-fitted curves based on equation for one site binding. Error bars represent the standard deviations of the mean. MFI_{max}, maximum median fluorescence intensity.

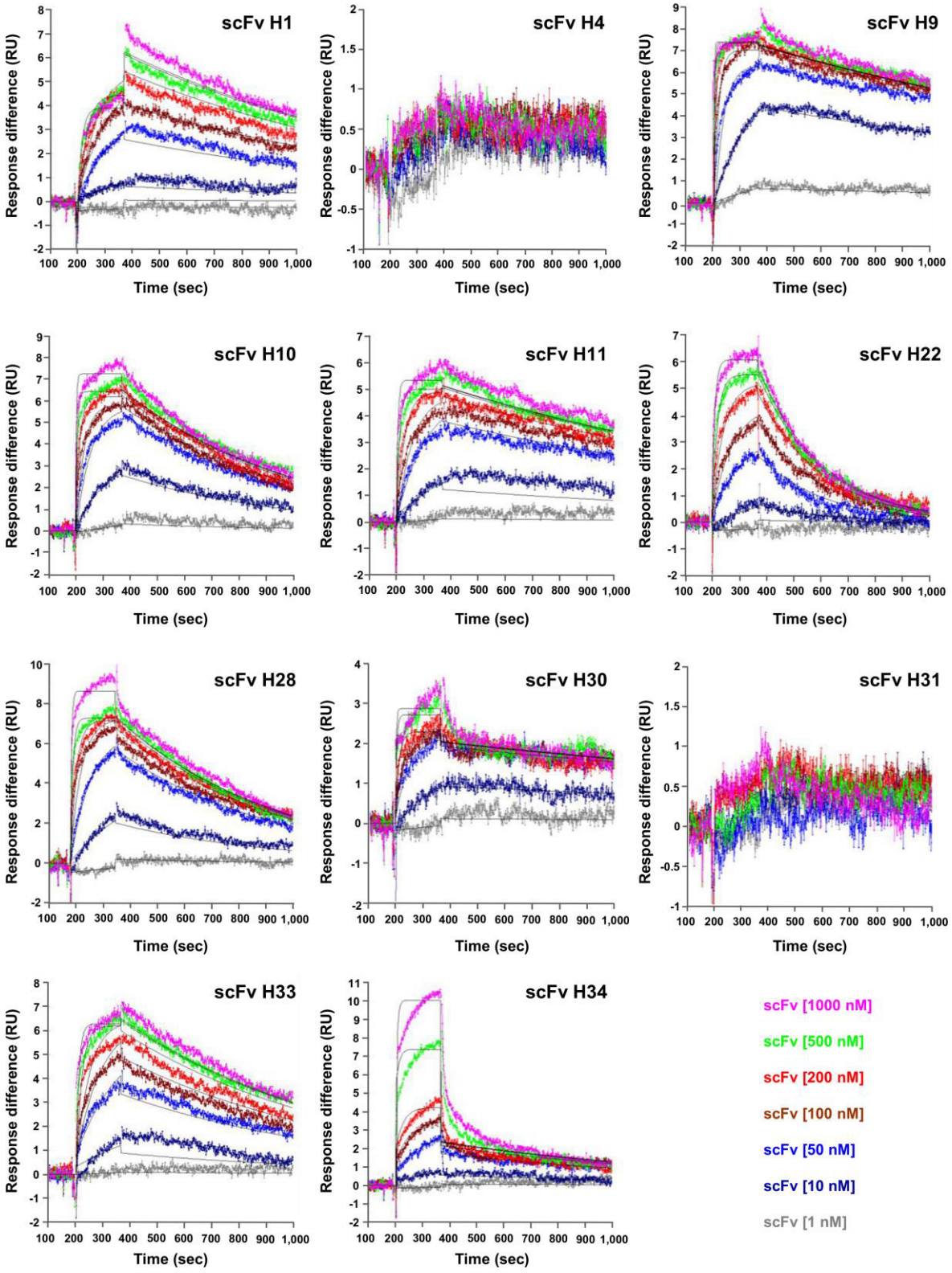

Figure 25. Binding properties of monomeric scFvs determined by SPR. Representative sensograms show the overlays of serial dilutions of monomeric scFvs injected over gB-1-coupled sensor chip. The y-axes of the sensograms exhibit the response differences after subtracting the background signals from gB-1 binding. The response differences were expressed as response units (RU). Biosensor data were fitted to a 1:1 Langmuir model (black curves) with exception of clone 4 and 31 due to less maximal response difference.

Table 20. Affinities of monomeric gB-specific scFvs.

ScFv	Flow cytometry[a]	Surface plasmon resonance[b]		
	EC_{50} ±SE [nM]	k_{on} ±SD [10^5 $M^{-1}s^{-1}$]	k_{off} ±SD [10^{-4} s^{-1}]	K_D ±SD [nM]
H1	19.1 ±1.0	0.73 ±0.07	8.67 ±0.36	12.0 ±1.6
H4	6.1 ±0.6	NC	NC	NC
H5	587.0 ±25.7	ND	ND	ND
H9	3.2 ±0.2	7.45 ±2.05	4.83 ±0.35	0.7 ±0.2
H10	11.6 ±0.8	3.58 ±0.26	15.30 ±0.28	4.3 ±0.4
H11	7.0 ±0.5	1.62 ±0.15	6.43 ±0.01	4.0 ±0.4
H22	28.9 ±3.2	0.95 ±0.01	40.45 ±2.33	42.6 ±2.3
H28	15.5 ±2.3	2.22 ±0.08	16.90 ±0.28	7.6 ±0.2
H30	8.5 ±0.4	4.27 ±0.59	3.95 ±0.43	0.9 ±0.1
H31	6.6 ±0.7	NC	NC	NC
H33	11.1 ±0.8	1.03 ±0.07	12.25 ±0.07	12.0 ±0.6
H34	7.2 ±0.3	2.41 ±0.95	8.82 ±1.24	4.1 ±2.1

[a]Binding affinities of SEC-purified scFvs to cell membrane-associated gB-1 were calculated from the equilibrium-binding curves as measured by flow cytometry. EC_{50}, half maximal effective concentration; SE, standard error. [b]Association and dissociation rate constants of monomeric scFvs were determined by SPR using amine coupled gB-1 as ligand. Affinity constant were calculated as $K_D = k_{off}/k_{on}$. Constants and errors were averaged from two independent determinations. SD, standard deviation; NC, not calculated; ND, not determined.

To evaluate whether the enriched antibodies can mediate therapeutically relevant antiviral activity, all gB-specific scFvs were tested for their capability to prevent HSV-infection *in vitro* using standard plaque neutralization assay. As illustrated in **Figure 26**, eight scFv showed detectable HSV-1 neutralizing activity (>10%) when concentration was kept constantly at 2 µM. Since the valency of gB-specific antibodies can strongly influence their HSV neutralizing capacity [144], scFvs were additionally cross-linked using an anti-myc tag-specific IgG in 2.5-fold molar excess. Several cross-linked scFvs revealed an increased neutralizing capacity (**Figure 26**). Highest antiviral potential after cross-linking was observed H4 and H31 which were derived from the same B cell clone sharing an overall amino acid homology of more than 99% (227 out of 228 aa). In contrast, high antiviral potency of scFv H28 completely vanished after cross-linking that may likely be caused by diminished accessibility of the larger antibody complex to its viral epitope. Since this clone showed formation of a monomeric scFv and a non-covalently linked $(scFv)_2$ fraction in the SEC profile (**Figure 22**), both antibody fractions were further characterized for their contribution to observed antiviral effect. Monovalent binding of scFv H28 to

membrane-associated gB of infected cells resulted in apparent equilibrium constants of 15.5 nM (±2.3) for HSV-1 and 14.8 nM (±0.8) for HSV-2, respectively (**Figure 27**). The $(scFv)_2$ dimer showed an increased avidity with equilibrium binding constants of 7.3 nM (±0.5) for HSV-1 and 6.8 nM (±0.4) for HSV-2, respectively. The comparable binding activities of the scFv and the $(scFv)_2$ for both HSV-1- and HSV-2-infected cells indicate that clone H28 may recognize a type common gB epitope. Driven by higher avidity, the dimeric $(scFv)_2$ indeed neutralized both serotypes significantly better than the monomeric scFv (**Figure 28**). Measurement of concentrations being needed for neutralization of 50% of the viruses ($PRNT_{50}$) revealed that both the monomeric scFv and the dimeric $(scFv)_2$ neutralized HSV-2 with a 14-fold and 7-fold increased efficacy than HSV-1. Noteworthy, the efficacy of antibody H28 as dimeric $(scFv)_2$ for neutralizing HSV-2 was even more favorable compared to that of a humanized mAb which is currently being developed for clinical applications in acyclovir-resistant disease [152].

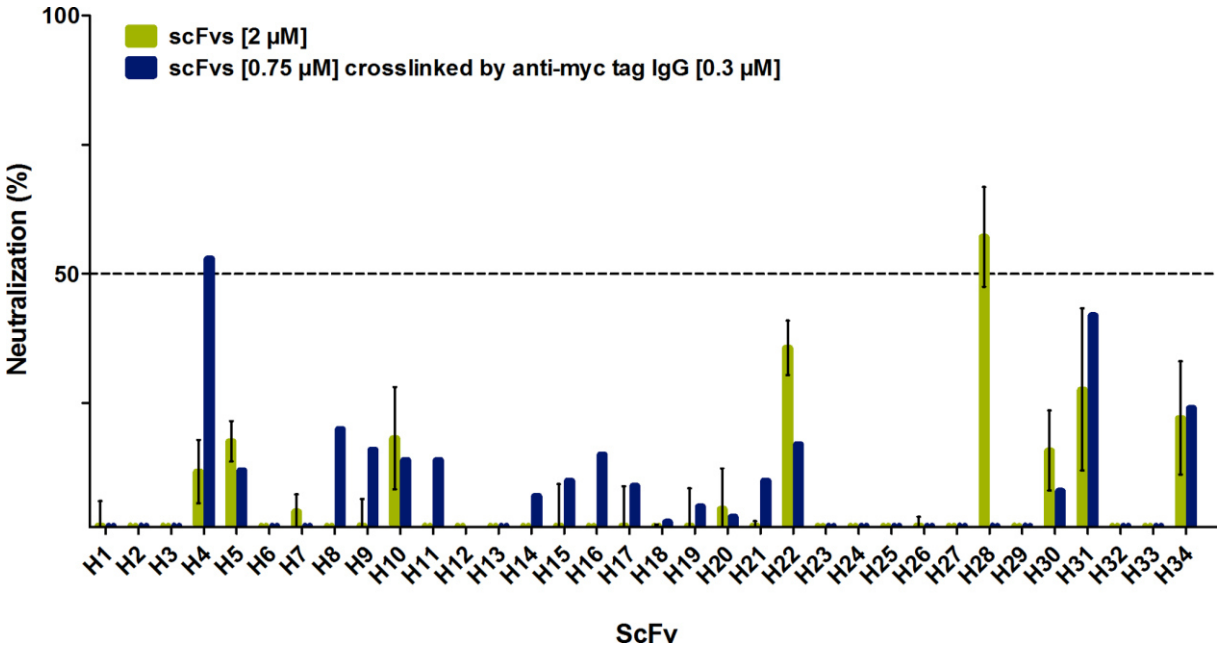

Figure 26. Capacity of gB-specific scFvs to neutralize HSV infections *in vitro*. Efficacy to neutralize infections of Vero cells with HSV strain 1F by LYNDAL-enriched antibodies was evaluated by plaque reduction neutralization test. IMAC-purified scFvs were tested with constant concentration of 2 µM (green). Data were averaged from four independent experiments showing error bars as standard error of the mean. To evaluate the neutralization capacity as bivalent constructs, the scFvs were additionally cross-linked with 2.5 molar excess of a myc tag-specific antibody (blue).

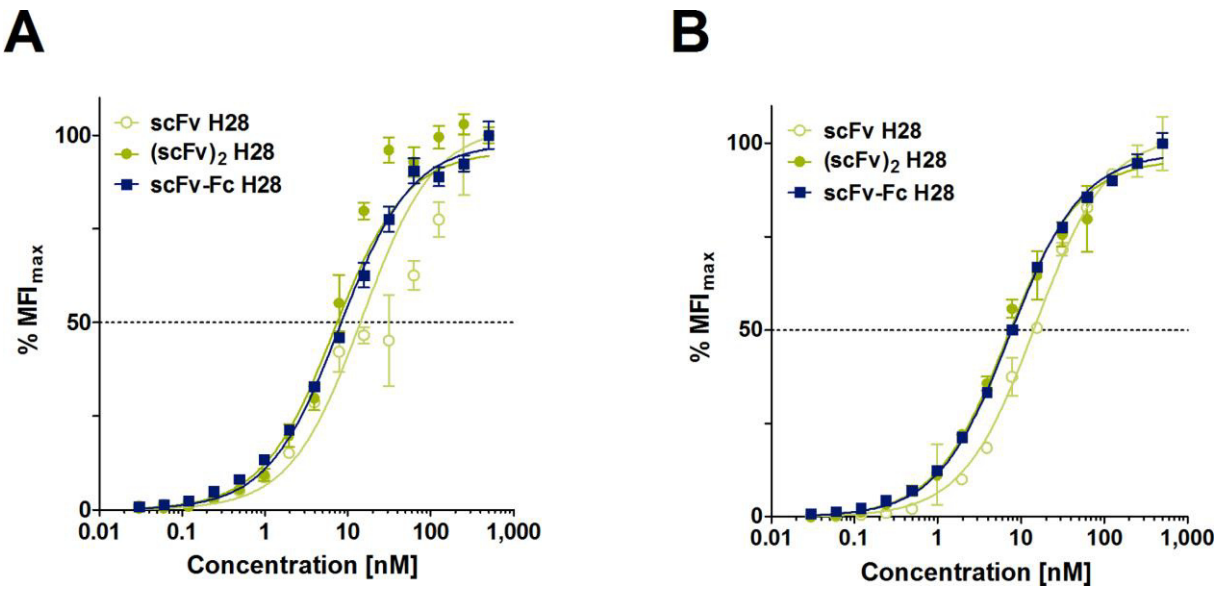

Figure 27. Equilibrium-binding curves for antibody H28. In flow cytomerty, binding activities of monovalent scFv, bivalent $(scFv)_2$, and bivalent scFv-Fc were determined on either (**A**) HSV-1- or (**B**) HSV-2-infected Vero cells. Error bars represent standard deviations of the mean values. MFI_{max}, maximum median fluorescence intensity.

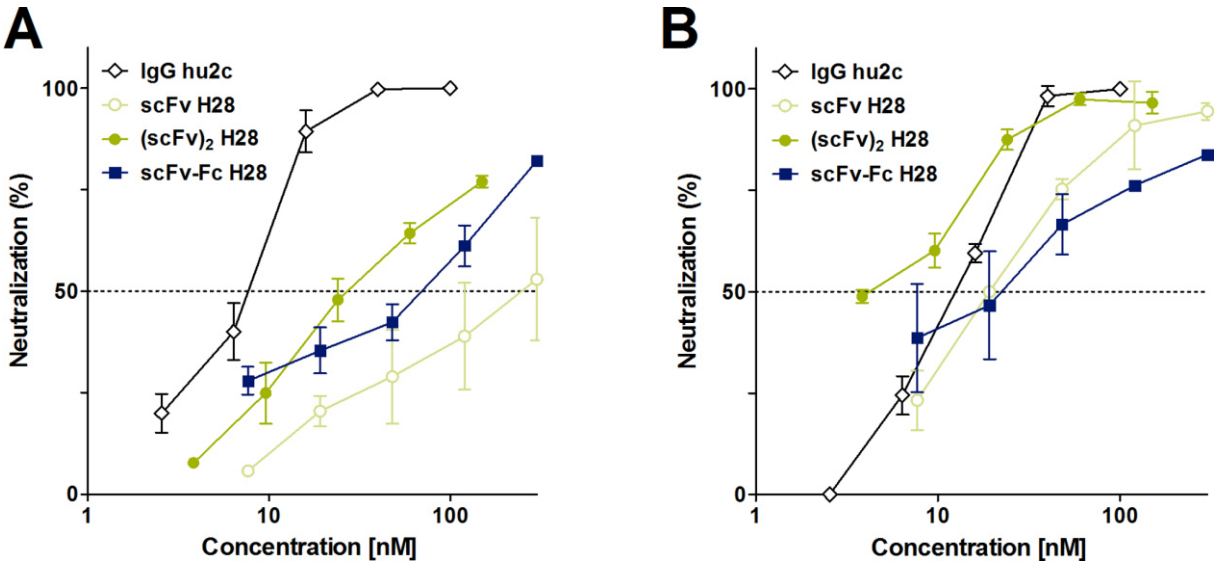

Figure 28. Concentration-dependent *in vitro* HSV neutralization of antibody H28. Antiviral capacity of clone H28 for neutralizing HSV-1 strain F (**A**) or HSV-2 strain G (**B**) was studied by plaque reduction neutralization tests (PRNT) using Vero cells. By using serial dilutions of monovalent scFv, bivalent $(scFv)_2$, or bivalent scFv-Fc, the concentrations were determined that neutralized 50% of viruses ($PRNT_{50}$). The humanized version of the monoclonal antibody 2c with known neutralizing property served as control. Experiments were performed in duplicate. Error bars represent standard deviations of the mean values.

To further assess the contribution of the antibody format to the neutralizing activity of H28, this antibody was reformatted into a bivalent scFv-Fc format. The reamplified scFv gene was therefore subcloned as NarI/EcoRV fragment into mammalian cell vector pYD11 that containes an intrinsic region encoding for a C-terminal-located human Fc antibody segment (**Figure 29A**). Covalently linkage via two disulfide bridges within the hinge region allows dimerization thus forming a bivalent scFv-Fc antibody fragment (**Figure 29B**, **Figure 29C**). Transiently expressed scFv-Fc was purified from mammalian cell culture supernatant by protein A chromatography obtaining high yield (~160 mg/l) of pure (**Figure 30A**, **Figure 30B**) and monomeric product (**Figure 30C**). The scFv-Fc format revealed similar binding affinities for HSV-1 and HSV-2 with 8.0 nM (±0.4) and 7.4 nM (±0.2) respectively when compared to bivalent dimeric $(scFv)_2$ (**Figure 27**). Similar to the other investigated formats, scFv-Fc revealed an increased capacity (3-fold) for neutralizing HSV-2 compared to HSV-1 (**Figure 28**). However, the scFv-Fc was less potent in neutralizing HSV-1 and HSV-2 than the dimeric $(scFv)_2$. In conclusion, smaller bivalent antibody constructs may be superior for the HSV neutralizing activity of H28.

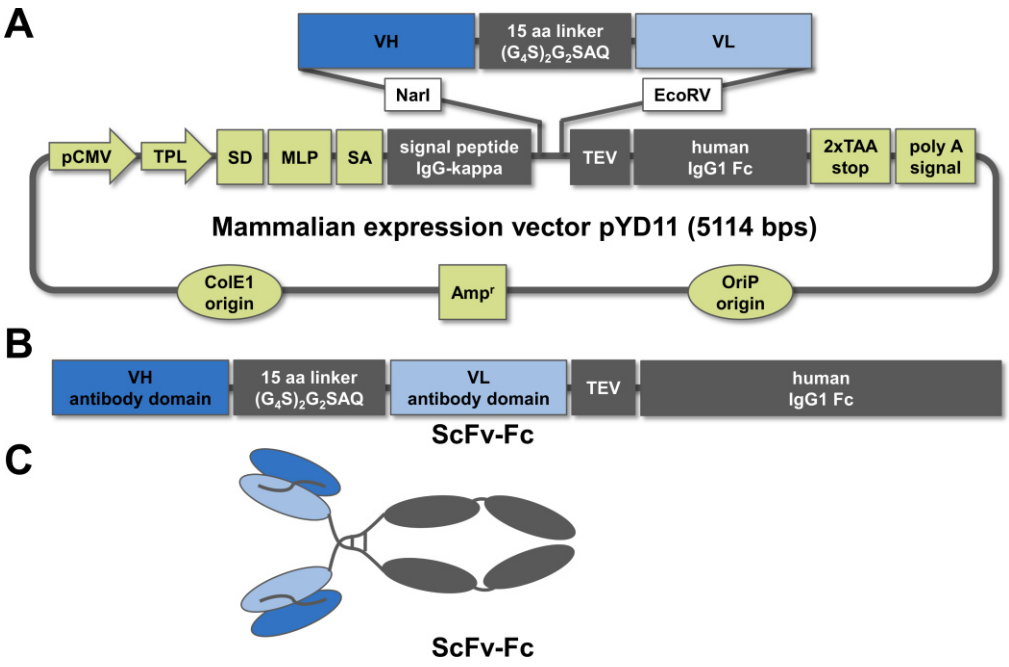

Figure 29. Maps of expression vector pYD11 and derived proteins. Target-enriched scFv genes were reamplified and subcloned into bacterial expression vector pYD11 as NarI/EcoRV fragments (**A**). After induction of the cytomegalovirus promoter (pCMV), translated proteins (**B**) are directed by the signal peptide IgG kappa into the cellular endoplasmic reticulum and, after folding to soluble scFv-Fc antibody fragments, released into the culture medium (**C**). MLP, adenovirus major late promoter; pCMV, cytomegalovirus promoter; SA, splice acceptor sequence; SD, splice donor sequence; TEV, tobacco etch virus protease cleavage site; TPL, adenovirus tripartite leader sequence.

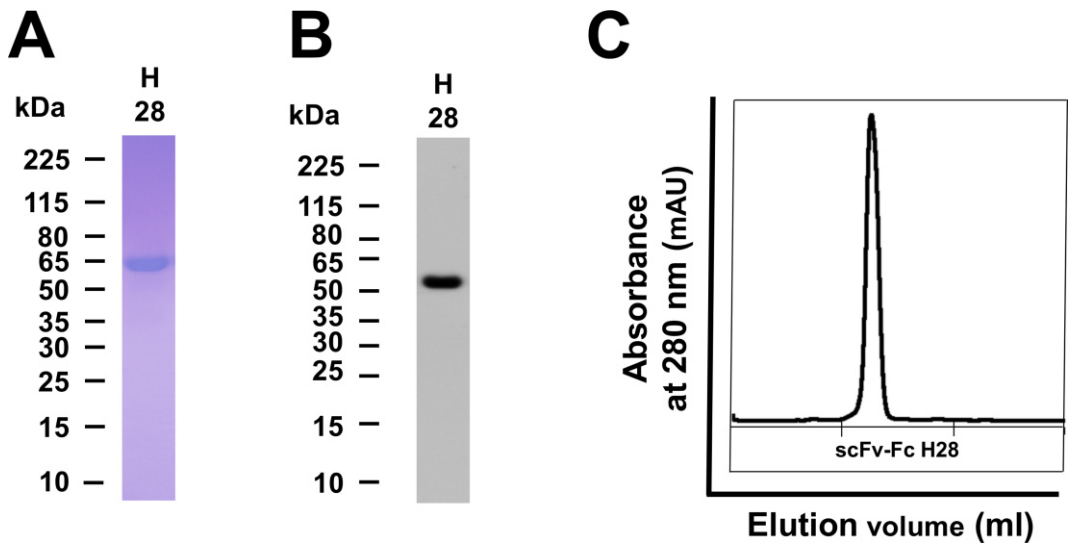

Figure 30. Characterization of gB-specific scFv-Fc H28. ScFv-Fc was transiently expressed in HEK 293-6E cells and purified by protein A chromatography before analyzing of 2 µg/lane of reduced protein by Coomassie-stained SDS-PAGE (**A**). For corresponding immunoblot, 1 µg of reduced scFv-Fc was loaded per lane and detected with a human Fc-specific peroxidase-conjugated IgG (**B**). ScFv-Fc was separated on SEC column Superdex 200 10/300 GL (**C**). The x-axe shows the elution volumes ranging from 0-30 ml and being segmented in 10 ml increments.

3.5 Selection of tumor-associated autoantibodies

In previous section, the value of LYNDAL for recovering antiviral antibody fragments from naturally immunized repertoires was confirmed. Of note, at least one antibody showed promising HSV neutralizing properties *in vitro* indicating that biological functional antibodies can be efficiently isolated from LYNDAL donors who were previously exposed to infectious diseases. In a next step, it was analyzed whether the presented concept is extendable to cancer-related autoantigens. Since the significance of the human immune system in the context of antitumor immune response has become evident [215-219], several immunogenic human tumor antigens have been identified that can elicit cellular and/or humoral immune responses in cancer patients [220]. Beside the antibody formation against a wide range of tumor-associated intracellular proteins, IgG-specific responses against strongly overexpressed extracellular regions of therapeutically relevant targets, such as HER2 [221] or EpCAM [222], has been reported. Considering that the most patients suffering from head and neck cancers exhibit an EGFR overexpression [223,224], this receptor tyrosine kinase was chosen as next target for antibody selection. First, sera of 19 LYNDAL donors with head and neck cancer were

screened by ELISA for identifying LYNDAL donors with an IgG response against the extracellular domain of recombinant human EGFR (**Figure 31**). The average response was comparable between the LYNDAL donors and a healthy control group (both mean = 1.1) indicating that autoantibodies are not exclusively produced in the context of a cancer-induced EGFR upregulation. EGFR-specific signals differed significantly within LYNDAL as well as the healthy control group (both SD = 0.6). Although autoantibody formation may be driven by EGFR overexpression in cancer patients, an antibody response against this ubiquitously expressed receptor seems to be also common under non-cancer conditions in some individuals.

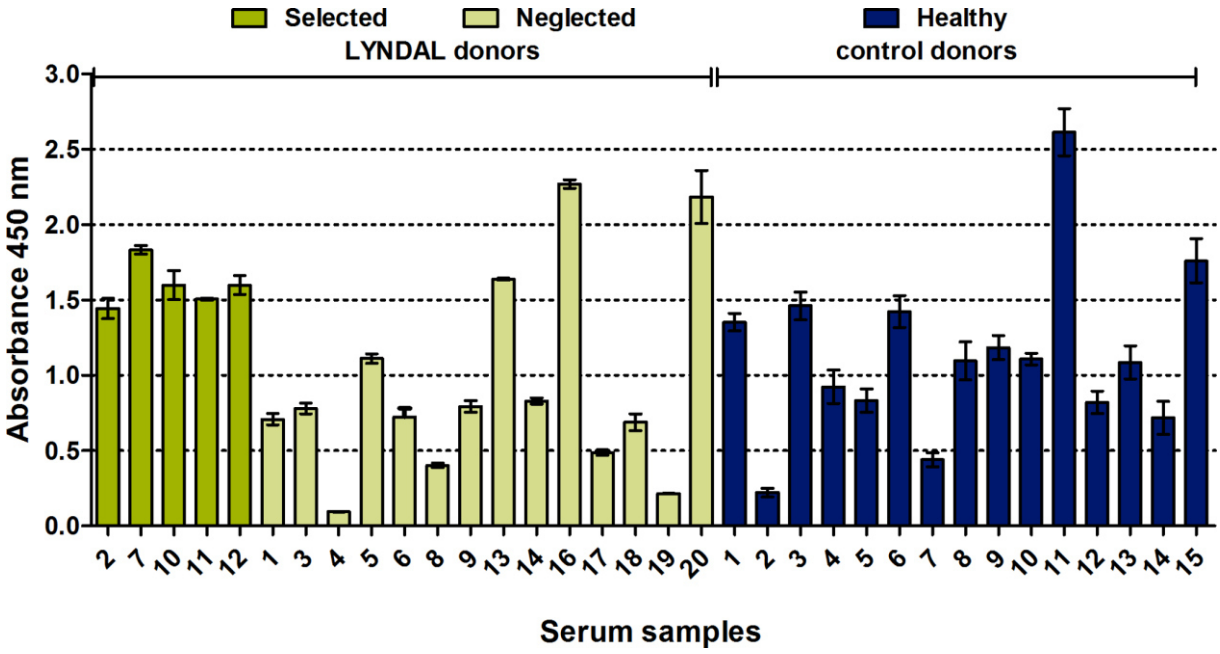

Figure 31. Serum-screening against target EGFR. Sera of LYNDAL donors with head and neck cancer and healthy control individuals were screened for IgG response towards the extracellular domain of EGFR. Recombinant EGFR was coated with 1 µg/ml and incubated with sera diluted 1:100 in MPBS. EGFR-specific IgG response was detected by using a peroxidase-conjugated antibody specifically recognizing human IgG Fc. EGFR-specific antibody response of LYNDAL donors (green) was compared to that of control individuals without cancer (blue). Bars of LYNDAL donors who were chosen for antibody selection are marked in dark green whereas all bars of neglected donors are colored in bright green. Error bars represent the standard deviations of the mean.

Finally, five LYNDAL comprising of $8.0x10^8$ different antibody clones from donors with increased EGFR-specific IgG titer were chosen for antibody panning (donor 2, 7, and 10-12). As target antigen, the extracellular domain of EGFR being fused to human IgG1 Fc was coated onto immunotubes and used for two independent selection experiments by employing different helper phage systems for phage assembly. Additionally, produced phages were preincubated with human Fc protein prior panning to reduce enrichment of Fc-specific antibodies. Under my supervision, Bachelor student Jonathan Kiefer performed biopanning experiments to investigate the efficacy of both phage systems for antibody selection. **Table 21** shows a summary of the obtained results. EGFR-specific binders were successfully enriched during three rounds of panning as evident from calculated enrichment factors. For identification of unique binders, individual clones that had been tested positive in ppELISA were screened by mpELISA. Taken both selection experiments together, the percentage of target-specific antibodies increased from the second to the third round by 12% (23 out of 192) and 76% (146 out of 192), respectively. Subsequent fingerprint analysis of clones with confirmed scFv genes finally resulted in identification of seven EGFR-specific antibody fragments with unique gene sequence [225].

Table 21. Summary of performed antibody selections towards EGFR.

Target antigen		EGFR-Fc	
Selection experiment number		1	2
Employed LYNDAL		2, 7, 10-12	
Combined LNYDAL size [$x10^8$]		8.0	
Used phage system for superinfection		Helper	Hyper
EGFR concentration (µg/ml)	R1	12	
	R2	4	
	R3	4	
Enrichment factor	R2	2	4
	R3	109	124
Specific clones	R2	3/96	20/96
	R3	85/96	61/96
Number of unique scFvs		6	1

Variable gene analysis revealed that the enriched EGFR-specific scFvs were derived from different germline genes (11 out of 117) and antibody families (8 out of 22). As observed previously for the gB selection experiment, scFv genes carried predominantly the VH1 or VH3 family sequences and showed a preference for

lambda light chains (**Figure 32**). Most clones (5 out of 7) had unique VH/VL pairings and two antibody fragments (E1 and E6) seemed to be clonally related because they possessed 95% identical amino acid positions (215 out of 228) with strong homology within the VH domain (117 out of 118, i.e., 99%). Analogous to gB-specific LYNDAL antibody fragments, the VH domains of EGFR-enriched scFvs had a higher accumulated number of somatic hypermutations on the nucleotide (**Figure 18A**) and the amino acid level (**Figure 18B**) than the VL domains. On average, variable domains possessed 14.4 and 7.3 amino acid exchanges in their VH and VL domains leading to exchange mutation frequencies of averaged 15% (VH) and 8% (VL). Considering the number of nucleotide mutations (VH: 28.0, VL: 12.1), frequencies for non-silent mutations were in the same range as previously observed for the gB-specific scFvs (VH: 51%, VL: 60%). Excluding CDR3 and FR4 regions for analysis, these mutations were predominantly accumulated within the CDRs (26%) and to a lower extent within the framework regions (8%) with highest mutation frequencies for the CDRH1 and CDRL2 followed by CDRH2 and CDRL1 (**Figure 33C**).

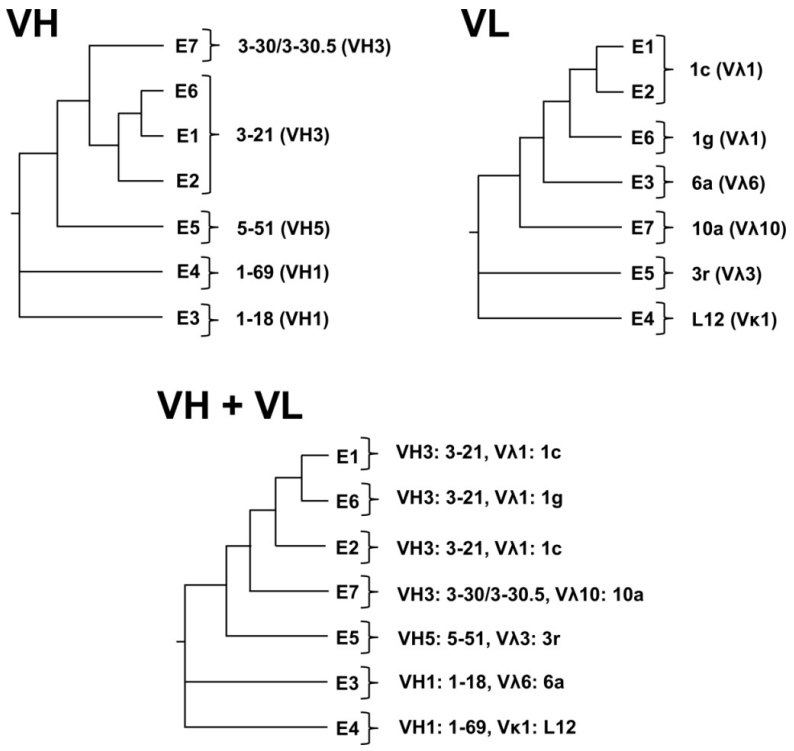

Figure 32. Sequence analysis of EGFR-specific LYNDAL scFvs. Germline sequences of the seven enriched scFvs were determined and phylogenic relationships analyzed by drawing phenograms employing the Phylogenic.fr web tool. Germline sequences as well as corresponding antibody families are shown for each clone.

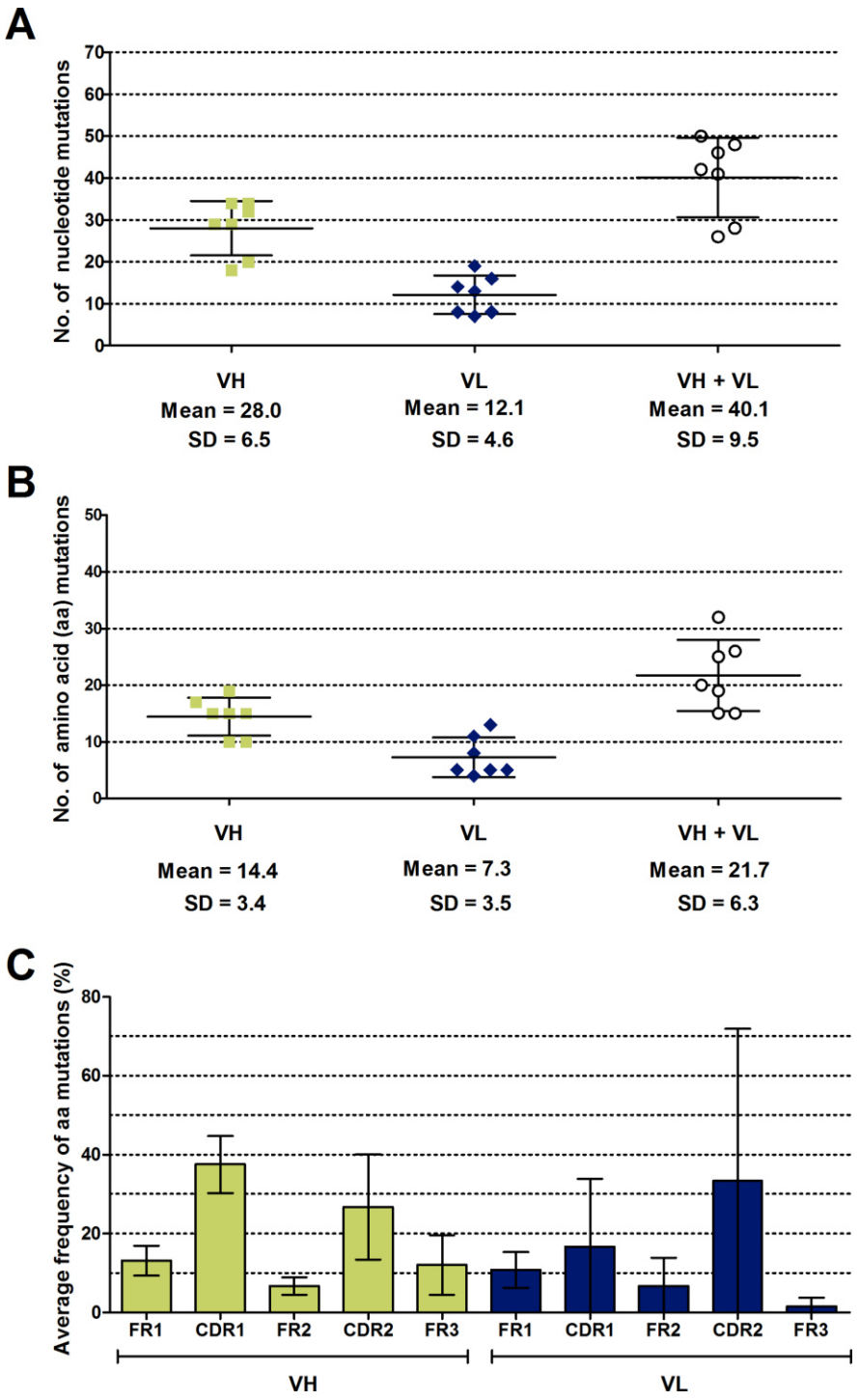

Figure 33. Analysis of somatic mutations within enriched EGFR-specific LYNDAL scFvs. Variable genes of the seven enriched scFvs were aligned to the closest respective germline sequences and the number of nucleotide (**A**) and amino acid (**B**) mutations was determined. Mean values and corresponding standard deviation are shown for the VH (green squares), VL (blue diamonds), and combined VH/VL genes (black circles). The distribution of exchange mutations encoded by the variable genes was analyzed separately for the VH (green) and VL (blue) domains (**C**). Mutation numbers of framework region (FR) 1-3 and complementarity determining region (CDR) 1+2 were determined and normalized to the length of each corresponding region. Results are presented as mean mutation frequency. Error bars represent standard deviations of mean values.

Genes of EGFR-specific scFvs were subcloned in expression vector pAB1 and subsequently expressed in the periplasm of TG1 *E. coli* bacteria. After IMAC separation, purity of antibody fragments was more than 95% as analyzed by SDS-PAGE under reducing conditions and Commassie staining (**Figure 34A**). Integrity of purified products was additionally confirmed in an immunoblot by specifically detecting myc tags of the fragments (**Figure 34B**). As seen in **Figure 35**, the yield of bacterially expressed EGFR-specific scFvs varied between 0.5 and 2.2 mg per liter of bacterial culture. Compared to the antiviral LYNDAL scFvs, the average yield for anti-EGFR scFvs was 50% less (2 mg/l versus 1.0 mg/l, respectively). In accordance with the gB-specific scFvs, more than 70% of EGFR-specific antibody fragments eluted mainly as monomers after SEC separation, and only clone E3 and E4 additionally formed dimeric $(scFv)_2$ fragments (**Figure 36**).

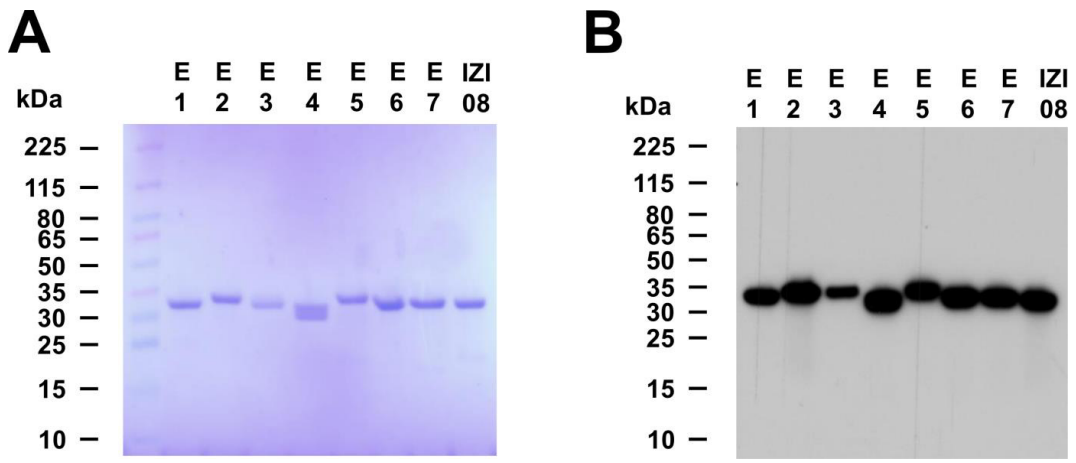

Figure 34. Characterization of EGFR-specific LYNDAL scFvs. Solubly expressed scFvs were purified by IMAC and 2 µg/lane analyzed under reducing conditions by Coomassie-stained SDS-PAGE (**A**). For corresponding immunoblot, 1 µg of reduced scFv was loaded per lane and detected with an anti-myc tag-specific mouse IgG and secondary anti-mouse peroxidase conjugate (**B**). A humanized version of the approved EGFR-specific antibody cetuximab, termed IZI08, was expressed and purified under comparable conditions and served as control.

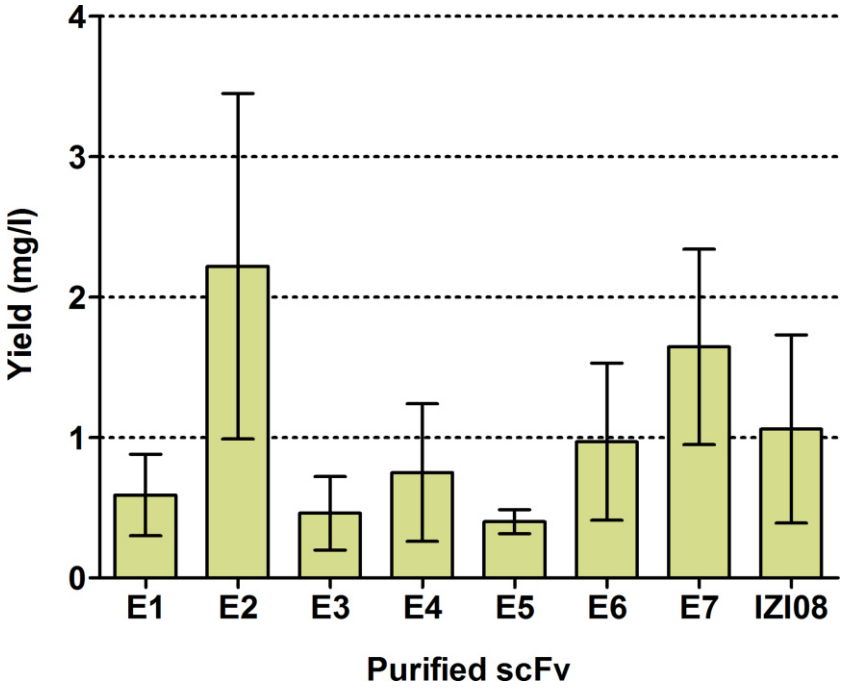

Figure 35. Expression yields of EGFR-specific LYNDAL scFvs. Antibody fragments were produced in the periplasm of TG1 *E. coli* cells, IMAC-purified, and filter-sterilized. Yields are presented as mg protein per liter bacteria culture. Error bars represent the standard deviations of at least two independent productions.

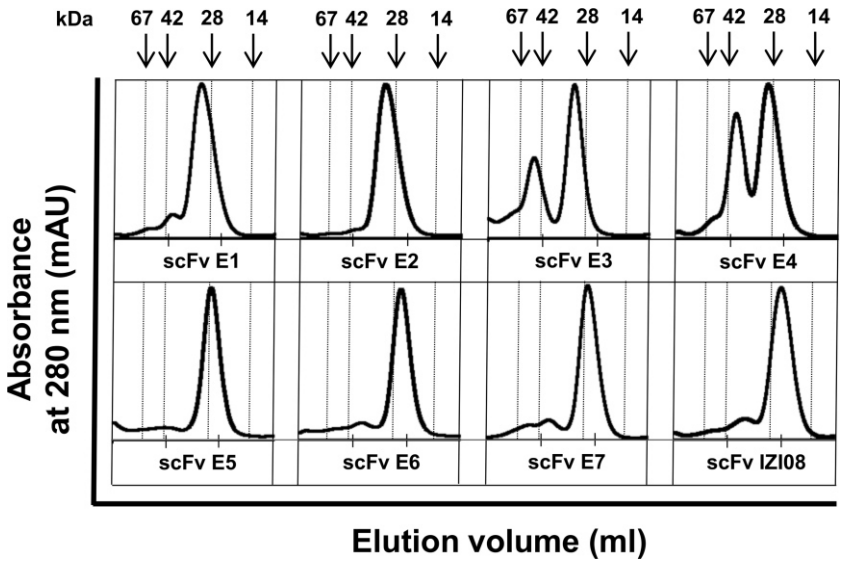

Figure 36. FPLC profiles of EGFR-specific LYNDAL scFvs. Antibody fragments were purified from periplasmic extracts by IMAC and separated on SEC column Superdex 75 10/300 GL. The x-axes show the elution volumes ranging from 8-14 ml and being segmented in 2 ml increments. All analyzed fragments exhibited a main peak corresponding to monomeric protein. Some fragments exhibited additionally peaks for dimeric fractions. EGFR-specific scFv IZI08 was used as control. Arrows indicate molecular weights of the used calibration reference proteins BSA (67 kDa, 9.07 ml), ovalbumin (42 kDa, 9.86 ml), control scFv (28 kDa, 11.50 ml), and RNase A (14 kDa, 12.98 ml).

Specific recognition of target epitopes with as less as possible unspecific binding and cross-reactivity to human self antigens are prerequisites for therapeutically applicable mAbs. Specificity of LYNDAL-enriched antibody fragments to cellular-expressed EGFR was therefore evaluated by flow cytometer experiments using various established human cancer cell lines showing differences in EGFR protein expression. In a first step, relative EGFR expression levels of various cell lines were assessed by flow cytometry using a receptor-saturating concentration (10 µg/ml) of therapeutically approved antibody cetuximab as specificity control. As seen in **Figure 37A**, highest level of EGFR-specific expression was detected for the well-established epidermoid carcinoma cell line A431 that is frequently used as model system for EGFR expression due to its aberrant high expression level of ≥2x10^6 EGF receptors/cell [226,227]. EGFR overexpression was also detected for the ovarian cancer cell line SKOV-3 as well as for different head and neck carcinoma cell lines showing mostly intermediate expression of the EGF receptor. In contrast, carcinoma breast cancer cell line MCF7, leukemia cell lines Jurkat (T cell-derived) and NALM-6 (B cell-derived), and Burkitt's lymphoma cell line Raji showed no expression of EGFR. To assess the specificity of LNYDAL-derived antibody fragments to cellular-expressed EGFR, monomeric scFvs of clone E3 and E4 were first SEC-separated since the FPLC profile showed additional formation of $(scFv)_2$ dimers (**Figure 36**). By using potentially receptor-saturating concentrations of scFvs monomers at 300 nM, all LYNDAL scFvs exhibited highly specific binding to EGFR-expressing tumor cell lines and no detectable signals on the EGFR-negative tumor cell lines (**Figure 37B**). Of note, fluorescence intensities were thereby dependent on the cellular expression levels and correlated well with the relative EGFR status. Compared with scFv IZI08, a humanized version of cetuximab being used as monovalent positive control, the fluorescence signals of scFvs E1-E4 were significantly lower and detectable signals were only obtained for cell lines with strong EGFR overexpression, i.e., HNO211, SKOV-3, and A431. In contrast, the other three LYNDAL scFvs E5-E7 delivered detectable signals for all investigated EGFR-positive cell lines that were in the range of positive control IZI08.

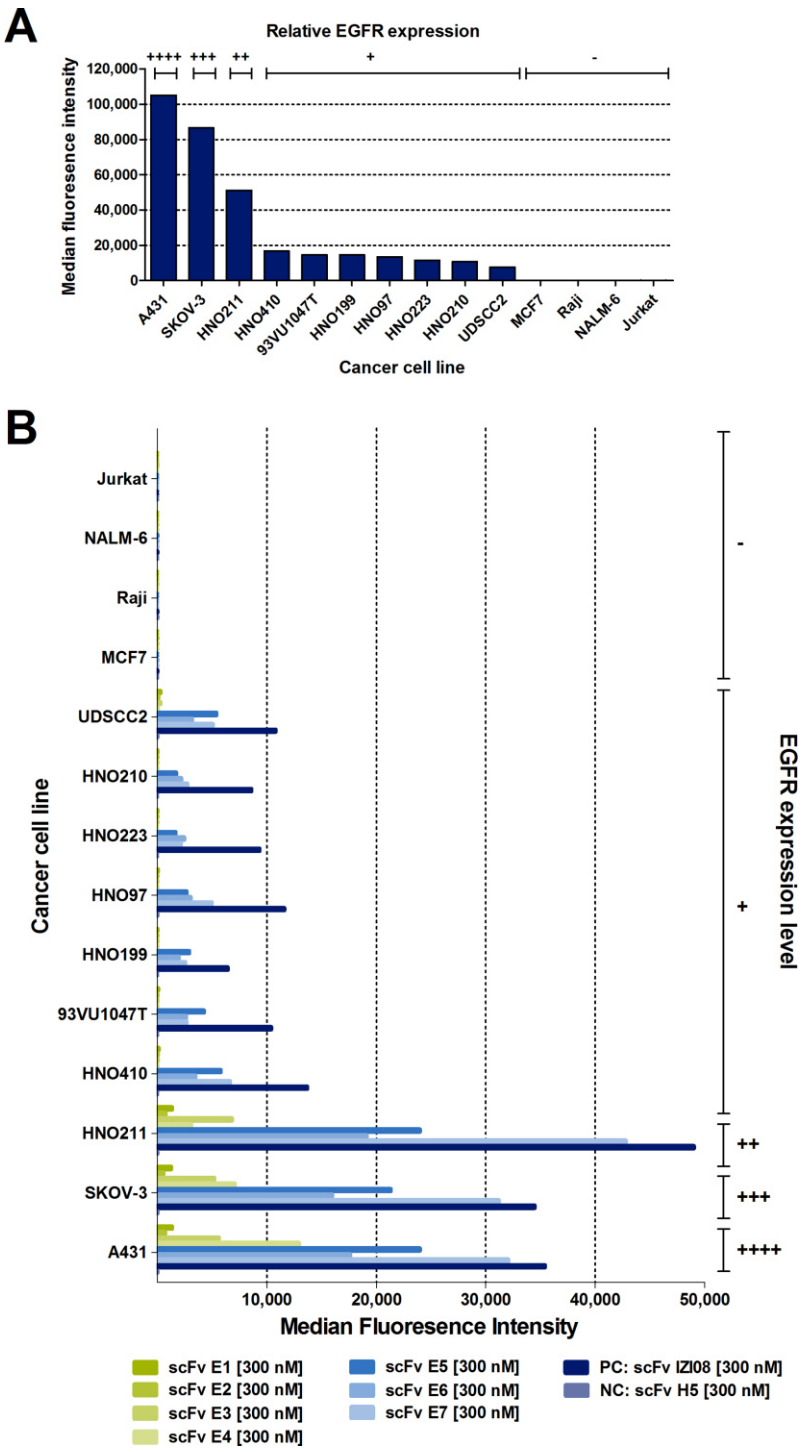

Figure 37. Specificity analysis of EGFR-selected LYNDAL scFvs. To determine receptor status of cell lines that were used for specificity analysis, $5x10^5$ cells/sample were incubated with EGFR-specific cetuximab (10 µg/ml) and binding was subsequently detected by an anti-human IgG FITC conjugate in flow cytomtry. By setting the FITC channel to constant 350 Volts, measured median fluorescence intensities were used for assessing relative expression levels that reached from very high (++++) to not detectable (-) (**A**). Specificity of scFv monomers for binding to cellular-expressed human EGFR was evaluated by flow cytometry on receptor-positive or negative tumor cells (**B**). Bound fragments were detected with myc tag-specific mouse antibody followed by anti-mouse FITC conjugate. HSV-specific scFv H5 and EGFR-specific scFv IZI08 served as controls for specific binding.

Binding activities of LYNDAL-derived scFvs were first assessed by determination the equilibrium constants for binding to cancer cell-expressed EGFR. As target cell line, A431 was chosen due to its mainly monomeric EGFR receptor status that allows determination of 1:1 interactions in contrast to, for example, SKOV-3 with a known higher level of receptor dimerization [227]. Median fluorescence intensities of serial-diluted scFv monomers were measured in triplicate by flow cytomertry and used for calculation of equilibrium binding curves using a 1:1 fit model (**Figure 38**). Apparent affinities were calculated as EC_{50} values with exception for scFvs E1 and E2 where no saturation of the equilibrium binding curves could be achieved in the investigated concentration range (**Table 22**). Calculated equilibrium constants of the other LYNDAL scFvs were, with exception of one, all in the low nanomolar range with 19 nM for the most affine binder. To confirm binding affinities of scFvs E5-E7, binding kinetics were measured by SPR using recombinant EGFR-Fc as ligand (**Figure 39**). Excluding scFv E7 due to progressively accumulation on the chip surface, calculated K_Ds of scFv E5 and scFv E6 were 32 nM and 11 nM, respectively (**Table 9**). Thus, binding of both scFvs seemed to be stronger to recombinant EGFR than to cellular expressed receptor. Accordingly, control scFv IZI08 possessed an increased affinity to recombinant than to cellular expressed EGFR (K_D = 0.9 nM versus EC_{50} = 6.5 nM). Despite the higher apparent affinity of IZI08, LYNDAL-derived antibody E6 showed slower dissociation rate than IZI08 ($7.9x10^3$ versus $4.0x10^3$) which ought to be beneficial for the development of anticancer mAbs being intended for treating solid tumors.

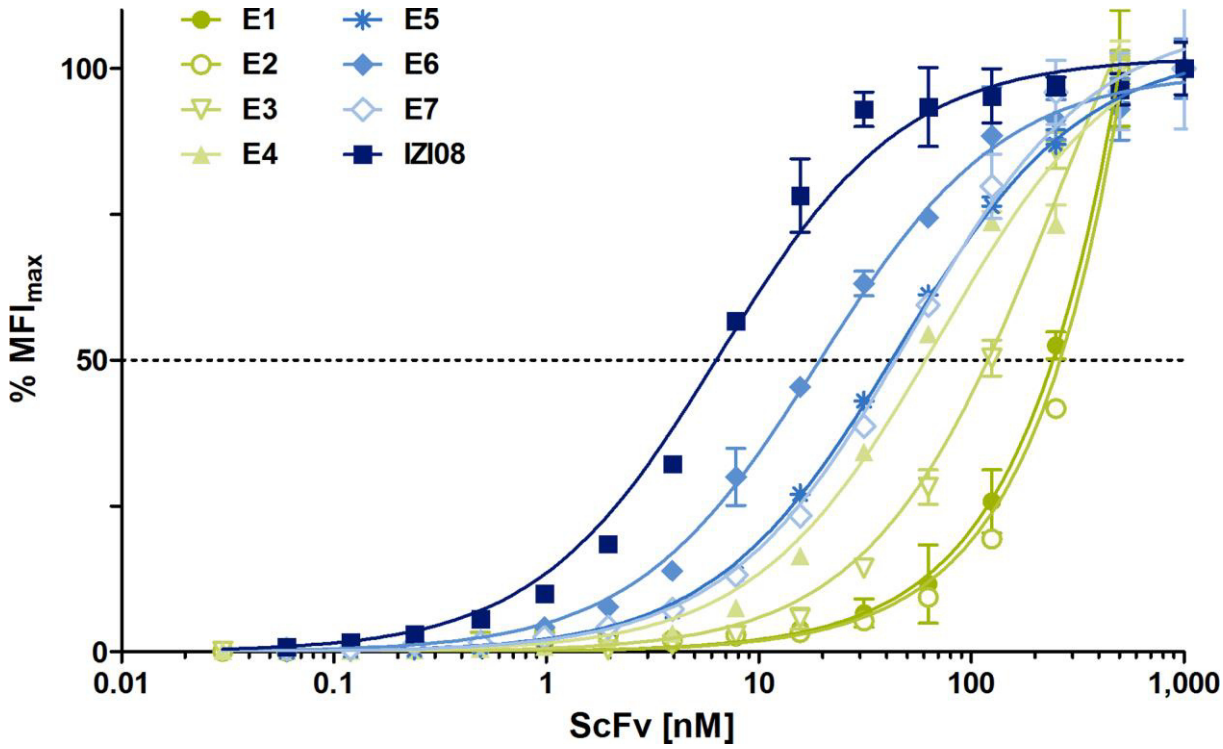

Figure 38. Equilibrium-binding curves for EGFR-specific scFvs. Binding activities of LYNDAL scFvs to cellular-presented human EGFR was measured by flow cytometry. Monomeric scFvs were titrated in triplicate on A431 cancer cells and binding detected using a myc tag-specific mouse IgG followed by mouse-specific FITC conjugate. After subtracting background fluorescence, averaged median fluorescence intensities were normalized to measured maximum median fluorescence intensities (MFI_{max}) and used for calculating nonlinear-fitted curves based on equation for one site binding. Error bars represent the standard deviations of the mean.

Table 22. Apparent affinities of EGFR-specific scFvs.

ScFv	Equillibrium binding[a]	Surface plasmon resonance[b]		
	EC_{50} ±SE [nM]	K_D ±SD [nM]	k_{on} ±SD [x10^5 $M^{-1}s^{-1}$]	k_{off} ±SD [x10^{-4} s^{-1}]
E3	257.2 ±21.2	ND	ND	ND
E4	70.8 ±5.9	ND	ND	ND
E5	45.0 ±1.3	32.2 ±1.2	2.5 ±0.1	79.0 ±0.1
E6	19.2 ±1.0	10.8 ±0.2	37.6 ±9.3	403.5 ±106.8
E7	51.5 ±3.2	NC	NC	NC
IZI08	6.5 ±0.4	0.9 ±0.1	371.0 ±217.8	343.0 ±220.6

[a]Binding affinities of monomeric scFv to A431-expressed EGFR were calculated from the equilibrium-binding curves after flow cytometry. EC_{50}, half maximal effective concentration; SE, standard error. [b]Association and dissociation rate constants of monomeric scFvs were determined by SPR using protein A-captured ligand EGFR-Fc. Affinity constant were calculated as $K_D = k_{off}/k_{on}$. Constants and errors were averaged from two independent determinations. SD, standard deviation; NC, not calculated; ND, not determined.

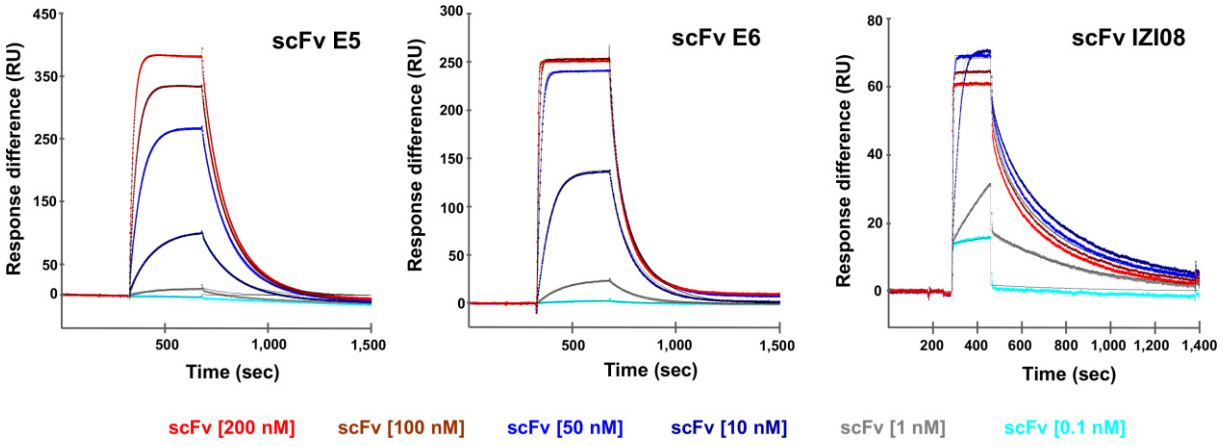

Figure 39. Kinetic analysis of EGFR-specific scFvs. Surface plasmon resonance measurements were performed by capturing EGFR-Fc on a protein A-covered sensor chip. Representative sensograms show the overlays of serial dilutions of injected monomeric scFvs. The y-axes of the sensograms exhibit the response differences after subtracting the background signals from EGFR binding. The response differences were expressed as response units (RU). Biosensor data were fitted with the 1:1 binding mass transfer model.

To evaluate the potential of LYNDAL for delivering anticancer autoantibodies with therapeutic value, the capacity of scFvs E3-E7 for induction of anti-proliferative effects was tested *in vitro*. Due to proliferating effects of the natural ligand EGF, it was first analyzed weather EGF-induced cell growth can be inhibited by antibody binding. Therefore, a constant number of SKOV-3 carcinoma cells was cultured in serum-reduced medium (0.3% FCS) before induction of cell proliferation by addition of 1 nM EGF. As summarized in **Figure 40**, scFv-titration up to 1 µM to activated cells revealed that scFv E6 can mediate a similar anti-proliferative effect (-13% versus -26%) as control scFv IZI08. The other investigated LYNDAL scFvs could not prevent EGF-induced tumor cell growth. In contrast, they partially enhanced tumor cell proliferation, e.g., scFv E5 and scFv E7 mediated a relatively increased proliferation effect of 69% and 229%, respectively.

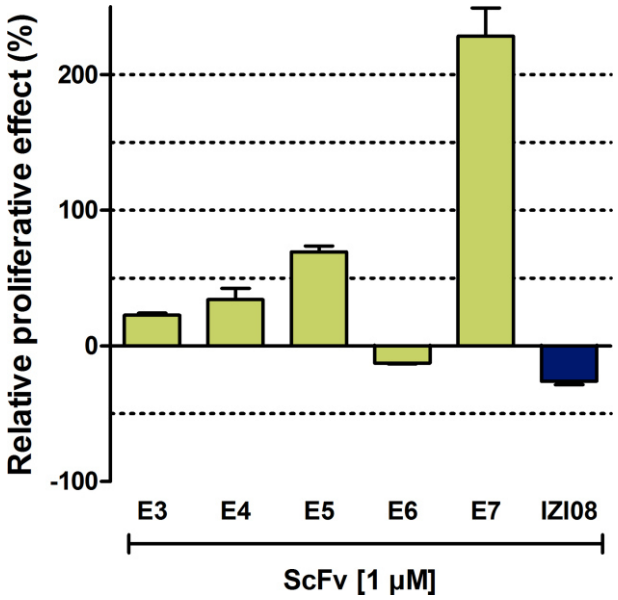

Figure 40. Effects of EGFR-specific scFvs on cell proliferation. Proliferative properties of EGFR-specific scFv monomers were tested on carinoma cell line SKOV-3 (5000 cells/well) that had been cultured for 24 hours in medium with reduced FCS concentration (0.3%). After replacement with medium containing 0.3% FCS and 1 nM EGF, 1 µM of the monomeric scFvs were added and incubated for 96 h until measurement of cell metabolism by resazurin reagent. Relative proliferative effect was calculated by comparison of measured fluorescence signal to that of control without antibody. Experiment was performed by Master student Philipp Kuhn.

To further evaluate the observed pro-proliferative and anti-proliferative effects, the three most potent scFvs E5-E7 were characterized in respect of EGF competition for receptor binding. In a flow cytometry experiment, EGF diminished binding of all three scFvs to EGFR being expressed on both A431 (**Figure 41A**) and SKOV-3 (**Figure 41B**). On average, the strongest relative reduction of antibody-specific binding was obtained for scFv E5 (95%) followed by scFv E6 (89%) and scFv E7 (77%). The reduction of measured fluorescence signals indicates that the epitopes on EGFR were no longer accessible for the investigated scFvs. Observed reduction might be either mediated by ligand-dependent blockage of antibody binding sites or by EGF-induced conformation changes of the receptor thus leading to blockage of antibody epitopes. Although parental antibody cetuximab directly occlude the EGF binding site [180], reduction of fluorescence signal by EGF for control scFv IZI08 was only 20%. In contrast to LYNDAL-derived scFvs, control IZI08 possesses a higher affinity to EGFR than its endogenous ligand that may result in an efficient masking of the EGF binding site [228].

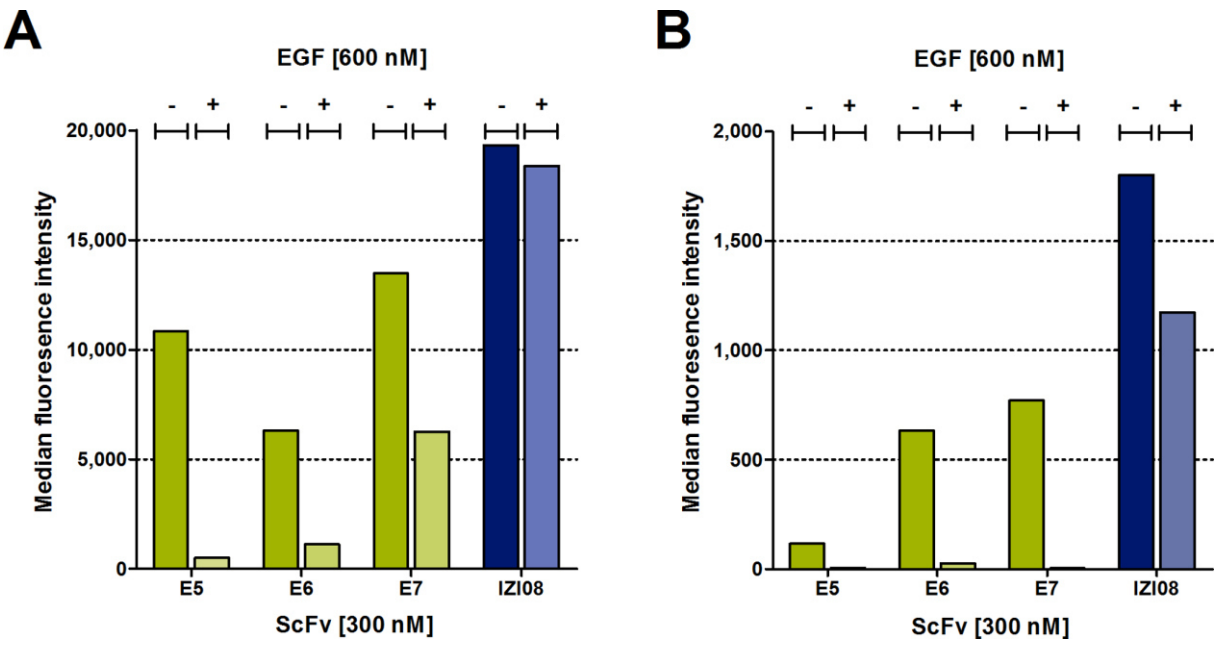

Figure 41. Competition assay for EGFR binding. In flow cytometry, LYNDAL scFvs (green) were tested for their ability to compete with epidermal growth factor for binding to cellular-expressed EGFR. Monomeric scFvs were preincubated (bright) with 2-fold molar excess of EGF, and binding to either A431 (**A**) or SKOV-3 (**B**) cells was detected by a myc tag-specific mouse antibody followed by an anti-mouse FITC conjugate. Competition was compared to binding of scFvs monomers without preincubation of EGF (dark). ScFv IZI08 was used as control (blue). Incubation steps were performed at 4°C to prevent EGF-induced receptor internalization.

To further assess the potential of antibody E6 for mediating anti-proliferating effects towards cancer cells, this clone and control IZI08 were reformatted into the bivalent scFv-Fc antibody format and transiently expressed in HEK 293-6E cells. ScFv-Fcs were purified from cell culture supernatants by protein A chromatography and characterized by Coomassie-stained SDS-PAGE (**Figure 42A**) and immunoblot (**Figure 42B**) showing a high purity (>95%) of specific detectable proteins. Protein A purification of scFv-Fcs yielded 28.3 mg and 35.5 mg per liter culture medium for E6 and IZI08, respectively. Analytical size exclusion chromatography showed highly monomeric profiles for both scFv-Fc antibody fragments (**Figure 42C**).

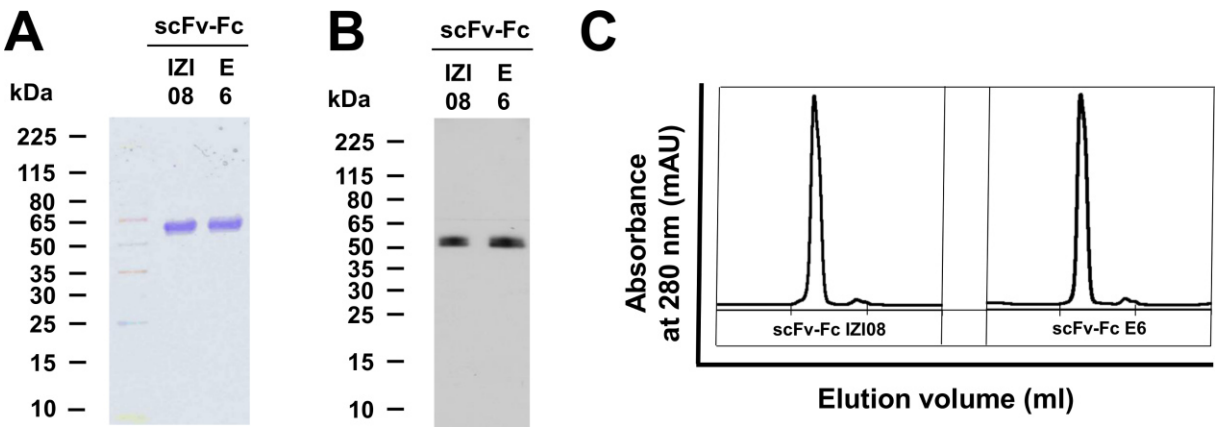

Figure 42. Characterization of EGFR-specific scFv-Fcs. Antibody fragments were transiently expressed in HEK 293-6E cells and purified by protein A chromatography before analyzing of 2 µg/lane of reduced protein by Coomassie-stained SDS-PAGE (**A**). For corresponding immunoblot, 1 µg of reduced scFv-Fc was loaded per lane and detected with an anti-human Fc-specific peroxidase-conjugated IgG (**B**). ScFv-Fcs were separated on SEC column Superdex 200 10/300 GL (**C**). The x-axes show the elution volumes ranging from 0-30 ml and being segmented in 10 ml increments.

Before analyzing within a proliferation assay, the apparent affinities of both constructs for binding to EGFR were determined on A431 cells. As calculated from the equilibrium binding curves, scFv-Fc E6 had a similar affinity (1.6 nM ±0.2) than scFv-Fc IZI08 and its parental IgG cetuximab (2.4 nM ±0.2 and 2.0 nM ±0.2, respectively) (**Figure 43**). Analyzing the anti-proliferating activity on SKOV-3 cells using the same settings as reported for the prescreening, scFv-Fc E6 showed a concentration-dependent anti-proliferative effect on the EGF-induced SKOV-3 growth which was comparable to that of scFv-Fc IZI08 (IC_{50}s of 6.2 nM versus 3.6 nM) (**Figure 44**). Using parental cetuximab as control, this IgG was even more potent as scFv-Fc IZI08 (IC_{50} of 0.2 nM) most likely due to a better steric hindrance of the EGF/EGFR binding.

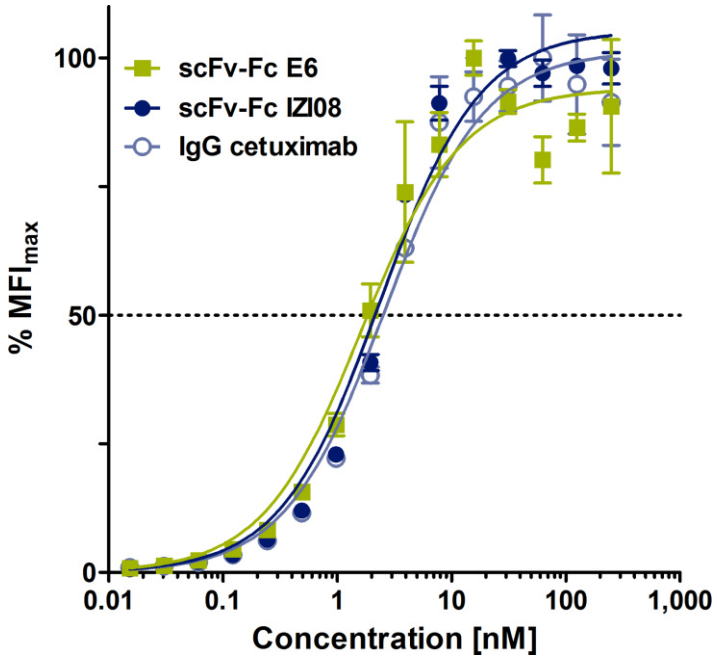

Figure 43. Equilibrium-binding curves for EGFR-specific bivalent antibodies. In flow cytomerty, binding activities of bivalent scFv-Fc E6 and IZI08 as well as IgG cetuximab was determined on EGFR-positive carinoma cell line A431. Error bars represent standard deviations of the mean values. MFI_{max}, maximum median fluorescence intensity.

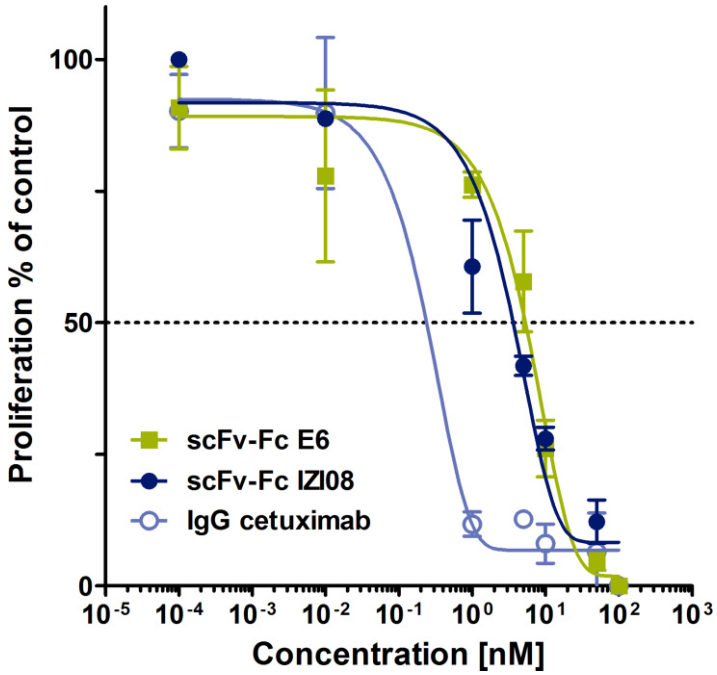

Figure 44. Anti-proliferation capacity of antibody E6. ScFv-Fc E6 was tested on carcinoma cell line SKOV-3 (5000 cells/well) for its capacity to mediate anti-proliferative effects. Cells were grown in serum-reduced medium (0.3% FCS) for 24 h. The next day, fresh medium that had been supplemented with 1 nM of EGF was added to promote tumor cell growth. EGF-induced proliferation was blocked by adding serial dilutions of anti-proliverative scFv-Fc E6. ScFv-Fc IZI08 and IgG cetuximab served as controls. Cell metabolism was measured after 96 h employing resazurin reagent.

4 Discussion

4.1 Underlying idea of LYNDAL

Somatically hypermutated antibodies that have been developed during a secondary immune response can possess advantageous biological properties, e.g., improved virus neutralizing properties when compared to germline antibodies from primary responses [64,65]. Unfortunately, such antibodies are usually underrepresented in the bulk immune response and the most potent antibodies might emerge late in an infection as a result of various evolutionary attempts [56]. However, cloning of the "fossil record" as combinatorial library, i.e., the entire antibody repertoire of an individual including its immunological history, allows in principle the resurrection of any antibody that the individual has ever made [229]. Using this approach, it has been previously reported that anti-metastatic antibodies can be recovered from cancer patient libraries at a frequency of one to 10^8 library members [230] that might be valuable for therapeutic developments.

Following this idea, this thesis aimed in the development of an efficient concept for generating human monoclonal antibodies that were produced during the course of a natural immune response and therefore might possess advantageous biological properties being exploitable for therapeutic purposes. The presented approach includes the generation of 20 individual "LYmph Node Derived Antibody Libraries" (LYNDAL) that were cloned from the entire IgG repertoire of 20 single tumor-draining lymph nodes of head and neck cancer patients. By combination of seropositive donor libraries for target panning, the successful translation of the concept was validated by test selection employing both a viral (gB of HSV-1) and a cancer-related target (EGFR).

4.2 Library diversity

Capturing the fossil record by combinatorial antibody libraries required the cloning of an appropriate number of VH/VL combinations since random V gene cloning produces a high number of novel non-natural combinations. Small-size immune libraries (10^5-10^6 members) are generally sufficient for selecting high affinity mAbs when they are cloned from plasmablasts that have been captured during the course

of an ongoing antibody response. Contrary, individual LYNDAL possessed larger repertoires (~10^8 members) because the presented concept requires the cloning of the past immunological memory of included donors to enable the selection of affinity-matured antibodies from seropositive repertoires. As demonstrated previously, combinatorial libraries can be closely related to the immune response of the included donor(s) [58,231,232], and the possibility to obtain HuMAbs with original VH/VL pairings and identical sequences as found in single B cells depends on the construction of large random immune libraries. Thus, cloning highly diverse and functional donor repertoires that preferably cover all functional germline sequences may increase the success for isolating of originally paired and naturally affinity-matured mAbs. Although cloning of incomplete antibody repertoires has been reported [76], e.g., to exclude unstable or rarely used antibody frameworks, LYNDAL cloning implemented all known functional antibody genes. Since the human immune system is not a steady state system, “useless” antibody gene segments are supposed to be efficiently removed by evolutionary pressure. In conclusion, the most of existing human gene segments may be valuable for generation natural mAbs against current and/or former pathogenic structures, and antibody libraries that not include the diversity of all gene families may be limited in paratope diversity [85]. Actually, some of the selected LYNDAL antibody fragments based on rare sequences from the Vλ5 and Vλ6 families that have sometimes been excluded for library construction [76] and thus would be missed in the current antibody selection.

4.3 Library primer

To include all functional antibody genes for LYNDAL construction, a novel primer set has been designed that possessed not more than two degenerated positions per primer to enable highest quality during repertoire amplification. For library cloning, the first sets of primer described in literature were based on V gene sequence information that had been extracted from different sources, e.g., Kabat, EMBL, and literature, and thus did not amplify the complete human antibody gene repertoires [40,233-235]. Based on more detailed sequence information supplied by the VBASE, subsequently refined and larger primer sets have been published that include all known functional sequences [84,85,236-238]. Actually, the VBASE is predominantly used to design primers for cloning naïve repertoires [70,85] because this database

provides a structured overview about sequence alignments of all functional human V genes. In accordance, LYNDAL primers were designed by employing the VBASE thus enabeling the amplification of all listed 117 functional V gene sequences. As shown by the analysis of the PCR products (**Figure 10**), indeed the most primer combinations exhibited a high efficacy in primary V gene amplification. Most importantly, the utilized primer set delivered a high sequence diversity as obvious from the V gene analysis identifying 77% of annotated functional sequences (**Figure 12**, **Figure 13B**). Actually, the extensive V gene diversity within LYNDAL is remarkable when compared to the V gene usage of other repertoires such as the commercial CAT2.0 library [84], one of the largest antibody libraries to date ($1.3x10^{11}$ clones). Although the germline diversity of the CAT2.0 library is higher than for LYNDAL (90% versus 77%), a 3-fold higher sample size has been used for the CAT2.0 analysis (841 versus 280). Including the sequences of all selected clones, the diversity increased for both LYNDAL and CAT2.0 to 79% and 94%, respectively. Keeping in mind that much more additional sequences were included for CAT2.0 analysis than for LYNDAL (5044 versus 41), the final library diversities might be comparable. Another example is Affitech´s NBL library which was cloned using a primer set for amplifying all known V genes presented within the VBASE [236]. Compared to the LYNDAL primers, the primer set used for the NBL library possessed a higher level of degeneracy [239]. By analyzing 96 random scFvs that had been cloned with the NBL strategy, only 61% of the antibody families could be identified [239] whereas all families are present in the LYNDAL collection (**Figure 13A**). In conclusion, an optimized primer design with less degenerated positions as well as performing elevated numbers of initial V gene amplification steps (e.g., 39 for LYNDAL cloning) might provide antibody repertoires with larger diversity compared to those amplified with the commonly used primer sets.

4.4 Frequency of antibody frameworks

The success of the LYNDAL concept depends on the cloning of the immunological donor history which is mainly recorded in the IgG (memory) B cell population. To assess the quality of the cloned repertoires, it was first proved whether the cloned functional sequences within LYNDAL possess a naturally occurring distribution pattern. A universal distribution pattern of the functional human antibody repertoire is in general difficult to define because the existing databases of human functional antibody genes all derive from various independent sources and individuals. To obtain a natural distribution pattern which reflects the situation in human individuals, the framework frequency of functional entries from three large antibody gene databases (VBASE, VBASE2, and IMGT) were used to define a reference. Compared with this, the LYNDAL distribution was similar for most of the analyzed antibody families with exception for four families where major differences occurred (VH2, VH6, Vκ4, and Vλ5) (**Figure 13C**). As reported by others [84,85], pooling the amplified gene products according the predicted natural family distribution patterns, e.g., according the VBASE, allows cloning of distribution patterns that may match nicely with the natural situation [85]. LYNDAL strategy was adopted to give maximal yields of V gene PCR products for library cloning. The obtained LYNDAL distribution was more nature-related as reported for other libraries that also refrain from pooling V genes according natural patterns [239,240]. In conclusion, the LYNDAL primer set and cloning strategy can be used for cloning of a nature-like framework distribution. However, pooling along the theoretical human representation seems to be also reasonable.

4.5 Functional repertoire

In general, library clones encoding for aberrant and non-productive antibody fragments, for example VL-pIII fusions, are often very well-expressed within antibody libraries and can lead to growth disadvantages for clones expressing functional rearrangements [241]. Successful antibody selection therefore requires cloning of highly functional repertoires, i.e., the percentage of clones encoding for producible full-length antibody-pIII fusions should be maximized, for example by optimizing gene amplification and cloning. As a common problem during gene amplification,

degenerated primers, mismatches, or PCR errors are known to cause point mutations or even out-of-frame deletions within the cloned repertoires. Moreover, errors occurring subsequent to PCR amplification, e.g., restriction digest, dephosphorylation, and ligation, can result in incomplete cloning of both antibody chains. By optimization of each cloning step for LYNDAL generation including the conditions for PCR amplification, digest, ligation, and transformation, the final libraries possessed a high percentage (~73%) of functional clones (**Figure 11**). Comparison of LYNDAL with other scFv libraries using similar cloning approaches confirmes the high quality of the cloned repertoires. For example, the commercial NBL library possesses a clearly reduced functional protein expression with estimated 37% and 26% for VH/VL-lambda and VH/VL-kappa sublibraries, respectively as analyzed from produced model libraries [239]. Other commercial libraries using cloning strategies different to that of LYNDAL achieved comparable or increased functional complexities. MorphoSys' HuCAL GOLD library for instance, a synthetic human Fab library based on frequently used V gene consensus sequences, was reported to contain a functional antibody repertoire of 77% [78]. For the second generation library HuCAL PLATINIUM, MorphoSys reported an even improved percentage of functional clones of about 83% [79]. In the end, optimizing the gene amplification steps and the cloning procedure allowed the generation of highly functional LYNDAL repertoires that are qualitatively comparable with the current commercial libraries.

4.6 Cloning strategy

Various approaches have been applied for cloning genetically diverse antibody repertoires. Independently whether naïve or immune libraries were produced, most antibody libraries were generated by using a one, two, or even three step cloning strategy. In the one step technique, the rearranged VH and VL genes are combined by PCR assembly [40,50,68] and cloned into an appropriate library vector. In the two step approach, VH and VL repertoires are successively cloned whereby the heavy chain repertoire is usually inserted into a vector containing the inserted light chain repertoire [51,237,239,240]. In the rarely used three step strategy, separate VH and VL libraries are prepared, and the excised VH repertoire is inserted into the vectors containing the VL repertoire [70]. LYNDAL was cloned using a modified two-step

cloning strategy (**Figure 7**) to reduce steps leading to loss of diversity, i.e., PCR-based errors during assembly PCR in the one step strategy or additional restriction digest and transformation steps in the three-step strategy. In contrast to most two-step strategies, LYNDAL was cloned vice versa, i.e., the heavy chain genes were cloned first followed by insertion of the light chain repertoires, with the aim to increase the light chain diversity within LYNDAL. Although heavy chain binding is commonly regarded to be of higher relevance, recent insights revealed the importance of light chain binding, and in fact, such isolated binder are expected to be exploitable for developing VL-based immunotherapeutics [242-245]. Additionally, cloning of the lambda and kappa repertoires was performed separately which allows the control of the light chain selection process, for example, when selection of one certain light chain group is preferred. By panning LYNDAL against the test antigens, lambda light chain-derived scFvs were preferably selected (90%, n = 41) although VH/VL-kappa and VH/VL-lambda sublibraries of similar sizes had been combined. This phenomenon has also been observed by Hust and coworkers when combined VH/VL-lambda and VH/VL-kappa repertoires were applied for selection yielding mainly binders that originated from the lambda library (91%, n = 400). Based on the observation that lambda scFvs are expressed in higher yields in *E.coli* than kappa scFvs [239], it has been speculated that this leads to a selection advantage of lambda scFvs in phage display [240]. When employing exclusively the kappa library, Hust et al. obtained binders even in cases where no kappa antibodies were initially isolated from the combined repertoires [240]. In the end, this simple strategy is also applicable for LYNDAL to further increase the number of kappa-derived binders.

4.7 Antibody format

Cloning of phage-displayed antibody repertoires is normally restricted on smaller antibody fragments, preferentially Fabs and scFvs, since folding of larger antibody formats in the periplasm of *E. coli* is mostly inefficient. For generation of LYNDAL, the scFv format was chosen because it usually yields higher expression levels in *E. coli* than Fabs [246]. Moreover, scFvs can be more easily engineered than Fabs which have to be reformatted in usually two cloning steps. LYNDAL-derived scFvs can be subcloned in one step into the bivalent scFv-Fc antibody format (**Figure 29**). Like the natural occurring IgGs, scFv-Fcs contain two antigen binding sites and can therefore

mediate natural antibody effector functions, such as ADCC and CDC. A recent comparison between Fab and scFv libraries of comparable size and diversity showed that the latter format can yield a higher percentage of unique binders [85]. However, reformatting both formats into IgGs revealed that more Fabs retained their specific binding capability finally leading to a balanced number of unique clones from both types of libraries [85]. In conclusion, LYNDAL is expected to be especially favorable for the development of scFv-based and diabody-derived therapeutics.

4.8 V domain linkage

To stabilize the naturally weak VH/VL interaction, linkage of both variable domains by an appropriate peptide linker can be applied to produce the scFv format. In the case of LYNDAL, this was done by a 15 aa long $(G_4S)_2G_2SAQ$ peptide (**Figure 8**). Thus far, a range of different linkers has been tested for connecting the variable domains of scFv fragments that differed in composition and length [247-249]. Although the scFv linker seems to be a passive entity during protein folding [246], linker peptides can strongly influence the properties of the fragments, e.g., the extent of multimerization or the conformational and proteolytic stability [250]. In general, scFvs are predominantly monomeric when the V domains are joined by polypeptides of at least 12 residues, and shorter linkers enhance the formation of bivalent diabody constructs by non-covalent linkage of two protein chains [251]. Usually hydrophilic and flexible linkers with small side chains are preferred for V domain linkage, and the most common composition consists of three (G_4S) repeats. LYNDAL repertoires were cloned into the pHEN-derived vector pHENIS that encodes for a 14 aa $(G_4S)_2G_2SA$ linker with highly hydrophilic and flexible character (**Figure 8**). This linker was completed by a C-terminal-located glutamine that had been introduced during light chain cloning because the utilized ApaLI restriction site encoded for an additional cytosine. Although other codons would be possible, the CAA triplet was chosen due to the hydrophilic and uncharged character of encoded glutamine. Indeed, the designed LYNDAL linker seems to be useful because selected scFvs could be expressed in high yields (**Figure 21**, **Figure 35**), were proteolytic resistant, and most selected fragments showed predominately formation of monomeric products in SEC profiles (**Figure 22**, **Figure 36**).

Formation of additional dimers and even higher aggregates in some cases of LYNDAL-derived scFvs is in line with previous reports stating that various scFvs tend to form dimers or higher molecular weight species especially after periplasmic production [252-259]. Dimer formation has been described for scFvs of limited stability and is caused by dissociation of the two variable domains due to destabilization of their interface [253,260]. Conversion from monomer to dimer depends on many factors, such as presence of the antigen, ion strength, and buffer pH. Furthermore, dimer formation can be promoted by other conditions, e.g., increasing protein concentration [255], short linker lengths of 15-20 aa [261], and thawing of frozen preparations [256]. It was speculated that dimers most likely exist in the form of domain–swapped diabodies [260], and indeed the two functional binding sites of the dimeric fraction of LNYDAL-derived scFv H28 indicates that at least this fragment exist as defined diabody.

4.9 Source of antibody genes

Access to human antibody genes is generally restricted to B cells of the peripheral blood. Actually, the majority of both naïve and immune libraries were cloned from this source [52,57-60,262-264]. To include the rarely mutated germline genes of rearranged antibodies, naïve libraries were mostly prepared from the IgM and/or IgD repertoires because mature naïve B cells express both classes on their surfaces. In contrast, immune libraries aimed at cloning antibody genes from antigen-activated B cells after somatic hypermutation and are therefore mostly prepared from class-switched IgGs representing the most of serum immunoglobulins. In fact, peripheral blood was frequently used for immune library cloning because it contains a high number of antigen-specific plasmablast [49] and is therefore highly appropriate for capturing HuMAbs from ongoing infections. However, cloning of past immunological responses, as needed for the LYNDAL concept, requires a high diversity and number of activated (memory) B cells that are rarely found in the peripheral blood. Actually, other sources being rich in activated B cells have been applied for immune library cloning, e.g., bone marrow [51,56,148,149], spleen [265,266], and lymph nodes [267-270]. Until now there are only limited examinations comparing the quality of different B cell sources for library cloning. However, lymph nodes have been reported to be a superior source for library cloning as assessed by

the number of mature and activated B cells as well as the amount of PCR-amplifiable antibody genes [271]. Furthermore, the highly hypermutated nature of such selected mAbs has been confirmed [272] indicating that they were derived from B cells being generated during an antigen-encountered immune response. Moreover, two publications have shown that libraries being derived from (draining) murine lymph nodes are superior for selecting diverse and high affinity antibodies [273,274]. As a matter of fact, fundamental processes of the humoral immunity take place within the lymph node germinal centers, such as somatic hypermutation, class switch recombination, and differentiation of clonally expanded B cells into memory B and plasma cells [275,276]. Furthermore, lymph nodes per se contain a high number of antigen-encountered and activated B lymphocytes [277,278] including a conceptually interesting subset of re-entered and re-activated IgG-positive memory cells harboring extensive somatic hypermutation [279]. Indeed, all selected LYNDAL antibodies thus far have accumulated a particularly high level of somatic hypermutations. As a result, the average number of mutated amino acids from the high affinity LYNDAL antibodies was higher than that reported for hyperimmunized vaccinated individuals (25.3, n = 41 versus 20.5, n = 594) that was hypothesized to represent a fully-matured humoral immune response [280]. Most importantly, this thesis shows for the first time that cloning of entirely lymph node-derived libraries can deliver high affinity antiviral antibodies that partly possess promising neutralizing properties. Thus far, such human antibodies were exclusively obtained from (sorted) blood [19,22,23,57,58,281] or bone marrow B cells [54,149,282]. Moreover, it has been shown that cloning of immune libraries from tumor-draining lymph nodes can deliver high affinity antitumoral autoantibodies that were produced during a natural immune response in tumor patients. Latter strategy was additionally confirmed by a recent publication showing that antitumor antibodies can be selected from lymph nodes of cancer patients, e.g., against the tumor-associated antigens HER2 and CEA [270]. Furthermore, the LYNDAL concept shows for the first time that autoantibodies against the extracellular region of EGFR can be recovered from tumor patient repertoires. In conclusion, cloning the fossil record from donor lymph nodes is highly valuable for selecting human mAbs against a broad range of targets where a natural immune response has occurred within donors. Moreover, employing tumor-draining lymph nodes from cancer patients increases the chance to select tumor-related autoantibodies. In future, performing antibody selections using novel or refined

approaches, e.g. library panning on intact tumor cells [283], are expected to further improve the selection success for LYNDAL.

4.10 Selection of antiviral neutralizing antibodies

Based on novel approaches or technical improvements within the last decades, various potent human neutralizing mAbs against a range of viral diseases have been isolated. The majority was derived from immunized or vaccinated repertoires employing humanized transgenic mice [284], human hybridomas [285-288], immortalized human B cells [289-291], single-cell cloning [22,23,281,292], and combinatorial immune libraries [293]. In general, latest technological proceedings even allowed the isolation of broadly neutralizing antibodies against complex targets, such as influenza virus [286,288,292], HIV [22,23,281], and HCV [284]. Particularly, combinatorial immune libraries delivered therapeutically interesting antiviral mAbs against a wide range of antiviral targets like measles [54], influenza [56], rotavirus [294], rabies [58], hepatitis A, B, and C [57,63,295], RSV [296], HIV [51,297,298], rubella, CMV, VZV, and HSV [149]. In contrast, only a few reports exist about the isolation of antiviral mAbs from non-immunized repertoires [299,300] indicating that in general immunized human sources are preferred for the development of antiviral human mAbs. Indeed, as shown by the group of Rolf Zinkernagel analyzing B cell repertoires from vesicular stromatitis virus (VSV)-infected mice, antiviral human mAbs from immunized repertoires may possess superior neutralizing properties when derived from secondary or hyperimmune responses compared to naïve or primary repertoires [64,65]. Employing LYNDAL from seropositive donors (**Figure 14**) a broad range of specific (**Figure 23**) and high affinity scFvs (**Figure 24**, **Figure 25**, **Table 20**) against gB-1 could be isolated that partially possessed neutralizing activities (**Figure 26**). In fact, all such isolated scFv showed extensive somatic hypermutations in the range of a secondary or hyperimmune response (**Figure 18**) [280]. Moreover, several scFvs revealed clonal relation of the identified VH/VL pairings indicating that they were derived from the same host as response to the apparent HSV infection (**Figure 17**). All of the gB-1-selected LNYDAL scFvs showed cross-reactivity to HSV-2 (**Figure 23**) that may be attributed to the overall amino acid homology of both viral gB proteins of about 87%. Based on the presented data, it is speculated that this sequence

similarity is directly translated into a high structural similarity of both serotypes although only the crystal structure of HSV-1 has been resolved yet [93]. As a matter of fact, LYNDAL selection of HSV-specific scFvs was highly efficient although only few seropositive donor libraries were combined for panning. In conclusion, more high affinity binders with therapeutic relevance for HSV neutralization is supposed to be expected after panning of further seropositive LYNDAL donors. Thus far, there are only limited reports about generated human monoclonal antibodies against glycoprotein B of HSV [150,301] despite it is the main fusogenic protein, and targeting this protein seems to be highly promising for immunotherapy [144,152]. In fact, this thesis represents the first report about such a broad panel of human gB-specific mAbs that may be valuable for investigation of the natural immune response against herpes simplex virus in future. Although several HSV-specific scFvs with nanomolar binding affinities could be isolated from LYNDAL, only a few (24%), however, showed neutralizing activity (**Figure 26**).

It has previously been shown that valency of gB-specific antibodies can have a strong effect on their HSV neutralizing capacity [144]. It is therefore conceivable that testing of bivalent formats possibly reveals neutralizing potential. In the presented thesis, it has been shown that for some monovalent fragments neutralizing activities improved after cross-linking. Nevertheless, only the best neutralizing antibody H28 was further investigated in different formats. In this case, both bivalent formats, the dimeric $(scFv)_2$ and the scFv-Fc, showed indeed higher neutralizing efficacy. The larger scFv-Fc was less effective than the smaller, dimeric $(scFv)_2$ supporting the conclusion that smaller, bivalent constructs, such as diabodies, are favorable for the neutralizing activity of antibody H28. To achieve improved therapeutic effects of H28, further optimization is necessary, e.g., by increasing the antibody affinity or evaluation of the best V domain linker length and composition. The similar binding affinities of H28 to HSV-1 and HSV-2 (**Figure 27**) indicate that a serotype common epitope may be recognized. Surprisingly, H28 revealed differences in the neutralizing efficacy for both HSV serotypes showing better neutralizing activity for HSV-2 (**Figure 28**). Excluding the binding affinity, other biological reasons may be responsible for the different neutralizing behaviors that have to be investigated in the future. As an outlook for the therapeutic development of antibody H28, it is interesting to evaluate whether Fc-dependent effector functions or the combination of several

potent therapeutic antibodies, such as hu2c [144,152], can further increase the therapeutic effect.

4.11 Selection of tumor-associated autoantibodies

One foremost goal of this thesis was the selection of autoantibodies against cancer-associated targets that possess therapeutic value. Therefore, the LNYDAL repertoires were cloned from exclusively tumor-draining lymph nodes from head and neck cancer patients. As shown by other researchers, antibody responses against tumor-associated self antigens may be a common phenomenon during cancer diseases as a result of cancer immunosurveillance [302-305], and their use as biomarkers for early detection of cancer or prognosis markers has already been evaluated [304,306-309]. Autoantibody formation might be caused by increased immunogenicity of tumor cell-derived proteins that have undergone different alterations, e.g., overexpression, mutations, misfolding, or aberrant expression [304]. Thus far, less is known how these modifications can trigger antibody responses. One hypothesis is based on the fact that many autoantibodies are generated against modified intracellular proteins [310] which are released from tumor cells in an inflammatory environment after aberrant tumor cell death, e.g., by apoptosis or necrosis [311,312]. However, formation of autoantibodies against extracellular membrane proteins, such as HER2 and CEA, has also been reported [313-317]. These autoantibodies have been proven to be useful as diagnostic markers [317,318] and seem even to be valuable as drugs for immunotherapy. Using cloned antibody repertoires from cancer patients, several groups could identify antibodies with specificities to cancer-related antigens including extracellular membrane proteins [52,270,319-321]. However, EGFR-specific autoantibodies from cancer patient repertoires have not been reported yet, and human EGFR-specific antibodies were so far only recovered from naïve repertoires [322-326]. In general, the human EGF receptor is a valuable target for cancer immunotherapy because of its strong overexpression in many cancers including those of the head and neck. The overexpression of EGFR in head and neck carcinoma therefore may also induce autoantibody formation in these patients. Indeed, the LYNDAL concept allowed the selection of several EGFR-specific scFvs from seropositive head and neck cancer patient repertoires. Although one could argue that these antibodies might be the

product of randomly parings of non-target-specific antibodies, the development of such antibodies as the result of an autoimmune response is very likely for the following reasons. First, the recovered scFvs all accumulated a high level of somatic mutations that is in the range of a secondary immune response [280]. Next, the selected scFvs revealed highly specific recognition to a broad range of EGFR overexpressing cell lines and showed no cross-reactivity towards EGFR-negative cell lines. Finally, the analyzed scFvs possessed good monovalent binding affinities (11 nM to 257 nM) despite the limited size of the applied LYNDAL repertoire ($8x10^8$ members). In contrast, EGFR-selection of non-immune libraries with comparable or even larger repertoires delivered lower affinity scFvs, e.g., 200-600 nM ($1x10^9$ members) [36], 246 nM ($2x10^9$ members) [76], 217 nM–300 nM ($7x10^9$ members) [322], and 472 nM ($6.5x10^{10}$ members) [323]. In fact, much larger naïve repertoires had to be screened to isolate antibodies with similar affinities. For example, panning the commercial CAT1.0 library with $1.4x10^{10}$ fragments delivered six scFvs with binding affinities between 2-120 nM [327]. Selection of murine phage display libraries that had been prepared from EGFR-immunized mice [273] did not outperform LYNDAL thus indicating that the full potential of the immunized LYNDAL repertoires might be exploited for this target. In this previous study, only four out of ten murine scFvs recognized both recombinant and cellularly expressed EGFR with an affinity of about 19 nM for the best bivalent antibody. In contrast, all seven LYNDAL scFvs were highly specific in recognition of cellular EGFR (**Figure 37**), and the best bivalent antibody possessed a similar binding affinity to EGFR on A431 tumor cells than approved cetuximab (1.6 nM versus 2.0 nM) (**Figure 43**).

To investigate the therapeutic potential of the EGFR-specific autoantibodies, EGF-dependent *in vitro* proliferation assays were performed. These revealed that 80% of the investigated scFv may induce proliferative effects on tumor cells and only 20% prevent tumor proliferation (**Figure 40**). Although the analyzed number of EGFR autoantibodies is not significant (n = 5), this result is a hint that EGFR autoantibodies in common possess biological functions that can influence the natural EGFR signaling and may mainly stimulate tumor growth in tumor patients. These findings are in accordance with Olsen et al. who observed that increased concentration of EGFR autoantibodies in tumor patients resulted in worse prognosis and reduced disease-free survival times [328]. Nevertheless, although the most antibody fragments showed tumor-growth activation, scFv-Fc E6 mediated anti-proliferative

effects on EGF-sensitive SKOV-3 tumor cells that were comparable with the humanized scFv-Fc version of cetuximab (**Figure 44**). Moreover, cytotoxicity assays revealed promising cell inhibiting effects on different head and neck cancer cell lines (Stefan Kiesgen, personal communication) indicating that further exploration of antibody E6 for clinically development is warranted.

LYNDAL serum screening revealed not only EGFR autoantibody formation within head and neck cancer patients but also within the healthy control cohort (**Figure 31**). Although EGFR autoantibodies were mainly reported in diseased individuals [329,330], measurable levels of such antibodies were also observed within healthy populations [328,329]. The reasons for occurring of such autoantibodies in healthy individuals are not clear, however, the obtained results may indicate that the immune system in general possesses the capability for modulating EGFR signaling by autoantibodies that can mediate growth inhibitory and stimulating effects. Indeed, the opportunities of autoantibodies for influencing the EGFR signaling are diverse because the extracellular domain of EGFR contains binding sites for several natural ligands, such as EGF [186]. Competition of autoantibodies with these natural ligands for binding or antibody-induced receptor internalization may modulate the EGFR signaling. Indeed, three of the here investigated LYNDAL antibodies interfere with EGF binding and mediate both proliferative and anti-proliferative effects on human tumor cells. However, the underlying mechanisms for these effects have not been investigated yet and should be analyzed in the future. In conclusion, the LYNDAL concept is appropriate to isolate tumor-related autoantibodies that possess biological functions. As observed for LYNDAL donors, cancer patient repertoires in common might predominantly possess EGFR autoantibodies of proliferating nature, and extensive screening might be therefore required to isolate scFvs with therapeutically exploitable properties from such repertoires.

4.12 Selection of antibodies against further therapeutic targets

Although not explicitly shown within the result section, the LYNDAL concept was additionally evaluated on other human self antigens. For example, much effort was done for selecting therapeutically valuable antibodies against the human MET receptor, a RTK and protooncogene that is frequently overexpressed in human cancers, e.g., in head and neck cancer with about 42% [331]. Aberrant activation of

the MET receptor triggers signaling cascades that promote tumor growth, angiogenesis, and metastasis, and MET overexpression is generally correlated with poor prognosis [332,333]. Several selection experiments against recombinant MET-Fc has been performed using LYNDAL that not exceeded altogether $8.0x10^8$ clones. However, the used LYNDAL were all derived from donors with limited antigen-specific IgG response that were comparable with those of included healthy control individuals. As a result, MET selections mainly delivered antibody fragments with incomplete VH genes. These so selected binders possessed sequence-similar, hypermutated VL genes that were all derived from the same germline sequence (6a). Performing further selections with libraries possessing a fixed MET-specific VL gene and randomly combined VH genes, scFvs with nanomolar affinities to the MET receptor were finally selected. Based on these results, it is likely that the final VH/VL combinations of the MET-specific scFvs were not derived from naturally occurring combinations that had been developed within employed donors. In conclusion, LYNDAL selection should be preferably performed with libraries from donors with high antigen-specific IgG titers. Otherwise, the complete LYNDAL collection can be utilized for panning to increase the chance to isolate high affinity scFvs with non-naturally occurring VH/VL sequence combinations.

4.13 Summary and prospects

The herein presented LYNDAL concept is an applicable approach for recovering fully human antibody fragments with therapeutic potential. Cloning of antigen-encountered, lymph node-derived B cell repertoires from several donors provides a valuable alternative for selecting high affinity human antibody fragments with immunological unique functional properties. In fact, prepared donor libraries possessed high diversity and functional quality and cloned repertoires may therefore represent the antibody immune history of the included donors. Proof-of-concept was shown by selection of high affinity scFvs with high binding specificity against two completely different targets, i.e., one viral and one cancer-related antigen. As a sign for antigen-driven affinity maturation within donors, all scFvs possessed a high level of somatic hypermutations. The primary goal, the selection of biologically functional and therapeutically interesting antibody fragments, was confirmed for both investigated targets delivering antibodies with either virus-neutralizing (H28) or tumor

cell growth reducing property (E6). In future, LYNDAL can be further utilized to characterize the antibody response to natural infections and the autoimmune response against cancer-related targets as well. By employing the immune repertoires for panning against autologous tumor material, LYNDAL can be also applied for the identification of novel tumor-associated antigens including the selection of appropriate human monoclonal antibodies for immunotherapy. Moreover, in cases where no immunization occurred in LYNDAL donors, antibodies are expected to be still selectable when the whole LNYDAL collection is employed for panning then acting as large non-immunized library. In contrast to antibodies being derived from naïve repertoires, these binders may possess high levels of somatic mutations and it remains to be seen whether such antibodies can be exploited for therapeutic applications. Using the efficient system of the human antibody response, however, scFvs with unique functional properties might be preferentially selected from immunized LYNDAL repertoires. In conclusion, the herein presented concept has been shown to be valuable for recovering human scFvs with therapeutic potential. These antibody fragments should be further developed for therapeutic application, e.g., by investigation of the modes of action, improving affinities, and coupling to novel effector functions. Showing the value of LYNDAL for isolating of *in vivo*-matured antibody fragments with promising therapeutic properties, the concept is expected to be extendable to other B cell sources (e.g., tumor infiltrating B cells), patient cohorts, and other disease-specific targets, especially for other viral and head and neck tumor-related antigens.

References

1. Kohler G, Milstein C (1975) Continuous cultures of fused cells secreting antibody of predefined specificity. Nature 256: 495-497.
2. Sears HF, Atkinson B, Mattis J, Ernst C, Herlyn D, et al. (1982) Phase-I clinical trial of monoclonal antibody in treatment of gastrointestinal tumours. Lancet 1: 762-765.
3. Dillman RO, Shawler DL, Dillman JB, Royston I (1984) Therapy of chronic lymphocytic leukemia and cutaneous T-cell lymphoma with T101 monoclonal antibody. J Clin Oncol 2: 881-891.
4. Klee GG (2000) Human anti-mouse antibodies. Arch Pathol Lab Med 124: 921-923.
5. Boulianne GL, Hozumi N, Shulman MJ (1984) Production of functional chimaeric mouse/human antibody. Nature 312: 643-646.
6. Morrison SL, Johnson MJ, Herzenberg LA, Oi VT (1984) Chimeric human antibody molecules: mouse antigen-binding domains with human constant region domains. Proc Natl Acad Sci U S A 81: 6851-6855.
7. Jones PT, Dear PH, Foote J, Neuberger MS, Winter G (1986) Replacing the complementarity-determining regions in a human antibody with those from a mouse. Nature 321: 522-525.
8. Nelson AL, Dhimolea E, Reichert JM (2010) Development trends for human monoclonal antibody therapeutics. Nat Rev Drug Discov 9: 767-774.
9. Reichert JM (2013) Antibodies to watch in 2013: Mid-year update. MAbs 5: 513-517.
10. Reichert JM (2013). http://www.antibodysociety.org/news/approved_mabs.php. Data current as of December, 2013.
11. Wilson PC, Andrews SF (2012) Tools to therapeutically harness the human antibody response. Nat Rev Immunol 12: 709-719.
12. Green LL (1999) Antibody engineering via genetic engineering of the mouse: XenoMouse strains are a vehicle for the facile generation of therapeutic human monoclonal antibodies. J Immunol Methods 231: 11-23.
13. Lonberg N (2005) Human antibodies from transgenic animals. Nat Biotechnol 23: 1117-1125.
14. Harel Inbar N, Benhar I (2012) Selection of antibodies from synthetic antibody libraries. Arch Biochem Biophys 526: 87-98.
15. Kwakkenbos MJ, Diehl SA, Yasuda E, Bakker AQ, van Geelen CM, et al. (2010) Generation of stable monoclonal antibody-producing B cell receptor-positive human memory B cells by genetic programming. Nat Med 16: 123-128.
16. Traggiai E, Becker S, Subbarao K, Kolesnikova L, Uematsu Y, et al. (2004) An efficient method to make human monoclonal antibodies from memory B cells: potent neutralization of SARS coronavirus. Nat Med 10: 871-875.
17. Yu X, McGraw PA, House FS, Crowe JE, Jr. (2008) An optimized electrofusion-based protocol for generating virus-specific human monoclonal antibodies. J Immunol Methods 336: 142-151.
18. Wardemann H, Yurasov S, Schaefer A, Young JW, Meffre E, et al. (2003) Predominant autoantibody production by early human B cell precursors. Science 301: 1374-1377.
19. Wrammert J, Smith K, Miller J, Langley WA, Kokko K, et al. (2008) Rapid cloning of high-affinity human monoclonal antibodies against influenza virus. Nature 453: 667-671.
20. Yu X, Tsibane T, McGraw PA, House FS, Keefer CJ, et al. (2008) Neutralizing antibodies derived from the B cells of 1918 influenza pandemic survivors. Nature 455: 532-536.
21. Walker LM, Phogat SK, Chan-Hui PY, Wagner D, Phung P, et al. (2009) Broad and potent neutralizing antibodies from an African donor reveal a new HIV-1 vaccine target. Science 326: 285-289.

22. Scheid JF, Mouquet H, Feldhahn N, Seaman MS, Velinzon K, et al. (2009) Broad diversity of neutralizing antibodies isolated from memory B cells in HIV-infected individuals. Nature 458: 636-640.

23. Scheid JF, Mouquet H, Ueberheide B, Diskin R, Klein F, et al. (2011) Sequence and structural convergence of broad and potent HIV antibodies that mimic CD4 binding. Science 333: 1633-1637.

24. Walker LM, Huber M, Doores KJ, Falkowska E, Pejchal R, et al. (2011) Broad neutralization coverage of HIV by multiple highly potent antibodies. Nature 477: 466-470.

25. Corti D, Voss J, Gamblin SJ, Codoni G, Macagno A, et al. (2011) A neutralizing antibody selected from plasma cells that binds to group 1 and group 2 influenza A hemagglutinins. Science 333: 850-856.

26. Hoogenboom HR (2005) Selecting and screening recombinant antibody libraries. Nat Biotechnol 23: 1105-1116.

27. Smith GP (1985) Filamentous fusion phage: novel expression vectors that display cloned antigens on the virion surface. Science 228: 1315-1317.

28. McCafferty J, Griffiths AD, Winter G, Chiswell DJ (1990) Phage antibodies: filamentous phage displaying antibody variable domains. Nature 348: 552-554.

29. Zahnd C, Amstutz P, Pluckthun A (2007) Ribosome display: selecting and evolving proteins in vitro that specifically bind to a target. Nat Methods 4: 269-279.

30. Hanes J, Pluckthun A (1997) In vitro selection and evolution of functional proteins by using ribosome display. Proc Natl Acad Sci U S A 94: 4937-4942.

31. Freudl R, Schwarz H, Stierhof YD, Gamon K, Hindennach I, et al. (1986) An outer membrane protein (OmpA) of Escherichia coli K-12 undergoes a conformational change during export. J Biol Chem 261: 11355-11361.

32. Fuchs P, Breitling F, Dubel S, Seehaus T, Little M (1991) Targeting recombinant antibodies to the surface of Escherichia coli: fusion to a peptidoglycan associated lipoprotein. Biotechnology (N Y) 9: 1369-1372.

33. Harvey BR, Georgiou G, Hayhurst A, Jeong KJ, Iverson BL, et al. (2004) Anchored periplasmic expression, a versatile technology for the isolation of high-affinity antibodies from Escherichia coli-expressed libraries. Proc Natl Acad Sci U S A 101: 9193-9198.

34. Mazor Y, Van Blarcom T, Mabry R, Iverson BL, Georgiou G (2007) Isolation of engineered, full-length antibodies from libraries expressed in Escherichia coli. Nat Biotechnol 25: 563-565.

35. Boder ET, Wittrup KD (1997) Yeast surface display for screening combinatorial polypeptide libraries. Nat Biotechnol 15: 553-557.

36. Feldhaus MJ, Siegel RW, Opresko LK, Coleman JR, Feldhaus JM, et al. (2003) Flow-cytometric isolation of human antibodies from a nonimmune Saccharomyces cerevisiae surface display library. Nat Biotechnol 21: 163-170.

37. Ho M, Nagata S, Pastan I (2006) Isolation of anti-CD22 Fv with high affinity by Fv display on human cells. Proc Natl Acad Sci U S A 103: 9637-9642.

38. Akamatsu Y, Pakabunto K, Xu Z, Zhang Y, Tsurushita N (2007) Whole IgG surface display on mammalian cells: Application to isolation of neutralizing chicken monoclonal anti-IL-12 antibodies. J Immunol Methods 327: 40-52.

39. Rondot S, Koch J, Breitling F, Dubel S (2001) A helper phage to improve single-chain antibody presentation in phage display. Nat Biotechnol 19: 75-78.

40. Marks JD, Hoogenboom HR, Bonnert TP, McCafferty J, Griffiths AD, et al. (1991) By-passing immunization. Human antibodies from V-gene libraries displayed on phage. J Mol Biol 222: 581-597.

41. Barbas CF, 3rd, Kang AS, Lerner RA, Benkovic SJ (1991) Assembly of combinatorial antibody libraries on phage surfaces: the gene III site. Proc Natl Acad Sci U S A 88: 7978-7982.

42. Kontermann RE (2010) Chapter 9: Immunotube selections. In: Antibody Engineering. Volume 1. Edited by Kontermann RE, Dübel S. Second edition: Springer Protocols. pp. 127-137.

43. Hawkins RE, Russell SJ, Winter G (1992) Selection of phage antibodies by binding affinity. Mimicking affinity maturation. J Mol Biol 226: 889-896.

44. Chames P, Hufton SE, Coulie PG, Uchanska-Ziegler B, Hoogenboom HR (2000) Direct selection of a human antibody fragment directed against the tumor T-cell epitope HLA-A1-MAGE-A1 from a nonimmunized phage-Fab library. Proc Natl Acad Sci U S A 97: 7969-74.

45. Robert R, Jacobin-Valat MJ, Daret D, Miraux S, Nurden AT, et al. (2006) Identification of human scFvs targeting atherosclerotic lesions: selection by single round in vivo phage display. J Biol Chem 281: 40135-40143.

46. Giordano RJ, Cardo-Vila M, Lahdenranta J, Pasqualini R, Arap W (2001) Biopanning and rapid analysis of selective interactive ligands. Nat Med 7: 1249-1253.

47. Ruan W, Sassoon A, An F, Simko JP, Liu B (2006) Identification of clinically significant tumor antigens by selecting phage antibody library on tumor cells in situ using laser capture microdissection. Mol Cell Proteomics 5: 2364-2373.

48. Geyer CR, McCafferty J, Dubel S, Bradbury AR, Sidhu SS (2012) Recombinant antibodies and in vitro selection technologies. Methods Mol Biol 901: 11-32.

49. Fink K (2012) Origin and Function of Circulating Plasmablasts during Acute Viral Infections. Front Immunol 3: 78.

50. Clackson T, Hoogenboom HR, Griffiths AD, Winter G (1991) Making antibody fragments using phage display libraries. Nature 352: 624-628.

51. Burton DR, Barbas CF, 3rd, Persson MA, Koenig S, Chanock RM, et al. (1991) A large array of human monoclonal antibodies to type 1 human immunodeficiency virus from combinatorial libraries of asymptomatic seropositive individuals. Proc Natl Acad Sci U S A 88: 10134-10137.

52. Cai X, Garen A (1995) Anti-melanoma antibodies from melanoma patients immunized with genetically modified autologous tumor cells: selection of specific antibodies from single-chain Fv fusion phage libraries. Proc Natl Acad Sci U S A 92: 6537-6541.

53. Chapal N, Chardes T, Bresson D, Pugniere M, Mani JC, et al. (2001) Thyroid peroxidase autoantibodies obtained from random single chain FV libraries contain the same heavy/light chain combinations as occur in vivo. Endocrinology 142: 4740-4750.

54. de Carvalho Nicacio C, Williamson RA, Parren PW, Lundkvist A, Burton DR, et al. (2002) Neutralizing human Fab fragments against measles virus recovered by phage display. J Virol 76: 251-258.

55. Gabibov AG, Belogurov AA, Jr., Lomakin YA, Zakharova MY, Avakyan ME, et al. (2011) Combinatorial antibody library from multiple sclerosis patients reveals antibodies that cross-react with myelin basic protein and EBV antigen. FASEB J 25: 4211-4221.

56. Kashyap AK, Steel J, Oner AF, Dillon MA, Swale RE, et al. (2008) Combinatorial antibody libraries from survivors of the Turkish H5N1 avian influenza outbreak reveal virus neutralization strategies. Proc Natl Acad Sci U S A 105: 5986-5991.

57. Kim SJ, Jang MH, Stapleton JT, Yoon SO, Kim KS, et al. (2004) Neutralizing human monoclonal antibodies to hepatitis A virus recovered by phage display. Virology 318: 598-607.

58. Kramer RA, Marissen WE, Goudsmit J, Visser TJ, Clijsters-Van der Horst M, et al. (2005) The human antibody repertoire specific for rabies virus glycoprotein as selected from immune libraries. Eur J Immunol 35: 2131-2145.

59. Mao S, Gao C, Lo CH, Wirsching P, Wong CH, et al. (1999) Phage-display library selection of high-affinity human single-chain antibodies to tumor-associated carbohydrate antigens sialyl Lewisx and Lewisx. Proc Natl Acad Sci U S A 96: 6953-6958.

60. Persson MA, Caothien RH, Burton DR (1991) Generation of diverse high-affinity human monoclonal antibodies by repertoire cloning. Proc Natl Acad Sci U S A 88: 2432-2436.

61. Raats JM, Wijnen EM, Pruijn GJ, van den Hoogen FH, van Venrooij WJ (2003) Recombinant human monoclonal autoantibodies specific for citrulline-containing peptides from phage display libraries derived from patients with rheumatoid arthritis. J Rheumatol 30: 1696-1711.

62. Thie H, Toleikis L, Li J, von Wasielewski R, Bastert G, et al. (2011) Rise and fall of an anti-MUC1 specific antibody. PLoS One 6: e15921.

63. Zebedee SL, Barbas CF, 3rd, Hom YL, Caothien RH, Graff R, et al. (1992) Human combinatorial antibody libraries to hepatitis B surface antigen. Proc Natl Acad Sci U S A 89: 3175-3179.

64. Kalinke U, Bucher EM, Ernst B, Oxenius A, Roost HP, et al. (1996) The role of somatic mutation in the generation of the protective humoral immune response against vesicular stomatitis virus. Immunity 5: 639-652.

65. Kalinke U, Oxenius A, Lopez-Macias C, Zinkernagel RM, Hengartner H (2000) Virus neutralization by germ-line vs. hypermutated antibodies. Proc Natl Acad Sci U S A 97: 10126-10131.

66. Hammond PW (2010) Accessing the human repertoire for broadly neutralizing HIV antibodies. MAbs 2: 157-164.

67. Weiss-Ottolenghi Y, Gershoni JM (2014) Profiling the IgOme: Meeting the challenge. FEBS Lett 588: 318-325.

68. Vaughan TJ, Williams AJ, Pritchard K, Osbourn JK, Pope AR, et al. (1996) Human antibodies with sub-nanomolar affinities isolated from a large non-immunized phage display library. Nat Biotechnol 14: 309-314.

69. Sheets MD, Amersdorfer P, Finnern R, Sargent P, Lindquist E, et al. (1998) Efficient construction of a large nonimmune phage antibody library: the production of high-affinity human single-chain antibodies to protein antigens. Proc Natl Acad Sci U S A 95: 6157-6162.

70. de Haard HJ, van Neer N, Reurs A, Hufton SE, Roovers RC, et al. (1999) A large non-immunized human Fab fragment phage library that permits rapid isolation and kinetic analysis of high affinity antibodies. J Biol Chem 274: 18218-18230.

71. Ackerman ME, Lai JI, Pastan I, Wittrup KD (2011) Exploiting bias in a non-immune human antibody library to predict antigenicity. Protein Eng Des Sel 24: 845-853.

72. Griffiths AD, Williams SC, Hartley O, Tomlinson IM, Waterhouse P, et al. (1994) Isolation of high affinity human antibodies directly from large synthetic repertoires. EMBO J 13: 3245-3260.

73. Pini A, Viti F, Santucci A, Carnemolla B, Zardi L, et al. (1998) Design and use of a phage display library. Human antibodies with subnanomolar affinity against a marker of angiogenesis eluted from a two-dimensional gel. J Biol Chem 273: 21769-21776.

74. Hoet RM, Cohen EH, Kent RB, Rookey K, Schoonbroodt S, et al. (2005) Generation of high-affinity human antibodies by combining donor-derived and synthetic complementarity-determining-region diversity. Nat Biotechnol 23: 344-348.

75. Soderlind E, Strandberg L, Jirholt P, Kobayashi N, Alexeiva V, et al. (2000) Recombining germline-derived CDR sequences for creating diverse single-framework antibody libraries. Nat Biotechnol 18: 852-856.

76. Knappik A, Ge L, Honegger A, Pack P, Fischer M, et al. (2000) Fully synthetic human combinatorial antibody libraries (HuCAL) based on modular consensus frameworks and CDRs randomized with trinucleotides. J Mol Biol 296: 57-86.

77. Silacci M, Brack S, Schirru G, Marlind J, Ettorre A, et al. (2005) Design, construction, and characterization of a large synthetic human antibody phage display library. Proteomics 5: 2340-2350.

78. Rothe C, Urlinger S, Lohning C, Prassler J, Stark Y, et al. (2008) The human combinatorial antibody library HuCAL GOLD combines diversification of all six CDRs according to the natural immune system with a novel display method for efficient selection of high-affinity antibodies. J Mol Biol 376: 1182-1200.

79. Prassler J, Thiel S, Pracht C, Polzer A, Peters S, et al. (2011) HuCAL PLATINUM, a synthetic Fab library optimized for sequence diversity and superior performance in mammalian expression systems. J Mol Biol 413: 261-278.

80. Tiller T, Schuster I, Deppe D, Siegers K, Strohner R, et al. (2013) A fully synthetic human Fab antibody library based on fixed VH/VL framework pairings with favorable biophysical properties. MAbs 5.

81. Perelson AS, Oster GF (1979) Theoretical studies of clonal selection: minimal antibody repertoire size and reliability of self-non-self discrimination. J Theor Biol 81: 645-670.

82. Perelson AS (1989) Immune network theory. Immunol Rev 110: 5-36.

83. Sblattero D, Bradbury A (2000) Exploiting recombination in single bacteria to make large phage antibody libraries. Nat Biotechnol 18: 75-80.

84. Lloyd C, Lowe D, Edwards B, Welsh F, Dilks T, et al. (2009) Modelling the human immune response: performance of a 1011 human antibody repertoire against a broad panel of therapeutically relevant antigens. Protein Eng Des Sel 22: 159-168.

85. Schwimmer LJ, Huang B, Giang H, Cotter RL, Chemla-Vogel DS, et al. (2013) Discovery of diverse and functional antibodies from large human repertoire antibody libraries. J Immunol Methods 391: 60-71.

86. Arama V, Cercel AS, Vladareanu R, Mihai C, Mihailescu R, et al. (2010) Type-specific herpes simplex virus-1 and herpes simplex virus-2 seroprevalence in Romania: comparison of prevalence and risk factors in women and men. Int J Infect Dis 14 Suppl 3: e25-31.

87. Doi Y, Ninomiya T, Hata J, Yonemoto K, Tanizaki Y, et al. (2009) Seroprevalence of herpes simplex virus 1 and 2 in a population-based cohort in Japan. J Epidemiol 19: 56-62.

88. Kramer MA, Uitenbroek DG, Ujcic-Voortman JK, Pfrommer C, Spaargaren J, et al. (2008) Ethnic differences in HSV1 and HSV2 seroprevalence in Amsterdam, the Netherlands. Euro Surveill 13.

89. Lupi O (2011) Prevalence and risk factors for herpes simplex infection among patients at high risk for HIV infection in Brazil. Int J Dermatol 50: 709-713.

90. Xu F, Markowitz LE, Gottlieb SL, Berman SM (2007) Seroprevalence of herpes simplex virus types 1 and 2 in pregnant women in the United States. Am J Obstet Gynecol 196: 43 e41-46.91. Taylor TJ, Brockman MA, McNamee EE, Knipe DM (2002) Herpes simplex virus. Front Biosci 7: d752-764.

91. Taylor TJ, Brockman MA, McNamee EE, Knipe DM (2002) Herpes simplex virus. Front Biosci 7: d752-764.

92. Connolly SA, Jackson JO, Jardetzky TS, Longnecker R (2011) Fusing structure and function: a structural view of the herpesvirus entry machinery. Nat Rev Microbiol 9: 369-381.

93. Heldwein EE, Lou H, Bender FC, Cohen GH, Eisenberg RJ, et al. (2006) Crystal structure of glycoprotein B from herpes simplex virus 1. Science 313: 217-220.

94. Carter JB, Saunders VA (2010) Chapter 11: Herpesviruses (and other dsDNA viruses. In: Virology: principles and applications. Second edition: John Wiley & Sons. pp. 121-133.

95. Johnson DC, Huber MT (2002) Directed egress of animal viruses promotes cell-to-cell spread. J Virol 76: 1-8.

96. Mellerick DM, Fraser NW (1987) Physical state of the latent herpes simplex virus genome in a mouse model system: evidence suggesting an episomal state. Virology 158: 265-275.

97. Chentoufi AA, Kritzer E, Yu DM, Nesburn AB, Benmohamed L (2012) Towards a rational design of an asymptomatic clinical herpes vaccine: the old, the new, and the unknown. Clin Dev Immunol 2012: 187585.

98. Looker KJ, Garnett GP, Schmid GP (2008) An estimate of the global prevalence and incidence of herpes simplex virus type 2 infection. Bull World Health Organ 86: 805-812, A.

99. Straface G, Selmin A, Zanardo V, De Santis M, Ercoli A, et al. (2012) Herpes simplex virus infection in pregnancy. Infect Dis Obstet Gynecol 2012: 385697.

100. Mindel A, Marks C (2005) Psychological symptoms associated with genital herpes virus infections: epidemiology and approaches to management. CNS Drugs 19: 303-312.

101. Freeman EE, Weiss HA, Glynn JR, Cross PL, Whitworth JA, et al. (2006) Herpes simplex virus 2 infection increases HIV acquisition in men and women: systematic review and meta-analysis of longitudinal studies. AIDS 20: 73-83.

102. Johnston C, Saracino M, Kuntz S, Magaret A, Selke S, et al. (2012) Standard-dose and high-dose daily antiviral therapy for short episodes of genital HSV-2 reactivation: three randomised, open-label, cross-over trials. Lancet 379: 641-647.

103. Flagg EW, Weinstock H (2011) Incidence of neonatal herpes simplex virus infections in the United States, 2006. Pediatrics 127: e1-8.

104. Whitley RJ, Nahmias AJ, Visintine AM, Fleming CL, Alford CA (1980) The natural history of herpes simplex virus infection of mother and newborn. Pediatrics 66: 489-494.

105. Whitley RJ (2006) Herpes simplex encephalitis: adolescents and adults. Antiviral Res 71: 141-148.

106. Farooq AV, Shukla D (2012) Herpes simplex epithelial and stromal keratitis: an epidemiologic update. Surv Ophthalmol 57: 448-462.

107. Dawson CR, Togni B (1976) Herpes simplex eye infections: clinical manifestations, pathogenesis and management. Surv Ophthalmol 21: 121-135.

108. Elion GB, Furman PA, Fyfe JA, de Miranda P, Beauchamp L, et al. (1977) Selectivity of action of an antiherpetic agent, 9-(2-hydroxyethoxymethyl) guanine. Proc Natl Acad Sci U S A 74: 5716-5720.

109. Danve-Szatanek C, Aymard M, Thouvenot D, Morfin F, Agius G, et al. (2004) Surveillance network for herpes simplex virus resistance to antiviral drugs: 3-year follow-up. J Clin Microbiol 42: 242-249.

110. Stranska R, Schuurman R, Nienhuis E, Goedegebuure IW, Polman M, et al. (2005) Survey of acyclovir-resistant herpes simplex virus in the Netherlands: prevalence and characterization. J Clin Virol 32: 7-18.

111. Bacon TH, Levin MJ, Leary JJ, Sarisky RT, Sutton D (2003) Herpes simplex virus resistance to acyclovir and penciclovir after two decades of antiviral therapy. Clin Microbiol Rev 16: 114-128.

112. Griffiths PD (2009) A perspective on antiviral resistance. J Clin Virol 46: 3-8.

113. Morfin F, Thouvenot D (2003) Herpes simplex virus resistance to antiviral drugs. J Clin Virol 26: 29-37.

114. Birch CJ, Tachedjian G, Doherty RR, Hayes K, Gust ID (1990) Altered sensitivity to antiviral drugs of herpes simplex virus isolates from a patient with the acquired immunodeficiency syndrome. J Infect Dis 162: 731-734.

115. Darville JM, Ley BE, Roome AP, Foot AB (1998) Acyclovir-resistant herpes simplex virus infections in a bone marrow transplant population. Bone Marrow Transplant 22: 587-589.

116. Lolis MS, Gonzalez L, Cohen PJ, Schwartz RA (2008) Drug-resistant herpes simplex virus in HIV infected patients. Acta Dermatovenerol Croat 16: 204-208.

117. Blot N, Schneider P, Young P, Janvresse C, Dehesdin D, et al. (2000) Treatment of an acyclovir and foscarnet-resistant herpes simplex virus infection with cidofovir in a child after an unrelated bone marrow transplant. Bone Marrow Transplant 26: 903-905.

118. Saint-Leger E, Fillet AM, Malvy D, Rabanel B, Caumes E (2001) [Efficacy of cidofovir in an HIV infected patient with an acyclovir and foscarnet resistant herpes simplex virus infection]. Ann Dermatol Venereol 128: 747-749.

119. Bryant P, Sasadeusz J, Carapetis J, Waters K, Curtis N (2001) Successful treatment of foscarnet-resistant herpes simplex stomatitis with intravenous cidofovir in a child. Pediatr Infect Dis J 20: 1083-1086.

120. Levin MJ, Bacon TH, Leary JJ (2004) Resistance of herpes simplex virus infections to nucleoside analogues in HIV-infected patients. Clin Infect Dis 39 Suppl 5: S248-257.

121. Biswas S, Field HJ (2008) Herpes simplex virus helicase-primase inhibitors: recent findings from the study of drug resistance mutations. Antivir Chem Chemother 19: 1-6.

122. Martinez V, Molina JM, Scieux C, Ribaud P, Morfin F (2006) Topical imiquimod for recurrent acyclovir-resistant HSV infection. Am J Med 119: e9-11.

123. Kleymann G, Fischer R, Betz UA, Hendrix M, Bender W, et al. (2002) New helicase-primase inhibitors as drug candidates for the treatment of herpes simplex disease. Nat Med 8: 392-398.

124. Field HJ, Huang ML, Lay EM, Mickleburgh I, Zimmermann H, et al. (2013) Baseline sensitivity of HSV-1 and HSV-2 clinical isolates and defined acyclovir-resistant strains to the helicase-primase inhibitor pritelivir. Antiviral Res 100: 297-299.

125. Roth K, Ferreira VH, Kaushic C (2013) HSV-2 vaccine: current state and insights into development of a vaccine that targets genital mucosal protection. Microb Pathog 58: 45-54.

126. Lee AJ, Ashkar AA (2012) Herpes simplex virus-2 in the genital mucosa: insights into the mucosal host response and vaccine development. Curr Opin Infect Dis 25: 92-99.

127. Awasthi S, Friedman HM (2013) A Paradigm Shift: Vaccine-Induced Antibodies as an Immune Correlate of Protection Against Herpes Simplex Virus Type 1 Genital Herpes. J Infect Dis.

128. Kern AB, Schiff BL (1964) Vaccine Therapy in Recurrent Herpes Simplex. Arch Dermatol 89: 844-845.

129. Kutinova L, Benda R, Kalos Z, Dbaly V, Votruba T, et al. (1988) Placebo-controlled study with subunit herpes simplex virus vaccine in subjects suffering from frequent herpetic recurrences. Vaccine 6: 223-228.

130. Mertz GJ, Ashley R, Burke RL, Benedetti J, Critchlow C, et al. (1990) Double-blind, placebo-controlled trial of a herpes simplex virus type 2 glycoprotein vaccine in persons at high risk for genital herpes infection. J Infect Dis 161: 653-660.

131. Skinner GR, Turyk ME, Benson CA, Wilbanks GD, Heseltine P, et al. (1997) The efficacy and safety of Skinner herpes simplex vaccine towards modulation of herpes genitalis; report of a prospective double-blind placebo-controlled trial. Med Microbiol Immunol 186: 31-36.

132. Corey L, Langenberg AG, Ashley R, Sekulovich RE, Izu AE, et al. (1999) Recombinant glycoprotein vaccine for the prevention of genital HSV-2 infection: two randomized controlled trials. Chiron HSV Vaccine Study Group. JAMA 282: 331-340.

133. Stanberry LR, Spruance SL, Cunningham AL, Bernstein DI, Mindel A, et al. (2002) Glycoprotein-D-adjuvant vaccine to prevent genital herpes. N Engl J Med 347: 1652-1661.

134. Belshe RB, Leone PA, Bernstein DI, Wald A, Levin MJ, et al. (2012) Efficacy results of a trial of a herpes simplex vaccine. N Engl J Med 366: 34-43.

135. Whitley RJ, Roizman B (2002) Herpes simplex viruses: is a vaccine tenable? J Clin Invest 110: 145-151.

136. Dropulic LK, Cohen JI (2012) The challenge of developing a herpes simplex virus 2 vaccine. Expert Rev Vaccines 11: 1429-1440.

137. Johnston C, Koelle DM, Wald A (2014) Current status and prospects for development of an HSV vaccine. Vaccine 32(14):1553-60.

138. Johnston C, Koelle DM, Wald A (2011) HSV-2: in pursuit of a vaccine. J Clin Invest 121: 4600-4609.

139. Hemming VG (2001) Use of intravenous immunoglobulins for prophylaxis or treatment of infectious diseases. Clin Diagn Lab Immunol 8: 859-863.

140. Marasco WA, Sui J (2007) The growth and potential of human antiviral monoclonal antibody therapeutics. Nat Biotechnol 25: 1421-1434.

141. Both L, Banyard AC, van Dolleweerd C, Wright E, Ma JK, et al. (2013) Monoclonal antibodies for prophylactic and therapeutic use against viral infections. Vaccine 31: 1553-1559.

142. Law M, Hangartner L (2008) Antibodies against viruses: passive and active immunization. Curr Opin Immunol 20: 486-492.

143. Flego M, Ascione A, Cianfriglia M, Vella S (2013) Clinical development of monoclonal antibody-based drugs in HIV and HCV diseases. BMC Med 11: 4.

144. Krawczyk A, Krauss J, Eis-Hubinger AM, Daumer MP, Schwarzenbacher R, et al. (2011) Impact of valency of a glycoprotein B-specific monoclonal antibody on neutralization of herpes simplex virus. J Virol 85: 1793-1803.

145. Drew PD, Moss MT, Pasieka TJ, Grose C, Harris WJ, et al. (2001) Multimeric humanized varicella-zoster virus antibody fragments to gH neutralize virus while monomeric fragments do not. J Gen Virol 82: 1959-1963.

146. Zhu Q, McAuliffe JM, Patel NK, Palmer-Hill FJ, Yang CF, et al. (2011) Analysis of respiratory syncytial virus preclinical and clinical variants resistant to neutralization by monoclonal antibodies palivizumab and/or motavizumab. J Infect Dis 203: 674-682.

147. Co MS, Deschamps M, Whitley RJ, Queen C (1991) Humanized antibodies for antiviral therapy. Proc Natl Acad Sci U S A 88: 2869-2873.

148. Burioni R, Williamson RA, Sanna PP, Bloom FE, Burton DR (1994) Recombinant human Fab to glycoprotein D neutralizes infectivity and prevents cell-to-cell transmission of herpes simplex viruses 1 and 2 in vitro. Proc Natl Acad Sci U S A 91: 355-359.

149. Williamson RA, Burioni R, Sanna PP, Partridge LJ, Barbas CF, 3rd, et al. (1993) Human monoclonal antibodies against a plethora of viral pathogens from single combinatorial libraries. Proc Natl Acad Sci U S A 90: 4141-4145.

150. Sanna PP, Williamson RA, De Logu A, Bloom FE, Burton DR (1995) Directed selection of recombinant human monoclonal antibodies to herpes simplex virus glycoproteins from phage display libraries. Proc Natl Acad Sci U S A 92: 6439-6443.

151. Sanna PP, De Logu A, Williamson RA, Hom YL, Straus SE, et al. (1996) Protection of nude mice by passive immunization with a type-common human recombinant monoclonal antibody against HSV. Virology 215: 101-106.

152. Krawczyk A, Arndt MA, Grosse-Hovest L, Weichert W, Giebel B, et al. (2013) Overcoming drug-resistant herpes simplex virus (HSV) infection by a humanized antibody. Proc Natl Acad Sci U S A 110: 6760-6765.

153. Klein F, Mouquet H, Dosenovic P, Scheid JF, Scharf L, et al. (2013) Antibodies in HIV-1 vaccine development and therapy. Science 341: 1199-1204.

154. Hefferon KL (2014) Broadly neutralizing antibodies and the promise of universal vaccines: where are we now? Immunotherapy 6: 51-57.

155. (2008) WHO World Cancer Report. Lyon: International Agency for Resarch on Cancer.

156. Jemal A, Bray F, Center MM, Ferlay J, Ward E, et al. (2011) Global cancer statistics. CA Cancer J Clin 61: 69-90.

157. Reichert JM, Dhimolea E (2012) The future of antibodies as cancer drugs. Drug Discov Today 17: 954-963.

158. Pardoll DM (2012) The blockade of immune checkpoints in cancer immunotherapy. Nat Rev Cancer 12: 252-264.

159. Kubota T, Niwa R, Satoh M, Akinaga S, Shitara K, et al. (2009) Engineered therapeutic antibodies with improved effector functions. Cancer Sci 100: 1566-1572.

160. Ducry L, Stump B (2010) Antibody-drug conjugates: linking cytotoxic payloads to monoclonal antibodies. Bioconjug Chem 21: 5-13.

161. Petersdorf SH, Kopecky KJ, Slovak M, Willman C, Nevill T, et al. (2013) A phase 3 study of gemtuzumab ozogamicin during induction and postconsolidation therapy in younger patients with acute myeloid leukemia. Blood 121: 4854-4860.

162. Alley SC, Okeley NM, Senter PD (2010) Antibody-drug conjugates: targeted drug delivery for cancer. Curr Opin Chem Biol 14: 529-537.

163. Lambert JM (2013) Drug-conjugated antibodies for the treatment of cancer. Br J Clin Pharmacol 76: 248-262.

164. Tomblyn M (2012) Radioimmunotherapy for B-cell non-hodgkin lymphomas. Cancer Control 19: 196-203.

165. Maher J, Adami AA (2013) Antitumor immunity: easy as 1, 2, 3 with monoclonal bispecific trifunctional antibodies? Cancer Res 73: 5613-5617.

166. Kontermann RE (2012) Dual targeting strategies with bispecific antibodies. MAbs 4: 182-197.

167. Arndt A, Diebolder P, Krauss J (2010) Neuentwicklungen in der Antikörpertherapie. In: Zeller WJ, zur Hausen H, editors. Onkologie: Grundlagen, Diagnostik, Therapie.

168. Shim H (2011) One target, different effects: a comparison of distinct therapeutic antibodies against the same targets. Exp Mol Med 43: 539-549.

169. Vokes EE, Chu E (2006) Anti-EGFR therapies: clinical experience in colorectal, lung, and head and neck cancers. Oncology (Williston Park) 20: 15-25.

170. Eccles SA (2011) The epidermal growth factor receptor/Erb-B/HER family in normal and malignant breast biology. Int J Dev Biol 55: 685-696.

171. Leemans CR, Braakhuis BJ, Brakenhoff RH (2011) The molecular biology of head and neck cancer. Nat Rev Cancer 11: 9-22.

172. Tan AR, Swain SM (2003) Ongoing adjuvant trials with trastuzumab in breast cancer. Semin Oncol 30: 54-64.

173. Bonner JA, Harari PM, Giralt J, Azarnia N, Shin DM, et al. (2006) Radiotherapy plus cetuximab for squamous-cell carcinoma of the head and neck. N Engl J Med 354: 567-578.

174. Vermorken JB, Mesia R, Rivera F, Remenar E, Kawecki A, et al. (2008) Platinum-based chemotherapy plus cetuximab in head and neck cancer. N Engl J Med 359: 1116-1127.

175. Citri A, Yarden Y (2006) EGF-ERBB signalling: towards the systems level. Nat Rev Mol Cell Biol 7: 505-516.

176. Ferguson KM, Berger MB, Mendrola JM, Cho HS, Leahy DJ, et al. (2003) EGF activates its receptor by removing interactions that autoinhibit ectodomain dimerization. Mol Cell 11: 507-517.

177. Garrett TP, McKern NM, Lou M, Elleman TC, Adams TE, et al. (2002) Crystal structure of a truncated epidermal growth factor receptor extracellular domain bound to transforming growth factor alpha. Cell 110: 763-773.

178. Ogiso H, Ishitani R, Nureki O, Fukai S, Yamanaka M, et al. (2002) Crystal structure of the complex of human epidermal growth factor and receptor extracellular domains. Cell 110: 775-787.

179. Burgess AW, Cho HS, Eigenbrot C, Ferguson KM, Garrett TP, et al. (2003) An open-and-shut case? Recent insights into the activation of EGF/ErbB receptors. Mol Cell 12: 541-552.

180. Schmitz KR, Ferguson KM (2009) Interaction of antibodies with ErbB receptor extracellular regions. Exp Cell Res 315: 659-670.

181. Oda K, Matsuoka Y, Funahashi A, Kitano H (2005) A comprehensive pathway map of epidermal growth factor receptor signaling. Mol Syst Biol 1: 2005 0010.

182. Seshacharyulu P, Ponnusamy MP, Haridas D, Jain M, Ganti AK, et al. (2012) Targeting the EGFR signaling pathway in cancer therapy. Expert Opin Ther Targets 16: 15-31.

183. Yarden Y, Sliwkowski MX (2001) Untangling the ErbB signalling network. Nat Rev Mol Cell Biol 2: 127-137.

184. Mendelsohn J, Baselga J (2006) Epidermal growth factor receptor targeting in cancer. Semin Oncol 33: 369-385.

185. Herbst RS, Shin DM (2002) Monoclonal antibodies to target epidermal growth factor receptor-positive tumors: a new paradigm for cancer therapy. Cancer 94: 1593-1611.

186. Normanno N, De Luca A, Bianco C, Strizzi L, Mancino M, et al. (2006) Epidermal growth factor receptor (EGFR) signaling in cancer. Gene 366: 2-16.

187. Salomon DS, Normanno N, Ciardiello F, Brandt R, Shoyab M, et al. (1995) The role of amphiregulin in breast cancer. Breast Cancer Res Treat 33: 103-114.

188. Pines G, Kostler WJ, Yarden Y (2010) Oncogenic mutant forms of EGFR: lessons in signal transduction and targets for cancer therapy. FEBS Lett 584: 2699-2706.

189. Nagane M, Coufal F, Lin H, Bogler O, Cavenee WK, et al. (1996) A common mutant epidermal growth factor receptor confers enhanced tumorigenicity on human glioblastoma cells by increasing proliferation and reducing apoptosis. Cancer Res 56: 5079-5086.

190. Sugawa N, Ekstrand AJ, James CD, Collins VP (1990) Identical splicing of aberrant epidermal growth factor receptor transcripts from amplified rearranged genes in human glioblastomas. Proc Natl Acad Sci U S A 87: 8602-8606.

191. Frederick L, Wang XY, Eley G, James CD (2000) Diversity and frequency of epidermal growth factor receptor mutations in human glioblastomas. Cancer Res 60: 1383-1387.

192. Pao W, Miller V, Zakowski M, Doherty J, Politi K, et al. (2004) EGF receptor gene mutations are common in lung cancers from "never smokers" and are associated with sensitivity of tumors to gefitinib and erlotinib. Proc Natl Acad Sci U S A 101: 13306-13311.

193. Geyer CE, Forster J, Lindquist D, Chan S, Romieu CG, et al. (2006) Lapatinib plus capecitabine for HER2-positive advanced breast cancer. N Engl J Med 355: 2733-2743.

194. Yarden Y, Pines G (2012) The ERBB network: at last, cancer therapy meets systems biology. Nat Rev Cancer 12: 553-563.

195. Alvarenga ML (2010) Innovative analytical tools in the biopharmaceutical development [Dissertation]. Bonn: Rheinische Friedrich-Wilhelms-Universität.

196. Sunada H, Magun BE, Mendelsohn J, MacLeod CL (1986) Monoclonal antibody against epidermal growth factor receptor is internalized without stimulating receptor phosphorylation. Proc Natl Acad Sci U S A 83: 3825-3829.

197. Li S, Schmitz KR, Jeffrey PD, Wiltzius JJ, Kussie P, et al. (2005) Structural basis for inhibition of the epidermal growth factor receptor by cetuximab. Cancer Cell 7: 301-311.

198. Kimura H, Sakai K, Arao T, Shimoyama T, Tamura T, et al. (2007) Antibody-dependent cellular cytotoxicity of cetuximab against tumor cells with wild-type or mutant epidermal growth factor receptor. Cancer Sci 98: 1275-1280.

199. Hoyle M, Crathorne L, Peters J, Jones-Hughes T, Cooper C, et al. (2013) The clinical effectiveness and cost-effectiveness of cetuximab (mono- or combination chemotherapy), bevacizumab (combination with non-oxaliplatin chemotherapy) and panitumumab (monotherapy) for the treatment of metastatic colorectal cancer after first-line chemotherapy (review of technology appraisal No.150 and part review of technology appraisal No. 118): a systematic review and economic model. Health Technol Assess 17: 1-237.

200. Kim GP, Grothey A (2008) Targeting colorectal cancer with human anti-EGFR monoclonocal antibodies: focus on panitumumab. Biologics 2: 223-228.

201. Hocking CM, Price TJ (2014) Panitumumab in the management of patients with KRAS wild-type metastatic colorectal cancer. Therap Adv Gastroenterol 7: 20-37.

202. Hecht JR, Mitchell E, Chidiac T, Scroggin C, Hagenstad C, et al. (2009) A randomized phase IIIB trial of chemotherapy, bevacizumab, and panitumumab compared with chemotherapy and bevacizumab alone for metastatic colorectal cancer. J Clin Oncol 27: 672-680.

203. Larkin MA, Blackshields G, Brown NP, Chenna R, McGettigan PA, et al. (2007) Clustal W and Clustal X version 2.0. Bioinformatics 23: 2947-2948.

204. Gasteiger E HC, Gattiker A, Duvaud S, Wilkins MR, Appel RD, Bairoch A (2005) The Proteomics Protocols Handbook: Humana Press.

205. Giudicelli V, Chaume D, Lefranc MP (2005) IMGT/GENE-DB: a comprehensive database for human and mouse immunoglobulin and T cell receptor genes. Nucleic Acids Res 33: D256-261.

206. Brochet X, Lefranc MP, Giudicelli V (2008) IMGT/V-QUEST: the highly customized and integrated system for IG and TR standardized V-J and V-D-J sequence analysis. Nucleic Acids Res 36: W503-508.

207. Dereeper A, Guignon V, Blanc G, Audic S, Buffet S, et al. (2008) Phylogeny.fr: robust phylogenetic analysis for the non-specialist. Nucleic Acids Res 36: W465-469.

208. Retter I, Althaus HH, Munch R, Muller W (2005) VBASE2, an integrative V gene database. Nucleic Acids Res 33: D671-674.

209. Kontermann RE, Martineau P, Cummings CE, Karpas A, Allen D, et al. (1997) Enzyme immunoassays using bispecific diabodies. Immunotechnology 3: 137-144.

210. Hoogenboom HR, Griffiths AD, Johnson KS, Chiswell DJ, Hudson P, et al. (1991) Multi-subunit proteins on the surface of filamentous phage: methodologies for displaying antibody (Fab) heavy and light chains. Nucleic Acids Res 19: 4133-4137.

211. Durocher Y, Perret S, Kamen A (2002) High-level and high-throughput recombinant protein production by transient transfection of suspension-growing human 293-EBNA1 cells. Nucleic Acids Res 30: E9.

212. Ejercito PM, Kieff ED, Roizman B (1968) Characterization of herpes simplex virus strains differing in their effects on social behaviour of infected cells. J Gen Virol 2: 357-364.

213. Johnson G, Wu TT (2001) Kabat Database and its applications: future directions. Nucleic Acids Res 29: 205-206.

214. Hellenbrand W, Thierfelder W, Muller-Pebody B, Hamouda O, Breuer T (2005) Seroprevalence of herpes simplex virus type 1 (HSV-1) and type 2 (HSV-2) in former East and West Germany, 1997-1998. Eur J Clin Microbiol Infect Dis 24: 131-135.

215. Swann JB, Smyth MJ (2007) Immune surveillance of tumors. J Clin Invest 117: 1137-1146.

216. Zitvogel L, Apetoh L, Ghiringhelli F, Andre F, Tesniere A, et al. (2008) The anticancer immune response: indispensable for therapeutic success? J Clin Invest 118: 1991-2001.

217. Jaras K, Anderson K (2011) Autoantibodies in cancer: prognostic biomarkers and immune activation. Expert Rev Proteomics 8: 577-589.

218. Heo CK, Bahk YY, Cho EW (2012) Tumor-associated autoantibodies as diagnostic and prognostic biomarkers. BMB Rep 45: 677-685.

219. Shishido SN, Varahan S, Yuan K, Li X, Fleming SD (2012) Humoral innate immune response and disease. Clin Immunol 144: 142-158.

220. Stockert E, Jager E, Chen YT, Scanlan MJ, Gout I, et al. (1998) A survey of the humoral immune response of cancer patients to a panel of human tumor antigens. J Exp Med 187: 1349-1354.

221. Cheever MA, Disis ML, Bernhard H, Gralow JR, Hand SL, et al. (1995) Immunity to oncogenic proteins. Immunol Rev 145: 33-59.

222. Kim JH, Herlyn D, Wong KK, Park DC, Schorge JO, et al. (2003) Identification of epithelial cell adhesion molecule autoantibody in patients with ovarian cancer. Clin Cancer Res 9: 4782-4791.

223. Grandis JR, Tweardy DJ (1993) Elevated levels of transforming growth factor alpha and epidermal growth factor receptor messenger RNA are early markers of carcinogenesis in head and neck cancer. Cancer Res 53: 3579-3584.

224. Ang KK, Berkey BA, Tu X, Zhang HZ, Katz R, et al. (2002) Impact of epidermal growth factor receptor expression on survival and pattern of relapse in patients with advanced head and neck carcinoma. Cancer Res 62: 7350-7356.

225. Kiefer JD (2012) Generation of fully human anti-EGFR antibody fragments using Phage-Display: Ruprechts-Karls Universität Heidelberg. Bachelor Thesis.

226. Gamou S, Kim YS, Shimizu N (1984) Different responses to EGF in two human carcinoma cell lines, A431 and UCVA-1, possessing high numbers of EGF receptors. Mol Cell Endocrinol 37: 205-213.

227. Bjorkelund H, Gedda L, Barta P, Malmqvist M, Andersson K (2011) Gefitinib induces epidermal growth factor receptor dimers which alters the interaction characteristics with (1)(2)(5)I-EGF. PLoS One 6: e24739.

228. Goldstein NI, Prewett M, Zuklys K, Rockwell P, Mendelsohn J (1995) Biological efficacy of a chimeric antibody to the epidermal growth factor receptor in a human tumor xenograft model. Clin Cancer Res 1: 1311-1318.

229. Lerner RA, Barbas CF, 3rd, Kang AS, Burton DR (1991) On the use of combinatorial antibody libraries to clone the "fossil record" of an individual's immune response. Proc Natl Acad Sci U S A 88: 9705-9706.

230. Felding-Habermann B, Lerner RA, Lillo A, Zhuang S, Weber MR, et al. (2004) Combinatorial antibody libraries from cancer patients yield ligand-mimetic Arg-Gly-Asp-containing immunoglobulins that inhibit breast cancer metastasis. Proc Natl Acad Sci U S A 101: 17210-17215.

231. Caton AJ, Koprowski H (1990) Influenza virus hemagglutinin-specific antibodies isolated from a combinatorial expression library are closely related to the immune response of the donor. Proc Natl Acad Sci U S A 87: 6450-6454.

232. Zhou J, Lottenbach KR, Barenkamp SJ, Lucas AH, Reason DC (2002) Recurrent variable region gene usage and somatic mutation in the human antibody response to the capsular polysaccharide of Streptococcus pneumoniae type 23F. Infect Immun 70: 4083-4091.

233. Larrick JW, Danielsson L, Brenner CA, Abrahamson M, Fry KE, et al. (1989) Rapid cloning of rearranged immunoglobulin genes from human hybridoma cells using mixed primers and the polymerase chain reaction. Biochem Biophys Res Commun 160: 1250-1256.

234. Watkins BA, Davis AE, Fiorentini S, Reitz MS, Jr. (1995) V-region and class specific RT-PCR amplification of human immunoglobulin heavy and light chain genes from B-cell lines. Scand J Immunol 42: 442-448.

235. Welschof M, Terness P, Kolbinger F, Zewe M, Dubel S, et al. (1995) Amino acid sequence based PCR primers for amplification of rearranged human heavy and light chain immunoglobulin variable region genes. J Immunol Methods 179: 203-214.

236. Sblattero D, Bradbury A (1998) A definitive set of oligonucleotide primers for amplifying human V regions. Immunotechnology 3: 271-278.

237. Little M, Welschof M, Braunagel M, Hermes I, Christ C, et al. (1999) Generation of a large complex antibody library from multiple donors. J Immunol Methods 231: 3-9.

238. Hust M, Dübel S (2010) Chapter 5: Human antibody gene libraries. In: Antibody Engineering. Volume 1. Edited by: Kontermann RE, Dübel S. Second edition: Springer Protocols. pp. 65-84.

239. Loset GA, Lobersli I, Kavlie A, Stacy JE, Borgen T, et al. (2005) Construction, evaluation and refinement of a large human antibody phage library based on the IgD and IgM variable gene repertoire. J Immunol Methods 299: 47-62.

240. Hust M, Meyer T, Voedisch B, Rulker T, Thie H, et al. (2011) A human scFv antibody generation pipeline for proteome research. J Biotechnol 152: 159-170.

241. de Bruin R, Spelt K, Mol J, Koes R, Quattrocchio F (1999) Selection of high-affinity phage antibodies from phage display libraries. Nat Biotechnol 17: 397-399.

242. Ewert S, Huber T, Honegger A, Pluckthun A (2003) Biophysical properties of human antibody variable domains. J Mol Biol 325: 531-553.

243. Hussack G, Keklikian A, Alsughayyir J, Hanifi-Moghaddam P, Arbabi-Ghahroudi M, et al. (2012) A V(L) single-domain antibody library shows a high-propensity to yield non-aggregating binders. Protein Eng Des Sel 25: 313-318.

244. Dubnovitsky AP, Kravchuk ZI, Chumanevich AA, Cozzi A, Arosio P, et al. (2000) Expression, refolding, and ferritin-binding activity of the isolated VL-domain of monoclonal antibody F11. Biochemistry (Mosc) 65: 1011-1018.

245. Kim DY, To R, Kandalaft H, Ding W, van Faassen H, et al. (2014) Antibody light chain variable domains and their biophysically improved versions for human immunotherapy. MAbs 6: 219-235.

246. Pluckthun A (1992) Mono- and bivalent antibody fragments produced in Escherichia coli: engineering, folding and antigen binding. Immunol Rev 130: 151-188.

247. Glockshuber R, Malia M, Pfitzinger I, Pluckthun A (1990) A comparison of strategies to stabilize immunoglobulin Fv-fragments. Biochemistry 29: 1362-1367.

248. Plückthun A (1991) Strategies for the Expression of Antibody Fragments in Echerichia coli. In METHODS: A Comparison to Methods in Enzymology Volume 2. Number 2. pp.88-96.

249. Huston JS, McCartney J, Tai MS, Mottola-Hartshorn C, Jin D, et al. (1993) Medical applications of single-chain antibodies. Int Rev Immunol 10: 195-217.

250. Turner DJ, Ritter MA, George AJ (1997) Importance of the linker in expression of single-chain Fv antibody fragments: optimisation of peptide sequence using phage display technology. J Immunol Methods 205: 43-54.

251. Kortt AA, Dolezal O, Power BE, Hudson PJ (2001) Dimeric and trimeric antibodies: high avidity scFvs for cancer targeting. Biomol Eng 18: 95-108.

252. Holliger P, Prospero T, Winter G (1993) "Diabodies": small bivalent and bispecific antibody fragments. Proc Natl Acad Sci U S A 90: 6444-6448.

253. Essig NZ, Wood JF, Howard AJ, Raag R, Whitlow M (1993) Crystallization of single-chain Fv proteins. J Mol Biol 234: 897-901.

254. Griffiths AD, Malmqvist M, Marks JD, Bye JM, Embleton MJ, et al. (1993) Human anti-self antibodies with high specificity from phage display libraries. EMBO J 12: 725-734.

255. Whitlow M, Filpula D, Rollence ML, Feng SL, Wood JF (1994) Multivalent Fvs: characterization of single-chain Fv oligomers and preparation of a bispecific Fv. Protein Eng 7: 1017-1026.

256. Kortt AA, Malby RL, Caldwell JB, Gruen LC, Ivancic N, et al. (1994) Recombinant anti-sialidase single-chain variable fragment antibody. Characterization, formation of dimer and higher-molecular-mass multimers and the solution of the crystal structure of the single-chain variable fragment/sialidase complex. Eur J Biochem 221: 151-157.

257. Raag R, Whitlow M (1995) Single-chain Fvs. FASEB J 9: 73-80.

258. Schier R, Bye J, Apell G, McCall A, Adams GP, et al. (1996) Isolation of high-affinity monomeric human anti-c-erbB-2 single chain Fv using affinity-driven selection. J Mol Biol 255: 28-43.

259. Wu AM, Chen W, Raubitschek A, Williams LE, Neumaier M, et al. (1996) Tumor localization of anti-CEA single-chain Fvs: improved targeting by non-covalent dimers. Immunotechnology 2: 21-36.

260. Arndt KM, Muller KM, Pluckthun A (1998) Factors influencing the dimer to monomer transition of an antibody single-chain Fv fragment. Biochemistry 37: 12918-12926.

261. Desplancq D, King DJ, Lawson AD, Mountain A (1994) Multimerization behaviour of single chain Fv variants for the tumour-binding antibody B72.3. Protein Eng 7: 1027-1033.

262. Schmaljohn C, Cui Y, Kerby S, Pennock D, Spik K (1999) Production and characterization of human monoclonal antibody Fab fragments to vaccinia virus from a phage-display combinatorial library. Virology 258: 189-200.

263. Kausmally L, Waalen K, Lobersli I, Hvattum E, Berntsen G, et al. (2004) Neutralizing human antibodies to varicella-zoster virus (VZV) derived from a VZV patient recombinant antibody library. J Gen Virol 85: 3493-3500.

264. Tikunova N, Dubrovskaya V, Morozova V, Yun T, Khlusevich Y, et al. (2012) The neutralizing human recombinant antibodies to pathogenic Orthopoxviruses derived from a phage display immune library. Virus Res 163: 141-150.

265. Salonen EM, Parren PW, Graus YF, Lundkvist A, Fisicaro P, et al. (1998) Human recombinant Puumala virus antibodies: cross-reaction with other hantaviruses and use in diagnostics. J Gen Virol 79 (Pt 4): 659-665.

266. Kowal C, Weinstein A, Diamond B (1999) Molecular mimicry between bacterial and self antigen in a patient with systemic lupus erythematosus. Eur J Immunol 29: 1901-1911.

267. Ward RL, Clark MA, Lees J, Hawkins NJ (1996) Retrieval of human antibodies from phage-display libraries using enzymatic cleavage. J Immunol Methods 189: 73-82.

268. Roovers RC, van der Linden E, Zijlema H, de Bruine A, Arends JW, et al. (2001) Evidence for a bias toward intracellular antigens in the local humoral anti-tumor immune response of a colorectal cancer patient revealed by phage display. Int J Cancer 93: 832-840.

269. Rothe A, Klimka A, Tur MK, Pfitzner T, Huhn M, et al. (2004) Construction of phage display libraries from reactive lymph nodes of breast carcinoma patients and selection for specifically binding human single chain Fv on cell lines. Int J Mol Med 14: 729-735.

270. Ayat H, Burrone OR, Sadghizadeh M, Jahanzad E, Rastgou N, et al. (2013) Isolation of scFv antibody fragments against HER2 and CEA tumor antigens from combinatorial antibody libraries derived from cancer patients. Biologicals 41: 345-354.

271. Yip YL, Hawkins NJ, Clark MA, Ward RL (1997) Evaluation of different lymphoid tissue sources for the construction of human immunoglobulin gene libraries. Immunotechnology 3: 195-203.

272. Clark MA, Hawkins NJ, Papaioannou A, Fiddes RJ, Ward RL (1997) Isolation of human anti-c-erbB-2 Fabs from a lymph node-derived phage display library. Clin Exp Immunol 109: 166-174.

273. Kettleborough CA, Ansell KH, Allen RW, Rosell-Vives E, Gussow DH, et al. (1994) Isolation of tumor cell-specific single-chain Fv from immunized mice using phage-antibody libraries and the re-construction of whole antibodies from these antibody fragments. Eur J Immunol 24: 952-958.

274. Venet S, Kosco-Vilbois M, Fischer N (2013) Comparing CDRH3 diversity captured from secondary lymphoid organs for the generation of recombinant human antibodies. MAbs 5: 690-698.

275. Shlomchik MJ, Weisel F (2012) Germinal center selection and the development of memory B and plasma cells. Immunol Rev 247: 52-63.

276. Victora GD, Nussenzweig MC (2012) Germinal centers. Annu Rev Immunol 30: 429-457.

277. McHeyzer-Williams LJ, McHeyzer-Williams MG (2005) Antigen-specific memory B cell development. Annu Rev Immunol 23: 487-513.

278. Tangye SG, Tarlinton DM (2009) Memory B cells: effectors of long-lived immune responses. Eur J Immunol 39: 2065-2075.

279. Bende RJ, van Maldegem F, Triesscheijn M, Wormhoudt TA, Guijt R, et al. (2007) Germinal centers in human lymph nodes contain reactivated memory B cells. J Exp Med 204: 2655-2665.

280. Poulsen TR, Jensen A, Haurum JS, Andersen PS (2011) Limits for antibody affinity maturation and repertoire diversification in hypervaccinated humans. J Immunol 187: 4229-4235.

281. Mouquet H, Klein F, Scheid JF, Warncke M, Pietzsch J, et al. (2011) Memory B cell antibodies to HIV-1 gp140 cloned from individuals infected with clade A and B viruses. PLoS One 6: e24078.

282. Kashyap HK, Biswas R (2008) Dipolar solvation dynamics in room temperature ionic liquids: an effective medium calculation using dielectric relaxation data. J Phys Chem B 112: 12431-12438.

283. Pavoni E, Vaccaro P, Anastasi AM, Minenkova O (2014) Optimized selection of anti-tumor recombinant antibodies from phage libraries on intact cells. Mol Immunol 57: 317-322.

284. Broering TJ, Garrity KA, Boatright NK, Sloan SE, Sandor F, et al. (2009) Identification and characterization of broadly neutralizing human monoclonal antibodies directed against the E2 envelope glycoprotein of hepatitis C virus. J Virol 83: 12473-12482.

285. Keck ZY, Sung VM, Perkins S, Rowe J, Paul S, et al. (2004) Human monoclonal antibody to hepatitis C virus E1 glycoprotein that blocks virus attachment and viral infectivity. J Virol 78: 7257-7263.

286. Kubota-Koketsu R, Mizuta H, Oshita M, Ideno S, Yunoki M, et al. (2009) Broad neutralizing human monoclonal antibodies against influenza virus from vaccinated healthy donors. Biochem Biophys Res Commun 387: 180-185.

287. Smith SA, de Alwis AR, Kose N, Harris E, Ibarra KD, et al. (2013) The potent and broadly neutralizing human dengue virus-specific monoclonal antibody 1C19 reveals a unique cross-reactive epitope on the bc loop of domain II of the envelope protein. MBio 4: e00873-00813.

288. Yasugi M, Kubota-Koketsu R, Yamashita A, Kawashita N, Du A, et al. (2013) Human monoclonal antibodies broadly neutralizing against influenza B virus. PLoS Pathog 9: e1003150.

289. Burioni R, Canducci F, Mancini N, Clementi N, Sassi M, et al. (2009) Molecular cloning of the first human monoclonal antibodies neutralizing with high potency swine-origin influenza A pandemic virus (S-OIV). New Microbiol 32: 319-324.

290. Matsumoto T, Yamada K, Noguchi K, Nakajima K, Takada K, et al. (2010) Isolation and characterization of novel human monoclonal antibodies possessing neutralizing ability against rabies virus. Microbiol Immunol 54: 673-683.

291. Costin JM, Zaitseva E, Kahle KM, Nicholson CO, Rowe DK, et al. (2013) Mechanistic study of broadly neutralizing human monoclonal antibodies against dengue virus that target the fusion loop. J Virol 87: 52-66.

292. Hu W, Chen A, Miao Y, Xia S, Ling Z, et al. (2013) Fully human broadly neutralizing monoclonal antibodies against influenza A viruses generated from the memory B cells of a 2009 pandemic H1N1 influenza vaccine recipient. Virology 435: 320-328.

293. Duan T, Ferguson M, Yuan L, Xu F, Li G (2009) Human Monoclonal Fab Antibodies Against West Nile Virus and its Neutralizing Activity Analyzed in Vitro and in Vivo. J Antivir Antiretrovir 1: 36-42.

294. Itoh K, Nakagomi O, Suzuki K, Inoue K, Tada H, et al. (1999) Recombinant human monoclonal Fab fragments against rotavirus from phage display combinatorial libraries. J Biochem 125: 123-129.

295. Johansson DX, Voisset C, Tarr AW, Aung M, Ball JK, et al. (2007) Human combinatorial libraries yield rare antibodies that broadly neutralize hepatitis C virus. Proc Natl Acad Sci U S A 104: 16269-16274.

296. Barbas CF, 3rd, Crowe JE, Jr., Cababa D, Jones TM, Zebedee SL, et al. (1992) Human monoclonal Fab fragments derived from a combinatorial library bind to respiratory syncytial virus F glycoprotein and neutralize infectivity. Proc Natl Acad Sci U S A 89: 10164-10168.

297. Zhang MY, Choudhry V, Sidorov IA, Tenev V, Vu BK, et al. (2006) Selection of a novel gp41-specific HIV-1 neutralizing human antibody by competitive antigen panning. J Immunol Methods 317: 21-30.

298. Zhang MY, Shu Y, Phogat S, Xiao X, Cham F, et al. (2003) Broadly cross-reactive HIV neutralizing human monoclonal antibody Fab selected by sequential antigen panning of a phage display library. J Immunol Methods 283: 17-25.

299. Saokaew N, Poungpair O, Panya A, Tarasuk M, Sawasdee N, et al. (2013) Human monoclonal single-chain antibodies specific to dengue virus envelope protein. Lett Appl Microbiol.

300. Zhu Z, Dimitrov AS, Bossart KN, Crameri G, Bishop KA, et al. (2006) Potent neutralization of Hendra and Nipah viruses by human monoclonal antibodies. J Virol 80: 891-899.

301. Fujinaga S, Sugano T, Matsumoto Y, Masuho Y, Mori R (1987) Antiviral activities of human monoclonal antibodies to herpes simplex virus. J Infect Dis 155: 45-53.

302. Baldwin RW (1971) Tumour-associated antigens and tumour-host interactions. Proc R Soc Med 64: 1039-1042.

303. Anderson KS, LaBaer J (2005) The sentinel within: exploiting the immune system for cancer biomarkers. J Proteome Res 4: 1123-1133.

304. Tan EM (2001) Autoantibodies as reporters identifying aberrant cellular mechanisms in tumorigenesis. J Clin Invest 108: 1411-1415.

305. Finn OJ (2005) Immune response as a biomarker for cancer detection and a lot more. N Engl J Med 353: 1288-1290.

306. Chapman C, Murray A, Chakrabarti J, Thorpe A, Woolston C, et al. (2007) Autoantibodies in breast cancer: their use as an aid to early diagnosis. Ann Oncol 18: 868-873.

307. Desmetz C, Bascoul-Mollevi C, Rochaix P, Lamy PJ, Kramar A, et al. (2009) Identification of a new panel of serum autoantibodies associated with the presence of in situ carcinoma of the breast in younger women. Clin Cancer Res 15: 4733-4741.

308. Xu C, Yu C, Ma H, Xu L, Miao M, et al. (2013) Prevalence and risk factors for the development of nonalcoholic fatty liver disease in a nonobese Chinese population: the Zhejiang Zhenhai Study. Am J Gastroenterol 108: 1299-1304.

309. Zhou SL, Yue WB, Fan ZM, Du F, Liu BC, et al. (2013) Autoantibody detection to tumor-associated antigens of P53, IMP1, P16, cyclin B1, P62, C-myc, Survivn, and Koc for the screening of high-risk subjects and early detection of esophageal squamous cell carcinoma. Dis Esophagus.

310. Zinkernagel RM (2000) What is missing in immunology to understand immunity? Nat Immunol 1: 181-185.

311. Sahin U, Tureci O, Schmitt H, Cochlovius B, Johannes T, et al. (1995) Human neoplasms elicit multiple specific immune responses in the autologous host. Proc Natl Acad Sci U S A 92: 11810-11813.

312. Scanlan MJ, Chen YT, Williamson B, Gure AO, Stockert E, et al. (1998) Characterization of human colon cancer antigens recognized by autologous antibodies. Int J Cancer 76: 652-658.

313. Pupa SM, Menard S, Andreola S, Colnaghi MI (1993) Antibody response against the c-erbB-2 oncoprotein in breast carcinoma patients. Cancer Res 53: 5864-5866.

314. Disis ML, Pupa SM, Gralow JR, Dittadi R, Menard S, et al. (1997) High-titer HER-2/neu protein-specific antibody can be detected in patients with early-stage breast cancer. J Clin Oncol 15: 3363-3367.

315. Ward RL, Hawkins NJ, Coomber D, Disis ML (1999) Antibody immunity to the HER-2/neu oncogenic protein in patients with colorectal cancer. Hum Immunol 60: 510-515.

316. Haidopoulos D, Konstadoulakis MM, Antonakis PT, Alexiou DG, Manouras AM, et al. (2000) Circulating anti-CEA antibodies in the sera of patients with breast cancer. Eur J Surg Oncol 26: 742-746.

317. Lu H, Ladd J, Feng Z, Wu M, Goodell V, et al. (2012) Evaluation of known oncoantibodies, HER2, p53, and cyclin B1, in prediagnostic breast cancer sera. Cancer Prev Res (Phila) 5: 1036-1043.

318. Ostendorff HP, Awad A, Braunschweiger KI, Liu Z, Wan Z, et al. (2013) Multiplexed VeraCode bead-based serological immunoassay for colorectal cancer. J Immunol Methods 400-401: 58-69.

319. Pereira S, Van Belle P, Elder D, Maruyama H, Jacob L, et al. (1997) Combinatorial antibodies against human malignant melanoma. Hybridoma 16: 11-16.

320. Lee KJ, Mao S, Sun C, Gao C, Blixt O, et al. (2002) Phage-display selection of a human single-chain fv antibody highly specific for melanoma and breast cancer cells using a chemoenzymatically synthesized G(M3)-carbohydrate antigen. J Am Chem Soc 124: 12439-12446.

321. Dantas-Barbosa C, Faria FP, Brigido MM, Maranhao AQ (2009) Isolation of osteosarcoma-associated human antibodies from a combinatorial Fab phage display library. J Biomed Biotechnol 2009: 157531.

322. Heitner T, Moor A, Garrison JL, Marks C, Hasan T, et al. (2001) Selection of cell binding and internalizing epidermal growth factor receptor antibodies from a phage display library. J Immunol Methods 248: 17-30.

323. Zhao X, Dai W, Cao L, Zhu H, Yu Y, et al. (2007) Selection and characterization of an internalizing epidermal-growth-factor-receptor antibody. Biotechnol Appl Biochem 46: 27-33.

324. Chang C, Takayanagi A, Yoshida T, Shimizu N (2011) Screening of scFv-displaying phages recognizing distinct extracellular domains of EGF receptor by target-guided proximity labeling method. J Immunol Methods 372: 127-136.

325. Kurosawa G, Sumitomo M, Ukai Y, Subere J, Muramatsu C, et al. (2011) Selection and analysis of anti-cancer antibodies for cancer therapy obtained from antibody phage library. Cancer Sci 102: 175-181.

326. Rust S, Guillard S, Sachsenmeier K, Hay C, Davidson M, et al. (2013) Combining phenotypic and proteomic approaches to identify membrane targets in a 'triple negative' breast cancer cell type. Mol Cancer 12: 11.

327. Souriau C, Rothacker J, Hoogenboom HR, Nice E (2004) Human antibody fragments specific for the epidermal growth factor receptor selected from large non-immunised phage display libraries. Growth Factors 22: 185-194.

328. Olsen DA, Jakobsen EH, Brandslund I (2013) Quantification of EGFR autoantibodies in the amplification phenomenon of HER2 in breast cancer. Clin Chem Lab Med 51: 2325-2329.

329. Planque S, Zhou YX, Nishiyama Y, Sinha M, O'Connor-Mccourt M, et al. (2003) Autoantibodies to the epidermal growth factor receptor in systemic sclerosis, lupus, and autoimmune mice. FASEB J 17: 136-143.

330. Liu M, Subramanian V, Christie C, Castro M, Mohanakumar T (2012) Immune responses to self-antigens in asthma patients: clinical and immunopathological implications. Hum Immunol 73: 511-516.

331. Choe JY, Yun JY, Nam SJ, Kim JE (2012) Expression of c-Met Is Different along the Location and Associated with Lymph Node Metastasis of Head and Neck Carcinoma. Korean J Pathol 46: 515-522.

332. Peng Z, Zhu Y, Wang Q, Gao J, Li Y, et al. (2014) Prognostic Significance of MET Amplification and Expression in Gastric Cancer: A Systematic Review with Meta-Analysis. PLoS One 9: e84502.

333. Abou-Bakr AA, Elbasmi A (2013) c-MET overexpression as a prognostic biomarker in colorectal adenocarcinoma. Gulf J Oncolog 1: 28-34.

Appendix

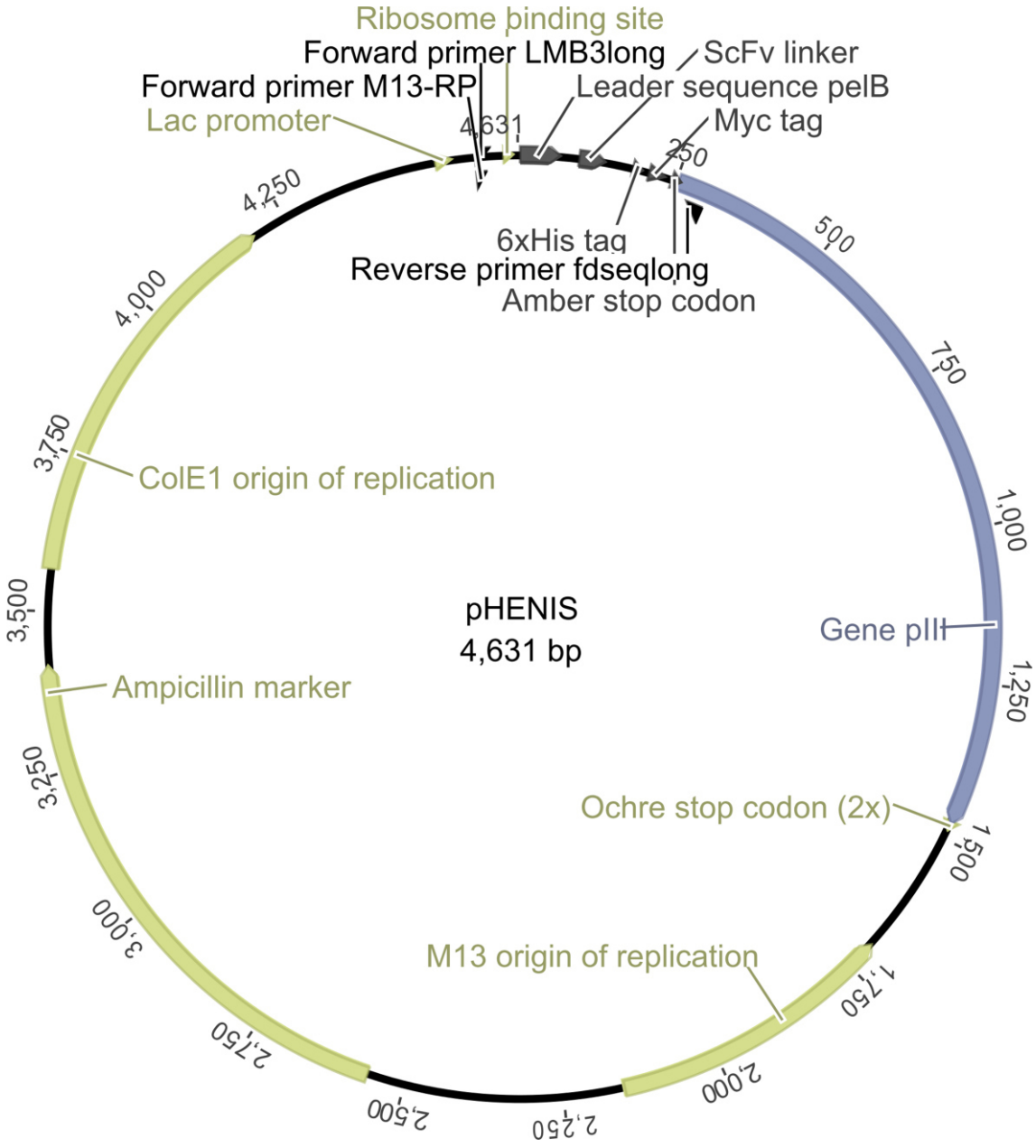

Figure 45. Map of phagemid vector pHENIS.

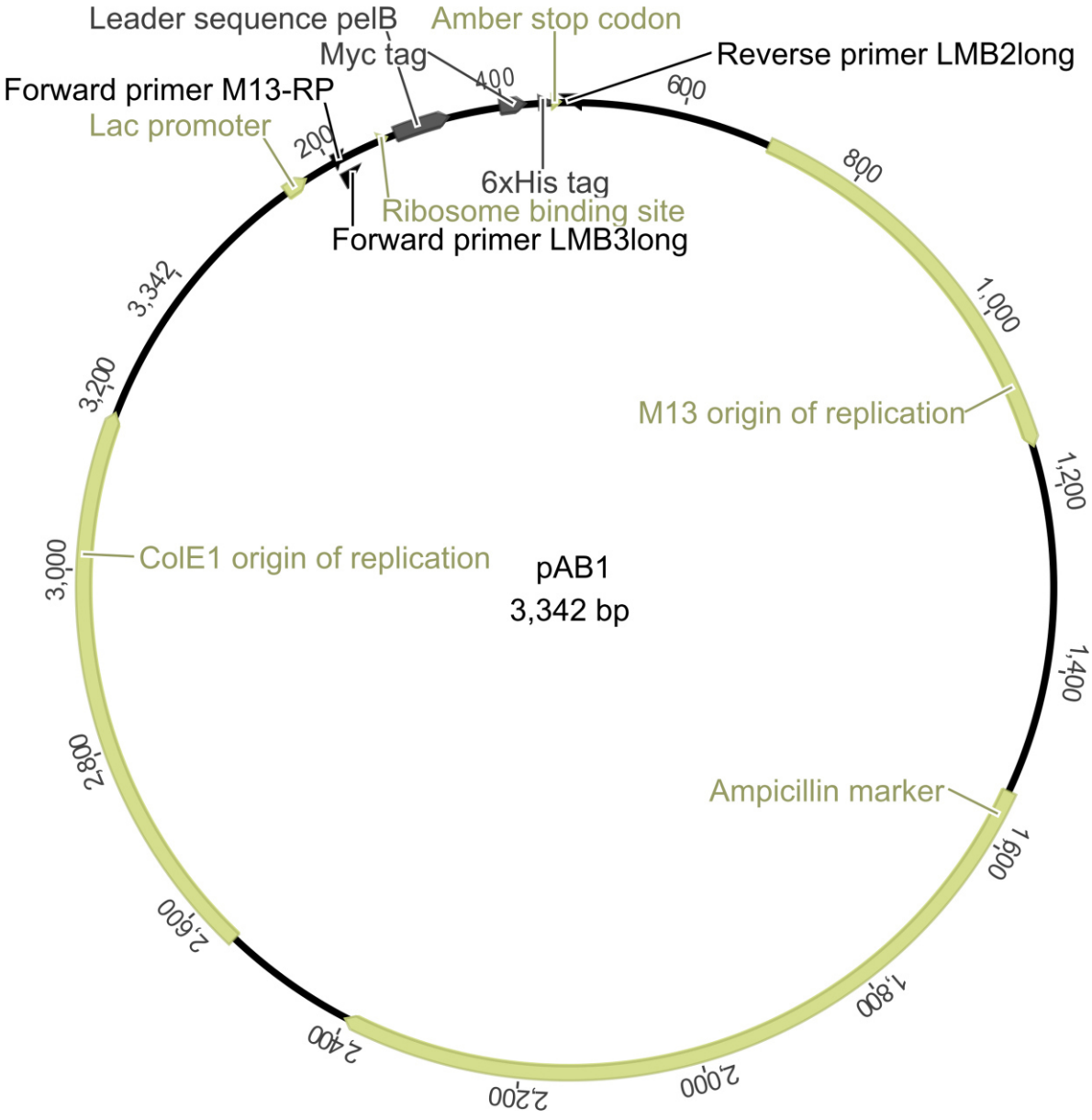

Figure 46. Map of bacterial expression vector pAB1.

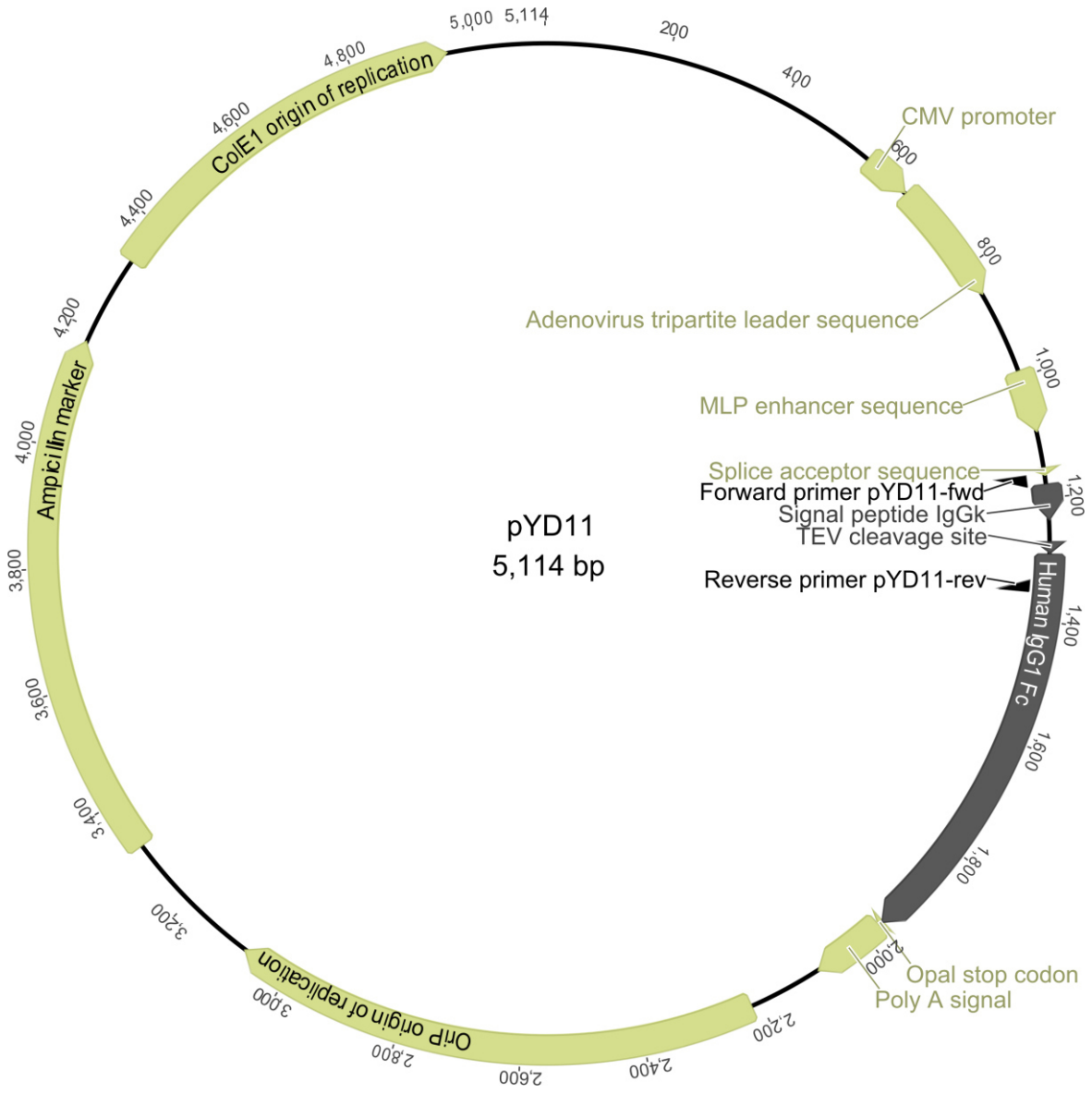

Figure 47: Map of mammalian expression vector pYD11.

Acknowledgements

First, I would like to thank Prof. Dr. Roland E. Kontermann for accepting me as external PhD student at the University of Stuttgart, for his valuable feedbacks, ideas, and helpful discussions.

Furthermore, I thank Prof. Dr. Dirk Jäger for the opportunity to work at the Department of Medical Oncology at the National Center for Tumor Diseases (NCT) in Heidelberg and the support of this project.

Special thanks go to Dr. Michaela A. E. Arndt and PD. Dr. Jürgen Krauss for giving me the opportunity to work in their group “Antibody-based Immunotherapeutics” at the NCT Heidelberg. Thanks a lot for your encouraged support throughout the last years, for your trust for giving me the freedom to develop and conduct my own ideas, and the support of the project.

I am grateful to our cooperation partners from the Heidelberg University Hospital Prof. Dr. Christel Herold-Mende, Dr. Gerhard Dyckhoff, PD Dr. Philippe A. Federspil, and their group members for providing the patient lymph nodes and blood samples. I express my sincere gratitude to all patients who agreed to participate to this project.

I would like to thank Dr. Gerhard Moldenhauer for providing the detection antibody and Dr. Roland Kehm for the support concerning viral issues.

Furthermore, I thank the members of the other groups from the Medical Oncology Department for support, discussion, and enjoyable atmosphere.

Moreover, many thanks to the research groups of the Institute for Anatomy and Cell Biology of the University Heidelberg for kind welcoming in our new laboratory.

I express my gratitude to all former and current members of the research group “Antibody-based Immunotherapeutics” for their support and creating a pleasant and motivating atmosphere: Tobias Weber, Stefan Kiesgen, Anne Schlegelmilch, Armin Keller, Stephanie Haase, Benedikt Bötticher, Evelyn Exner, Athanasios Mavratzas, Claudia Bollinger, Daniela Behling, Martin Cremer, Raphael Bleiler, Nora Liebers, Mira Alt, Richard Schneider, Philipp Kuhn, Jonathan Kiefer, and Tamana Karimi.

Especially, I want to thank Stephanie and Armin for their great help and constant support during library construction and selection, and Anne for her help with the virus work.

Last but not least, I thank my family and friends, especially my beloved parents, my brothers Christoph and Jörg, and Tammy for their love, support, and encouragement.

Erklärung

Ich erkläre hiermit, dass ich die vorgelegte Dissertation selbst verfasst und mich keinen anderen als den von mir ausdrücklich bezeichneten Quellen und Hilfen bedient habe. Des Weiteren erkläre ich, dass ich an keiner anderen Stelle ein Prüfungsverfahren beantragt oder die Dissertation in dieser oder einer anderen Form bereits anderweitig als Prüfungsarbeit verwendet habe.

Heidelberg, den 20.01.2014

Philipp J. Diebolder